

**CALLOSE-MEDIATED REGULATION OF PLASMODESMATA
DURING THE ESTABLISHMENT OF *MEDICAGO TRUNCATULA*-
SINORHIZOBIUM MELILOTI SYMBIOTIC INTERACTION**

Rocio Gaudioso-Pedraza

Submitted in accordance with the requirements for the degree of Doctor of
Philosophy (Ph.D.)

The University of Leeds

Faculty of Biological Sciences

September 2017

The candidate confirms that the work submitted is his/her own and that appropriate credit has been given where reference has been made to the work of others.

This copy has been supplied on the understanding that it is copyright material and that no quotation from the thesis may be published without proper acknowledgement.

The right of Rocio Gaudioso-Pedraza to be identified as Author of this work has been asserted by her in accordance with the Copyright, Designs and Patents Act 1988.

A mis padres

Acknowledgements

I would like to thank my supervisor, Dr Yoselin Benitez-Alfonso, for her support during these years. Thank you for the discussions, for all the learning experiences and above all, all the fun. Thank you for opening the door to your lab but also to your home. You have been much more than a thesis supervisor. Thanks for everything.

Thanks to all members of the lab that have shared time, discussions and coffee with me over the time of my PhD.

I would also like to thank everyone in the Centre for Plant Sciences, but especially Prof. Paul Knox, Sue Marcus and his group. They have been extremely helpful during my PhD. Many thanks to Prof. Giles Oldroyd and his group at the John Innes Centre, their expertise in *Medicago truncatula* and resources have been instrumental in this thesis.

I am very grateful to the University of Leeds for funding my PhD and supporting my work during these years.

I would like to thank those without I doubt I would have made it. Thanks to Ambra, Gloria, Kasia, Yoselin and Mercedes. The time of Hijas at Leeds has been some of my happiest years. I feel inspired by you every day and I am incredibly grateful to count you among my friends.

Thanks to Carlos, thank you for accompanying me every day, thank you for your unconditional support and thank you for sharing your life with me.

Thanks to my family a thousand times and for a thousand reasons. Thanks to my mum for her mitochondrial DNA, thanks to my dad for his pep talks, thanks to my sister for all her encouragement and love. I will always be overwhelmed by your support, patience and, above all, your unwavering love.

Abstract

Legumes, such as *Medicago truncatula*, can fix atmospheric nitrogen by forming symbiotic associations with soil-borne bacteria collectively called rhizobia. As a result of this relationship, specific roots organs called nodules, are developed that houses rhizobia and where the nitrogen fixation process occurs. Nodule formation is tightly regulated by complex signalling mechanisms and environmental cues, such as nitrate availability. Molecular signals move between the site of infection and the cortex/pericycle to coordinate nodule organogenesis and also systemically along the vascular system to coordinate root and shoot responses. Despite recent progress in the identification of some of these signals very little is known about the pathways for intercellular transport.

In this project, the role of the cell-wall polysaccharide callose in the establishment of symbiotic interaction between *Medicago truncatula* and *Sinorhizobium meliloti* was addressed. Callose metabolism regulates transport through plasmodesmata: intercellular channels that form a symplastic path for transport. Using immuno-histochemistry we found that callose is downregulated as early as 16 hours post-bacterial inoculation. Concomitantly, the expression of a plasmodesmata located callose degrading enzyme (Medtr3g083580), identified using phylogeny, was induced. Roots constitutively expressing either Medtr3g083580 or its Arabidopsis orthologue PdBG1, showed reduced callose levels and a higher rate of infection and nodulation, even when grown in nitrate concentrations that inhibit nodulation. The effects were stronger when using a promoter active early after rhizobial infection and were mimicked, in high nitrate conditions, by the ectopic expression of a novel plasmodesmata receptor-like kinase (Medtr1g073320).

The results suggest an important role for callose in the control of nodulation, both under nitrate deprived or sufficient conditions, likely associated with the regulation of transport via plasmodesmata. The relevance of the findings is discussed in light of potential applications in crop improvement and in reducing the use of nitrogen fertilizers.

Table of Contents

| | |
|---|-------------|
| Acknowledgements | iii |
| List of figures | xi |
| List of Appendices | xv |
| List of abbreviations | xvii |
| Chapter 1 –Introduction | 2 |
| 1.1 Brief introduction to symbiosis | 2 |
| 1.2 Brief introduction to biological nitrogen fixation | 3 |
| 1.2.1 Sequential steps in the formation of nitrogen fixing symbiosis | 5 |
| 1.2.2 Key regulators of rhizobia infection and nodulation in Medicago truncatula | 8 |
| 1.2.3 The regulation of symbiosis by the host plant | 15 |
| 1.2.4 Spontaneous nodulation | 21 |
| 1.3 Brief introduction to the symplastic pathway | 23 |
| 1.3.1 Role of the symplastic pathway in plant development | 25 |
| 1.3.2 Regulation of plasmodesmata transport | 26 |
| 1.3.3 Role of plasmodesmata in plant-microorganism interactions | 29 |
| 1.4 Aims and objectives of this thesis | 36 |
| Chapter 2 –Materials and Methods | 39 |
| 2.1 Plant Methods | 39 |
| 2.1.1 Plant materials, seed sterilisation and vernalisation | 39 |
| 2.1.2 Plant growth conditions | 39 |
| 2.1.3 Generation of M. truncatula transgenic roots by A. rhizogenes | 39 |
| 2.1.4 Plant growth media | 40 |
| 2.2 Bacterial Methods | 41 |
| 2.2.1 Bacterial strains | 41 |
| 2.2.2 Plasmid preparation and bacterial transformation | 41 |
| 2.2.3 Growth curve | 41 |
| 2.2.4 Bacterial growth media | 42 |
| 2.2.5 Nodule occupancy assay | 43 |
| 2.3 Microscopy Methods | 43 |
| 2.3.1 Confocal Microscopy | 43 |

| | | |
|---|---|-----------|
| 2.3.2 | Light Microscopy | 43 |
| 2.4 | Molecular Biology Methods | 43 |
| 2.4.1 | Standard PCR | 43 |
| 2.4.2 | Agarose gel electrophoresis | 44 |
| 2.4.3 | Golden Gate designs and cloning system | 44 |
| 2.4.4 | Primer design | 47 |
| 2.4.5 | Gateway designs and cloning system | 48 |
| 2.4.6 | Primer design | 50 |
| 2.4.7 | Quantitative Real-Time Reverse Transcription PCR | 52 |
| 2.5 | Phenotyping <i>M. truncatula</i> roots development | 54 |
| 2.5.1 | 2-Deoxy-D-glucose (DDG) treatment | 54 |
| 2.5.2 | Root hair length measurement | 54 |
| 2.5.3 | Root length, weight and width measurement | 54 |
| 2.6 | Nodulation and infection assays | 55 |
| 2.6.1 | β -Galactosidase staining | 55 |
| 2.6.2 | Flood infection in plates | 55 |
| 2.6.3 | Spot inoculation | 55 |
| 2.6.4 | Infection in soil | 56 |
| 2.6.5 | Counting Infection Threads, Infection Pockets and Nodule Primordia | 56 |
| 2.6.6 | Assaying nodulation in soil | 56 |
| 2.7 | Phylogenetic and structural analyses of proteins | 57 |
| 2.7.1 | Retrieval of β -1,3-glucanases, GSL and PDLP-like sequences and analysis of protein domains | 57 |
| 2.7.2 | Alignments and phylogenetic analysis | 57 |
| 2.7.3 | Selection of candidates | 58 |
| 2.8 | Biochemistry Methods | 58 |
| 2.8.1 | Immunolocalisation | 58 |
| 2.8.2 | Aniline blue staining | 59 |
| 2.8.3 | Histochemical localisation of GUS | 60 |
| 2.8.4 | Toluidine blue staining | 60 |
| 2.9 | Statistical analysis of the data | 60 |
| Chapter 3 – Regulation of callose in cell walls of <i>M.truncatula</i> roots in response to rhizobia | | 63 |
| 3.1 | Summary | 63 |

| | | |
|--|---|------------|
| 3.2 | Results | 65 |
| 3.2.1 | Immunolocalisation experiments show that callose is down-regulated after inoculation of <i>M. truncatula</i> roots with rhizobia | 65 |
| 3.2.2 | Callose regulation appears not to be essential for the inhibition of nodulation in nitrate conditions..... | 67 |
| 3.2.3 | Identification of callose metabolic enzymes regulated in response to rhizobia infection in <i>Medicago</i> roots | 76 |
| 3.2.4 | MtBG2 (Medtr3g083580) is a novel plasmodesmata located callose degrading enzyme induced in response to rhizobia .. | 85 |
| 3.3 | Discussion | 89 |
| 3.3.1 | Establishment of <i>Medicago</i> -rhizobia symbiosis involves down-regulation of callose in cell walls | 89 |
| 3.3.2 | Callose regulation upon inoculation suggest changes in symplastic communication | 90 |
| 3.3.3 | Newly identified plasmodesmata located protein plays a role in regulating callose during the establishment of the <i>Medicago</i> -rhizobia endosymbiotic interaction | 92 |
| 3.3.4 | Nitrate availability inhibits nodule development but may not affect callose regulation | 94 |
| Chapter 4 -Altering callose turnover affects infection and nodulation in <i>M. truncatula</i>-rhizobia interaction | | 97 |
| 4.1 | Summary | 97 |
| 4.2 | Results | 98 |
| 4.2.1 | Effect of the callose synthase inhibitor 2-Deoxy-D-Glucose in rhizobial infection and nodulation | 98 |
| 4.2.2 | Ectopic expression of a plasmodesmata-located callose degrading enzyme affects infection and nodulation | 111 |
| 4.3 | Discussion | 122 |
| 4.3.1 | The regulation of callose is probably required to control nodule number in both nitrate depleted and sufficient conditions ... | 122 |
| 4.3.2 | The increase in infection thread formation in callose depleted roots suggests a positive feedback linking infection and nodulation | 126 |
| Chapter 5 – Using symbiotic promoters to determine the temporal and spatial requirements for callose regulation during nodulation ... | | 129 |
| 5.1 | Summary | 129 |
| 5.2 | Results | 131 |
| 5.2.1 | PDBG1, a bona-fide β -1,3-glucanase as a tool to reduce plasmodesmata-associated callose in <i>M. truncatula</i> | 131 |

| | | |
|---|---|------------|
| 5.2.2 | Expressing PdBG1 under infection and nodulation promoters leads to a higher number of nodules | 134 |
| 5.2.3 | Roots expressing the pMtERN1-AtPdBG1 construct show a higher number of infection threads..... | 136 |
| 5.2.4 | Root phenotype, nodule development and colonisation are not affected in roots expressing PdBG1 | 138 |
| 5.3 | Discussion | 143 |
| 5.3.1 | Ectopic degradation of callose in rhizobia infected epidermal tissues is sufficient to regulate nodulation | 143 |
| Chapter 6 -A novel receptor-like kinase targets plasmodesmata to regulate nodulation in nitrogen sufficient conditions | | 148 |
| 6.1 | Summary | 148 |
| 6.2 | Results | 150 |
| 6.2.1 | Phylogenetic analysis identifies MtPDLP1 (Medtr1g073320) as evolutionary related to PDLP proteins | 150 |
| 6.2.2 | MtPDLP1 co-localises with callose deposits around plasmodesmata in <i>M. truncatula</i> roots | 152 |
| 6.2.3 | Expression profile indicates up-regulation of MtPDLP1 after rhizobial infection. | 153 |
| 6.2.4 | Constitutive expression of MtPDLP1 improves plant biomass in soil..... | 155 |
| 6.2.5 | Over-expression of MtPDLP1 does not affect callose, nodule number or infection threads in nitrogen-depleted conditions 158 | |
| 6.2.6 | Constitutive expression of MtPDLP1 affects response to rhizobia in nitrate sufficient conditions..... | 163 |
| 6.3 | Discussion | 169 |
| 6.3.1 | Overexpression of the receptor-like kinase MtPDLP1 positively regulates plant growth | 169 |
| 6.3.2 | MtPDLP1 plays a role in signalling responses to full-nitrate conditions..... | 170 |
| Chapter 7 -General discussion and conclusions | | 177 |
| 7.1 | Callose regulates symplastic communication in <i>M. truncatula</i> roots upon rhizobia inoculation..... | 177 |
| 7.2 | The ectopic expression of callose degrading enzymes in rhizobia infected and nodulating tissues increases the number of nodules | 178 |
| 7.3 | A plasmodesmata-located RLK regulated signalling affecting nodule number under high nitrate conditions | 180 |
| 7.4 | Conclusions..... | 182 |

| | |
|--------------------------|------------|
| Appendices..... | 184 |
| Bibliography..... | 202 |

List of tables

| | |
|---|-----|
| Table 1.1-Table summarising some of the genes identified up-to date that play a role in the regulation of the nodulation process in legumes. | 20 |
| Table 2.1-Recipe of plant growth media used in this work | 40 |
| Table 2.2-Recipe of bacterial growth media used in this work | 42 |
| Table 2.3-Standard PCR reaction conditions | 44 |
| Table 2.4: Standard reaction mixture for GoldenGate cloning system . | 44 |
| Table 2.5: List of vectors generated by GoldenGate in this study | 47 |
| Table 2.6: List of primers used in the generation or confirmation of GoldeGate clones | 47 |
| Table 2.7: List of Gateway vectors used in this study | 49 |
| Table 2.8: List of expression vectors generated and used in this study | 49 |
| Table 2.9: List of primers used in the generation of clones by Gateway system. Adapters for Gateway donor vectors are underlined. | 51 |
| Table 2.10: Primers used in QPCR and RTPCR assays..... | 52 |
| Table 2.11 CFX96 Touch™ program setting designed for optimal output and used in PCR cycling for the QPCR analysis. | 53 |
| Table 4.1- DDG treatment does not affect the percentage of nodulating plants. | 105 |
| Table 4.2- DDG treatment does not affect the percentage of colonised nodules..... | 105 |
| Table 4.3- Infectability of rhizobia is not affected by DDG. | 106 |
| Table 4.4- Percentage of infected nodules in composite plants expressing pUb-MtBG2-mcherry construct..... | 113 |
| Table 4.5-Effect of nitrate in infection and nodulation in control and overexpressing MtBG2 plants. | 118 |
| Table 4.6- Percentage of infected nodules in composite plants expressing pUb-MtBG2-mcherry construct and growing in 5mM potassium nitrate.)..... | 118 |
| Table 5.1- Percentage of infected nodules in composite plants expressing pMtERN1-AtPdBG1 construct..... | 138 |
| Table 6.1- Percentage of infected nodules in composite plants expressing p35S- MtPDL1-YFP construct.. | 162 |
| Table 6.2- Percentage of infected nodules in composite plants expressing p35S- MtPDL1-YFP construct and growing in full nitrate conditions..... | 168 |

List of figures

| | |
|---|----|
| Figure 1.1-Chemical reaction of the biological nitrogen fixation that occurs in legume nodules..... | 4 |
| Figure 1.2- Diagram showing the steps involved in rhizobia infection and nodule formation in <i>Medicago truncatula</i> | 7 |
| Figure 1.3 Epidermal Nod factor (NF) signalling pathway and components of the cortical signalling transduction in <i>M. truncatula</i> | 12 |
| Figure 1.4- Diagram showing the structure of a simple (A) and branched (B) plasmodesmata..... | 24 |
| Figure 1.5-Structure of callose. Callose molecules are conformed by n repetitions of β -1,3 linked molecules of glucose. | 27 |
| Figure 1.6- Schematic model on callose regulation of plasmodesmata permeability..... | 28 |
| Figure 1.7-Schematic model showing the possible role of the symplastic pathway in the symbiotic process.. | 36 |
| Figure 2.1- Map of the <i>pMtERN1-PdBG1-GFP</i> vector..... | 45 |
| Figure 2.2- Map of the untagged vectors generated with specific infection and nodulation promoters <i>MtNFBx</i> , <i>MtERN1</i> and <i>MtNIN</i> | 46 |
| Figure 2.3- Map of <i>pUb- Medtr3g083580-mcherry</i> vector generated by GateWay cloning system. | 50 |
| Figure 2.4: Drawing showing infection zone in a <i>M. truncatula</i> root. The infection zone is where root hairs start to develop and are susceptible to be infected by rhizobia. | 56 |
| Figure 3.1- Callose levels are globally reduced 24 hours post-inoculation with rhizobia in <i>M. truncatula</i> | 66 |
| Figure 3.2- Callose is downregulated upon inoculation..... | 67 |
| Figure 3.3- Nitrate inhibits nodulation and infection in <i>M.truncatula</i> roots..... | 68 |
| Figure 3.4- Nitrate does not have an effect in <i>M. truncatula</i> root length.. | 69 |
| Figure 3.5- Aniline blue staining suggest that callose is not regulated by nitrate..... | 70 |
| Figure 3.6- Immunolocalisation indicates that 5mM nitrate does not regulate callose in <i>M. truncatula</i> roots. | 71 |
| Figure 3.7- Callose is downregulated upon inoculation in <i>M. truncatula</i> roots growing in nitrate..... | 73 |
| Figure 3.8 <i>ENOD11</i> expression is not completely inhibited by nitrate in <i>M. truncatula</i> roots. | 75 |

| | |
|--|-----|
| Figure 3.9- Full majority-rule consensus tree of GHL17s using sequences isolated from <i>M. truncatula</i> (Medtr) and <i>Arabidopsis thaliana</i> (At) generated by Bayesian inference of phylogeny..... | 78 |
| Figure 3.10 Full majority-rule consensus tree of Glucan Synthase Like (GSL) protein family using sequences isolated from <i>M. truncatula</i> (Medtr) and <i>Arabidopsis thaliana</i> (At) generated by Bayesian inference of phylogeny..... | 79 |
| Figure 3.11- Phylogenetic studies identify potential <i>Medicago</i> orthologues to <i>Arabidopsis</i> Plasmodesmata located β -1,3-glucanases. | 80 |
| Figure 3.12- Expression profiles of potential BGs in <i>M. truncatula</i> root hairs suggest a role in early stages of infection..... | 81 |
| Figure 3.13- The genes MtBG2 and MtBg1 are upregulated upon rhizobia inoculation of <i>M. truncatula</i> roots | 82 |
| Figure 3.14- Expression profiles of potential callose synthase orthologues in <i>M. truncatula</i> do not suggest a role in early stages of infection.. | 84 |
| Figure 3.15- MtBG2 localises at plasmodesmata. <i>MtBG2</i> fused to mcherry was expressed under the Ubiquitin promoter (<i>pUb</i>) in transgenic <i>M. truncatula</i> roots. | 86 |
| Figure 3.16- MtBG2 expressed under the ubiquitin promoter affects callose deposition in <i>M. truncatula</i> transgenic roots. | 87 |
| Figure 3.17- Immunolocalisation experiments confirms reduced callose in plants overexpressing <i>MtBG2</i> | 88 |
| Figure 4.1 2- Deoxy-D Glucose treatment affects callose deposition in <i>M. truncatula</i> roots. | 100 |
| Figure 4.2- Effect of DDG treatment in <i>Medicago truncatula</i> root length. | 101 |
| Figure 4.3- DDG does not seem to affect root hair development in <i>M. truncatula</i> | 102 |
| Figure 4.4- Continuous treatment with DDG affects the number of emerged lateral root in <i>M. truncatula</i> | 103 |
| Figure 4.5- DDG does not affect rhizobia growth..... | 104 |
| Figure 4.6- DDG treatment affects the density of nodules and infection threads in <i>M. truncatula</i> roots inoculated with rhizobia..... | 107 |
| Figure 4.7 Examples of nodule primordia and infection threads (IT) in wild-type <i>M. truncatula</i> treated with 100 μ M DDG for 5 days or water (control)..... | 108 |
| Figure 4.8- DDG treatment can recover infection and nodulation phenotype in nitrate sufficient conditions..... | 110 |

| | |
|---|-----|
| Figure 4.9- <i>M. truncatula</i> transgenic roots constitutively expressing MtBG2 show higher density of infection thread and nodule primordia compared to control roots expressing an empty vector. | 112 |
| Figure 4.10- Root length is not affected by the expression of <i>pUb-MtBG2-mcherry</i> | 113 |
| Figure 4.11- <i>M. truncatula</i> composite roots 14 days post inoculation. | 114 |
| Figure 4.12- Nitrate does not affect root length in <i>M. truncatula</i> roots expressing <i>pUb-MtBG2-mcherry</i> | 116 |
| Figure 4.13- <i>M. truncatula</i> roots constitutively expressing MtBG2 show inhibition of nodulation and in infection thread in high nitrate conditions..... | 117 |
| Figure 4.14- <i>M. truncatula</i> transgenic roots 14 days post inoculation in nitrate conditions..... | 119 |
| Figure 4.15- Callose remains the same in <i>M. truncatula</i> transgenic roots expressing <i>pUb-MtBG2-mcherry</i> inoculated with mock or rhizobia cultures in no nitrate and nitrate sufficient conditions.. | 121 |
| Figure 5.1- <i>Arabidopsis thaliana</i> β -1, 3-glucanase PdBG1 localises in the cell periphery in a pattern that resembles plasmodesmata sites in <i>M. truncatula</i> roots. | 132 |
| Figure 5.2- <i>Arabidopsis</i> PdBG1 displays callose degrading activity in <i>M. truncatula</i> | 133 |
| Figure 5.3- Ectopic expression of the <i>Arabidopsis</i> β -1, 3- glucanase PdBG1 improves nodulation..... | 135 |
| Figure 5.4- The majority of <i>M. truncatula</i> plants show more than 4 nodules per plant. | 136 |
| Figure 5.5- PdBG1 expression in <i>M. truncatula</i> affects the number of infection threads..... | 137 |
| Figure 5.6- Phenotype of <i>Medicago</i> transgenic roots expressing PdBG1 under different promoters..... | 139 |
| Figure 5.7- <i>M. truncatula</i> shoots appear normal in <i>PdBG1</i> transgenic. Pictures were taken of the general aspect of <i>M. truncatula</i> composite plants growing for 24 days in pots containing an equal mixture of sand and Terragreen. | 140 |
| Figure 5.8- Example of nodule architecture 14 days post inoculation in <i>M. truncatula</i> control and roots expressing <i>Arabidopsis</i> PdBG1. | 141 |
| Figure 5.9- Example pictures of infection thread, infection pocket, nodule primordia and nodule in <i>M. truncatula</i> roots 14 days post inoculation with <i>lacZ</i> expressing rhizobia..... | 142 |

| | |
|--|-----|
| Figure 6.1 Full majority-rule consensus tree of Arabidopsis (At) PDLPs and <i>M. truncatula</i> (Medtr) genes identified putative orthologues. | 151 |
| Figure 6.2- Alignment of the <i>Medicago truncatula</i> PDLP-like protein Medtr1g073320, and the <i>Arabidopsis thaliana</i> PDLP proteins AtPDLP1 and AtPDLP2 sequences. | 152 |
| Figure 6.3- Intercellular localisation of MtPDLP1 in <i>M. truncatula</i> roots.. | 153 |
| Figure 6.4-Expression profile of <i>MtPDLP1</i> in <i>M. truncatula</i> inoculated root hairs. | 154 |
| Figure 6.5- <i>MtPDLP1</i> is upregulated upon inoculation in <i>M. truncatula</i> roots..... | 155 |
| Figure 6.6- <i>MtPDLP1</i> overexpression does not affect root length in <i>M. truncatula</i> | 156 |
| Figure 6.7- <i>MtPDLP1</i> overexpression affects plant development..... | 157 |
| Figure 6.8- Over expression of <i>MtPDLP1</i> does not affect callose deposition in <i>M. truncatula</i> grown in depleted nitrate..... | 159 |
| Figure 6.9- Plants expressing <i>p35S-MtPDLP1-YFP</i> are not affected in infection or nodulation 7 days post inoculation in low nitrate conditions..... | 160 |
| Figure 6.10- Plants overexpressing <i>MtPDLP1</i> nodulate normally in soil in low nitrate conditions..... | 161 |
| Figure 6.11 <i>MtPDLP1</i> plants experience callose downregulation upon inoculation in <i>M. truncatula</i> in nitrate-depleted conditions | 165 |
| Figure 6.12- <i>MtPDLP1</i> affects callose regulation upon inoculation in full-nitrate conditions. | |
| Figure 6.13- <i>M. truncatula</i> roots constitutively expressing <i>MtPDLP1</i> do not show inhibition of nodulation and infection in full nitrate conditions..... | 166 |
| Figure 6.14- Root phenotype of infected <i>M. truncatula</i> transgenic roots expressing <i>p35S- MtPDLP1-YFP</i> | 167 |
| Figure 6.15-Expression pattern of MtCLE13 in response to rhizobia. | 171 |
| Figure 6.16- Expression pattern of <i>MtPDLP1</i> in response nitrate. | 173 |
| Figure 6.17 Schematic proposed model of the role of <i>MtPDLP1</i> in the control of nodulation in <i>M. truncatula</i> | 175 |
| Figure 7.1-Schematic model of callose-mediated regulation of root nodule development in <i>M. truncatula</i> | 183 |

List of Appendices

| | |
|--|-----|
| Appendix 1 List of sequences used in the phylogenetic analysis of β -1,3-glucanases from the GHL17 protein family in <i>Arabidopsis thaliana</i> and <i>M. truncatula</i> . <i>Picea sitchensis</i> sequence was included as an outgroup. Table includes predicted domains (See Material and Methods)..... | 184 |
| Appendix 2- List of sequences used in the phylogenetic analysis of callose synthase protein family in <i>Arabidopsis thaliana</i> and <i>Medicago truncatula</i> | 186 |
| Appendix 3 List of sequences used in the phylogenetic analysis of PDLP protein family in <i>Arabidopsis thaliana</i> and <i>M. truncatula</i> . <i>Picea sitchensis</i> was included as an outgroup. Table include predicted domains (See Material and Methods)..... | 187 |
| Appendix 4- Phylogenetic reconstruction using β -1,3-glucanases from GHL17 family protein sequences isolated from <i>A. thaliana</i> and <i>M. truncatula</i> orthologues generated by Maximum Likelihood algorithm. Bootstrap values for 500 repetitions are included. | 190 |
| Appendix 5- Phylogenetic reconstruction using β -1,3-glucanases from GHL17 family protein sequences isolated from <i>A. thaliana</i> and <i>M. truncatula</i> orthologues generated by Neighbour Joining algorithm. Bootstrap values for 500 repetitions are included..... | 191 |
| Appendix 6- Phylogenetic reconstruction using CALs sequences isolated from <i>A. thaliana</i> and <i>M. truncatula</i> orthologues generated by Maximum Likelihood algorithm. Bootstrap values for 500 repetitions are included. | 192 |
| Appendix 7- Phylogenetic reconstruction using CALs sequences isolated from <i>A. thaliana</i> and <i>M. truncatula</i> orthologues generated by Neighbour Joining algorithm..... | 193 |
| Appendix 8- Phylogenetic reconstruction using PDLPs sequences isolated and <i>A. thaliana</i> and <i>M. truncatula</i> orthologues generated by Maximun Likelihood algorithm..... | 194 |
| Appendix 9- Phylogenetic reconstruction using PDLPs sequences isolated and <i>A. thaliana</i> and <i>M. truncatula</i> orthologues generated by Neighbour Joining algorithm..... | 195 |
| Appendix 10- Phylogenetic reconstruction using β -1,3-glucanases from GHL17 family protein sequences isolated from <i>A. thaliana</i> and <i>M. truncatula</i> orthologues generated by Neighbour Joining algorithm in Newick format. | 196 |
| Appendix 11: Phylogenetic reconstruction using β -1,3-glucanases from GHL17 family protein sequences isolated from <i>A. thaliana</i> and <i>M. truncatula</i> orthologues generated by Maximum likelihood algorithm in Newick format. Bootstrap values for 1000 repetitions are included..... | 196 |

| | |
|---|------------|
| Appendix 12 Phylogenetic reconstruction using β-1,3-glucanases from GHL17 family protein sequences isolated from <i>A. thaliana</i> and <i>M. truncatula</i> orthologues generated by Bayesian inference of phylogeny algorithm in Newick format. Posterior probabilities are included..... | 197 |
| Appendix 13- Phylogenetic reconstruction using CALs sequences isolated from <i>A. thaliana</i> and <i>M. truncatula</i> orthologues generated by Neighbour Joining algorithm in Newick format. Bootstrap values for 500 repetitions are included..... | 198 |
| Appendix 14-Phylogenetic reconstruction using CALs sequences isolated from <i>Arabidopsis thaliana</i> and <i>M. truncatula</i> orthologues generated by Maximum Likelihood algorithm in Newick format. Bootstrap values for 500 repetitions are included..... | 199 |
| Appendix 15- Phylogenetic reconstruction using CALs sequences isolated from <i>Arabidopsis thaliana</i> and <i>M. truncatula</i> orthologues generated by Bayesian inference of phylogeny algorithm in Newick format. Posterior probabilities are included. | 199 |
| Appendix 16- Phylogenetic reconstruction using PDLPs sequences isolated and <i>A. thaliana</i> and <i>M. truncatula</i> orthologues generated by Neighbour Joining algorithm in Newick format. Bootstrap values for 500 repetitions are included..... | 199 |
| Appendix 17- Phylogenetic reconstruction using PDLPs sequences isolated and <i>A. thaliana</i> and <i>M. truncatula</i> orthologues generated by Maximun Likelihood algorithm in Newick format. Bootstrap values for 500 repetitions are included..... | 200 |
| Appendix 18- Phylogenetic reconstruction using PDLP sequences isolated from <i>Arabidopsis thaliana</i> and <i>Medicago truncatula</i> orthologues generated by Bayesian inference of phylogeny algorithm in Newick format. Posterior probabilities are included. | 201 |

List of abbreviations

| | |
|-------|--|
| ABA | Abscisic acid |
| AM | Arbuscular Mycorrhiza |
| AON | Autoregulation of Nodulation |
| At | <i>Arabidopsis thaliana</i> |
| AVG | Aminoethoxyvinylglycine |
| BG | Beta Glucanases |
| BLAST | Basic local alignment search tool |
| BNM | Buffered Nodulation Medium |
| CALS | Callose Synthases |
| CCaMK | Calcium Calmodulin Dependent Kinase |
| CEPS | C-Terminally Encoded Peptides |
| CFDA | 5-Carboxyfluorescein Diacetate, Acetoxymethyl Ester |
| DDG | 2-Deoxy-D Glucose |
| DMF | Dimethylformamide |
| DMI3 | Does not make infections protein 3 |
| dpi | Days post inoculation |
| DWA | Distilled Water |
| ENOD | Early Nodulin |
| ER | Endoplasmic Reticulum |
| ERN1 | Ethylene Response Factor Required for Nodulation1 |
| FP | Fahraeus plant |
| GFP | Green Fluorescence Protein |
| GHL17 | Glycosyl hydrolase family 17 |
| GPI | Glycosylphosphatidyl inositol |
| hpi | Hours post inoculation |
| IT | Infection thread |
| Kb | Kilo bases |
| LB | Lysogeny broth |

| | |
|------|--|
| LRR | Leucine rich repeat |
| MM | Minimal Media |
| Mt | <i>Medicago truncatula</i> |
| NARK | Nodule autoregulation receptor-like protein kinase precursor |
| NFB | Nod Factor Box |
| NFP | Nod factor perception |
| NFRI | Nod factor receptor |
| NIC | Nitrate-induced |
| NIN | Nodule Inception |
| OD | Optical density |
| PBS | Phosphate-buffered saline |
| PCR | Polymerase Chain Reaction |
| PDLP | Plasmodesmata Located Protein |
| RIC | Rhizobia-induced |
| RLK | Receptor-like kinase |
| RPM | Revolution per minute |
| RT | Room temperature |
| SP | Signal peptide |
| SUNN | Super numeric nodules |
| Ub | Ubiquitin |
| X8 | Carbohydrate binding module |

Chapter 1

Chapter 1 –Introduction

1.1 Brief introduction to symbiosis

Symbiosis is a biological interaction between two different organisms living in physical association, often to the advantage of both. Symbiosis can be established between plants and some soil microorganisms. Through exploiting these interactions, the plant can improve its capacity to obtain water and essential macronutrients (including nitrogen and phosphorus) that sustain growth and development. With a human population growing at a fast rate and the impacts of climate change in agriculture, it is required that the food industry reduce the inputs of water, fertilisers and pesticides in crop production. Improving traits that affect symbiosis, or extending the number of plants that can engage in these beneficial associations, can be used as an alternative to overcome these challenges.

In beneficial plant-microbe interactions, two symbiotic systems have been mostly studied: interactions involving arbuscular mycorrhizal fungus (AM) or bacteria of the genus *Rhizobium* (rhizobia). More than 80% of all land plants families are able to form symbiosis with AM fungi (Bonfante and Genre, 2010). AM interactions have an important impact on nutrient uptake, especially nitrogen and phosphate, and on the global carbon cycle (Gherbi et al., 2008).

The origin of AM symbiosis is dated approximately 400 million years ago, hence might be the precursors of other symbiotic systems, such as the one established between legumes and rhizobia (Gherbi et al., 2008). In fact, some mutants unable to engage in symbiosis with rhizobia are also defective in forming associations with AM fungus. This suggests a genetic link between bacterial and fungal symbiosis. Common symbiosis genes have been successfully cloned and characterised, proteins involved in several steps in the recognition of the symbiotic partner and in the establishment of the symbiosis are shared among these two symbiotic systems (Denarie et al., 1996; Madsen et al., 2003; Gherbi et al., 2008; Maillet et al., 2011).

Different from AM, rhizobia can fix atmospheric nitrogen in symbiosis with only a few plant species belonging mainly to the Fabaceae family. In the next chapters,

the features that distinguish the legume-rhizobia symbiosis from other systems will be revised. By understanding these plant-microbe systems, the aim is to develop new environmentally sustainable technologies and tools to improve biological nitrogen fixation, a crucial process that will be introduced in the next section.

1.2 Brief introduction to biological nitrogen fixation

Nitrogen is an essential element for appropriate plant growth, representing around 2% of the total plant dry matter that will enter the food chain (Santi et al., 2013). Although the dinitrogen gas state is highly represented in the atmosphere, making about 78.1% of the earth's atmosphere, plants are not able to directly acquire it and metabolise it in that form. Plants can uptake nitrogen in the form of nitrate, nitrites and ammonium that become available after lightning storms and from decomposition of animal depositions and plant residues (Bernhardt et al., 2003). Only 1-4% of the nitrogen required for crop production is naturally available and this forces the use of nitrogen fertilisers to optimise yield. Nitrogen fertilizers are produced using the Haber-Bosch process which is energetically and economically expensive. Fertilizers production has other environmental consequences: important amounts of CO₂ are generated during production and, after periods of heavy rain or extensive irrigation, the excess of these fertilizers can run-off into waterways, contributing to eutrophication (Silva et al., 1978; Andersen et al., 2014). Due to these issues, the Department for Environment, Food and Rural Affairs determines the amount of nitrogen fertilisers that can be used and controls and fines those farms that do not comply with current regulations¹.

Some plants have evolved to overcome nitrogen limitation by establishing beneficial symbiotic associations with nitrogen-fixing soil-borne micro-organisms. Four different orders of flowering plants (Rosales, Fagales, Cucurbitales and Fabales) are able to associate with nitrogen-fixing micro-

¹Last visited 08/08/2017: <https://www.gov.uk/guidance/using-nitrogen-fertilisers-in-nitrate-vulnerable-zones#inspections>

organism, but legumes are the group of plants with the highest representation within these groups (Doyle, 2011).

In this symbiotic interaction, the bacteria is hosted intracellularly within highly specialised organs, known as root nodules, that are formed on the roots of host plants, and within which the bacteria have the optimal environment to fix nitrogen for the host plant in exchange for photosynthates (Li et al., 2012). Bacteria have an enzymatic complex, called nitrogenase, that mediates the reduction of atmospheric N_2 to ammonia (Figure 1.1) but that only function effectively in the low oxygen environment created within the nodules.

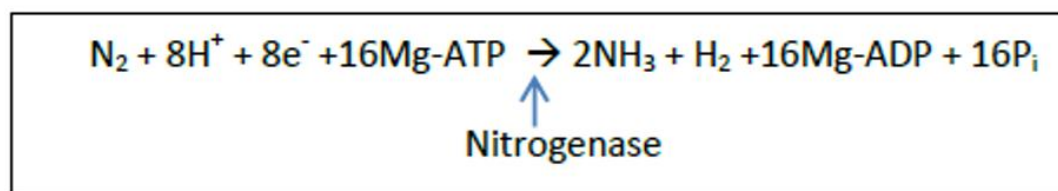


Figure 1.1-Chemical reaction of the biological nitrogen fixation that occurs in legume nodules. The bacterial enzyme nitrogenase catalyses the reaction that converts di-nitrogen gas into assimilable forms of nitrogen, such as NH_3 . The process is coupled to the hydrolysis of 16 equivalents of ATP and is accompanied by the co-formation of one molecule of H_2 .

Rather than relying on the use of external N sources, alternative ways to supply crops with the required nitrogen are the basis of developing more sustainable farming. A popular alternative is intercropping, a farming technique that relies on growing legumes able to fix nitrogen in arable soils aiming to improve the nitrogen content of the soil, positively impacting the growth of future crops harvested in the same land (Searle et al., 1981; Murray et al., 2017; Qin et al., 2017).

Understanding how legumes interact with soil bacteria to establish this beneficial interaction is essential in order to optimise the process and, in the future, engineer other economically important crops to enter in similar relationships. This would be especially important in terms of improving crops yield while reducing the use of contaminant fertilisers.

1.2.1 Sequential steps in the formation of nitrogen fixing symbiosis

Symbiotic nitrogen fixation accounts for about 175×10^6 tons of N fixed globally (Maximising the Use of Biological Nitrogen Fixation in Agriculture, report of a FAO/IAEA meeting 2001²). The process involves a series of concatenated events that starts with the recognition of the bacteria by the plant and finishes with the creation of a fully functional nitrogen-fixing nodule. Bacterial infection and organogenesis are highly specialised programmes that require the supply of important energetic resources, hence they are tightly regulated. In legumes, such as in *M. truncatula*, rhizobia symbiotic interaction begins with the exchange of chemical signals, leading to bacterial infection and nodule differentiation. This is a complex process, involving reprogramming of different root tissues cell types to allow for bacterial infection, entry and dedifferentiation into nitrogen-fixing bacteroids.

In nitrogen deprivation, legume roots release specific flavonoid molecules that serve as chemoattractants for the soil bacteria (Zhang et al., 2009) and activate the expression of rhizobia nodulation genes (nod genes). Among others, bacterial Nod genes encode for biosynthesis of the Nod factors, chito-oligosaccharides that trigger a number of morphological and biochemical changes in the host plant necessary for the symbiosis to occur (Geurts and Bisseling, 2002; Kereszt et al., 2011). A well-characterized example is the Nod factor-induced expression of *ENOD11*, an early nodulin gene encoding for a putative cell wall-associated protein widely used as a marker for early infection-related symbiotic events (Journet et al., 2001; Boisson-Dernier et al., 2005). Infection is initiated in root hairs and rhizobia are entrapped within the root hair and enter the plant through the formation of a tubular compartment that grows into the host cell, known as the infection thread (IT) (Mitra et al., 2004) (Figure 1.2-A). A region of the root, at around 3 cm from the root tip coincident with root hair initiation, is called 'infection zone' and is where the host-bacteria recognition is believed to take place (Bhuvaneshwari et al., 1981). Bacteria can also enter the

² Maximising the use of Biological Nitrogen Fixation in Agriculture. Report of an FAO/IAEA Technical Expert Meeting held in Rome, 13-15 March 2001.

root by cracks in the epidermis, normally caused by the emergence of lateral roots, but this is a much less common method (Vega-Hernández et al., 2001).

Bacterial infection is associated with concomitant cortical and pericycle cell reprogramming and division that will lead to the creation of a new organ, the nodule primordia, situated directly below the infection site (Geurts and Bisseling, 2002; Jones et al., 2007; Cerri et al., 2012) (Figure 1.2 B-1).

Eventually, the infection thread reaches the nodule primordia, releasing the bacteria into the dividing cells (Figure 1.2 D-3). As the nodule develops and matures, the bacteria will then turn into bacteroids, the fully functioning form of nitrogen-fixing symbiont. These bacteroids are not directly in contact with the plant's cytoplasm as they remain enclosed by a host membrane (Haag et al., 2013; Farkas et al., 2014). All steps described in this section are schematized in (Figure 1.2).

Nodules can be classified into two main groups depending on their developmental pattern. Determinate nodules, like those observed in *Lotus japonicus*, are characterised by a non-persistent meristem, are round-shaped with a centric nitrogen fixation zone where the bacteroids are hosted (Hirsch, 1992; Mao et al., 2013). In determinate nodules, senescence develops radially, starting from inner layers of the nodule and slowly spreading toward the outer sections of the nodule (Van de Velde et al., 2006).

On the other hand, temperate legumes, such as the model used in this work *Medicago truncatula*, generate indeterminate nodules, phenotypically characterised by a cylindrical shape consisting in a gradient of developmental zones comprising a persistent meristem (where cell division occurs), infection zone (where rhizobia differentiate into bacteroids) and fixation zone (composed of infected rhizobia-filled cells interspersed with some uninfected cells) (Van de Velde et al., 2006). As the nodule ages, a new zone named the senescence zone is developed close to the infection zone. This developmental zone will develop gradually until it reaches the apical zone as the nodule degenerates (Van de Velde et al., 2006).

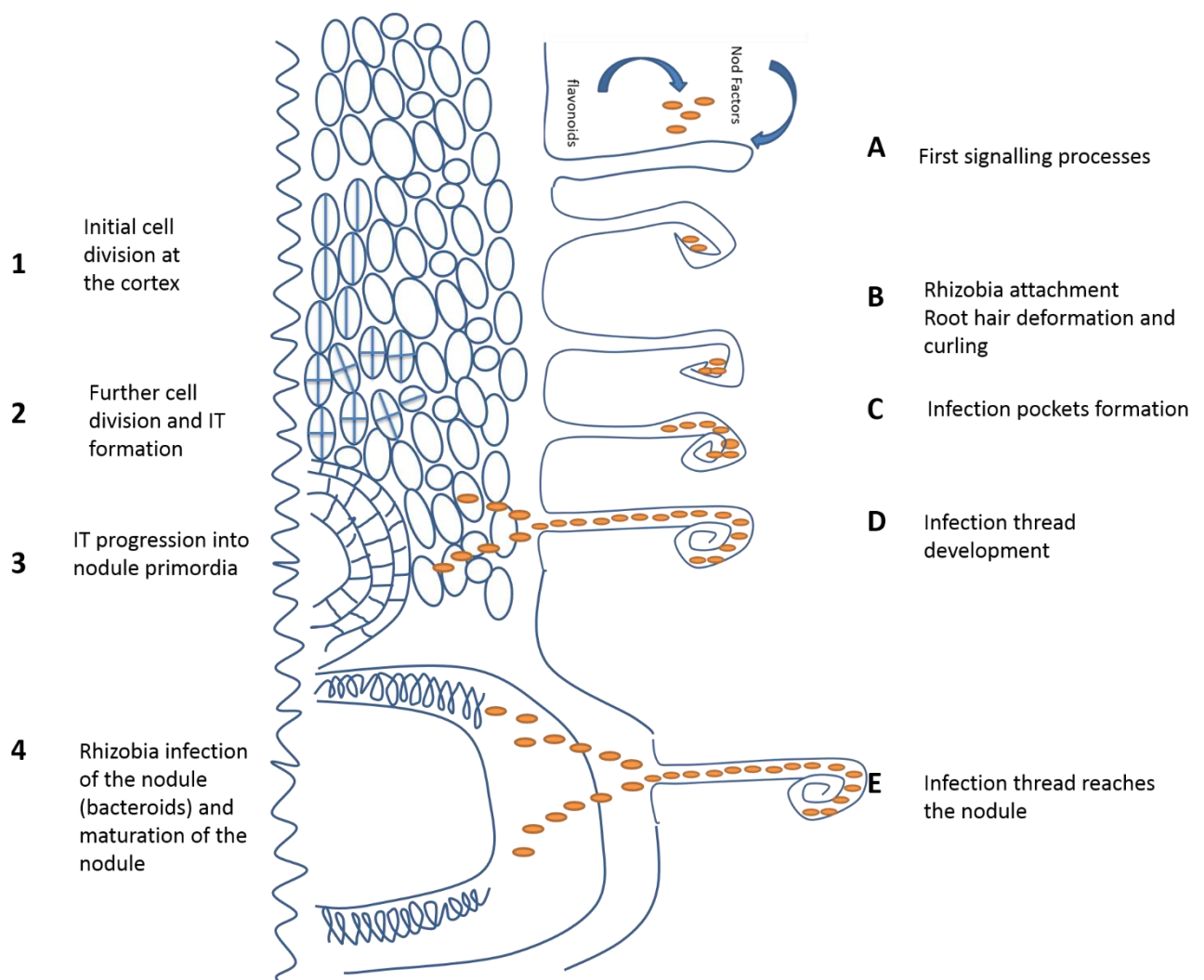


Figure 1.2- Diagram showing the steps involved in rhizobia infection and nodule formation in *Medicago truncatula*. A- The host plant secretes signalling compounds, called flavonoids, that are perceived by the bacteria and that will trigger the synthesis of bacterial Nod Factors. These factors are then perceived by the plant, triggering the start of the symbiosis. B and 1- Rhizobia attaches to the surface of the root hairs, which deform and curl for bacterial entrapment. Cell division start in the cortex in synchrony to bacterial infection in the epidermis. C and 2-Bacteria are entrapped in the root hair. A local hydrolysis of the plant cell wall takes place in the curled root hair and the plasma membrane invaginates. This results in the formation of a tubular structure, called the infection thread (IT), which transports the bacteria into the plant. The cortex

continues to divide and dedifferentiates into a nodule primordia. D and 3- Infection threads develop into the root epidermis, through inner plant's tissues and into the nodule primordia developing in the cortex. E and 4- Infection thread allows bacterial colonization of the nodule, where they differentiate into their symbiotic form, the bacteroids. These bacteroids remained enclosed by a host membrane. Nodules hosting the bacteroids reach their functional and mature stages and begin to fix nitrogen.

1.2.2 Key regulators of rhizobia infection and nodulation in *Medicago truncatula*

Important efforts have been made in the last years to identify the key genetic regulators orchestrating the processes of infection and nodulation in the *M. truncatula*-rhizobia symbiosis. The rise of plant genomics resources during the last decade allowed an impressive accumulation of datasets on gene identity, expression and regulation (Benedito et al., 2008; He et al., 2009). This has led to a more detailed understanding of the genetic programs associated/regulating the symbiotic process in legumes. Nevertheless, the biggest challenge remains focus on the regulatory hubs orchestrating the different stages of these programs.

Infection and nodulation are interconnected but independent programmes as they appear controlled by different regulatory mechanisms. This extra complexity hinders the complete understanding of the genetic pathway behind the symbiotic process and highlights the needs for more research in this area. The main regulatory pathways of infection and nodulation are reviewed in the next sections.

1.2.2.1 The Nod-factor signal transduction pathway

The initial stages of the symbiotic interaction involve a series of signalling events between the host plant and the soil-borne bacteria present in the rhizosphere. When the conditions for the symbiosis are appropriate, the plant will synthesize phenolic compounds, known as flavonoids, which will be perceived by the bacteria and will trigger the transcription of bacterial Nod-genes (Fisher and Long, 1992; Ehrhardt et al., 1996) (Figure 1.3). Nod-genes are primarily involved in the activation of Nod-factors, chitin-based compound that acts as powerful

signalling molecules (Cardenas et al., 1995). The specificity of the symbiotic interaction is determined by the nature of the plant phenolic signal and the structure of bacterial Nod factor (Cardenas et al., 1995; Ehrhardt et al., 1996).

Nod factors are necessary, and in some cases sufficient, to elicit a response in the host plant, as experiments with isolated Nod factors have proven (Wais et al., 2002; Oldroyd et al., 2005).

The first responses are observed within 1 min of treatment with Nod factors and involves perception by LysM receptor-like kinases (named Nod factor perception, NFP, in *M.truncatula* (Arrighi et al., 2006), and Nod factor receptor, NFR1/NFR5, in *L. japonicus* (Madsen et al., 2003). Recent studies focused on the regulatory pathways controlling the recognition step of the bacteria and subsequent formation of the infection thread in root hairs. In *L.japonicus* genetic approaches identified a LysM-receptor as necessary for the recognition step, for infection thread formation and development (Kawaharada et al., 2015). This receptor is initially regulated in the epidermal cell layer but controls the development of infection threads through inner cell layers in the root (Kawaharada et al., 2015).

After Nod factor perception in the epidermal cell layer, the first physiological changes include depolarization of the plasma membrane and changes in ion fluxes across it (Ehrhardt et al., 1992; Felle et al., 1999; D'Haese and Holsters, 2002) (Figure 1.3). This induces calcium spiking events in and around the nucleus (Ehrhardt et al., 1996). Mutants unable to trigger this calcium spiking were defective in nodulation highlighting the importance of this physiological response (Dudley et al., 1987; Ehrhardt et al., 1996). This calcium signal is deciphered by the calcium and calmodulin-dependant kinase, *DMI3* (Levy et al., 2004; Mitra et al., 2004; Miller et al., 2013), which triggers downstream signalling processes that will eventually lead to the transcriptional regulation of early nodulin genes. Mutants in *DMI3* are not able to induce Nod factor dependent gene expression but maintain Nod factor-induced calcium spiking, placing this kinase downstream of the first calcium spiking events (Wais et al., 2000).

Nod factor-dependent gene expression regulates infection and nodulation and activate, among others, the genes *ENOD11* and *ENOD12* in the epidermal cell

layer within hours of rhizobia inoculation or treatment with Nod factors (Journet et al., 2001). Analysis of the *ENOD11* promoter has identified a Nod-Factor responsive regulatory unit (also called the Nod Factor Box) sufficient to direct Nod Factor-elicited expression of *ENOD11* in root hairs soon after infection but not in later stages of the infection process (Andriankaja et al., 2007; Laloum et al., 2014). The expression of these genes (and the use of the Nod Factor Box regulatory unit) are nowadays used as markers for early-stages in the infection process.

1.2.2.2 Signalling crosstalk between infection and nodulation

Signalling in the root epidermis controls pre-infection and infection thread formation, but these signalling pathways also coordinate nodule organogenesis. The calmodulin-dependent protein CCaMK, encoded by *DMI3*, forms a complex with the regulator CYCLOPS upon inoculation that will decode the calcium spiking in the nucleus and affect the expression of two main symbiotic regulators (Cerri et al., 2012; Singh et al., 2014), *Nodule Inception (NIN)* (Singh et al., 2014) and *Ethylene Response Factor Required for Nodulation 1 (ERN1)* (Andriankaja et al., 2007; Marsh et al., 2007; Middleton et al., 2007).

NIN and *ERN1* are two of the first genes activated after inoculation, and are essential for the development of infection threads (Cerri et al., 2012; Xie et al., 2012; Fournier et al., 2015; Kawaharada et al., 2015). These factors also contribute to nodule organogenesis in the cortex although acting in different pathways (Middleton et al., 2007; Cerri et al., 2012; Kawaharada et al., 2015). Mutants in *ERN1* develop small nodules that arrest soon after initiation (Middleton et al., 2007).

On the other hand, *NIN* is both required and sufficient to initiate nodule organogenesis but is not essential in early Nod factor signalling (Schauser et al., 1999; Marsh et al., 2007; Soyano et al., 2013; Vernie et al., 2015). Some evidence suggest that *NIN* regulates pre-infection responses and nodulation steps in different root tissues (Vernie et al., 2015). For example, when *NIN* is expressed under the epidermal specific promoter *pEXP7* and in a *nin* mutant background, it can induce cortical cell division in response to rhizobia but at much lower efficiencies that when is expressed in the cortex. Additionally, when

expressed under the cortical specific promoter, *pNRT1.3*, *NIN* was able to promote spontaneous nodule organogenesis in wildtype plants (Vernie et al., 2015). *NIN* is also sufficient to promote the transcription of the essential cytokinin receptor *Cytokinin Response 1(CRE1)* in to the root cortex (Figure 1.3) (the role of cytokinins in nodule organogenesis will be reviewed in section 1.2.2.3.2 of this thesis).

NIN expression not only appears to regulate both infection and nodule organogenesis, but also nodule number. For proper functioning in all these different processes, expression of *NIN* should be spatially and temporally regulated, and *NIN* itself appears to be important for its regulation. How *NIN* is regulated and how it coordinates responses in these distant cell layers is still unknown.

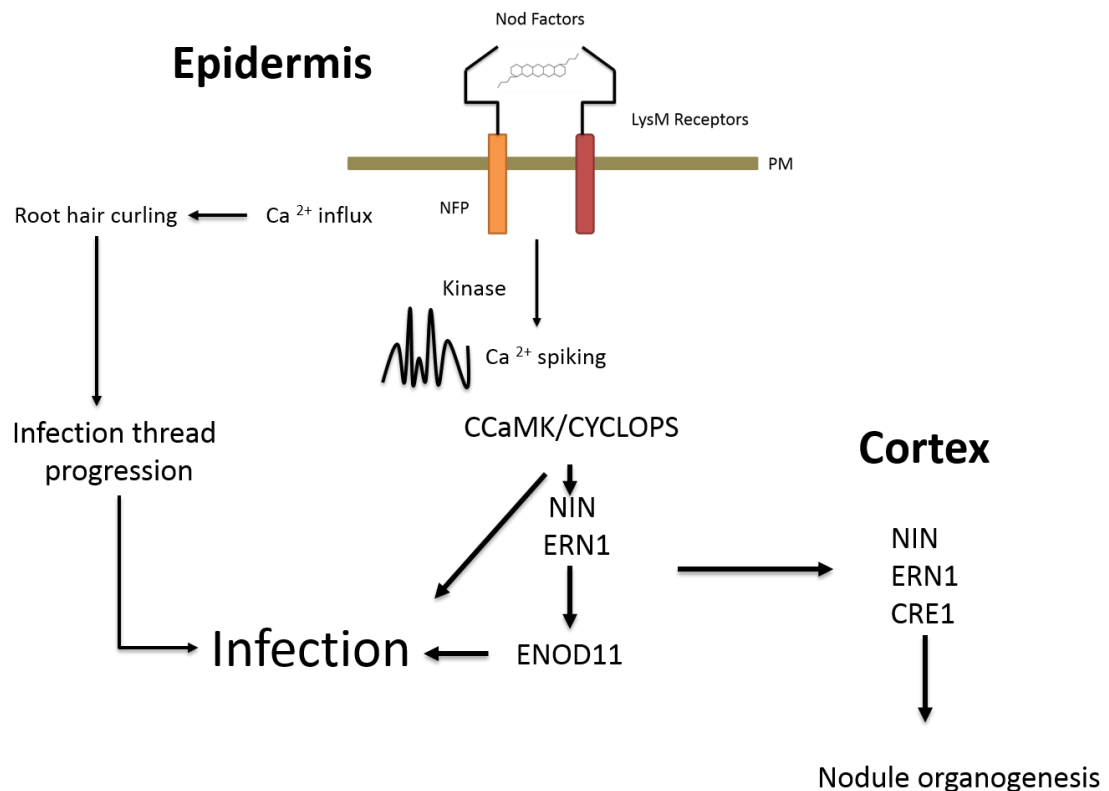


Figure 1.3 Epidermal Nod factor (NF) signalling pathway and components of the cortical signalling transduction in *M. truncatula*. Nod factors secreted by rhizobia are sensed by root epidermal cells that activate the LysM-type receptor-like kinases NFP. Receptor activation induces Ca²⁺ influx at the root hair tips, resulting in Caspiking, in root hair curling and rhizobia infection. The calcium-dependant calmodulin CCaMK, encoded by DMI3, form a complex with its partner CYCLOPS and decodes the calcium spiking signals in the nucleus, and trigger the expression of the transcription factors ERN1 and NIN. Together ERN1 and NIN activate the early nodulin gene *ENOD11*, important for infection. In parallel, a mobile signal, is activated/produced in the epidermis downstream of DMI3 and is translocated to the cortex where it activates the transcription factors ERN1, NIN and the cytokinin receptor CRE1 and induces cortical cell divisions leading to nodule organogenesis.

1.2.2.3 Control of nodulation by hormones

Hormones regulate a myriad of developmental processes in plants (Gray, 2004; Schaller, 2012; Locascio et al., 2014; Crook et al., 2016) including the establishment of nitrogen-fixing symbiosis and the development of nodules. In the next section, information on the role of specific hormones in the process of infection and nodulation will be reviewed.

1.2.2.3.1 Auxin

Auxin is thought to be a regulator of nodule organogenesis, being its accumulation correlated with an increase in the number of nodules and its long-distance transport appears regulated upon inoculation (Mathesius et al., 1998; van Noorden et al., 2006). Application of polar auxin transport inhibitors such as NPA or TIBA leads to the formation of spontaneous nodule-like structure in *Medicago* species (Hirsch et al., 1989; Rightmyer and Long, 2011). Furthermore, the application of a low concentration of auxin enhances nodulation in *M. truncatula* (van Noorden et al., 2006). Additionally, recent work from Roy et al (2017) shows that the *Medicago* paralogue of the Arabidopsis auxin transporter *AUX1*, *MtLAX2*, plays an important role in nodule organogenesis. Expression studies found the gene to be expressed in nodule primordia, the vasculature of developing nodules and at the apex of mature nodules (Roy et al, 2017). The characterisation of the mutant *mtlax2* showed that these plants had a defective lateral root development and fewer nodules than wild type plants (Roy et al 2017).

Auxin has also been proposed to play a role in the infection process. Research in the actinorhizal symbiosis *Frankia/Casuarina glauca* showed that the auxin transporter *CgAux1* was predominately expressed in infected cells and infected root hairs (Peret et al., 2007) and that auxin accumulated in the infected cells of the nodule (Krouk et al., 2010). In the legume/bacteria symbiosis interaction auxin signalling has been identified as essential for correct bacterial infection (Breakspear et al, 2014). A *Medicago* ortholog of the Arabidopsis *Arabidopsis thaliana Auxin Response Factor 16* is rapidly regulated upon infection in *Medicago* root hairs. A mutation in the gene results in reduced infection, potentially caused by a blocking in the stage of infection pocket, suggesting that the early stages of infection were affected in the mutant. Interestingly, nodule numbers and development were normal in the mutants, suggesting an essential role of the ARF16 in infection initiation (infection pocket formation) but not in infection thread extension and/or nodule organogenesis (Breakspear et al, 2014).

Auxin function in the development of infection threads has been proposed to be related to its effects in cell wall loosening and expansion (Perrot-Rechenmann, 2010) but so far little evidence support this theory.

1.2.2.3.2 Cytokinins

Cytokinins are known to control root development, shoot branching and lateral root formation (Laplaze et al., 2007; Bensmihen, 2015). In *Lotus*, cytokinins act in the root epidermis upon inoculation with rhizobia and throughout nodule development (Held et al., 2014). A gain of function mutation in the kinase domain of the cytokinin receptor gene (*LHK1*) in *L. japonicus* leads to spontaneous nodule development in absence of rhizobia (Tirichine et al., 2007), suggesting that cytokinin signalling is necessary and sufficient for nodule organogenesis. On the other hand, a loss of function in the same receptor in *Lotus* and its homologous in *M. truncatula* (*CRE1*) reduces nodulation (Gonzalez-Rizzo et al., 2006; Murray et al., 2007).

To further support an important role for cytokinins in nodule organogenesis, essential genes for nodulation were up-regulated upon the treatment with exogenous cytokinin and nodule primordia were visible in the absence of rhizobia (Heckmann et al., 2011). External application of cytokinin can also activate *NIN* in the cortex, but not in the epidermal cell layer, linking its function with cortical cell reprogramming (Heckmann et al., 2011). The role for cytokinin in infection has also been discussed and linked to auxin, where both hormones might be counteracting each other effects. Intriguingly, cytokinins appears to mediate bacterial attachment during infection, adding to the complexity of cytokinin's role during the establishment of symbiotic interactions (Liu et al., 2015).

The dual role of cytokinins in epidermal and cortical cell layers suggest that an intermediary partner might travel to the cortex to elicit *de novo* cytokinin synthesis. Alternatively, the hormone might act as a secondary signal synthesized in epidermal cell layer upon inoculation and Nod Factor perception and translocated to underlying cortex cells, where it triggers the initiation of nodule primordia (Frugier et al., 2008). Whether the initial response to Nod factors involves *de novo* cytokinin synthesis or cytokinin transport remains unclear.

1.2.2.3.3 Ethylene

The role of ethylene in nodulation has been largely studied. In most legumes, ethylene acts as a negative regulator of nodulation. External application of the ethylene precursor aminocyclopropane 1-carboxylic acid blocks the characteristic calcium spiking necessary for nodulation (Oldroyd et al., 2001). Consistent with this, the ethylene biosynthesis inhibitor aminoethoxyvinylglycine (AVG) enhances nodulation and infection in several legumes (Peters and Crist-Estes, 1989; Nukui et al., 2000; Benitez-Alfonso et al., 2013).

A mutation in *MtSk11*, the *M. truncatula* orthologue of the Arabidopsis *EIN2* gene (a component of the ethylene signalling pathway) leads to enhanced number of nodules and Nod factor response (Penmetsa et al., 2003; Combier et al., 2008; Penmetsa et al., 2008). Ethylene has also been linked to infection thread formation and development in pea and *Lotus* (Guinel and Larue, 1992; Nukui et al., 2004). For a complete review of the role of ethylene in nodulation see (Guinel, 2015).

1.2.3 The regulation of symbiosis by the host plant

1.2.3.1 The mechanism behind the Autoregulation of Nodulation

Legumes balance their need to enter in the symbiotic interaction with the energy expense that it requires by limiting the number of nodules through the Autoregulation Of Nodulation (AON), a negative feedback system that control systemically number of nodules and infection. This regulatory system starts functioning as soon as 4 days post inoculation and involves both local and systemic signalling. Split-root experiments showed that when a sector of the root was inoculated with rhizobia, nodulation in the second section of the root was inhibited when it was inoculated at a later time point with rhizobia, demonstrating that a systemic inhibitory signal is transported through the plant (Kosslak and Bohlool, 1984). Furthermore, *Medicago* plants showing spontaneous nodule-like structures in the absence of rhizobia suppressed the formation of rhizobia-elicited nodule formation, but this suppressive response was eliminated when the

spontaneous nodule-like structure were excised, suggesting that the inhibitory signal is originated in the nodules (Caetano-Anolles and Gresshoff, 1991) (spontaneous nodulation will be reviewed later in this chapter).

The best studied mutants in AON are the LRR-receptor kinase *har1* in *L. japonicus* (Wopereis et al., 2000), *sym29* in *Pisum sativum* (Krusell et al., 2002), *nark* in *Glycine max* (Searle et al., 2003) and *sunn* in *M. truncatula* (Schnabel et al., 2005). These genes encode for a leucine-rich repeat receptor protein kinase and their mutations result in supernodulating plants, with often about 10-fold increase in the number of nodules. Their orthologue in Arabidopsis is CLAVATA1, a receptor like kinase, which perceives the CLAVATA3 peptide and that regulates meristem and flower development (Clark et al., 1993; Stahl and Simon, 2013).

The currently proposed model for this receptor is as follows: soon after the initiation of nodulation, short CLAVATA3/ESR-related (CLE)-peptides are induced by rhizobia (also named rhizobia induced CLE peptides or RIC). GmRIC1 and GmRIC2 in *Glycine max* and MtRIC12 and MtRIC13 (MtCLE12 and MtCLE13) in *M. truncatula* are thought to be expressed in the root and move through the xylem to the shoot, where they are perceived by NARK in *Glycine max* and SUNN in *M. truncatula* (Searle et al., 2003; Schnabel et al., 2005; Mortier et al., 2010). The overexpression of these peptides in transgenic roots significantly inhibited nodulation 21 dpi (Mortier et al., 2010). Nodulation was also inhibited in untransformed roots on the same composite plants (*Medicago truncatula* roots that were not overexpressing CLE peptides), suggesting that the overexpression of *MtCLE12* and *MtCLE13* in transgenic roots might have a negative systemic effect on roots not overexpressing the peptides (Mortier et al., 2010). Additionally, the overexpression of MtCLE13 in the supernodulating *sunn* mutant background did not lead to an inhibition of nodulation, suggesting that the systemic effect of MtCLE13 in control of nodulation is SUNN dependent (Mortier et al., 2012).

The expression patterns suggest that GmRIC1 in *Glycine max* and MtCLE12 in *M. truncatula* are early signals of AON, signalling the degree of infection, while GmRIC2 and MtCLE13 are a later signal, determining the extent of successful

nodule organogenesis (Mortier et al., 2010; Ferguson et al., 2014). Analysis of *ENOD11* expression pattern 3 dpi in roots overexpressing both *MtCLE12* and 13 in *Medicago* shows a downregulation of the gene, suggesting that the peptides inhibit nodulation at the early stages of Nod factor signalling, before the onset of *ENOD11* expression. The combination of both RIC peptides is likely to orchestrate AON in legumes.

Alternatively to the systemic effect of CLE peptides in nodulation, it might be possible that the peptides are perceived locally in the root and control a separate from SUNN pathway to control nodule number. This second pathway might be auxin-related. Auxin transport assays post inoculation in the *sun* mutant showed that the amount of auxin loaded from shoot to root was not reduced, compared to what was seen in the wild type plants. This reduction of auxin transport also correlates with the start of the autoregulation of nodulation program (Mathesius et al., 1998; van Noorden et al., 2006). CLE peptides can modulate auxin in *Arabidopsis* (Whitford et al., 2008), suggesting that it is possible that they are regulating auxin levels in the root to restrict nodulation in *M. truncatula*.

Future experiments aimed at characterising the CLE peptides expression pattern, transport and components involved in CLE perception and signalling will enhance our understanding of their importance in AON in legumes.

1.2.3.2 Host mechanisms to control nodulation in response to nitrate availability

The symbiotic process is also regulated by nitrate availability in the soil. This is a homeostatic process that allows the plant to control the energy partition that will allocate to biological nitrogen fixation depending on its nitrogen requirements (Cho and Harper, 1991). External availability of readily assimilable forms of nitrogen, such as ammonia, heavily inhibits the formation of nodules (Streeter, 1985; Day et al., 1989; van Noorden et al., 2016). Agricultural soils often contain high levels of residual nitrogen due to the repeated addition of fertilisers to the soil, this limits the efficiency and the usefulness of legumes as an intercrop. Understanding the pathway by which legumes sense nitrogen status in the environment and how that signal is translated to the nodulation and nitrogen

fixation processes is essential to maximise the potential of legumes in the development of a more sustainable agriculture with fewer added fertilisers.

The early stages of nitrogen recognition and signalling are likely to be mediated by membrane receptors (Krouk et al., 2010; Criscuolo et al., 2012) of the family of nitrate transporters NRT1/NRT2. These family of proteins include more than 90 members in *L. japonicus* and in *M. truncatula* that are also involved in the control of root growth (Pellizzaro et al., 2014).

The signalling process downstream of sensing the nitrate status in the environment appears, as the AON pathway, to be both systemic and local and mediated by small peptides and perceived by a family of LRR-receptor kinases (Reid et al., 2011a).

Recent research in soybean identified a pathway where GmNIC1 (a nitrate-induced CLE peptide) controls infection and nodulation in response to the nitrate status but not to rhizobial infection (Reid et al., 2011a; Reid et al., 2011b). The proposed mechanism is that GmNIC1 interacts with a homolog of the LRR-receptor kinase GmNARK expressed in the root. It is not currently known how GmNARK can distinguish between CLE peptides induced by rhizobia and by nitrate. On the other hand, two CLE peptides have been identified in *L. japonicus*, *LjCLE-RS1* regulated by rhizobia and *LjCLE-RS2* regulated by both rhizobia and nitrate availability. In the case of the nitrate induced peptide, its expression pattern in response to nitrate was not affected in mutants deficient in the Nod factor signalling pathway, suggesting that it acts downstream of this pathway (Okamoto and Kawaguchi, 2015).

Currently, there is not a similar model in *M. truncatula*, nor are mutants available in encoding nitrate-induced CLE peptides in soybean. Therefore it is difficult to determine if the role of CLE peptides in the control of nodulation by nitrate is conserved in different plant systems.

Additionally, another class of small peptides called CEPs (C-Terminally Encoded Peptides) identified in *M. truncatula* are induced in a nitrogen dependent manner (Imin et al., 2013) The overexpression of these peptides promotes nodulation

(Delay et al., 2013) and in *M. truncatula* have also been identified as partners in the pathway that controls lateral root formation (Mohd-Radzman et al., 2016).

Finally, nitrate levels also appear to affect signalling via other important factors, such as ethylene, flavonoids, auxin and cytokinin (Coronado et al., 1995; Caba et al., 1998; Mathesius et al., 2000). The role that these factors play in nodulation has been introduced before in this work.

1.2.3.2.1 A shared pathway?

Mutants in the LRR-receptors SUNN in *M. truncatula* and NARK in *G. max* are, additionally to supernodulating, insensitive to nitrate in the media, meaning that they do not see an inhibition of nodulation in the presence of exogenous nitrate (Carroll et al., 1985a; Day et al., 1989; Schnabel et al., 2010). This suggests that the pathways involved in the autoregulation of nodulation and the inhibition by nitrate might have shared components. As described above, nitrate induced CLE peptides are potentially also signalling through NARK/SUNN in *G. max* and *M. truncatula*, but it appears that rhizobia-induced peptides are perceived in the shoots, whereas NICs are perceived locally in the root, at least in *G. max* (Reid et al., 2011a). To study the role of the shoot in the control of nodulation by nitrate, grafting experiments were carried out using as root stock either wild type or mutants in the AON pathway.

The number of nodules developed post inoculation were assessed after treatment with high levels of nitrate compared to the absence of nitrate. Plants with intact AON response (wild type shoot stock/nark root stock or wild type shoot stock/wild type root stock) were used to assess the role of NARK in the root as part of the nitrate-controlled regulation of nodulation. Plants with wt root stocks displayed a decreased number of nodules in high levels of nitrate compared to those having a supernodulating (*nark* mutation) rootstock (Reid et al., 2011a). There was not a significant difference in nodule number when nitrate was not applied between the different combinations of root and shoot stocks, suggesting that the role of NARK in the root is nitrate-dependant. These grafting experiments indicate the potential of dual action for NARK, in the local perception of nitrate-

induced CLE and in the systemic (shoot derived) response to rhizobia-induced CLE in no-nitrate (Reid et al., 2011a).

Structural studies showed that the rhizobia induced peptides feature a signal peptide domain, which is highly conserved across species (Reid et al., 2013) and it potentially serves a function in transport and/or cleavage. Interestingly, in soybean, the peptides induced by nitrate do not feature this domain. This might correlate with the fact that rhizobia induced peptides are transported long-distances, thus require modifications to enter the secretory pathway (Reid et al., 2013).

Little is known about this mechanism in *M.truncatula*, but *sun*n and other supernodulating mutants affected in the LRR-receptor also show nitrate insensitivity, nodulating in spite of its availability in the environment. As before, this suggests some shared steps and/or components in the autoregulation of nodulation and in the response to nitrate. The identification of nitrate-induced CLE peptides in *M. truncatula* is essential to discern the molecular mechanisms behind the control of nodulation by nitrate availability in this model legume.

1.2.3.2.2 Summary: Genetic control of nodulation

Great efforts have been made in recent years to decipher the partners regulating nodulation in legumes. Several mutants have been characterized which have helped to decode this mechanism (Table 1.1).

Table 1.1-Table summarising some of the genes identified up-to date that play a role in the regulation of the nodulation process in legumes.

| Gene | Gene product | Site of production | Site of action | Comments | References |
|--|--------------|--------------------|--------------------|---|--|
| GmNARK; GsNARK; LjHAR1; MtSUNN;P sSYM29 | LRR-RK | Shoot/root | Shoot/root | Acts in shoot (AON) and root (Nitrate inhibition) | (Krusell et al., 2002; Searle et al., 2003; Schnabel et al., 2005) |
| GmNIC1 | CLE | root | root | Nitrate induced CLE peptide | (Reid et al., 2011a) |
| GmRICI/2; LjCLE- RS1/2;MtC LE12/13 | CLE | root | probably the shoot | rhizobia-induced CLE-peptide | (Okamoto et al., 2009; Mortier et al., 2010; Lim et al., 2011; Reid et al., 2011a) |

| | | | | | |
|----------------------------|---------------------------------------|-------------|--------------|--|--|
| LjASTRAY | bZIP TF | | root | Supernodulation / early nodulation phenotype | (Nishimura et al., 2002) |
| LjCLV2; PsSYM28 | CLV2 (truncated LRR-receptor protein) | Shoot/root | Shoot/root ? | May interact with other AON LRR RKs | (Sagan and Duc, 1996; Krusell et al., 2002) |
| LJETR1 | ETR1 | Shoot/root | Shoot/root? | Ethylene receptor | (Gresshoff et al., 2009; Lohar et al., 2009) |
| LjKLV | LRR-RK | Shoot/root? | Shoot/root? | May interact with other AON LRR RKs | (Oka-Kira et al., 2005) |
| LjPLENTY | Unknown | root | root | Mutants show hypernodulation | (Yoshida et al., 2010) |
| LjRDH1 | Unknown | root | root | Mutants show hypernodulation | (Ishikawa et al., 2008) |
| LjTML | Unknown | root | root | Mutants show hypernodulation | (Magori et al., 2009) |
| MtEFD | Ap2-EREBP | root | root | positively regulates CK levels | (Vernie et al., 2008) |
| MtLSS | Unknown | Shoot/root? | Shoot/root? | A possible regulator of SUNN | (Schnabel et al., 2010) |
| MtSKL | EIN2 | Root | root | ethylene response factor | (Penmetsa and Cook, 1997; Penmetsa et al., 2008) |
| PsNOD3, MtRDN1 | RDN1 | Root | root | affects CLE synthesis and/or transport | (Engvild, 1987; Li et al., 2009; Novak, 2010; Schnabel et al., 2011) |

1.2.4 Spontaneous nodulation

Several legume mutants are able to produce nodule-like structures in the absence of rhizobia (Gleason et al., 2006; Tirichine et al., 2006a; Marsh et al., 2007; Suzaki et al., 2013; Saha and DasGupta, 2015). The study of these mutants is especially interesting as they are evidence that the Nod factor signalling and nodule organogenesis can be uncoupled. Their analysis establish the signalling and molecular mechanisms behind nodule organogenesis in the absence of rhizobia.

Experiments expressing the native promoter *pDMI3* and an autoactive version of DMI3 (generated by deletion of the the CaM binding/autoinhibition domain) in the mutant *dmi3* (unable to form infection threads and nodules) showed that as many as 43% of these plants would spontaneously nodulate (Gleason et al., 2006). Sectioning of these structures showed the absence of an infection zone in the nodule. Additionally, when inoculated with rhizobia, these plants were unable to form infection threads showing that the mutant phenotype is complemented, as compared to mutants complemented with the native promoter and a full version of DMI3 that showed regular infection thread and nodule development (Gleason et al., 2006). Additionally, a mutation in a single aminoacid in CCaMK (*snf1* mutant) is sufficient to trigger cortical cell dedifferentiation and form nodule primordia in *L. japonicus* (Tirichine et al., 2006b). In all cases spontaneous nodules were round in shape and smaller than control nodules developed after inoculation with rhizobia.

Research from Marsh et al (2017) showed that, unlike *dmi3* mutants, *nin* plants transformed with the autoactive version of DMI3 did not form spontaneous nodulation. This result suggests that the capacity of autoactive version of DMI3 to induce spontaneous nodule organogenesis is NIN-dependent in *M. truncatula* (Marsh et al., 2007).

A mutant in *L. japonicus* affected in the cytokinin receptor LHK1 (*snf2*) presents a constitutively activated cytokinin signalling. *snf2* mutants also showed nodule organogenesis in the absence of rhizobia (Tirichine et al., 2007). Further studies with this mutant showed that auxin was regulated during cortical cell proliferation, suggesting that this response appears downstream of the cytokinin signalling pathway (Suzaki et al., 2013). Additionally, and as described in section 1.2.2, expression of *NIN* in cortical cells of *nin* and *cre1* mutant backgrounds can promote spontaneous nodule organogenesis. Contrarily, when *NIN* was expressed in the epidermal cell layer no spontaneous nodulation could be seen, indicating that *NIN* can act independently of cytokinin signalling in the cortex to trigger organogenesis (Vernie et al., 2015).

Finally, other mutants, such as a mutation in the Symbiosis Receptor Kinase in *M. truncatula* (*symrk*, a member of the Nod factor signalling pathway and

essential for both nodule organogenesis and infection) were affected in nodule organogenesis. When this mutant is transformed with the kinase domain of SYMRK (*symrk-kd*), plants displayed spontaneous nodule organogenesis. Spontaneous organogenesis could not be seen when transformed with the full length version of the protein, suggesting that the kinase domain is responsible for the phenotype (Saha et al., 2014). Unlike the spontaneous nodules seen in the experiments using the CCaMK autoactive version, *symrk-kd* plants showed both a deregulation in the number of nodules and their spatial positioning.

The underlying mechanism of the miss-regulation of nodule organogenesis in the absence of rhizobia is not yet clear (Saha et al., 2014). Whatever the underlying mechanism, it is clear that deregulated *SYMRK*, *CCaMK* and *NIN* activity affects the signalling pathways that control nodule number and, in some cases, spatial positioning of nodules. Deciphering the mechanisms behind these phenotypes could help to understand how infection and nodulation processes regulated and to what extent they are genetically uncoupled.

1.3 Brief introduction to the symplastic pathway

In all multicellular organisms, cell to cell communication is essential for growth, response to the environment and defence. Intercellular communication can occur apoplastically, which implicates ligands and plasma-membrane localized receptors, transcellularly, involving protein channels (Chaumont and Tyerman, 2014; Adamowski and Friml, 2015) or exocytosis (Zarsky et al., 2013) of molecules that move in the apoplastic space or symplastically, where the molecules move through channels embedded in the cell walls called plasmodesmata. Plasmodesmata connect the cytoplasm of adjacent cells forming the symplast where small and large of molecules can move either by diffusion or actively via interactions with plasmodesmata proteins/modifiers (Ehlers and Kollmann, 2001; Turgeon and Wolf, 2009). Plasmodesmata also play an important role in long distance signalling by enabling the loading and unloading of molecules transported in the phloem (Turgeon and Wolf, 2009; Seville et al., 2013).

Plasmodesmata are lined by plasma membrane and, in the centre of the pores a structure called desmotubule, derived from the endoplasmic reticulum (ER), can be found (Lucas and Lee, 2004). Two types of plasmodesmata have been characterised based on their biogenesis: primary and secondary (Ehlers and Kollmann, 2001). Primary plasmodesmata originate in the developing cell wall during cytokinesis (Knox and Benitez-Alfonso, 2014), and secondary plasmodesmata originate *de novo*, independent of cell division, in already existing cell walls. Secondary plasmodesmata are thought to have more complex structures (Ehlers and Kollmann, 2001) as they can either be simple (a single channel) or branched (multiple channels connected) (Carlsbecker et al., 2010) (Figure 1.4). Plasmodesmata structure are regulated with age, with young tissues displaying more simple plasmodesmata and more complex structures arising during cell differentiation (Ehlers and Kollmann, 2001). The differences in the structure of simple and branched plasmodesmata can affect the transport capacity of the channels (Oparka et al., 1999).

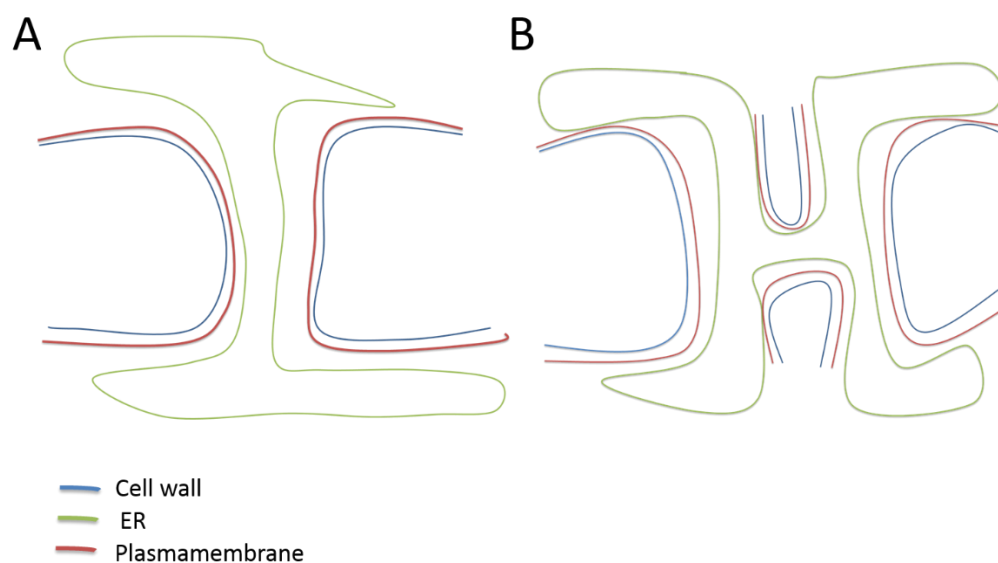


Figure 1.4- Diagram showing the structure of a simple (A) and branched (B) plasmodesmata. Simple plasmodesmata are formed after cytokinesis, and comprises a modified ER (green), the cell wall (blue), and the plasma membrane domain (red). Branched plasmodesmata appear post-cytokinesis presumably through modifications in already existing primary plasmodesmata and can comprise more than one channel aperture.

1.3.1 Role of the symplastic pathway in plant development

Plasmodesmata constitute an important pathway for the transport of proteins, RNAs and other signalling molecules that play a role in plant development (Sevilem et al., 2015; Otero et al., 2016). For example, the transcription factor LEAFY, that moves presumably via secondary plasmodesmata, to activate non-cell autonomously genes involved in flowering in the meristem and to determine flower organogenesis (Wu et al., 2003). Similarly, the Flowering Locus T protein is induced in response to environmental signals in leaves and its transported presumably via plasmodesmata into the phloem and up to the shoot where it promotes the differentiation of the apical meristem into floral meristems (McGarry and Kragler, 2013). Symplastic connectivity also regulates the activity of the transcription factors and miRNAs involved in the maintenance of the apical meristems (Vaten et al., 2011; Kitagawa and Jackson, 2017), in root hair patterning (Ishida et al., 2008) and is likely to control radial root patterning (Helariutta et al., 2000). Rinne et al. (2011) and Benitez-Alfonso et al (2013) suggested that some developmental transitions rely on symplastic communication, although the mobile factors affected are not yet identified. For instance, the formation of lateral root primordium (LRP) is miss-regulated when plasmodesmata are occluded (Benitez-Alfonso et al., 2013). The research indicates that for proper lateral root patterning, pericycle cells need to be symplastically connected prior lateral root specification and altering this connectivity produce lateral root clusters. Symplastic connectivity is temporally regulated as soon after the first round of cell division, the lateral root primordium appear symplastically isolated from the surrounding cells. Plasmodesmata are also temporarily closed during dormancy in poplar buds, being the recovery of symplastic connectivity associated with the transport of factors that trigger dormancy release (Rinne et al., 2011).

Despite their vital role in organogenesis and morphogenesis, the specific regulatory factors involved in the function of plasmodesmata during development remain mostly unknown. Research in plasmodesmata biology will provide deeper insights into how they are formed, structurally modified and the mechanisms regulating their function during plant development.

1.3.2 Regulation of plasmodesmata transport

Small molecules such as sugars, metabolites and RNAs are thought to move across plasmodesmata preferentially by diffusion through the cytoplasmic sleeve (the symplasm) (Lucas and Lee, 2004). Other molecules interact with partners to modify plasmodesmata aperture or transport capacity in order to be transported (Complainville et al., 2003). Plasmodesmata aperture are susceptible to modification of the architecture of the surrounding cell walls affecting symplastic transport. Specifically, the cell wall polysaccharide callose (β -1, 3-glucan polymer Figure 1.5) can accumulate in the neck region of plasmodesmata, in response to chemicals and environmental stresses, constricting the size and transport capacity of the channel (De Storme and Geelen, 2014). It is thought that the deposition of callose acts as a physical barrier to decrease the size of molecules that can go through (i.e. size exclusion limit, SEL). In contrast, the degradation of callose 'opens' plasmodesmata, increasing the molecular flux.

The study of proteins involved in plasmodesmata regulation is especially challenging since plasmodesmata localization in the cell walls difficult their accessibility for characterization and the isolation of pure plasmodesmata fractions (Fernandez-Calvino et al., 2011). Moreover, as these channels are essential for plant development, forward genetic screening only identified lethal alleles. Nevertheless, the collective effort of several research groups has produced a comprehensive list of putative plasmodesmata-located proteins identified by proteomic approaches (Fernandez-Calvino et al., 2011; Salmon and Bayer, 2012; Benitez-Alfonso et al., 2013). Some of these novel factors are callose synthases (CALS or Glucan Synthase Like protein, GSL) and β -1,3-glucanases, or BGs, which are directly involved in controlling callose synthesis and degradation respectively (Doxey et al., 2007; Vaten et al., 2011; Zavaliev et al., 2011; Benitez-Alfonso et al., 2013; De Storme and Geelen, 2014) (Figure 1.6). Other proteins such as Plasmodesmata-Callose Binding proteins (PDCBs) (Simpson et al., 2009), Plasmodesmata-Located Proteins (PDLPs) (Thomas et al., 2008) and other Receptor-like Kinases (RLKs) (Vaddepalli et al., 2014) were also identified and their function have been directly or indirectly linked to changes

in callose deposition. For example, the over-expression of PDLP1, PDLP5 and PDCB1 produces callose over-accumulation that decreases symplastic connectivity in *Arabidopsis thaliana* (Thomas et al., 2008; Lee et al., 2011). A mechanism involving PDLP and PDCB proteins has been shown to play a role in the response to bacterial and fungal pathogens and to abiotic stresses (Lee et al., 2011; Cui and Lee, 2016). PDLP1 has been associated with callose accumulation during the development of the haustorium, (a specialised feeding structure) during infection of *Arabidopsis* with *Hyaloperonospora arabidopsidis* (Caillaud et al., 2014). Recent work identified PDLP5 as partner for CALS1 and CALS8 in the regulation of callose in response to different stressors. Salicylic-acid regulates plasmodesmata permeability, expression analysis identified CALS1/PDLP5 as responsible for this regulation. On the other hand, the study of a pool of mutants identified a novel callose synthase, CALS8, required in the regulation of callose in response to reactive oxygen species (Cui and Lee, 2016).

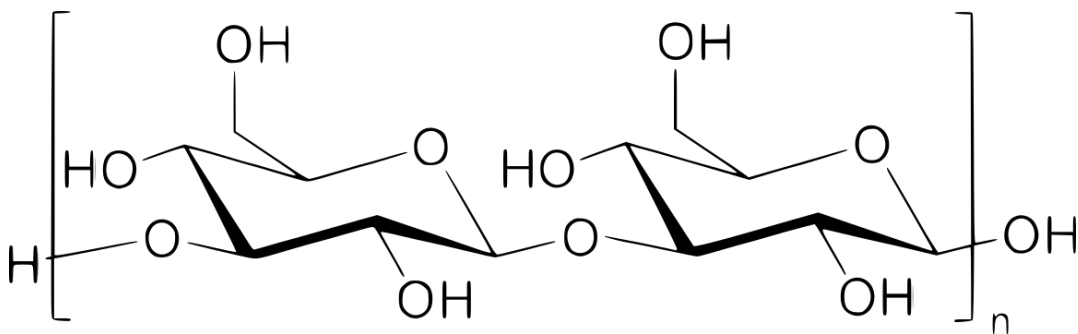


Figure 1.5-Structure of callose. Callose molecules are conformed by n repetitions of β -1,3 linked molecules of glucose.

In some cases, genetic screens have been successful in identifying proteins with a role in the regulation of callose at plasmodesmata affecting plant development (McGarry and Kragler, 2013). Loss of function mutation in *Arabidopsis* *CALS10*, named *chorus*, leads to a down regulation of callose in the epidermis (Chen et al., 2009; Cui and Lee, 2016) which appears to induce the spreading of the transcription factor *SPEECHLESS*, known to promote cellular entry into the stomatal lineage. As a result, *chorus* mutants show abnormal stomata development (Guseman et al., 2010; Simmons and Bergmann, 2016). *CALS10* is also involved in the phototropic response in hypocotyls, an effect that

correlates with changes in auxin distribution (Han et al., 2014). In addition, a loss of function *ca/s7* mutant shows defects in the formation of sieve plate in phloem cells thus affecting vascular transport (Xie et al., 2011).

Similarly, a gain of function mutants in *CALS3* result in an over accumulation of callose, decreased plasmodesmata aperture leading to defects in the transport of the transcription factor *SHORT-ROOT* and the microRNA165 (Vaten et al., 2011). *SHORT-ROOT* determines cell fate and root patterning (Nakajima et al., 2001), whereas, microRNA165 is involved in the radial patterning of the xylem (Carlsbecker et al., 2010; Vaten et al., 2011). As expected, these *ca/s3* hyperactive mutants displayed root developmental defects and altered vascular transport.

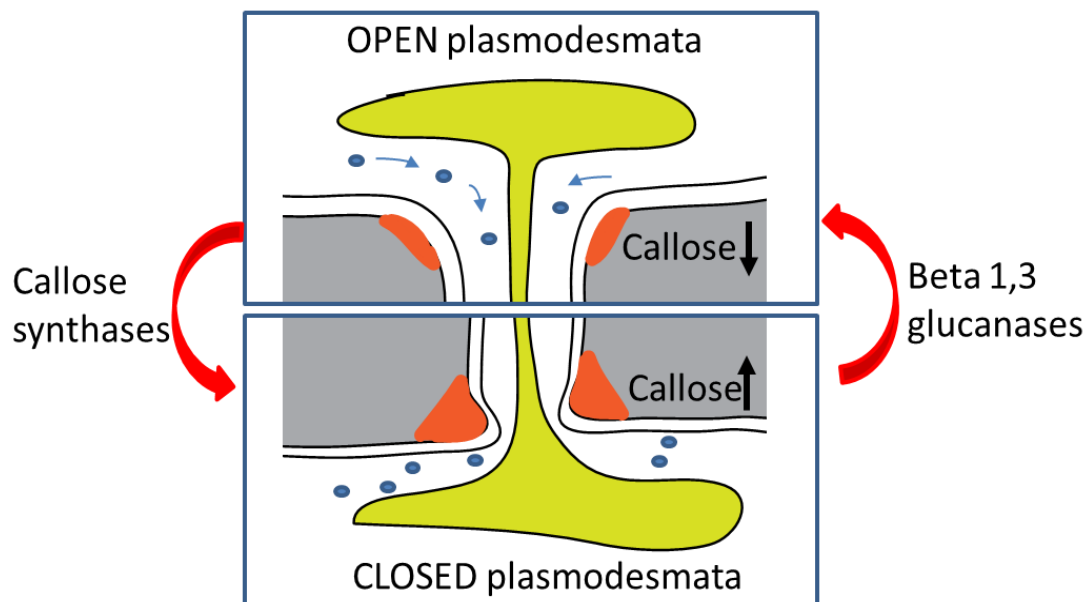


Figure 1.6- Schematic model on callose regulation of plasmodesmata permeability. Callose synthase promotes callose accumulation at the neck region of plasmodesmata, decreasing the pore permeability. On the other hand, β -1,3 glucanases digest callose, widening the pore and increasing molecular flux between cells.

Several genetic tools have been developed over the past years to modify callose at plasmodesmata sites aiming to alter symplastic communication under different cues (Muraro et al., 2011; Sevilem et al., 2013; Yadav et al., 2014). These approaches allowed the determination of spatial-temporal patterns of importance

for plasmodesmata regulation during plant development. Recent research exploiting one of these tools (the *icals3m* system, by which a mutated version of CALS3 was driven by the endodermis specific promoter *EN7*) has shown that the symplastic transport of signals is essential for the coordination of cell divisions and patterning in Arabidopsis roots (Wu et al., 2016). Wu et al. (2016) used the *icals3m* system to overexpress callose and block plasmodesmata-mediated transport to and from the endodermis in Arabidopsis roots. After reducing symplastic transport, the cells in the elongation zone of the root were shorter and wider compared to control plants not overexpressing callose. Additionally, cells in the meristem were affected in patterning and the endodermal cell lineage expanded to two cell layers, compared to control plants, where endodermal cell layer was still only one cell layer (Wu et al., 2016)

Symplastic transport can also be regulated by modifications in plasmodesmata branching and/or frequency (Burch-Smith et al., 2011; Sager and Lee, 2014). The molecular mechanism behind this dynamic regulation in plasmodesmata frequency/branching is mostly unknown. The genetic screen of PD-mutants has identified two mutants, *ise1* and *ise2*, affected in two RNA-helicases. These mutants display an increased symplastic transport and a higher proportion of branched plasmodesmata compared to wild type plants (Burch-Smith et al., 2011). More recent research has helped in the characterisation of a mutant in a choline transporter showing a reduction in the number of secondary plasmodesmata in the shoot apical meristem and in Arabidopsis leaves. Also, the number of highly branched plasmodesmata, characteristic of cellular differentiation, were reduced in this mutant (Kraner et al., 2017). These results suggest an essential role for this transporter in the formation and maturation of secondary plasmodesmata although the molecular mechanism involved remains unclear.

1.3.3 Role of plasmodesmata in plant-microorganism interactions

1.3.3.1 The regulation of the symplastic pathway during plant-pathogen interactions

Some microorganisms have evolved to exploit plasmodesmata for infection. Among plant pathogens manipulating plasmodesmata, viruses have been

studied more broadly (Benitez-Alfonso et al., 2010). Plant viruses produce specialised 'movement proteins' (MP) that interact with plasmodesmata and participate in virus spreading (Ward et al., 1997). MPs from tobamoviruses, bromoviruses or dianthoviruses are thought to increase plasmodesmata SEL by activation of BGs, the enzymes that degrade callose (Haupt et al., 2005; Sasaki et al., 2006; Su et al., 2010; Zavaliev et al., 2013). MPs from geminivirus can also associate with the synthesis of tubules that transverse the plant cell wall across plasmodesmata to facilitate virus spreading (Ward et al., 1997). Other viruses' MP, such as the tobacco mosaic virus can associate with the ER during early stages of infection and is then redistributed to plasmodesmata (Heinlein et al., 1998; Huang et al., 2001)

In some fungal invasions, plasmodesmata appear to be exploited as a way to spread the infection. Electromicroscopy pictures suggest that in the biotrophic invasion of the rice blast fungus, *Magnaporthe oryzae* develops an invasive hyphae (IH) that penetrates into the neighbouring cell through what appears to be plasmodesmata regions (Kankanala et al., 2007). The average plasmodesmata are too small to accommodate the IH, thus the appressed ER is thought to disintegrate, creating cytoplasmic pores, in order to make space for the passage of the fungus (Kankanala et al., 2007). There are literature reports that others fungi such as *Fusarium graminearum* move into neighbouring cells through pit pairs (cavities in lignified cell walls that resemble plasmodesmata) (Guenther and Trail, 2005; Kankanala et al., 2007). Fungus, and some pathogenic bacteria, can also affect the regulation of the molecular flux between cells presumably as a medium to limit plant defences (Lee et al., 2011). For example, the plasmodesmata protein Lym2, in concert with other receptors like kinases, appears to be required for regulating symplastic transport in response to the fungal elicitor chitin but not to the bacterial elicitor flagellin. Mutations in this receptor affect the defence response against the fungal pathogen *Botrytis cinerea* in *Arabidopsis* (Faulkner et al., 2013). More recently, a plasmodesmata-localised Ca²⁺ binding protein was identified to play a role in the regulation of plasmodesmata in response to bacterial flagellin through a mechanism involving changes in callose deposition (Xu et al., 2017). *Arabidopsis* responses to the fungus *Hyaloperonospora arabidopsidis* also trigger callose deposition at the site

of fungal penetration. Although in this case the role of plasmodesmata is not known, this regulation of callose depends on the expression of the plasmodesmata-located protein PDLP1 (Caillaud et al., 2014). The role of PDLP1 and PDLP5 in callose deposition and pathogenic responses has been dissected more recently (Lim et al., 2016). They regulate the symplastic transport of the signalling molecules azelaic acid and glycerol-3-phosphate which are involved in the systemic acquired resistance (SAR). Systemic acquired resistance refers to the priming that occurs in plants after a first encounter with pathogens, allowing plants that are primed to more quickly and more effectively activate defence responses. Overexpressing PDLP5 and PDLP1 drastically reduces plasmodesmata connectivity and impairs SAR in Arabidopsis (Cui and Lee, 2016; Lim et al., 2016). The role of CALS1 and CALS8, together with their partner PDLP5, in the regulation of callose in these responses was introduced in section 1.3.2.

The development of parasitic nematodes also appears influenced by plasmodesmata connectivity. Feeding occurs in highly specialised structures, called giant cells or syncytia depending if you are referring to root-knot nematodes or cyst nematodes. Many plasmodesmata connections form *de novo* between giant cells but between giant cells and the plant vascular system symplastic connectivity is reduced (Hofmann et al., 2010). In contrast, syncytia are massively connected to the phloem through plasmodesmata (Absmanner et al., 2013). When Arabidopsis mutant lines impaired in callose degradation were infected with cyst nematodes, histological analyses showed that feeding sites were smaller, indicating a crucial role for plasmodesmata in syncytia formation (Hofmann et al., 2010).

Plasmodesmata and callose also appears to regulate the plant response to herbivores. A triple PDLP mutant in Arabidopsis line (*pdko3*) challenged by herbivory caterpillars, is defective in some of the characteristic plant responses to pathogens, such as the K⁺ fluxes that trigger the depolarisation of the plasmamembrane of leaves cells 30 min post attack (Bricchi et al., 2013). These results suggest that PDLP, and likely plasmodesmata, are involved in the early responses to herbivory attack. Additionally, callose might be regulating response

to herbivores in a plasmodesmata-independent way. In response to herbivores, callose was deposited strongly on the sieve plates of a resistant rice variety compared to the susceptible one and his regulation was mediated by specific members of the CALS and BG family (Hao et al., 2008).

In summary, plasmodesmata and callose appear differentially regulated during plant interactions with viruses, fungal and bacterial pathogens but also after infection with nematodes and herbivores. Although the mechanism is not yet clear, plasmodesmata located proteins (PDLP), Lym receptors and callose metabolic enzymes appear to play a role in this response.

1.3.3.2 The regulation of the symplastic pathway during symbiotic interactions

The plant response to microbes is adjusted according to their nature (symbiont or pathogen) and the plant capacity to engage in these interactions (Soto et al., 2006; Vadassery and Oelmuller, 2009; Soto et al., 2011) (Zipfel and Oldroyd, 2017). In contrast to pathogenesis, the role that plasmodesmata or callose play in beneficial interactions it is not very well characterised (Rey and Schornack, 2013).

Research in the mutualistic symbiosis involving arbuscular mycorrhiza (AM) fungi with tobacco plants showed molecular trafficking between plant and AM fungus (Morales-Rayas et al., 2011). The symplastic tracer CFDA was applied in the leaves of the host plant, and it was transported to the fungus mycelia suggesting that there is a cytoplasm continuum between host plant cells and the fungus. However, no evidence for either plasmodesmata or other forms of tunnelling in the arbuscular interface was found (Morales-Rayas et al., 2011). On the other hand, AM was studied in the liverwort *Allisonia* and plasmodesmata-like structure were found in the fibrillary material that surrounds the colonizing fungus and separates them from the host plant plasmamembrane (Field et al., 2016). However, although these results suggest the symbiotic partners are symplastically connected, there is no evidence yet suggesting that the symplastic pathway in the host plant is regulated upon inoculation to facilitate this interaction.

In the legume-rhizobia symbiosis symplastic connectivity between the phloem and the nodule primordium has been shown to increase (Complainville et al., 2003) which was associated with an increase in plasmodesmata density in new and pre-existing cell walls. One day after infection of *M. truncatula* with rhizobium, reprogramming of cell division in the pericycle and in the cortex occurs and, concomitantly, the overall number of plasmodesmata between pericycle cells and the phloem companion cells increase in comparison to uninfected areas of the same root (Complainville et al., 2003). Cytoplasmic GFP, expressed under the companion cell-specific promoter AtSUC2, was normally restricted to the phloem in uninfected roots but it was transported into nodule initials and meristematic and invasion zones of the infected nodules (Complainville et al., 2003). As GFP, 6h after phloem loading, the symplastic fluorescent reporter 5 (6)-carboxy-fluorescein diacetate (CFDA) was transported into the nodule primordium but not into uninfected cortical tissues. These findings suggest the formation of a new symplastic domain between the phloem and the nodule initials after rhizobia inoculation coincident with an increase in plasmodesmata density (Complainville et al., 2003). Ectopic expression of a viral movement protein (MP from Tobacco Mosaic Virus) is known to increase plasmodesmata permeability and was used in this study to modify symplastic communication. A significant increase in nodule numbers two weeks post infection were counted in MP expressing transgenic roots, suggesting a role for plasmodesmata in nodule formation perhaps through interaction with the signalling pathways that regulate nodule number or infection sites (Beachy and Heinlein, 2000; Complainville et al., 2003).

Bederska et al. (2012) also used CFDA as a marker to determine changes in symplastic transport by loading the dye in the leaf and tracking its movement to the inner tissue of the nodules formed in *M. truncatula* roots infected with rhizobium. 42 days post infection CFDA was found to translocate to the pericycle and the endodermis of the nodule, but no fluorescence was detected in the nodule meristem or the invasion zone. This suggests that in older fully differentiated nodules symplastic continuity only occur between companion cells and the first layer of the parenchyma cells of the nodule. Further transport of molecules within the nodule is probably apoplastic (Bederska et al., 2012).

Plasmodesmata structure and frequency were also studied in other symbiotic systems. For instance, it was found that plasmodesmata frequency change between infected and uninfected cell types in the indeterminate nodules of *Vicia faba*, 5 weeks after the infection with rhizobium (Abd-Alla et al., 2000). Plasmodesmata were found 30 times more frequently between uninfected cells than between infected and uninfected cells and between infected cells. During actinorhizal symbiosis fully differentiated nodules of *D. glomerata* show abundant plasmodesmata between infected and uninfected cells (Schubert et al., 2011) although plasmodesmata density appears higher between mature infected cells than between younger ones.

1.3.3.3 Potential role of plasmodesmata in intercellular signalling during symbiosis

Communication of signals between epidermal and cortical cell layer might also play a role in legume-rhizobia symbiosis. Root hair bacterial infection and nodule primordia formation occur simultaneously in distant tissues, likely involving the transport of one or several mobile signals that coordinate these processes. However, the nature of these intercellular signal(s) and how they translocate from one cell layer to another remain poorly understood. The role of CCaMK in coordinating rhizobia infection and nodule organogenesis was introduced in section 1.2.2.2. Research from Rival et al., (2012) suggests that CCaMK also has a non-cell-autonomous function in coordinating the epidermis/cortex response to rhizobia infection. *M. truncatula dmi3* mutant plants were transformed with DMI3 driven by epidermal and cortical cell specific promoters. When DMI3 was only expressed in the epidermis infection threads but not nodule primordia could be seen (either at 7 dpi or 21 dpi), in contrast to when DMI3 was expressed in the cortex, neither infection threads nor nodule primordia could be seen at any time point analysed (Rival et al., 2012). Nodule organogenesis was achieved when *dmi3* plants were transformed with *DMI3* driven by both epidermal and cortical promoters, suggesting that nodule formation requires *DMI3* expression in both cell layers. These results suggest that, if nodule organogenesis requires a secondary signal between epidermis and cortex, *DMI3* might be involved at two levels: in the epidermis to generate this secondary signal and in the cortex to perceive it (Rival et al., 2012). Additionally, research

from Vernié et al (2015) reviewed in section 1.2.2.1, also suggested a non-cell autonomous role for *NIN* in nodule organogenesis. Regulators of *NIN*, or even *NIN* itself, might be transported intercellularly from the epidermis to the root cortex. Whether any of these mechanisms involve plasmodesmata is still unknown.

Finally, it was shown that epidermal expression of the early nodulin gene *ENOD40* that encodes two small peptides can induce division of cortical cells in *M. truncatula* roots (Sousa et al., 2001). This suggests that either the peptides encoded by *ENOD40* are moving from the epidermal cell layer to the cortex or alternatively, a secondary signal is triggered that transmits the information between cells to promote cell division. There is not enough evidence to support either of these hypothesis or to implicate plasmodesmata in the mobility of *NIN*, *ENOD40* or any other signalling molecule that coordinates the cross-talk between epidermal and cortical cell layers.

Although the nature of the signal is not yet known, together the findings suggest that symplastic communication is regulated during nodule initiation and that this regulation is crucial to control the number of nodules formed in *Medicago truncatula*. So far this regulation has been linked to a regulation in the number of plasmodesmata during the nodule organogenesis process, but the role of callose in this process has not yet been studied. Moreover the signal and pathways mediating communication between epidermis and cortex to coordinate infection and nodule organogenesis remain unclear. Although numerous transcriptional regulators have been identified to play a role in this process, so far there is no evidence that these move (or not) through plasmodesmata.

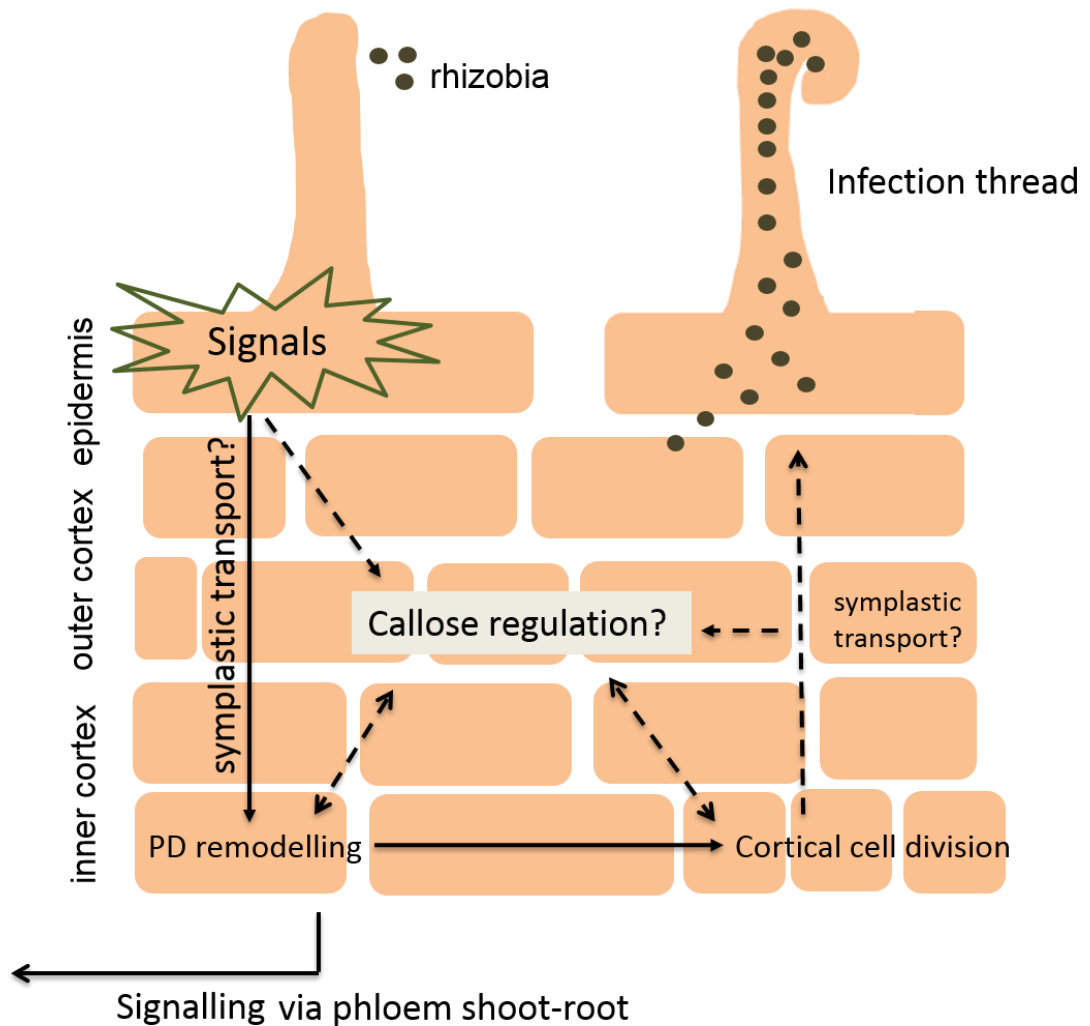


Figure 1.7-Schematic model showing the possible role of the symplastic pathway in the symbiotic process. Early signalling induced in response to rhizobia is perceived in the epidermal cell layer triggering further signalling to control infection and nodulation. It is hypothesised that these signals would regulate plasmodesmata and callose to control shoot-root signalling and to coordinate cortical cell division and the formation of infection threads. Solid lines refer to known changes in symplastic pathway and signalling pathway. Dotted lines refer to hypothesised changes in the root upon inoculation.

1.4 Aims and objectives of this thesis

The establishment of a symbiotic relation between legumes and nitrogen-fixing bacteria relies on a successful infection and the proper formation of nodules. These processes are independent but tightly coordinated through the transport

of signals between the site of bacteria recognition (epidermis) and the site of cell division in the cortex. Long distance communication (via the phloem) is also involved in regulating nodule formation (and infection) in relation to the plant nutritional status (and photosynthetic capacity) (Figure 1.7).

Previous research has demonstrated that the symplastic pathway is regulated upon inoculation by increasing number of plasmodesmata between cortex and phloem in infected roots, but until this day, there is no data regarding callose regulation or if there is any effect on epidermal-cortical communication. The following study is designed to fill these gaps in knowledge through characterising the role of callose and callose-modifying enzymes in rhizobia infection and nodulation in the model legume *M. truncatula*.

The specific objectives of this thesis are as follows:

1. To determine the patterns of callose deposition at the cell wall of *M. truncatula* roots upon inoculation with *S. meliloti*.
2. To identify genes/proteins regulating callose at plasmodesmata upon inoculation with rhizobia.
3. To determine how the infection and nodulation processes are affected when callose deposition is ectopically modified prior to inoculation by biochemical and genetic means.
4. To determine how the infection and nodulation processes are affected when callose deposition is spatially and locally modified using symbiotic promoters.
5. To determine the role of a novel plasmodesmata-located receptor like kinase protein in the response of *M. truncatula* to rhizobia in nitrate sufficient and depleted conditions.

Chapter 2

Chapter 2 –Materials and Methods

2.1 Plant Methods

2.1.1 Plant materials, seed sterilisation and vernalisation

M. truncatula ecotype Jemalong A17 (Barker et al., 1990) and Jester (Hill, 2000) were used in this study. *M. truncatula* line L416 containing the *pENOD11-GUS* (Boisson-Dernier et al., 2005) transgene was used to spatially and temporarily localise infection.

Seed coats were scarified by scratching the seeds between two sheets of sand paper, under sterile conditions 10% of sodium hypochlorite was added to the seeds. Bleach was removed after 3 minutes and the seeds washed with sterile water several times until all the bleach was removed. Sterile seeds were kept in water for 4 hours for imbibition prior placing them in Distilled Water Agar plates (DWA). Plates were covered in foil and placed at 4 °C for 4 days to synchronise germination.

2.1.2 Plant growth conditions

For phenotypic characterization and nodulation assays plants were grown in square plates containing Buffered Nodulation Medium (BNM) or Fahraeus plant medium (FP) supplemented with 1 µM L-α-(2-aminoethoxyvinyl)-Gly (AVG) in control environment chambers with 16h light/ 8h dark photoperiod (irradiance=418 µmol m⁻²s⁻¹) and 21°C/16°C day-night temperature regime. For nodulation assays in the presence of nitrate, Potassium Nitrate to a final concentration of 2 mM and 5mM was added to BNM media. *S. meliloti* strain 1021 pXLGD4 lacZ reporter was used for all the infection and nodulation assays. All recipes used in this work can be found in Table 2.1.

2.1.3 Generation of *M. truncatula* transgenic roots by *A. rhizogenes*

Seeds were sterilised as described above and let vernalize for 7 days. The day before transformation plates were kept at RT in an inverted position overnight. Under sterile conditions, germinated seeds were submerged in sterile water to avoid damaging the root tip prior transformation. A sterile scalpel was used to remove the root tip and the remaining seedling was dipped in the *Agrobacterium*

rhizogenes suspension. A total of three rows of 10 seedlings each were placed in squared plates containing FP medium and left in horizontal position and covered in foil overnight. The plates were then kept upright in controlled environment chambers for 7 days, covering the plates with blue paper to avoid direct exposure to light. Untransformed roots were cut and discarded and plants were transferred to fresh FP plates and let grown for three weeks before selection. For selection purposes, only plants expressing dsRED fluorescence or others fluorescence signals were transferred to fresh media (FP+AVG) or soil (sand+terragren) for further experiments.

2.1.4 Plant growth media

Recipes of plant growth media used in this work (Table 2.1).

Table 2.1-Recipe of plant growth media used in this work

| Media | Recipe for 1 L |
|-----------------------------------|--|
| DWA | 10 g Plant Agar (Sigma A4675) |
| Fahraeus plant | 0.1 g CaCl ₂ . 2H ₂ O, 0.12 g MgSO ₄ , 0.01g KHPO ₄ , 0.150 g NaHPO ₄ .12H ₂ O, 5 mg ferric citrate, 2.86 g H ₃ BO ₃ , 2.03 g MnSO ₄ , 0.22 g ZnSO ₄ .7H ₂ O, 0.08 g CuSO ₄ .5H ₂ O, 0.08 g H ₂ MoO ₄ .4H ₂ O, pH 6.3-6.7. For solid medium 0.5% (w/v) Plant agar (Sigma A4675) was added. pH 6 |
| Buffered Nodulation Medium | 390 mg MES, 344 mg CaSO ₄ .2H ₂ O, 0.125 g KH ₂ PO ₄ , 122 mg MgSO ₄ .7H ₂ O, 18.65 mg Na ₂ EDTA, 13.9 mg FeSO ₄ .7H ₂ O, 4.6 mg ZnSO ₄ .7H ₂ O, 3.1 mg H ₃ BO ₃ , 8.45 mg MnSO ₄ .H ₂ O, 0.25 mg Na ₂ MoO ₄ .2H ₂ O, 0.016 mg CuSO ₄ .5H ₂ O, 0.025 mg CoCl ₂ .6H ₂ O, pH 6.5. For solid medium 10 % (w/v) Plant agar (Sigma A4675) was added. pH 6 |

| | |
|---|--|
| Fahraeus Media supplemented with Nitrate | Fahraeus Media as above, KNO ₃ to 2mM or 5mM |
|---|--|

2.2 Bacterial Methods

2.2.1 Bacterial strains

Escherichia coli cultures were grown at 37°C overnight at 250 RPM in 7-10 ml cultures in LB media supplemented with the corresponding antibiotic. *A. rhizogenes* strain AR1193 (Stougaard, 1987) was used for hairy root transformation of *M. truncatula*. *A. rhizogenes* was grown in TY medium containing Rifampicin (50 µM), Carbenicillin (100 µM) and vector specific antibiotic at 28°C as and 250 RPM required.

S. meliloti strain 1021 pXLGD4 lacZ was grown overnight at 28°C and 250 RPM in the presence of tetracycline (5 µM).

2.2.2 Plasmid preparation and bacterial transformation

Overnight grown cultures of *E. coli* expressing the vector of interest were used to isolate the plasmid by the alkaline lysis method using the Qiagen Miniprep kit following manufacturer instructions.

E. coli and *Agrobacterium* cells were transformed by electroporation. In individual sterile cuvettes (Molecular Bioprobes 5510-11), 40 µl of competent cells and around 100 ng of plasmid were added. The current was applied at 2V for 10 seconds and sterile LB media added immediately after the shock. Transformed cells were recovered for 1 hour at 37°C in the case of *E. coli* and 2 hours at 28°C in the case of *Agrobacterium* cells. Cells were then plated on LB or TY medium respectively with appropriate antibiotics.

2.2.3 Growth curve

A preculture of *S. meliloti* was grown overnight in TY medium in presence of tetracycline at a final concentration of 500 µg/ml. When the OD₆₀₀ reached between 0.5 and 0.7 the culture was diluted to OD₆₀₀ 0.001 in TY media. 40 µl of

the bacterial dilution was added to 360 μ l of TY media with the appropriate inhibitor: 100 μ M DDG (Sigma D8375), 100 mM MgCl₂, water as a control for the solvent and TY alone. TY without bacterial inoculation was used as negative control. A 48 well plate was used (Cellstar) in a TECAN Infinite 200 (LifeSciences), and media for each condition was delivered in a randomised fashion to avoid mismeasurement from the machine. The absorbance was taken at 600 nm every 2 hours for 66 hours until the stationary phase was reached. The data was exported to GraphPad Prism 7 and the Log (10) of the average of all replicates per treatment used as each data point.

2.2.4 Bacterial growth media

Recipes of bacterial growth media used in this work (Table 2.2)

Table 2.2-Recipe of bacterial growth media used in this work

| Media | Recipe for 1 L |
|-----------|--|
| LB | 10 g Tryptone, 5 g Yeast Extract, 10 g NaCl. For solid media 10g, Bactoagar (Sigma 05040) was added. pH 7 |
| TY | 5 g Tryptone, 3 g Yeast Extract, 1.32 g CaCl ₂ 6H ₂ O. For solid media 10g, Bactoagar (Sigma 05040) was added |
| MM | 1 g MgSO ₄ 7H ₂ O, 2.2 g CaCl ₂ 6H ₂ O, 2.2g g K ₂ HPO ₄ , 0.2g FeCl ₃ , 10 ml 3% Mannitol, 1.1 g NaGlu, 0.5 mg Biotin, 0.5mg Thiamine, 0.5 mg Pantothenic Acid |

2.2.5 Nodule occupancy assay

Nodules were excised from each transgenic root and were surface-sterilized in 12% hypochlorite, followed by five washes in sterile water under sterile conditions. Nodules were crushed individually in 1 ml of sterile water. The suspension was plated on TY plates and was incubated at 28°C for 48 h. The same procedure was followed to use it to inoculate wild-type seedlings grown on BNM plates.

2.3 Microscopy Methods

2.3.1 Confocal Microscopy

Confocal analysis was performed on a Zeiss LSM700 Inverted and LSM800 Upright microscope using a 488 nm excitation laser for Alexa-488 and GFP. Emission was collected using the filters: BP 505–530 for GFP, the DAPI filter for Calcofluor (463 nm) and LP 615 for Pontamine Red staining. The images correspond to individual stacks of z- optical sections.

2.3.2 Light Microscopy

Light Microscopy Imaging was performed on a Zeiss AX10 light microscope and a Brunel Microscope Ltd BSR stereomicroscope. Pictures were taken with an Olympus -BH2 fitted with a QIMAGING camera (Canada).

2.4 Molecular Biology Methods

2.4.1 Standard PCR

Standard PCR was performed using Thermo 3 Prime in 0.2 ml PCR tubes with a final volume of 20 μ l. dNTPs were added to a final concentration of 10 μ M and MgCl₂ to 1.5mM. Reactions were run in a thermocycler with the following conditions (Table 2.3):

Table 2.3-Standard PCR reaction conditions

| Temperature | Time | Cycles |
|-------------|--------------|--------|
| 95°C | 2 minutes | 1 |
| 95°C | 0.5-1 minute | |
| 60-65°C | 0.5-1 minute | 25-35 |
| 72°C | 1 min/kb | |
| 72°C | 10 minutes | 1 |

2.4.2 Agarose gel electrophoresis

Nucleic acids were resolved by running the samples on 0.8-1% agarose gel at 70V in 1X TAE Buffer (tris-Acetate EDTA) and a final concentration of SYBR Safe of 1X (Invitrogen). Gels were photographed using SynGene GBox transilluminator and pictures analysed using GeneSys software.

2.4.3 Golden Gate designs and cloning system

Promoters and the genes necessary for generation of vectors mentioned were synthesised by GenScript. These include the sequences corresponding to the genes PdBG1 (At3g13560) and fragments for fusion constructs. To generate level 1 vectors 100 ng of the linearized backbone and equimolar amounts of each assembly pieces vectors were added to 15 µl total reaction volume (Table 2.4).

Table 2.4: Standard reaction mixture for GoldenGate cloning system

| |
|---|
| 100 ng backbone vector |
| Equimolar amount of each assembly piece |
| 1x NEB T4 Buffer |
| 1x BSA |
| 10 units <i>BsaI/BpiI</i> |
| 400 units T4 ligase |
| Water to 15 µl |

The tube was placed in a thermocycler and cycling parameters setup as follows: (37°C/ 3min//16°C/4min) x25 cycles (50°C/5min/80°C/5min) x1 cycle. 2 µl of the assembly reaction was transformed into 40 µl of competent *E. coli* cells. Colonies were checked using colony PCR and sequencing. Positive colonies were used to generate level 2 vectors using the same protocol replacing *Bsal* with *Bpil* restrictions enzyme. Selection of positive colonies was based on red/white phenotype, being the negative colonies red. Maps of the tagged version of the vector (Figure 2.1) and untagged versions of the construct (Figure 2.2) were generated.

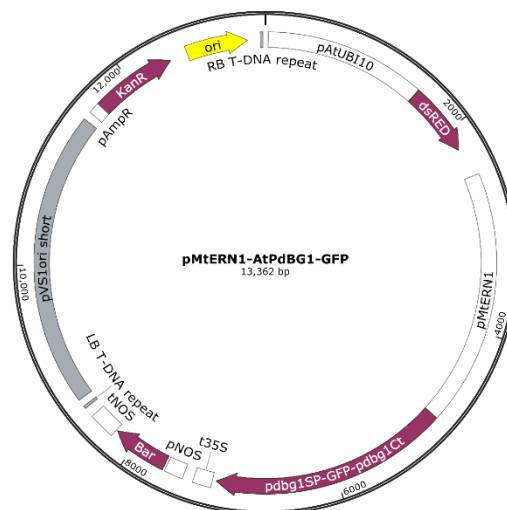


Figure 2.1- Map of the pMtERN1-PdBG1-GFP vector. A final binary vector carrying PdBG1 signal peptide (pdbgSP), GFP and PdBG1 C-terminal parts of the gene (PdBG1) driven by 2400 bp from the *MtERN1* promoter. The vector includes dsRED driven by the ubiquitin promoter (pAtUBI10) as a marker for transgenic root selection.

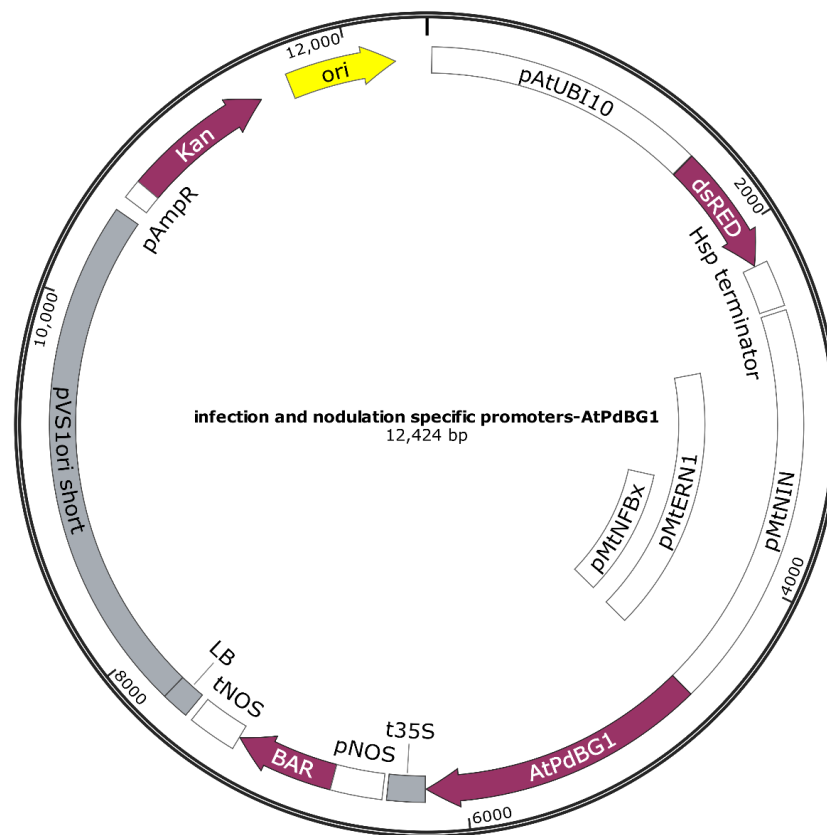


Figure 2.2- Map of the untagged vectors generated with specific infection and nodulation promoters *MtNFBx*, *MtERN1* and *MtNIN*. A final binary vector carrying PdBG1 gene driven by 2400 bp from the *MtERN1* promoter, 178 bp from the *MtNFBx* and 2180 bp from the *MtNIN*. The vector includes dsRED driven by the ubiquitin promoter (pAtUBI10) as a marker for transgenic root selection.

Constructs were obtained by GoldenGate cloning system (Engler et al., 2008), and contained the promoters of interest driving PdBG1 and the red fluorescent protein from the coral *Discosoma* (dsRED) driven by the ubiquitin promoter (Zhang et al., 2015). Constructs were transformed via *A. rhizogenes* in *M. truncatula* roots and transgenic roots were selected based on dsRed fluorescence. Vectors generated by GoldenGate are listed in Table 2.5.

Table 2.5: List of vectors generated by GoldenGate in this study

| Vector generated | Purpose/Description |
|----------------------------|---|
| <i>pMtERN1-AtPdBG1-GFP</i> | Cellular localisation and nodulation assays |
| <i>pMtNIN-AtPdBG1</i> | Nodulation assays |
| <i>pMtNFB-AtPdBG1</i> | Nodulation assays |
| <i>pMtERN1-AtPdBG1</i> | Nodulation assays |

2.4.4 Primer design

Primers were designed to confirm correct assembly of GoldenGate modules. Primers were designed using primer3 software (<http://primer3.ut.ee>). Sequences of primers of target genes are listed in Table 2.6.

Table 2.6: List of primers used in the generation or confirmation of GoldeGate clones

| Primer name | 5' to 3' primer sequence | Purpose | Target |
|--------------------|--|------------------------------------|--------------------------|
| PdBG1-C-Rv | CAG TGC CAA TGT TTA CAC CGA TA | Cloning confirmation/sequencing | At3g13560 |
| MtERN1-Fw | CTC ATA GCT TGC AAA TTA CAA CAT | Cloning confirmation/sequencing | EU038802(gene) |
| MtNIN-Fw | CGT ACG TGT TCT CCT CAA CTA C | Cloning confirmation/sequencing | Medtr5g099060(gene) |
| NFBx4-Fw | CGC TGA GCT CGA ATT CTA GTG | Cloning confirmation/sequencing | Synthetic NFB promoter |
| Right Border-Fw | GAT AAA CCT TTT | Cloning confirmation/sequencing | Backbone EC50505 pL2V |

| | | | |
|--------------------|-------------------------------------|------------------------------------|--------------------------|
| | CAC GCC CTT TTA | | |
| Left Border- Rv | CTG CCT GTA TCG AGT GGT GA | Cloning confirmation/sequencing | Backbone EC50505 pL2V |

2.4.5 Gateway designs and cloning system

Gateway cloning system is based in site-specific recombinases that catalyse the recombination of two DNA segments that carry specific and complementary sequences (Katzen, 2007). To create entry clones the target genes or gene fragments were amplified using primers containing the compatible adapters.

Primers were designed to amplify target genes *MtBG2* and *MtPDLP1* to generate fusion proteins with fluorescent proteins. In the case of Medtr3g083580, an internal fusion was required since the protein has a signal peptide and a GPI anchor, both needed for proper localisation and function of the protein. For that purpose, C-terminal and N-terminal section of the protein was amplified separately and cloned into different donor vector. In the case of Medtr1g073320, the whole protein was amplified in one single PCR reaction and cloned into the donor vector.

Amplification was purified by gel extraction using Qiagen Gel Extraction Kit (ID: 28706) and following the manufacturer's instructions and cloned into either pDONR201 or pDONR207 backbone. Ligation reaction with 1 µl BP clonase was incubated overnight at 25°C and stopped by adding 1 µl Proteinase K (Invitrogen). 1 µl of the ligation reaction was used to transform 50 µl of electrocompetent *E.coli* cells. Colonies were checked by PCR and positive colonies confirmed by sequencing. Confirmed positive clones were used for LR reaction, around 150 ng of each entry clone and destination vector was added to a PCR tube along with 1 µl of LR clonase to a maximum volume of 5 µl. The reaction was incubated at 25°C overnight. 1-2 µl of the reaction was used to transform electrocompetent *E.coli* cells. Colonies were screened by colony PCR and confirmed by sequencing. Gateway vectors used and generated are listed in Table 2.7 and Table 2.8 and schematized in Figure 2.3.

Table 2.7: List of Gateway vectors used in this study

| Vector used | Purpose/Description | Reference |
|-----------------------------|---|--------------------------------|
| pDNOR201 | Entry vector | Invitrogen® |
| pDNOR207 | Entry vector | Invitrogen® |
| pB7YWG2 | Destination, Binary vector, YFP tag at C-terminal | (Karimi et al., 2005) |
| pB7WG | Destination, Binary vector | Invitrogen® |
| p35s-PdBG1- <i>mcitrine</i> | Cellular localisation and nodulation assays | (Benitez-Alfonso et al., 2013) |

Table 2.8: List of expression vectors generated and used in this study

| Vector generated | Purpose/Description |
|--------------------------|---|
| <i>pUb-MtBG2-mcherry</i> | Cellular localization and nodulation assays |
| <i>p35s-MtPDL1-YFP</i> | Cellular localization and nodulation assays |

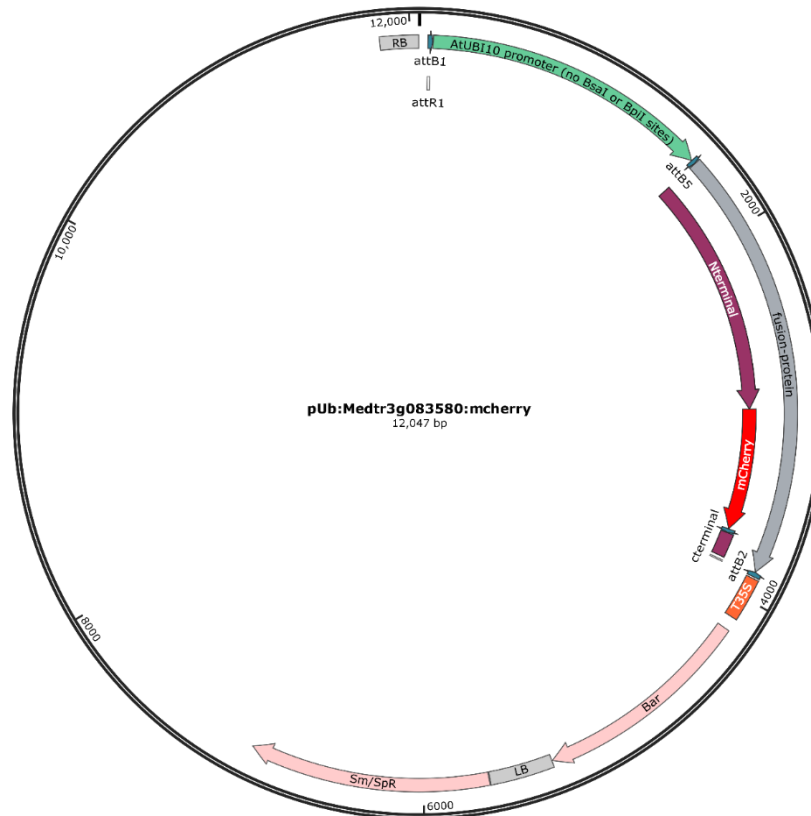


Figure 2.3- Map of *pUb-MtBG2-mcherry* vector generated by Gateway cloning system. A final vector carrying *MtBG2* Nt, mcherry fluorescent protein and *MtBG2* Ct driven by the Ubiquitin promoter (AtUB10).

2.4.6 Primer design

Primers were designed to amplify target genes with the necessary adapters. Primers were designed using primer3 software (<http://primer3.ut.ee>). Sequences of primers of target genes are listed in Table 2.9.

Table 2.9: List of primers used in the generation of clones by Gateway system. Adapters for Gateway donor vectors are underlined.

| Primer name | 5' to 3' primer sequence | Target |
|----------------|--|--|
| MtBG2-ATTB2 | <u>GGG GAC CAC TTT GTA</u> <u>CAA GAA AGC TGG GTT</u> TTA CAA CAT CAA AGC CAA AAG TAG | Medtr3g083580 |
| MtBG2-ATTB3 | <u>GGG GAC AAC TTT GTA</u> <u>TAA TAA AGT TGT AAC</u> TGG CGG TGA TGG GAG C | Medtr3g083580 |
| MtBG2-ATTB4 | <u>GGG GAC AAC TTT GTA</u> <u>TAG AAA AGT TGG GTG</u> GCT CAA GTT AGA ACT TCC TGC AT | Medtr3g083580 |
| MtPDLP1-ATTB5r | <u>GGG GAC AAC TTT GTA</u> <u>TAC AAA AGT TGT AAT</u> GAA GCT TCA AAA ATG GCT CAC | Medtr3g083580 |
| MtPDLP1-ATTB1 | <u>GGG GAC AAG TTT GTA</u> <u>CAA AAA AGC AGG CTC</u> CAT GTT TTG ATT CTC TCT CCA | Medtr1g073320 |
| MtPDLP1-ATTB2 | <u>GGG GAC CAC TTT GTA</u> <u>CAA GAA AGC TGG GTA</u> CCA CAA ATC TCT TTC AGC CAA AA | Medtr1g073320 |
| PUBIQ-ATTB1 | <u>GGG GAC AAG TTT GTA</u> <u>CAA AAA AGC AGG CTT</u> AGT CGT TGT GGT TGG TGC TTT | Ubiquitin promoter from Arabidopsis |
| PUBIQ-ATTB5r | <u>GGG GAC AAC TTT TGT</u> <u>ATA CAA AGT TGT TCT</u> GCA TCT GTT AAT CAG AAA AAC T | Ubiquitin promoter from Arabidopsis |

2.4.7 Quantitative Real-Time Reverse Transcription PCR

2.4.7.1 Primer design

Primers were designed to amplify around 200 bp of target genes. Primers were designed using primer3 software (<http://primer3.ut.ee>). Sequences of primers of target genes and housekeeping genes are listed in Table 2.10.

Table 2.10: Primers used in QPCR and RTPCR assays

| Primer name | 5' to 3' primer sequence |
|------------------|----------------------------------|
| QPCR-MtBG2-Fw | TGG TGG AAC TTG CGA CTT TG |
| QPCR- MtBG2-Rv | AGG GTA GAC ACT TGC AGG TT |
| QPCR- MtBG2-Fw | TGC AGC TAT TCA AGC AGG GA |
| QPCR- MtBG2-Rv | CCG CCA GTG CTC AAG TTA GA |
| QPCR-MtBG5-Fw | TGT TCT TTG TTG CAG GGA |
| QPCR-MtBG5-Rv | GAG CAG GGG CGT TAG AGA AG |
| QPCR-UBIQ-Fw | GCA GAT AGA CAC GCT GGG A |
| QPCR-UBIQ-Rv | AAC TGG GCA GGC AAT AA |
| RTPCR-MtACTIN-Fw | GAC AAT GGA ACT GGA ATG GTG |
| RTPCR-MtACTIN-Rv | CAA TAC CGT GCT CAA TGG GG |
| RTPCR-MtBG1-Fw | GCT CCT ATT CAA CAA GGA CAG C |
| RTPCR-MtBG1-Rv | GGG ACT TGA AGA AGG TCC AA |
| RTPCR-MtPDLP1-Fw | GGT TCC AAA GGG TGG TCA CT |
| RTPCR-MtPDLP1-Rv | GGC CTC CAC AGT AAA CCA TAT |

2.4.7.2 RNA extraction and cDNA synthesis

M. truncatula roots were spot inoculated and a window of 1 cm of root containing the inoculation point were collected at different time points and immediately frozen in liquid nitrogen. The samples were ground in liquid nitrogen in a chilled

mortar. RNA was extracted using the RNeasy Plant Mini Kit following the manufacturer's instructions (Qiagen, France). Quality and concentration of RNA were evaluated by electrophoresis and NanoDrop® Spectrometer ND-1000.

1 µg of RNA was used per sample to synthesise cDNA using SuperScript II (ThermoFisher-18064014) following manufacturer's protocol.

2.4.7.3 RT-PCR analysis

cDNA synthesised was used in standard PCR reactions to semi-quantify transcription. Primers were designed to amplify around 200 base pairs. Actin was used as internal housekeeping gene.

2.4.7.4 QPCR

Real time qPCR was carried out in a CFX Connect™ Real-Time PCR Detection System using CFX96 Touch™ program for recording the results (Bio-Rad). SYBR green was used for quantification of dsDNA synthesis during amplification. Reactions were carried out on whit optical 96 well plates. 3 wells were used per condition. The wells were as follows: 10 µl SYBR Green Jumpstart Taq ReadyMix for qPCR (Sigma), 2 µl cDNA (50ng), 1 µl of 10 µM gene specific forward primer and 1 µl of 10 µM gene specific reverse primer, and 6 µl of nuclease-free water (20 µl total volume)(Table 2.11).

Table 2.11 CFX96 Touch™ program setting designed for optimal output and used in PCR cycling for the QPCR analysis.

| | | |
|--|------|---------|
| 1 Cycle: | | |
| Initial Denaturation | 94°C | 2 mins |
| 40 Cycles: | | |
| Denaturation | 94°C | 15 secs |
| Annealing, Extension and Read Fluorescence. | 57°C | 1 min |

2.4.7.5 Relative Gene Expression Analysis

The relative gene expression levels were calculated using the comparative Ct ($\Delta\Delta\text{Ct}$) method (Schmittgen and Livak, 2008). The range for relative target gene expression, relative to the control calibrator sample, is calculated by: $2^{-\Delta\Delta\text{Ct}}$, where Ct represents the threshold cycle, with $\Delta\Delta\text{Ct} + s$ and $\Delta\Delta\text{Ct} - s$, where s is the standard deviation of the $\Delta\Delta\text{Ct}$ value.

2.5 Phenotyping *M. truncatula* roots development

2.5.1 2-Deoxy-D-glucose (DDG) treatment

100 μM DDG (Sigma D8375) diluted in water was used to treat 5 day-old wild type *M. truncatula* plants either 24 hours prior infection or during the inoculation process. In the case of transgenic roots, the treatment was applied 14 days after transformation. The treatment was delivered by placing a DDG soaked filter paper on top of the roots while growing in plates and removed prior the infection.

2.5.2 Root hair length measurement

Root hair length was measured using the Zeiss LSM700 Inverted Confocal Microscope and the ImageJ software. *Medicago* seeds were germinated and described above and seedlings were placed in plates with the treatment or water as a control between filter paper. Seedlings were allowed to grow for 5 days before imaging. To measure root hair length seedlings were imaged and root hairs measured using ImageJ. At least 3 seedlings were imaged for each condition. Average of all root hairs contained in the image was used to determine the difference.

2.5.3 Root length, weight and width measurement

Root length and width were measured using a D5200 Nikon Camera and ImageJ software. The widest point of the root was measured for width estimation.

2.6 Nodulation and infection assays

2.6.1 β -Galactosidase staining

M. truncatula roots were infected with *S. meliloti* strain 1021 pXLGD4 *lacZ*. Roots at different infection stages were fixed in Z buffer 2.5% Glutaraldehyde for 30 min under vacuum and further incubated for 1 hour. Roots were then trough fully washed with Z-Buffer. Roots were incubated at 30 °C for 4 hours (or until visible staining is seen) in staining solution. For 1 mL of staining solution, 50 μ l of 100 mM potassium ferrocyanide and potassium ferricyanide were added and 16 μ l of 50 mg/ml of X-gal in DMF (Promega) was made up in Z-buffer. Staining reaction was stopped by washing roots with Z-Buffer. The roots were then analysed under a microscope and the number of infection threads, infection pockets and nodule primordia quantified and/or imaged.

2.6.2 Flood infection in plates

For flood infection, 10 ml of liquid TY medium is inoculated with a single colony and grown overnight. The culture is pelleted, washed twice with 10 mM MgCl₂ and resuspended in 10 mM MgCl₂ to a final OD₆₀₀ of 0.05.

2.6.3 Spot inoculation

100 ml of liquid MM medium is inoculated with a saturated *S. meliloti* culture to a final OD of 0.007 and incubated for 16 hours. A final inoculum is prepared in FP (Fahraeus, 1957) medium to a final OD of 0.02. One single drop is deposited in the infection zone of the root (Figure 2.4) with Microloader tips (5242956003, Eppendorf). Plates were maintained in horizontal position for several minutes before sealing them with Micropore tape (3M) and cover the roots with foil.

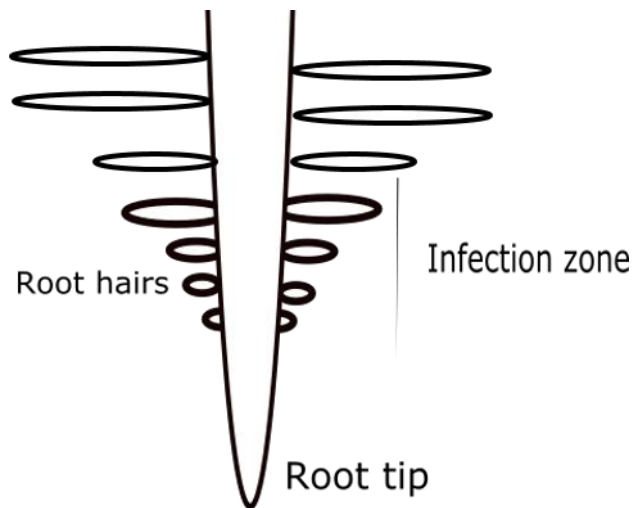


Figure 2.4: Drawing showing infection zone in a *M. truncatula* root. The infection zone is where root hairs start to develop and are susceptible to infection by rhizobia.

2.6.4 Infection in soil

Transformed *Medicago* roots growing in soil were infected ten days after the transplant with 1 ml of a saturated *S. meliloti* resuspension in water to a final OD₆₀₀ of 0.02-0.03.

2.6.5 Counting Infection Threads, Infection Pockets and Nodule Primordia

After lac Z staining infection threads, nodule primordia and older nodules were visualised and counted using a Zeiss Axio Scope.A1 and imaged using an Olympus -BH2 fitted with IMAGING camera (Canada). All nodule and nodule primordia were counted for the total number of nodule counting, but only nodules and nodule primordia showing blue staining were considered as 'infected' or 'colonised'. The ratio between blue nodules and the total number of nodules is the percentage of colonised nodules. All infection threads and infection pockets including the ones leading to a nodule primordia/ mature nodule were counted for the total number.

2.6.6 Assaying nodulation in soil

Composite plants were grown in a mixture of equal amounts of sand and terra green for 10 days before inoculation. For inoculation 1 ml of a saturated culture

of Sm1021 pXLGD4 (lacZ) at an OD₆₀₀ 0.05 per pot was used. Control plants were inoculated with 1 ml of water. Plants were watered as needed for 2 weeks after infection before harvesting the roots and assaying nodulation. The total number of mature nodules per composite plant were counted.

2.7 Phylogenetic and structural analyses of proteins

2.7.1 Retrieval of β -1,3-glucanases, GSL and PDLP-like sequences and analysis of protein domains

Isolation of sequences containing the β -1,3-beta glucosidase domain (GHL17) from *M. truncatula* and *A. thaliana* was performed as described in Gaudioso-Pedraza and Benitez-Alfonso, 2014. Only protein sequences containing the GHL17 domain (confirmed in SMART) and predicted to be complete were considered. To eliminate redundancies sequences obtained for each organism were aligned using MUSCLE (Edgar, 2004). The sequences were screened for characteristic features of this family, signal peptide (SP), glycosylphosphatidylinositol anchor (GPI) and carbohydrate-binding module (X8) in the case of GHL17, using the prediction programs SMART, SignalP 4.1 Serve, Phobius, GPI-SOM, FragAnchor, PredGPI and BIG-PI respectively (Eisenhaber et al., 2003; Fankhauser and Maser, 2005; Poisson et al., 2007; Pierleoni et al., 2008; Letunic et al., 2012). Sequences isolated are available in Appendix 1.

The same process was followed to retrieve orthologues of CALS and PDLP *Arabidopsis* family in *M. truncatula*. CALS proteins are characterised for their glucan-synthase domain. Sequences isolated are available in Appendix 2. On the other hand, PDLPs have a DUF26 domain and a transmembrane domain. Sequences isolated are available in Appendix 3

2.7.2 Alignments and phylogenetic analysis

All sequences isolated were aligned using Muscle 58 and phylogenetic trees calculated as described in Gaudioso-Pedraza and Benitez-Alfonso, 2014. The best model under the Akaike Information Criterion was LG+G. Majority-rule consensus trees convergence was reached after 90000 generations in all cases.

The trees were visualised using the software Figtree (<http://tree.bio.ed.ac.uk/software/figtree/>) and edited using TreeGraph2 (Stover and Muller, 2010). Trees generated are available in newick format in Appendices 10 to 18.

2.7.3 Selection of candidates

M. truncatula glucanases and PDLP that localised in the same clade as plasmodesmata Arabidopsis proteins were identified. Transcriptomic analyses available in The *Medicago truncatula* Gene Expression Atlas ((Benedito et al., 2008) were consulted. Candidate genes were further selected based on their expression pattern based on the following criteria: response to 1, 2, 3 or 5 dpi in root hairs, response to Nod factor treatment and/or lack of differential expression when infected with rhizobia mutants.

2.8 Biochemistry Methods

2.8.1 Immunolocalisation

2.8.1.1 Sample preparation

M. truncatula roots were cut into 1-2 cm pieces (to improve fixative infiltration) and fixed in 4% paraformaldehyde in PBS buffer at pH 7.0 and supplemented with 0.01% Triton-100. Ascending ethanol: water series (10:90, 30:70, 50:50 70:30 and 90:10) were used to dehydrate the samples. Samples were stained with a 2% eosin solution to facilitate sample positioning during embedding and sectioning. Wax embedding and sectioning

Samples are incubated overnight in a 1:1 solution paraffin wax (VWR) and ethanol at 37°C. Wax: ethanol is removed and replaced by 100% fresh wax and further incubated overnight at 37 °C. Wax was changed twice per day for at least 5 days. Roots were then oriented, taking care of avoiding bubbles. Sections of 10 µm were collected using a Rotatory Microtome HM 325 (MICROM) and recovered in polylysine slides (VWR International). Sections were stored at -20°C for further experiments.

When hand sections were needed, roots were sectioned with a razor blade (Wilkinson), exposing the inner tissue and were let dry for two hours at room temperature before immunolocalization.

2.8.1.2 Callose immunolocalisation

A drop of cell-wall degrading enzyme (2% pectinase (Sigma), 0.01% pectolyase Y23 (Sigma) in PBS) was added to each section and incubated at 37 C for 30 min, the enzyme was then removed and the section washes 3 times with PBS. A 3% BSA in PBS solution was used to block sections for 1 hour. After removing the blocking solution (3 washes with PBS) sections were incubated overnight at 4 C with a dilution 1:400 of anticalllose antibody (Biosupplies). The sections were washed 6 times with PBS prior incubation with secondary antibody (Alexa -488 antimouse Invitrogen dilution 1:200) for 4 hours. Sections were then washed six times with PBS prior counterstaining with DAPI (1µg/ml) or Calcofluor (1mg/ml). Sections were covered in mounting solution and were ready to image.

2.8.1.3 Fluorescence quantification

For quantification, z-stacks confocal images of callose immunolocalisation roots were taken. At least 3 roots per condition were used for quantification experiments. A region of interest of around 100 µm² was drawn in comparable areas of the root in every one of the stacks of each picture. Fluorescence intensity analysis was performed using ImageJ software (ImageJ, U.S. National Institutes of Health, Bethesda, MD; imagej.nih.gov/ij/). The integrated density was corrected for background differences by dividing the measured intensities with the average intensity of a cell-free region. Integrated density was averaged for all stacks and roots per conditions.

2.8.2 Aniline blue staining

Aniline blue was used to stain callose at the cell wall in whole roots. Roots were cut and rapidly submerged in 0.01% (w/v) aniline blue in phosphate buffer (pH 8) and incubated for 15 min under vacuum. Roots were then incubated in aniline blue solution overnight wrapped in foil at RT. Before imagining roots were washed thoughtfully with water.

2.8.3 Histochemical localisation of GUS

To localise spatial and temporal gene expression pattern *M. truncatula* plants expressing the transgene *pENOD11-GUS* were spot inoculated and samples taken at different time points. Plants were fixed in ice-cold 90% acetone in 15ml tubes for 30 min. Plants were then cover in GUS staining solution (50mM Sodium Phosphate pH 7, 0.5 mM potassium ferrocyanide, 0.5 mM potassium ferricyanide and Triton X-100 at 0.1 ml/100 ml) supplemented with 1mM 5-bromo-4-chloro-3-indolyl- β -D-glucuronic acid. Samples were incubated overnight at 37 °C in dark.

2.8.4 Toluidine blue staining

Wax sections of nodules were recovered in polylysine slides and dewaxed with increasing ethanol: water series. Sections were then submerged in a 5% toluidine blue solution until the tissue was stained (approximately 10 minutes). Sections were then washed several times with water.

2.9 Statistical analysis of the data

The significant differences between conditions were evaluated using the standard deviation of the mean (SDM) and P-values (Student's t-test). All data were analysed for normality using D'Agostino Pearson omnibus normality test. Differences were referred to as significant when *p-values*<0.05 and were all calculated using GraphPad Prism 7.

Data set were plotted using Box Plot where whiskers indicate maximum to minimum values, boxes delimit quartiles and central lines indicate the mean. Different letters were used to indicate statistically significant differences between datasets.

Normalised relative expressions and standard deviation were calculated using actin as an endogenous control using the Comparative Ct Method using Microsoft Excel Statistical package (Schmittgen and Livak, 2008) for QPCR experiments.

Chapter 3

Chapter 3 – Regulation of callose in cell walls of *M. truncatula* roots in response to rhizobia

3.1 Summary

The symplastic pathway is regulated during different processes of plant development to allow essential short and long distance signalling processes (Roberts and Oparka, 2003; Benitez-Alfonso et al., 2013; Stahl and Simon, 2013; Benitez-Alfonso, 2014). How this regulation is orchestrated remains not fully understood, but callose turnover at plasmodesmata has been shown one of the means by which symplastic connectivity is controlled. Callose degradation enhances cell-to-cell communication (Bucher et al., 2001; Rinne et al., 2005) and symplastic trafficking (Iglesias and Meins, 2000; Levy et al., 2007).

Previous research have shown that nodule formation in legumes is linked to a regulation of the symplastic pathway (Complainville et al., 2003). So far these changes have been associated with an increase in plasmodesmata density connecting the tissues but not with a regulation in callose (Complainville et al., 2003). Determining spatial and temporal changes in callose deposition in response rhizobia would help to discern the role of this polysaccharide in the regulation of the symplastic pathway during nitrogen-fixing symbiosis.

When nitrogen becomes available in the soil, legumes avoid interaction with rhizobia, the sites of infection are reduced and nodules formation is inhibited. Although the exact mechanism by which nitrogen regulates symbiosis is not fully understood, it is known to act both locally and systemically (Jeudy et al., 2010). Therefore, in this chapter is explored whether nitrogen would regulate callose deposition in roots, as a mechanism to affect colonisation by the bacteria.

This chapter focuses on the characterization of the role of callose during inoculation of *M. truncatula* roots with rhizobia in different growing conditions and the identification of potential callose modifying enzymes that might be regulating this process.

The sections 3.2.1 and 3.2.2 explore the levels of callose after inoculation in nitrogen-depleted conditions. Sections 3.2.2 and 3.2.4 refer to the identification of new *M. truncatula* plasmodesmata proteins potentially involved in callose regulation. Finally, sections 3.2.2.1 to 3.2.2.3 explore the role of callose in the inhibition of nodulation by nitrogen availability. The discussion section aims to bring together these results with current knowledge about the subject, as well as suggestions for future work.

3.2 Results

3.2.1 Immunolocalisation experiments show that callose is down-regulated after inoculation of *M. truncatula* roots with rhizobia

To determine if callose regulation correlates with rhizobia infection in *M. truncatula* roots, its deposition was immunodetected after spot-inoculation of the roots with mock (water) or with rhizobia. Sections of the root inoculated (a window of around 1 cm) with either mock (water) or rhizobia cultures were collected at two time points (16 h and 24 h post-inoculation). Callose antibody was used to detect the sites of deposition along the cell wall which were imaged using confocal microscopy as described in Materials and Methods. Images were used to quantify green fluorescence (using an Alexa 488-conjugate as secondary) to infer callose levels.

Callose appears strongly in inner root tissues of mock control roots (Figure 3.1-A). Punctate pattern of the signal was accumulated at the cortical, pericycle and endodermis cell layers, suggesting plasmodesmata labelling (Figure 3.1-G). Punctate signal is also present in the rhizobia-inoculated samples, but it appears reduced in comparison to mock-inoculated roots (Figure 3.1-D). Quantification of the fluorescence signal using ImageJ confirmed downregulation of callose at 16 and 24 hpi (Figure 3.2).

At this early stages of the infection process, the bacterial colonization of the host plant has not started, since infection threads typically appear between 24 and 36 hpi (Laplaze et al., 2015). Therefore, it is proposed that changes in the composition of the host plant cell walls occur prior bacterial infection, or even before root hair curling.

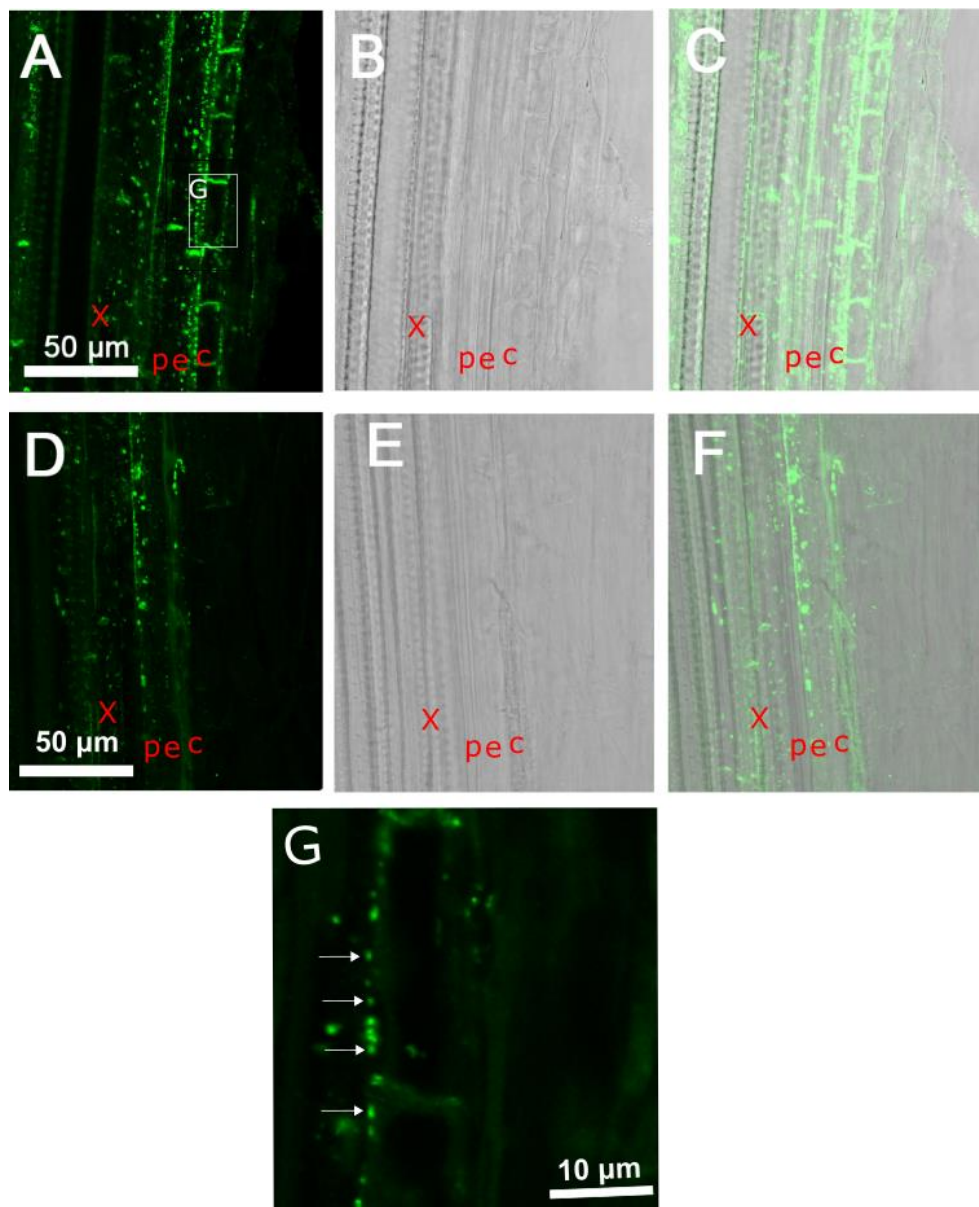


Figure 3.1- Callose levels are globally reduced 24 hours post-inoculation with rhizobia in *M. truncatula*. Immunolocalisation of callose revealed a down-regulation of the polysaccharide at the cell wall of *M. truncatula* roots spot-inoculated with rhizobia. Callose was detected using a monoclonal anti-callose antibody and an Alexa-488 (green) conjugated secondary antibody in longitudinal sections of roots 24 hours post inoculation with mock (water) (A to C) or rhizobia cultures (hpi) (D to F). Transmission light sections (B and E) are shown for signal co-localisation (C and (F). Callose signal is strongly visible in inner root tissues of control roots and reduced in the rhizobia-inoculated conditions. A close up of panel (A) is magnified in panel (G), showing plasmodesmata resembling punctated pattern (white arrows). Symbols in A to F refer to xylem vessel (x), pericycle (p), endodermis (e), and cortex (c). Panels C and F were brightened to improve signal localisation.

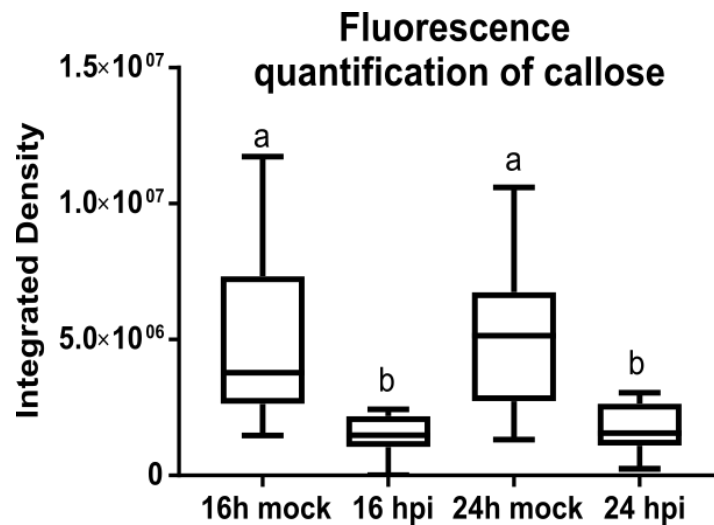


Figure 3.2- Callose is downregulated upon inoculation. Fluorescent immunolocalisation experiments using callose antibody were used to quantify callose levels at the cell wall at 16 hours and 24 hours post spot inoculation of *M. truncatula* roots with mock (water) and rhizobia cultures (hpi). Integrated density was calculated using ImageJ for each image in at least 3 roots per condition. Fluorescence was quantified in a region of interest of approximately 100 μ m². A Student's t-test was performed, different letters indicate significant differences ($p < 0.001$).

3.2.2 Callose regulation appears not to be essential for the inhibition of nodulation in nitrate conditions

3.2.2.1 Nitrate availability inhibits infection and nodule formation in *M. truncatula*

Symbiotic interactions and the formation of root nodules are a highly energetically demanding process, therefore must be tightly regulated. Plants regulate the number and location of new nodules by a diverse number of mechanisms (Reid et al., 2011b; Mortier et al., 2012; Bensmihen, 2015). Nitrate naturally available in the plant's surroundings is, unsurprisingly, one of the main signals that would determine the number of developed nodules (Carroll et al., 1985b; van Noorden et al., 2006). To verify the response of *M. truncatula* to nitrogen availability in our growing conditions, wild-type seedlings were grown in

FP medium plates with either depleted nitrate (no nitrate) or supplemented with 2mM KNO₃ or with 5mM KNO₃. Plants were inoculated with *S. meliloti* expressing the galactosidase gene and stained 7 dpi to identify infection sites and nodule primordia. *M. truncatula* plants showed a strong inhibition of both infection threads and nodule primordia under both concentrations of nitrate (Figure 3.3). 2 mM of nitrate appears to be enough to significantly inhibit symbiosis in *M. truncatula*. No significant differences in terms of root length could be seen between wildtype plants grown in no nitrate or nitrate supplemented media (Figure 3.4).

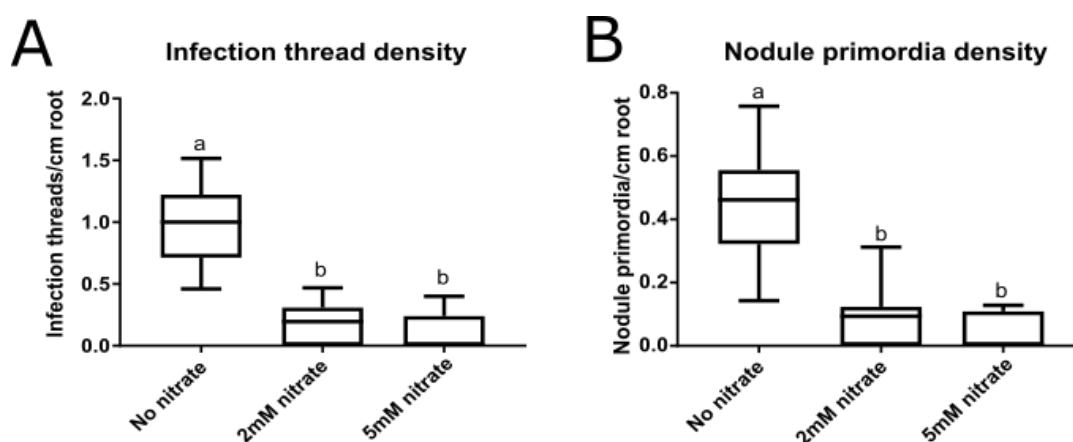


Figure 3.3- Nitrate inhibits nodulation and infection in *M. truncatula* roots.

M. truncatula plants were grown in the presence of 0, 2 and 5mM nitrate for 5 days prior to inoculation with rhizobia expressing the galactosidase gene. (A) 7 days post inoculation, roots were stained to dissect the number of infection threads. A significant decrease in the density of infection threads (number of infection threads and infection pockets/cm of root length) under these conditions was recorded. (B) 7 days post inoculation nodule primordia and young nodule number were counted. Nodule density decreased significantly in plants growing in plates with nitrate in the growth media. A Student's t-test was performed, different letters indicate significant differences ($p < 0.001$).

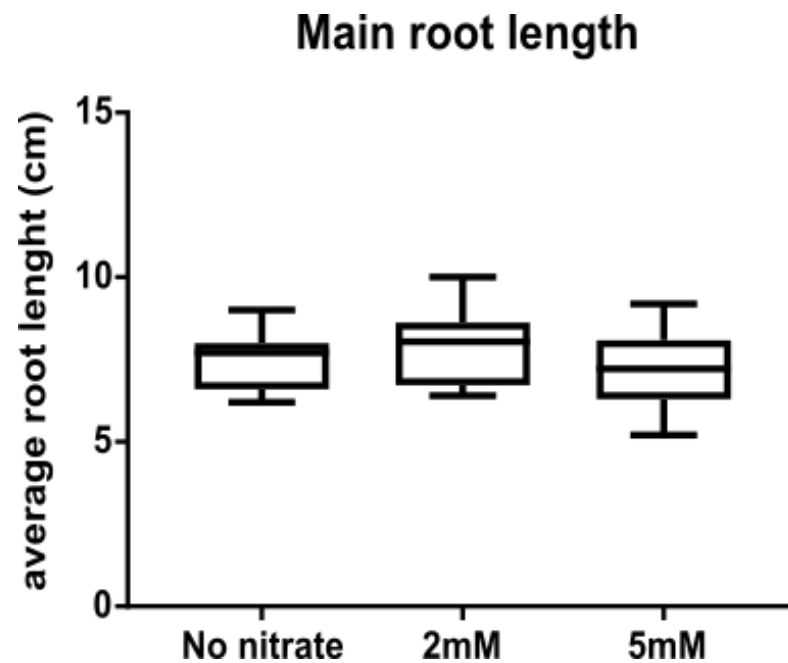


Figure 3.4- Nitrate does not have an effect in *M. truncatula* root length. Main root length of 12 day old *M. truncatula* growing in 2, 5 mM of nitrate and no nitrate, was measured. A Student's t-test was performed, no significant differences were seen ($p>0.05$).

3.2.2.2 Callose deposition in roots grown in the presence of nitrate and in no nitrate media do not appear significantly different

Callose is downregulated upon inoculation and potentially playing a role in the establishment of the symbiotic interaction (Figure 3.2). In order to assess whether callose also played a role in the root response to high nitrate, the callose content in roots grown under depleted (no nitrate) and added or full (2mM and 5mM KNO_3) nitrate conditions were compared. Wild-type *M. truncatula* seedlings were grown in nitrate conditions and aniline blue staining (Figure 3.5) and callose immunolocalisation (Figure 3.6) were carried out to compare callose levels. Quantification of fluorescence was measured in at least 3 roots per condition and method but no significant differences were observed (Figure 3.5-C and Figure 3.6-G). This suggests that callose turnover is not regulated by nitrate availability in the growth media and that potentially levels of callose in the root prior to inoculation is not a factor in the inhibition of nodulation by nitrate.

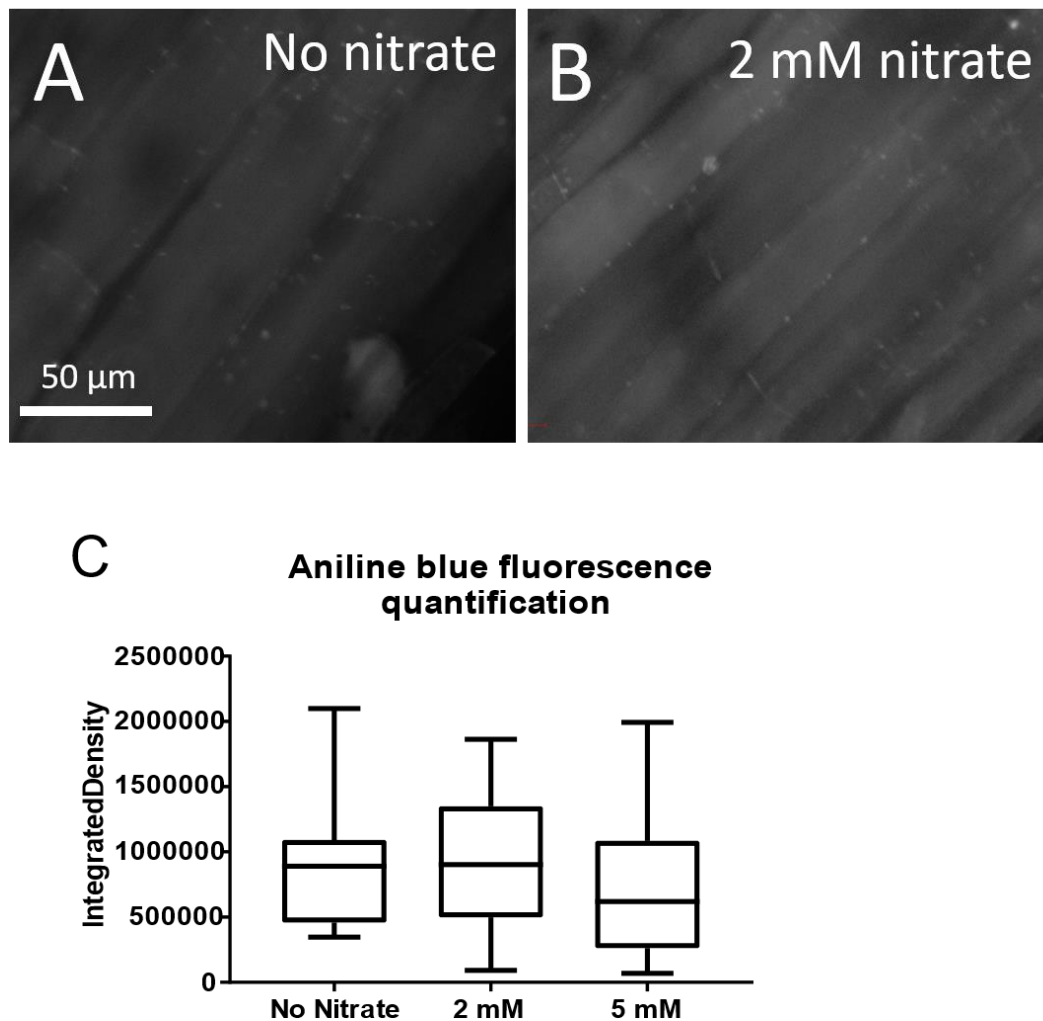


Figure 3.5- Aniline blue staining suggest that callose is not regulated by nitrate. Aniline blue was used to stain callose deposition (false coloured white) at plasmodesmata in wild-type *M. truncatula* roots growing in FP media and FP media supplemented with 2 mM and 5 mM KNO_3 . (A) Callose deposits in plants growing in nitrate-depleted media (FP) (B) Callose deposits in plants growing in FP media supplemented with 2mM KNO_3 . (C) Aniline blue fluorescence signal was measured by calculating integrated density using ImageJ for each image in at least 3 biological repetitions. The region of interest measured was approximately $100 \mu\text{m}^2$. A Student's t-test was performed, no significant differences were seen ($p > 0.05$).

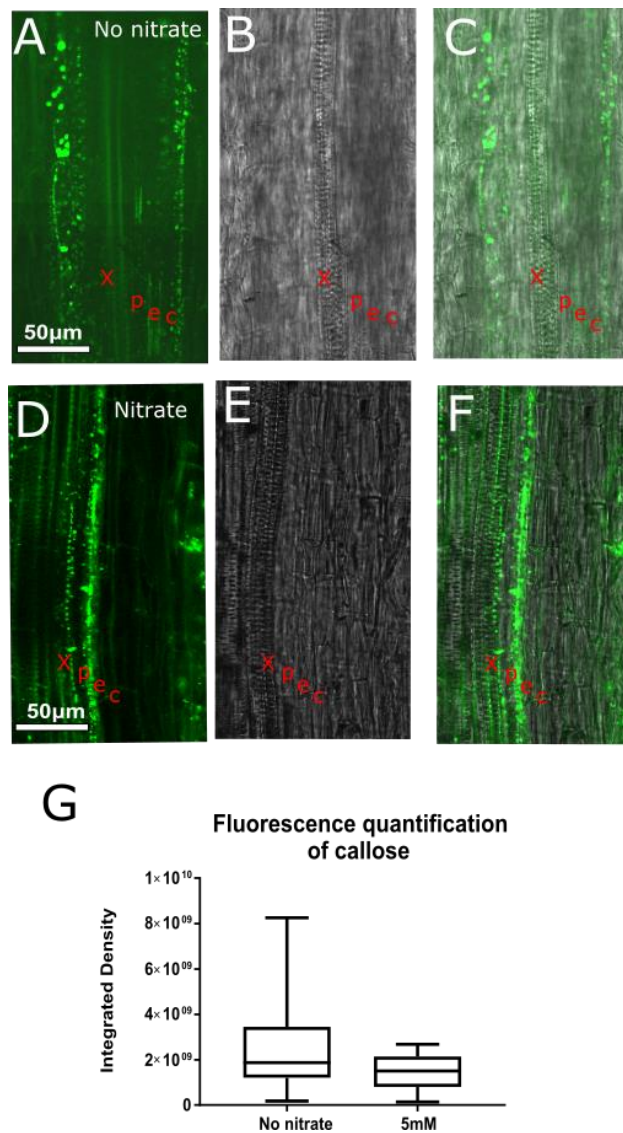


Figure 3.6- Immunolocalisation indicates that 5mM nitrate does not regulate callose in *M. truncatula* roots. Immunolocalisation of callose revealed that there is not a regulation of the polysaccharide due to nitrate availability. Callose was detected using a monoclonal antibody and Alexa-488 (green) conjugated antibody in *M. truncatula* roots longitudinal sections grown in no nitrate (A) and 5mM nitrate (D). Bright field (B and E) and composite images are shown for tissue localisation of the signal (C and F). (G) Fluorescence quantification of callose was performed by calculating the integrated density using ImageJ for each image in at least 3 biological repetitions per condition. Note that pictures do not show same sections of the roots. Fluorescence was quantified in a region of interests of approximately $100\mu\text{m}^2$. Symbols in A to F refer to, xylem vessel (x), pericycle (p), endodermis (e), and cortex (c). A Student's t-test was performed, no significant differences were seen ($p > 0.05$).

In order to determine whether callose downregulation reported after inoculation in nitrate-depleted conditions was maintained in nitrate media, *M.truncatula* transgenic roots expressing an empty vector were grown in media supplemented with 5 mM KNO₃ and inoculated with either water (mock) or rhizobia cultures. Roots were retrieved 24 hpi and used to localise callose deposits at plasmodesmata. Inoculation of *M. truncatula* roots with *S. meliloti* in the nitrate environment showed a reduction in callose deposition at the cell wall (Figure 3.7), resembling no nitrate conditions. This result supports the hypothesis that regulation of callose is not involved in the inhibition of rhizobia infection by nitrate at least at that time point post inoculation.

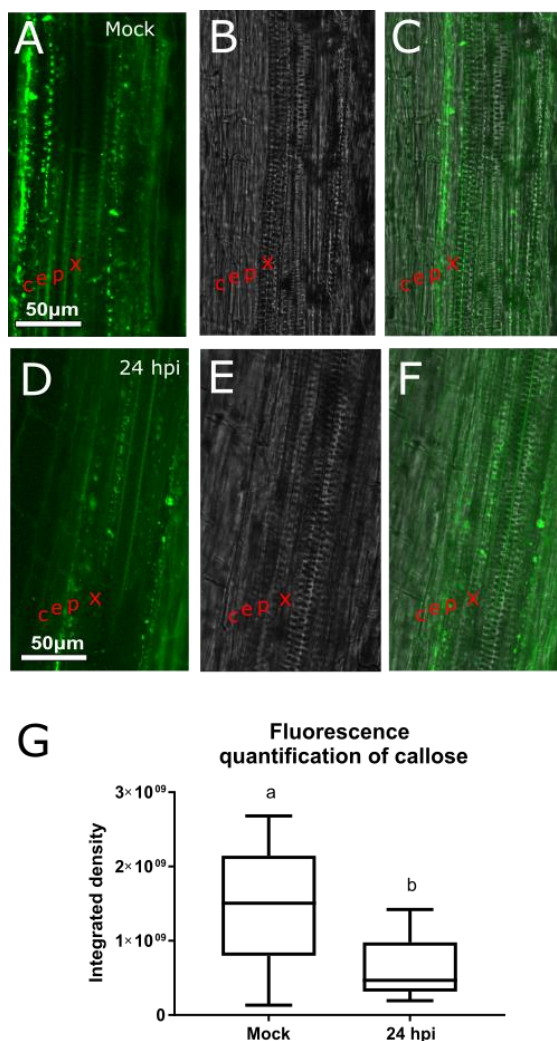


Figure 3.7- Callose is downregulated upon inoculation in *M. truncatula* roots growing in nitrate. Callose was detected using a monoclonal antibody and Alexa-488 (green) conjugated antibody in *M. truncatula* roots longitudinal sections grown in 5mM nitrate media and after 24 hours post spot-inoculation with either mock (water) (A) or rhizobia (hpi) solution (D). Bright field (B and E) and composite images are shown to help section localisation (C and F). (G) Fluorescence quantification of callose was performed by calculating the integrated density using ImageJ for each image in at least 3 biological repetitions per condition. Fluorescence was quantified in a region of interests of approximately 100μm². Symbols in A to F refer to xylem vessel (x), pericycle (p), endodermis (e), and cortex (c). A Student's t-test was performed, different letters indicate significant difference ($p < 0.001$).

3.2.2.3 *ENOD11* expression is regulated upon rhizobia infection in depleted and high nitrate conditions

To further support the hypothesis that, at least in the very early stages of the process after inoculation, nitrate is not inhibiting essential processes in the infection process and Nod factor signalling pathway, it was tested if nitrate operates by repressing the expression of symbiotic genes, such as *ENOD11* (Journet et al., 2001; Andriankaja et al., 2007; Svistoonoff et al., 2010).

M. truncatula plants expressing the GUS reporter gene driven by the *ENOD11* promoter were used to determine the spatial-temporal expression pattern of the gene upon inoculation in depleted and in full nitrate growing conditions (FP medium supplemented with 5mM nitrate). Seedlings were inoculated either with a mock solution or with rhizobia. Seedlings were stained 24 hpi to localise GUS expression. *GUS* expression appears in the epidermal cell layer and regulated by nitrogen availability. Roots that were exposed to nitrate in the growing media (N+) presented a patch-like expression pattern and staining was much less strong than plants growing under nitrated depleted conditions (N-) (Figure 3.8). This suggests that, although nitrate strongly affects *ENOD11* expression, does not completely inhibit it, thus infection still occur although at lower efficiency. These results agree with previous research that proved that *ENOD11* expression was regulated upon exposure to NodFactors in the presence of nitrate (Marsh et al., 2007).

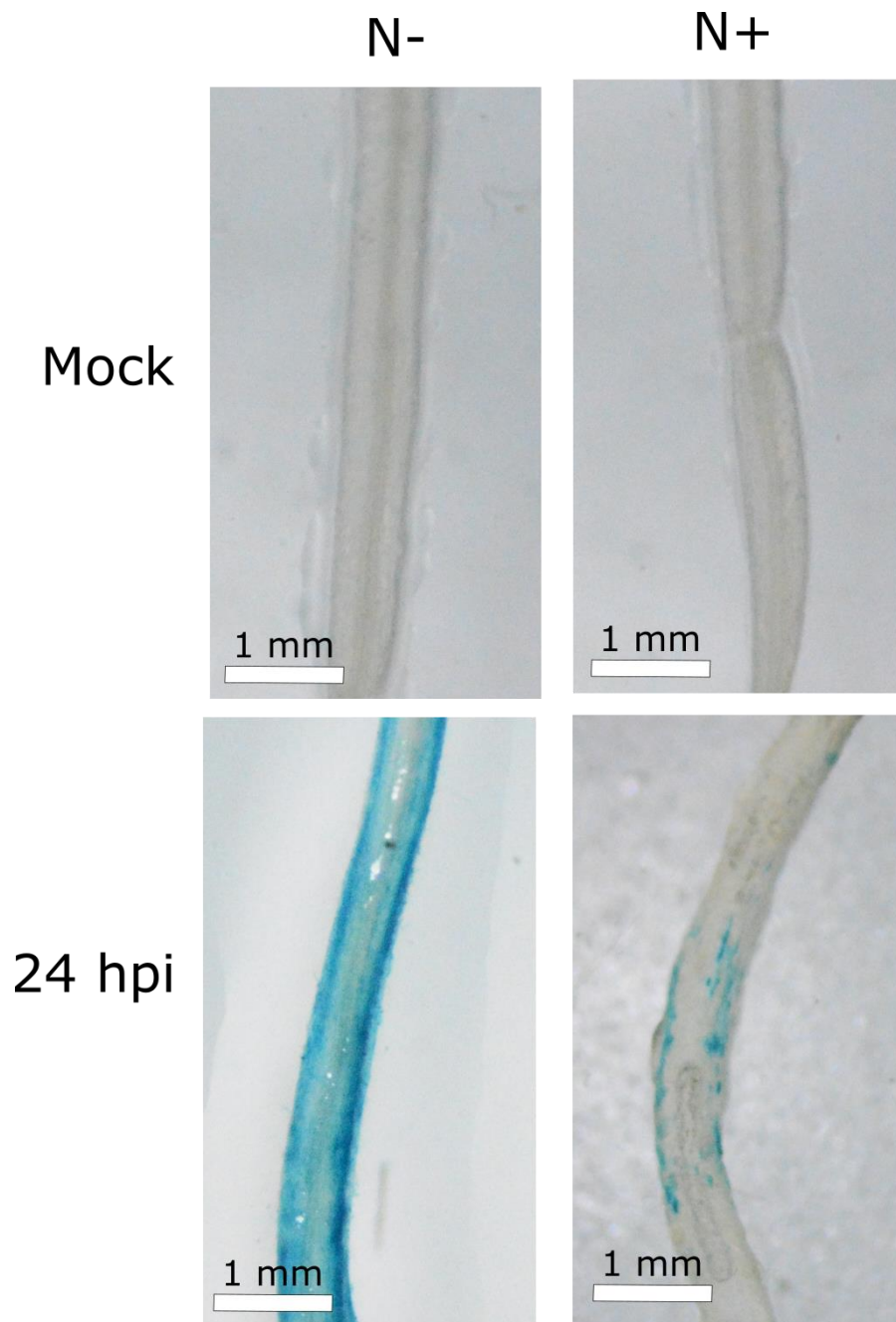


Figure 3.8 *ENOD11* expression is not completely inhibited by nitrate in *M. truncatula* roots. *M. truncatula* expressing the GUS reporter gene driven by the *ENOD11* promoter were grown in no nitrate (N-) or 5mM nitrate (N+) for 5 days and inoculated with either mock or rhizobia (24 hpi). Roots were stained 24 hpi to localise *ENOD11* expression pattern. GUS staining showed that in the absence of nitrate *ENOD11* is expressed widely in the infection zone epidermis but this expression is patchy and much less strong (although not completely inhibited) in the case of plants growing in high nitrate.

3.2.3 Identification of callose metabolic enzymes regulated in response to rhizobia infection in *Medicago* roots

It was shown that there is a downregulation of callose upon inoculation, and it was hypothesised that this downregulation is due to the activity of callose metabolic enzymes (such as BGs). Phylogenetic analyses have been recently applied to the preliminary screening of glycosyl hydrolases family 17, also known as β -1,3-glucanases (BGs) which include callose degrading enzymes in a range of plant representatives (Gaudioso-Pedraza and Benitez-Alfonso, 2014). Phylogenetic trees using three search algorithms were generated: Bayesian inference (Bayesian), Maximum Likelihood (ML) and Neighbour Joining (NJ) aiming to identify BG and CALS in *Medicago* by comparison with *Arabidopsis* orthologues.

For BG (GHL17 family) and CALS family members, identified as described in Material and Methods, the trees' topology were generally well supported by all 3 methods (Figure 3.9 and Figure 3.10 and Appendix 4, 5, 6, 7, 10, 11, 12, 13, 14 and 15).

Regarding BG, this approach allowed to pinpoint sequences with homology to plasmodesmata-located enzymes identified in *Arabidopsis*. Secretory signal peptides (SP) and a C-terminal glycosylphosphatidylinositol anchoring (GPI) domain are both present in plasmodesmata located GHL17 proteins identified in *Arabidopsis* (Thomas et al., 2008). Prediction tools were used to determine (the presence of a SP and GPI anchor in *Medicago* candidate orthologues. Out of 42 sequences containing the predicted GHL17 domain in *M. truncatula*, 14 have both a predicted SP and a GPI-anchor. All sequences retrieved, together with predicted domains can be found in the Appendix 1.

Out of the 42 GHL17 predicted proteins, MtBG1 (Medtr8g085720), MtBG2 (Medtr3g083580), MtBG4 (Medtr5g078200) and MtBG5 (Medtr3g065460) are phylogenetically more closely related to *Arabidopsis* glucanases that localised at plasmodesmata (At3G13560, At1G66250 and At2G01630) but only Medtr8g085720, Medtr3g083580 and Medtr3g065460 present SP and GPI, suggesting a membranous localisation (Figure 3.11-B).

On the other hand, microarray data shows an upregulation of the putative β -1,3-glucanase MtBG1 in root hairs upon inoculation (Figure 3.12-A), suggesting a role in infection and/or early stages of the signalling process (Breakspear et al., 2014).

To confirm results from microarrays experiments, inoculated roots were used for RT-PCR experiments. Due to the microarrays data and their close phylogenetic relationship with *Arabidopsis* PdBG1 (involved in post-embryonic developmental processes in *Arabidopsis*), MtBG1 and MtBG2 were selected for further experiments. Gene-specific primers for MtBG1 and MtBG2 were used to amplify around 200 bp of each gene. Actin was used as a housekeeping gene. Amplification of cDNA synthesised from extracted RNA shows that both genes are induced at early stages of infection (16 hpi) (Figure 3.13-A).

Additionally, and given the stronger regulation pattern of MtBG2 seen by RT-PCR, Q-PCR was also performed to study the expression pattern of the gene at 4, 8, 16 and 24 hpi with rhizobia (Figure 3.13-B). Relative expression of MtBG2 significantly increases at 24 hpi compared to roots inoculated with a mock solution (water). Earlier time points did not show any change in relative gene expression. The expression of MtBG2 was also assessed in 'full' nitrate conditions (5mM) and compared with control plants growing in no nitrate media but no significant differences were found (data not shown).

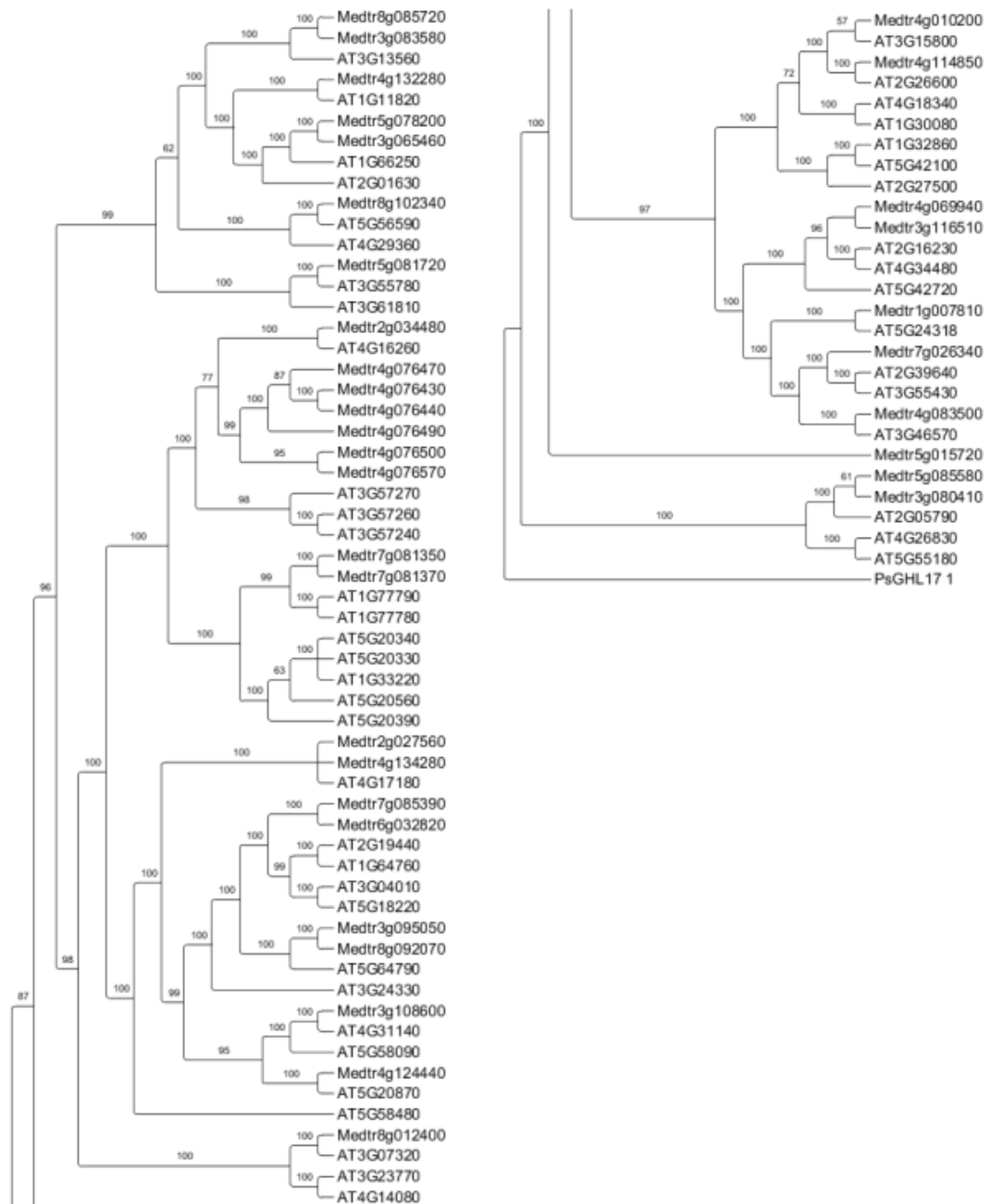


Figure 3.9- Full majority-rule consensus tree of GH17s using sequences isolated from *M. truncatula* (Medtr) and *Arabidopsis thaliana* (At) generated by Bayesian inference of phylogeny.

Phylogenetic relationship between *Medicago* and *Arabidopsis* Glycosyl hydrolase family 17 (GH17) family of proteins was determined using the Bayesian inference of phylogeny algorithm. A glucanase from *Picea sitchensis* (*PsGHL17_1*) was used as an outgroup. Bayesian posterior probabilities are indicated above the clades.

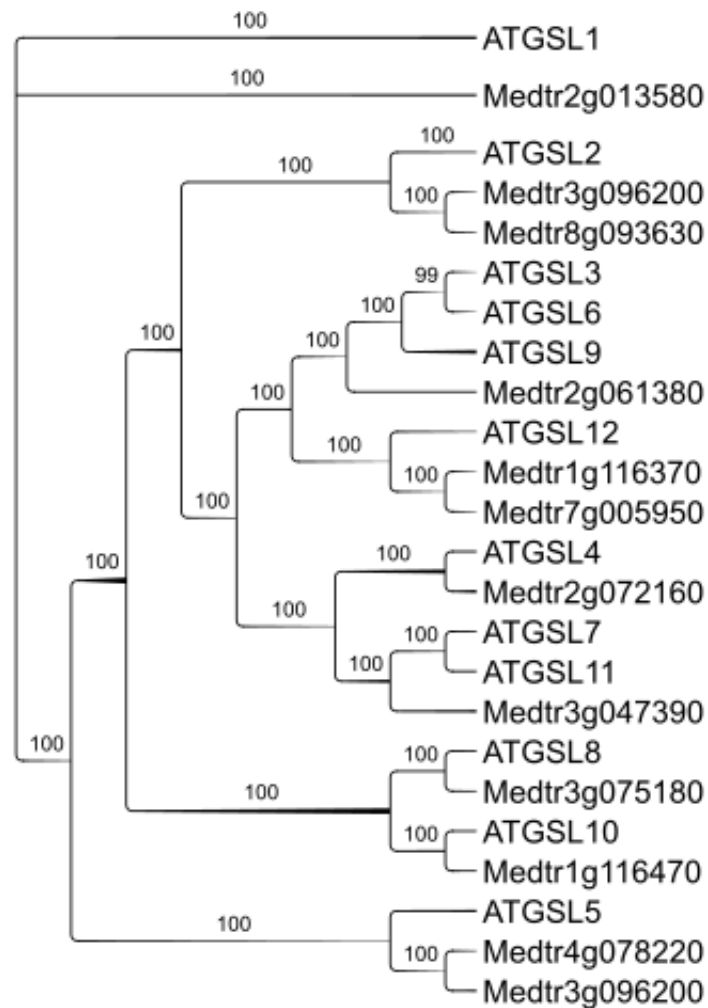


Figure 3.10 Full majority-rule consensus tree of Glucan Synthase Like (GSL) protein family using sequences isolated from *M. truncatula* (Medtr) and *Arabidopsis thaliana* (At) generated by Bayesian inference of phylogeny.

Phylogenetic relationship was determined using the Bayesian inference of phylogeny algorithm. Bayesian posterior probabilities are indicated above the clades.

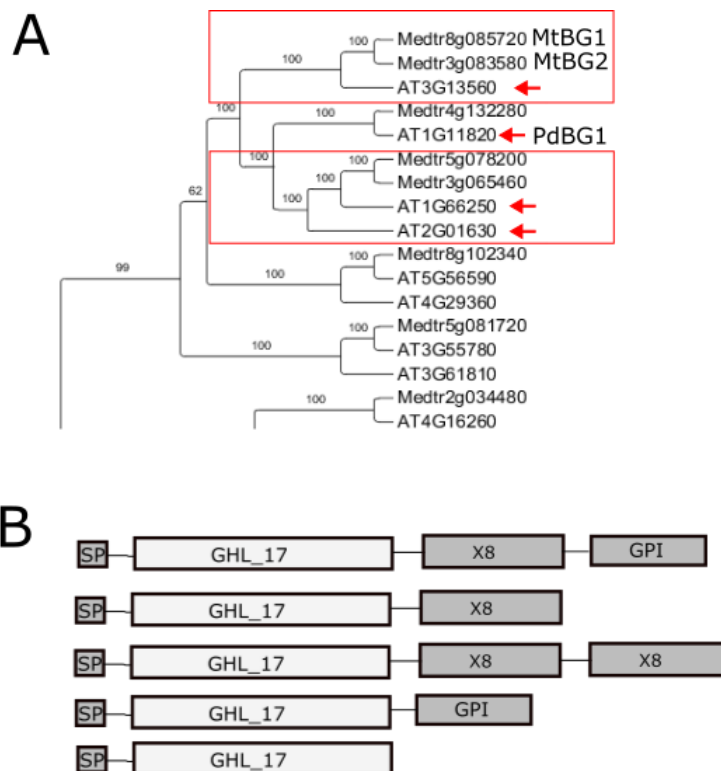


Figure 3.11- Phylogenetic studies identify potential *Medicago* orthologues to Arabidopsis Plasmodesmata located β -1,3-glucanases. (A) A fraction of phylogenetic tree indicating Bayesian posterior probabilities as a measurement of branch confidence. Proteins with known plasmodesmata localisation are arrowed. Red squares indicate *Medicago* glucanases closely related to Arabidopsis plasmodesmata β -1,3-glucanases. The whole tree is available in **Figure 3.9** (B) Protein domains in the β -1,3-glucanase family (also known as Glycosyl hydrolase family 17, GHL17) in *A. thaliana*. Protein domains include the core glycosyl hydrolase catalytic domain (GHL17) and the N-terminal signal peptide (SP) and might also include one or more carbohydrate binding modules (X8), and a hydrophobic C-terminal glycoposphatidylinositol anchoring sequence (GPI).

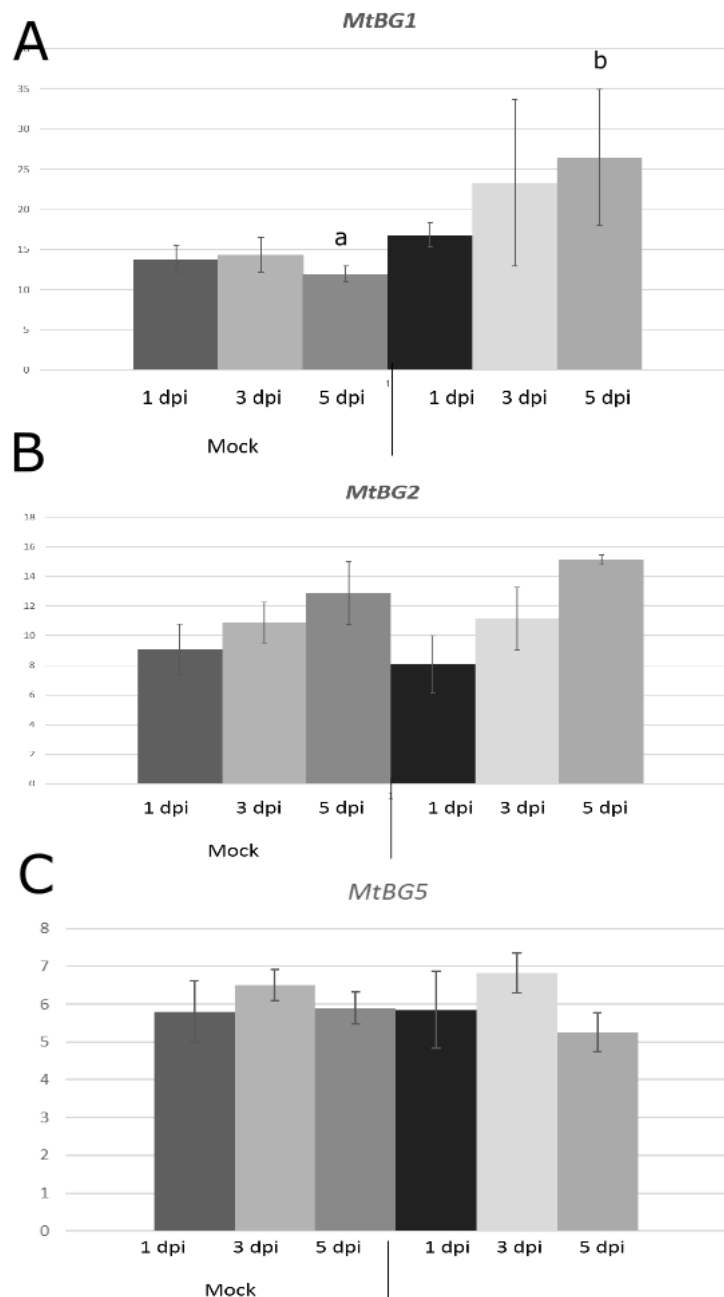


Figure 3.12- Expression profiles of potential BGs in *M. truncatula* root hairs suggest a role in early stages of infection. The profiles shown are extracted from Microarray data from <http://mtgea.noble.org/> (A) *MtBG1* shows a regulation in the expression in root hairs at 5 days post-inoculation with rhizobia compared to control experiments with a mutated rhizobia strain unable to form symbiosis (mock) (B) In contrast, *MtBG2* and *MtBG5* do not seem regulated in *M. truncatula* root hairs compared to mock conditions. Image adapted from <http://mtgea.noble.org/v3/>. Data published by (Breakspear et al., 2014).

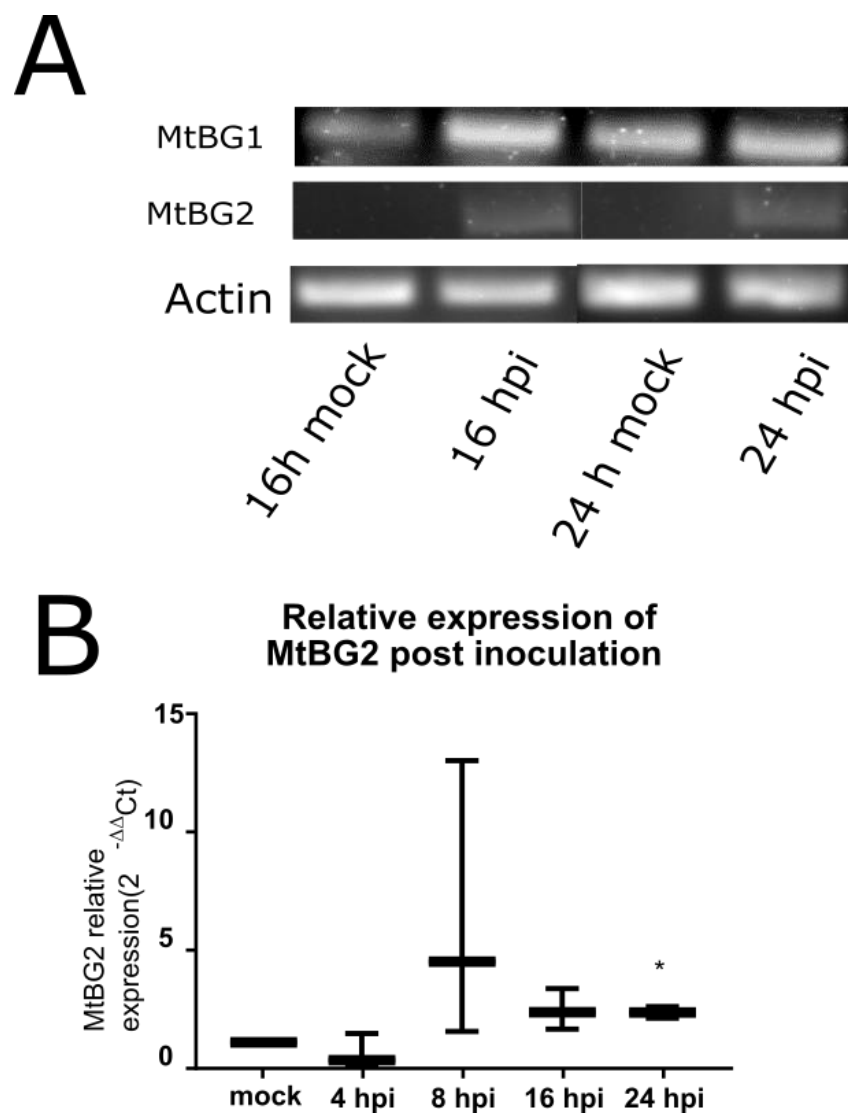


Figure 3.13- The genes MtBG2 and MtBg1 are upregulated upon rhizobia inoculation of *M. truncatula* roots. (A) *M. truncatula* roots were spot-inoculated with *S. meliloti* and samples collected at 16 and 24 hours post inoculation (hpi) RNA was extracted and cDNA synthesized. PCR was performed with Actin primers as housekeeping gene. MtBG1 shows an upregulation at 16 hpi, with steady expression at 24 hpi. On the other hand, MtBG2 shows an upregulation both at 16hi and 24 hpi. (B) Relative gene expression levels of MtBG2 at 4, 8, 16 and 24 hours post infection (hpi) with spot-inoculated rhizobia. Expression levels were detected using QPCR as described in Methods. Error bars represent $2^{-(\Delta\Delta Ct \pm \text{standard deviation})}$. Student's t-test between control and infected ΔCt values (* indicates a significant increase $p < 0.05$). Data obtained in collaboration with Callum Williams.

Phylogenetic analyses were also performed to study the Callose synthase protein family of *M. truncatula* and *A. thaliana*. Following the same protocol described above and in Material and Methods, the phylogeny of this protein family was reconstructed. General tree topology was maintained among the three algorithms (Appendix 6, 7, 13, 14 and 15).

Arabidopsis GSL12, also known as CALS3 is located at plasmodesmata and it is thought to control callose synthesis and symplastic trafficking during root development (Vaten et al., 2011). *M. truncatula* *MtGSL8* (Medtr1g116370) and *MtGSL10* (Medtr7g005950) are closely related to Arabidopsis *GSL12*, but expression data do not show a regulation of these genes upon inoculation (Figure 3.14), suggesting that they are not involved in the early stages of the symbiotic process.

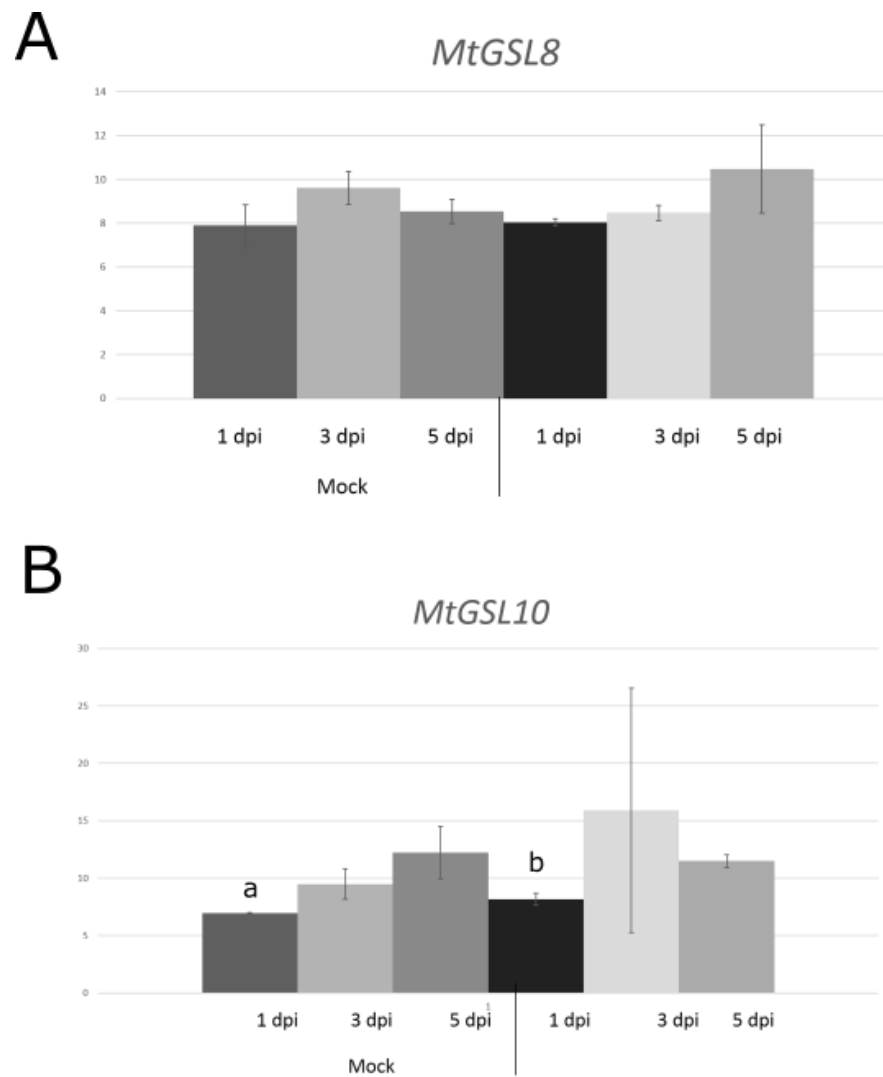


Figure 3.14- Expression profiles of potential callose synthase orthologues in *M. truncatula* do not suggest a role in early stages of infection. The profiles shown are extracted from Microarray data from <http://mtgea.noble.org/> (A) *MtGSL8* does not show a regulation in roots at 1, 3 and 5 days post-inoculation with rhizobia compared to control experiments with a mutated rhizobia strain (mock) (B) *MtGSL10* does not seem regulated in *M. truncatula* roots at 3 and 5 dpi, with a slight upregulation at 1 dpi. Student's t-test was performed. Different letters show statistical differences. Image adapted from <http://mtgea.noble.org/v3/>. Data published by (Breakspear et al., 2014).

3.2.4 MtBG2 (Medtr3g083580) is a novel plasmodesmata located callose degrading enzyme induced in response to rhizobia

Phylogenetic studies identified potential plasmodesmata-located glucanases in *M. truncatula* (Figure 3.9) which expression is affected after rhizobia inoculation (Figure 3.13). MtBG2 (Medtr3g083580) shows a strong expression profile linked to rhizobia inoculation, hence it was selected as a candidate gene. A fluorescent protein fusion was generated by placing the *mcherry* sequence between 462-463aa of MtBG2 (before the predicted omega site for GPI modification) and under the Arabidopsis *Ubiquitin* promoter to test the protein cellular localisation. *M. truncatula* transgenic roots expressing the fusion protein showed punctate localisation pattern (Figure 3.15-A) which co-localised with callose deposits revealed by aniline blue staining (Figure 3.15-B and C), suggesting that this newly identified protein is located at plasmodesmata.

To determine if the MtBG2-mcherry fusion is an active enzyme, callose levels in *M. truncatula* roots constitutively expressing the fusion protein were assessed. Aniline blue staining and callose immunolocalisation revealed that callose fluorescence signal was strongly reduced in transgenic roots overexpressing *MtBG2* in relation to control roots transformed with an empty vector (Figure 3.16 and Figure 3.17). Integration analysis of the signal in multiple sections indicates a significant decrease in callose in *MtBG2*-overexpressing roots supporting its role in callose degradation (Figure 3.16-C and Figure 3.17-C).

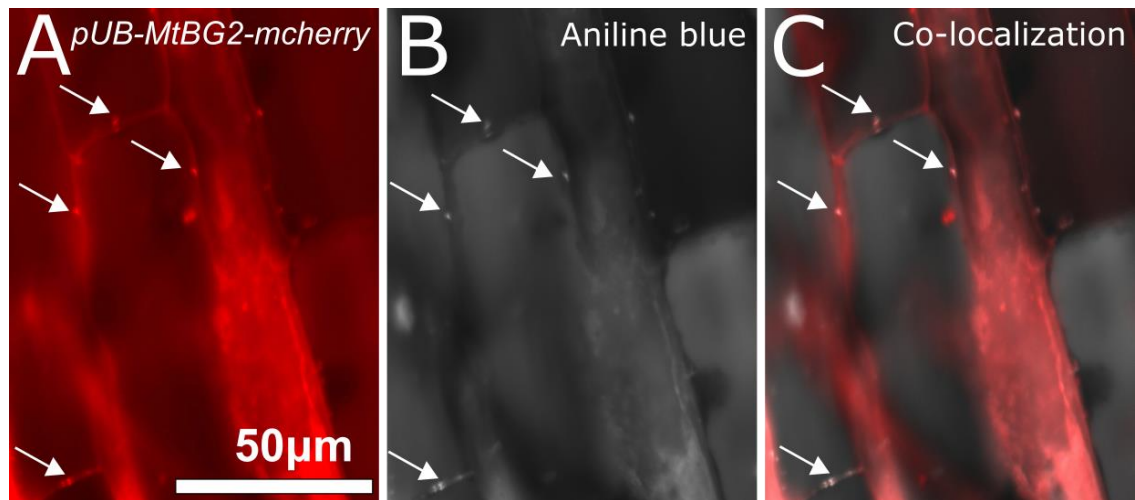


Figure 3.15- MtBG2 localises at plasmodesmata. *MtBG2* fused to *mcherry* was expressed under the Ubiquitin promoter (*pUb*) in transgenic *M. truncatula* roots. (A) Confocal microscopy picture showing *MtBG2-mcherry* localisation (red channel) (B) Callose deposits were revealed in the same root by aniline blue staining false coloured in white (C) Co-localisation of *MtBG2* with callose deposits suggesting plasmodesmata localisation (white arrows).

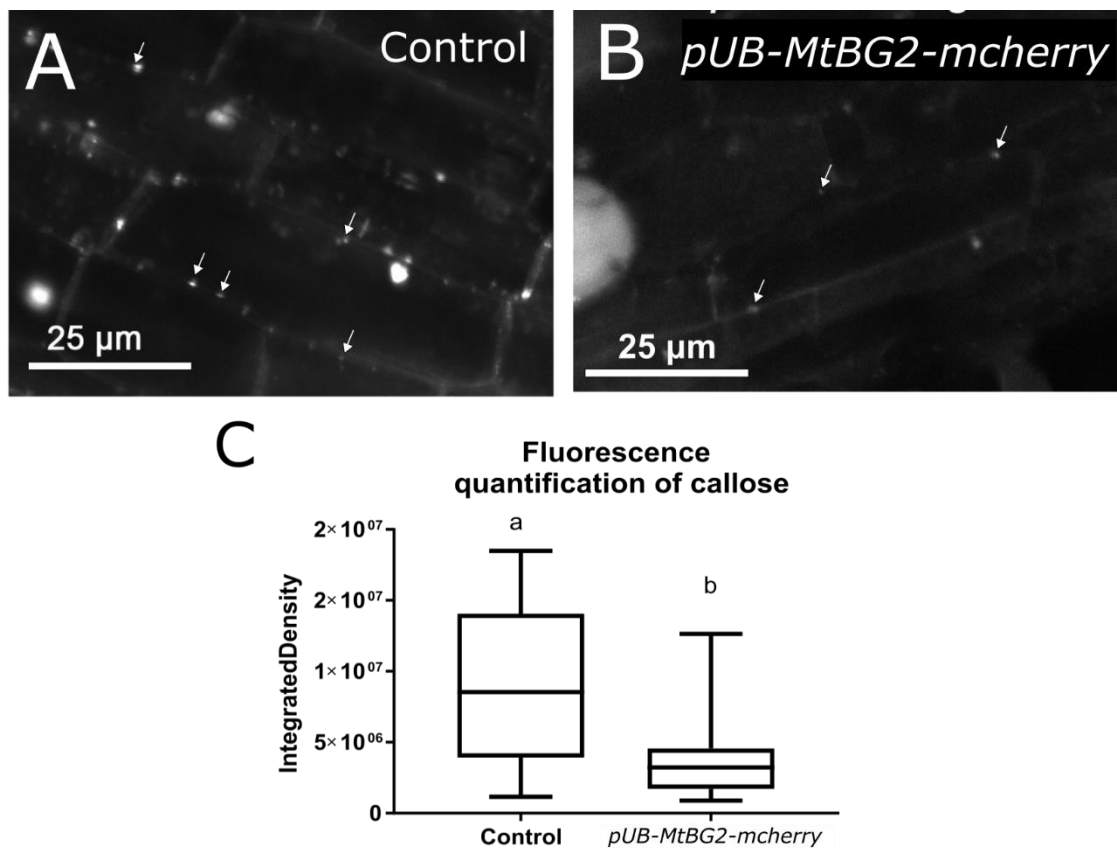


Figure 3.16- MtBG2 expressed under the ubiquitin promoter affects callose deposition in *M. truncatula* transgenic roots. Aniline blue was used to stain callose deposits at plasmodesmata (white spots highlighted by white arrows) in *Medicago* roots transformed with an empty vector as control (A) and with *pUb-MtBG2-mcherry* (B) (C) Aniline blue fluorescence signal was measured by calculating integrated density using ImageJ for each image in at least 3 biological repetitions. A Student's t-test was performed, different letters indicate significant differences ($p < 0.001$).

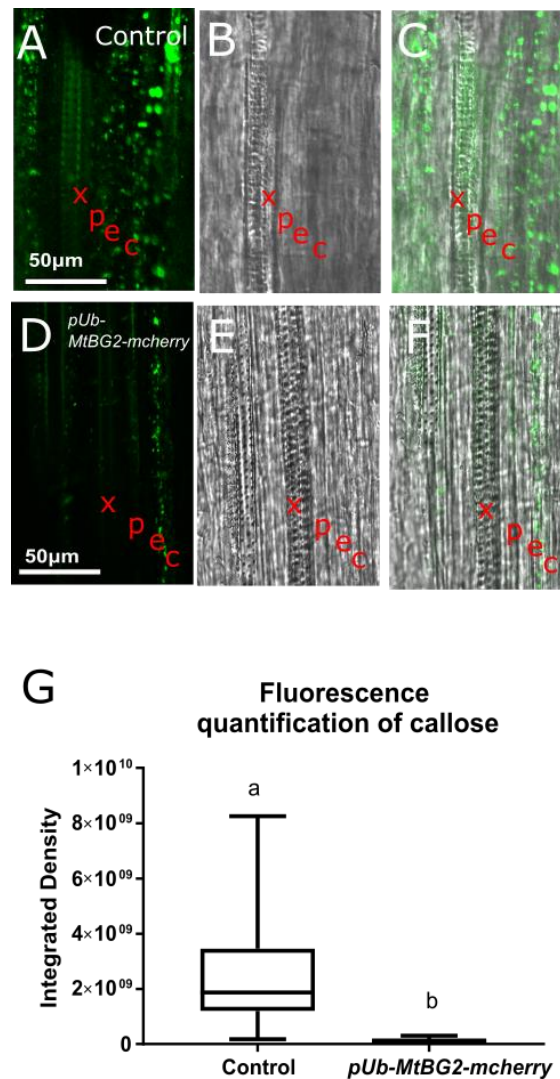


Figure 3.17- Immunolocalisation experiments confirms reduced callose in plants overexpressing *MtBG2*. Callose was localised with monoclonal antibodies and detected with a conjugated secondary antibody (Alexa-488). Bright field and composite image are shown to help section localisation. (A) Callose immunolocalisation in longitudinal sections of *M. truncatula* roots expressing an empty vector as control. (D) Callose immunolocalisation of *M. truncatula* roots constitutively (*pUB*) expressing *MtBG2-mcherry*. Bright field (B, C) and composite image (E, F) are shown to help with localisation. (G) Fluorescence quantification of callose. Integrated density was calculated using ImageJ for each image in at least 3 biological repetitions. Fluorescence was quantified in a region of interest of approximately $100\mu\text{m}^2$. Symbols in A to F refer to xylem vessel (x), pericycle (p), endodermis (e), and cortex (c). A Student's t-test was performed, different letters indicate significant differences ($p < 0.001$).

3.3 Discussion

3.3.1 Establishment of *Medicago*-rhizobia symbiosis involves down-regulation of callose in cell walls

The work presented in this chapter has provided insights into the changes in callose deposition at the cell wall that occur in *M. truncatula* roots after inoculation with rhizobia.

Through callose immunolocalisation it was confirmed that a down-regulation of this polysaccharide occurs throughout the first 24 hours post-inoculation. Although the conditions might affect the times for infection, the work from (Laplaze et al., 2015) indicates that infection threads are normally visible between 24 and 72 hours post-inoculation. The observed changes in callose, therefore, suggest that the plant arranges its cell wall structure before the infection thread starts developing. This timescale also suggests that these changes might be triggered by Nod factors secreted by the bacteria in the early stages of host-bacteria communication. Further experiments characterising callose deposition after Nod factors treatment or in mutants with defects in these signalling pathways will help to dissect this response.

Downregulation of callose differentiates the *Medicago*-rhizobia interaction from some plant-pathogens incompatible interactions where callose is deposited to fight the pathogen. Although the role of callose in non-pathogenic interactions has not been widely studied, callose is a well-known mechanism of plant defence against pathogens (Luna et al., 2011; Ellinger and Voigt, 2014; Voigt, 2014) where it plays a role in strengthening the cell wall. In addition, callose has been suggested to play an important role in the development of feeding sites during nematode infection of Arabidopsis plants, where it appears to be downregulated to allow the feeding site to develop (Hofmann et al., 2010). Also, and contrarily to other pathogens, some viruses have evolved to target the host glucanases to degrade callose, helping the spread of the infection (Iglesias and Meins, 2000; Benitez-Alfonso et al., 2010; Li et al., 2012). For a more in-depth review of the role of callose and plasmodesmata in pathogenic interactions, see Chapter 1 sections 1.3.3.

As in the response to rhizobia, the arbuscular mycorrhizal symbiosis does not trigger callose deposition (Bonfante-Fasolo et al., 1990; Peterson and Bonfante, 1994). Interestingly, a *Pisum sativum* mutant unable to form both nodules and arbuscular mycorrhizal showed an abnormal accumulation of callose when in contact with the beneficial fungus compared to wild-type plants (Gollotte et al., 1993). These observations suggest that callose is synthesized as a defence mechanism in AM non symbiotic pea mutant, contrary to interactions with wild-type pea plants. It is also interesting that a number of mutants unable to form arbuscular mycorrhizal symbiosis are also impaired in nodule formation (Resendes et al., 2001; Parniske, 2004; Breakspear et al., 2014). If callose regulation is involved in this response/common pathway still needs to be investigated.

3.3.2 Callose regulation upon inoculation suggest changes in symplastic communication

The early regulation of callose in the cell wall of roots undergoing inoculation/infection process can be associated with changes in plasmodesmata permeability. A de-novo symplastic continuum is generated upon infection (48 hpi) to connect the phloem and the cells in the inner cortex where the nodule primordia will form (Complainville et al., 2003). Research from Berderska et al., (2012) shows that, in older and fully differentiated nodules (40 dpi), symplastic continuity is maintained between companion cells and the first layer of the parenchyma cells within the nodule (Bederska et al., 2012). Together the results suggest that the symplastic continuum created between phloem and nodule in the early stages of nodulation (described by Complainville et al., 2003) is maintained during nodule maturation (Bederska et al., 2012). So far these changes were linked to an increase in plasmodesmata number not to changes in callose. Our results showing reduced callose levels early after inoculation suggest that regulation of symplastic communication during nodulation might occur through two mechanisms: callose degradation and formation of new plasmodesmata. Furthermore, this regulation appears induced in pericycle, endodermis and cortex upon infection as seen in immunolocalisation. Spot inoculated roots showed 24 hpi a downregulation of callose especially among these tissue layers that will form the nodule primordia. Interestingly, these results

are in concordance with previous literature that shows how a fluorescence probe that can only move through plasmodesmata was found in pericycle and cortex cell layers 48 hpi (Complainville et al., 2003). Further immunolocalisation experiments are needed to characterise the callose deposition pattern in outer cell layers (epidermis) upon inoculation.

Additionally, further studies focusing on changes in symplastic connectivity are required to fully understand the effect that this regulation has in cell-to-cell communication upon inoculation. The use of fluorescent mobile signals (GFP, CFDA, esculin...) has been useful in the past to dissect changes in symplastic connectivity (Knoblauch et al., 2015).

It has been recently demonstrated ³ that symplastic communication is, in fact, regulated upon inoculation and that new symplastic connections are created between epidermis and inner cell layers in *M. truncatula* roots 3 dpi. In short, this was demonstrated by monitoring the transport of a fluorescent tracer (CFDA) from epidermal cells towards inner cell layers in inoculated roots 3 days post inoculation. CFDA is a membrane permeable dye that only becomes fluorescence inside the cell where an endogenous esterase produces a non-membrane permeable fluorescent form that can only move between cells via plasmodesmata (Knoblauch et al., 2015). By these means, it was shown that the fluorescence signal was restricted to epidermal tissues in control roots (inoculated with water) but that it diffused from the epidermis to cortical cells in rhizobia-inoculated tissues.

Therefore, it can be hypothesised that this increase in symplastic permeability is due, at least partially, to a down-regulation of callose deposition in the cell wall around plasmodesmata sites. It would be interesting to explore if other modifications leading to changes in symplastic communication, such as the transitions from primary to secondary and/or branched plasmodesmata, play a role in this process.

³ Personal communication: Martina Beck and Fernanda de Carvalho-Niebel (LIPM, Université de Toulouse, INRA, CNRS, 31326 Castanet-Tolosan, France)

3.3.3 Newly identified plasmodesmata located protein plays a role in regulating callose during the establishment of the *Medicago-rhizobia* endosymbiotic interaction

Callose turnover at plasmodesmata is a dynamic process mainly carried out by two antagonist protein families, callose synthases and β -1, 3-glucanases. Here, it is reported a pool of putative glucanases and callose synthases in *M. truncatula* that might be involved in callose regulation upon inoculation by using phylogenetic and transcriptomic analyses. Identifying plasmodesmata proteins involved in the regulation of inoculation, infection and/or nodulation is an essential step to understand how symplastic communication and its regulation is involved in the establishment of symbiotic relationships and to identify the mobile signal(s) that orchestrate nodule organogenesis. Here, it is reported for the first time the plasmodesmata localisation of MtBG2, a protein with callose degrading activity.

Additionally, *MtBG2* and another prospective glucanase, *MtBG1*, are both upregulated after inoculation with rhizobia. This upregulation coincides in time (24 hpi) with the reduction in callose levels post inoculation reported in earlier sections of this thesis. Transcriptomic data from microarray experiments in root hairs (Breakspear et al., 2014) do not show upregulation in Medtr3g083580 expression but, if the expression of this gene coincides with the cortex and pericycle regions, where callose is downregulated, it would not show in the microarray data set. Studies from collaborators have confirmed that this is the case: the expression of the gene is mostly restricted to meristematic tissue, such as lateral roots in non-inoculated tissue and the root tip and to nodule primordia upon inoculation with rhizobia⁴. The expression of MtBG2 was localised to dividing inner root tissues localized below an infection site 3 dpi. In mature nodules, the expression was restricted to the apical zone, which includes both meristematic and early infection zones⁴. All these data together suggest that MtBG2, and potentially other β -1,3 glucanases, are involved in nodule formation, likely by mediating the regulation of callose and thereby the symplastic transport

⁴ Personal communication: Martina Beck and Fernanda de Carvalho-Niebel (LIPM, Université de Toulouse, INRA, CNRS, 31326 Castanet-Tolosan, France)

of signals that, ultimately, control the processes leading to nodule organogenesis.

The formation of lateral roots and nodules share some characteristics and regulatory signalling pathways, as has been pointed out by several authors (Imin et al., 2013; Moreira et al., 2013; Bensmihen, 2015). For example, hormonal control of both structures is alike, with an auxin gradient and the accumulation of auxin in the initiation area of both lateral roots and indeterminate nodule primordia being essential for their development (Hirsch et al., 1989; van Noorden et al., 2006; Overvoorde et al., 2010; Bensmihen, 2015). Additionally, the ectopic overexpression of the CLE peptides leads to both a reduction in nodule and lateral root primordia (Schnabel et al., 2005; Araya et al., 2014). Conversely, antagonist pathways, involving factors known to modulate meristem growth and maintenance, such as cytokinin or ethylene, have been identified where nodule formation is favoured while lateral root formation is negatively regulated (Huault et al., 2014; Bensmihen, 2015).

Arabidopsis orthologues of MtBG2 and MtBG1, PdBG1 and PDBG2, are plasmodesmata-located proteins that mediate callose degradation. Mutations in these genes restrict symplastic communication and increase lateral root density and distorting patterning (Benitez-Alfonso et al., 2013). This contrasts with our results where decreasing callose increased nodule density. Despite the essential role that callose is playing in these two postembryonic developmental processes, it seems clear that the downstream mechanisms behind the control of these systems differ (Benitez-Alfonso et al., 2013). *MtBG2* promoter expression was also seen in lateral root primordia⁵. In the absence of mutant lines, the role of *MtBG2* in lateral root formation and patterning was not addressed in this work but it has the potential to reveal interesting crosstalk between the mechanisms regulating nodules and lateral roots.

⁵ Personal communication: Martina Beck and Fernanda de Carvalho-Niebel (LIPM, Université de Toulouse, INRA, CNRS, 31326 Castanet-Tolosan, France)

3.3.4 Nitrate availability inhibits nodule development but may not affect callose regulation

The formation of nitrogen-fixing nodules is a tightly controlled process, regulated by several mechanisms and signals, including nitrate and the number of functioning nodules (Reid et al., 2011a; van Noorden et al., 2016). When plants can retrieve nitrate or ammonium directly from the soil, they will not form symbiotic association with rhizobia, thus nodules are inhibited. Some infection threads will be observed, but most of them will be arrested at the epidermal cell layer (Gage, 2004). The exact mechanism by which nitrate inhibits nodule formation is still unknown, but it includes both, local and systemic regulatory signals (Jeudy et al., 2010; Reid et al., 2011a; van Noorden et al., 2016).

High concentrations of nitrate have a similar effect on nodule and lateral root development and this inhibition has been associated with ABA signalling (Signora et al., 2001) and mutants in ABA have been characterised to have impaired nodulation (Tominaga et al., 2009).

Here, it is shown that, despite the availability of nitrate in plates, the effect of rhizobia in callose regulation appears the same than in no-nitrate conditions. In other words, roots that were grown in nitrate-depleted and full nitrate conditions did not show a significant difference in callose antibody labelling. However, it cannot be dismissed the possibility of nitrate having an effect on the length of the reduction, since both conditions were not compared in similar conditions. Further experiments characterising callose deposition in the same conditions would help discern this possibility. Additionally, *MtBG2* expression was not changed in roots growing under full nitrate (5mM) conditions and roots grown in full nitrate showed a downregulation of callose 24 hpi, just like roots inoculated in nitrate-depleted conditions. The expression of *ENOD11*, a reporter for early infection steps of the symbiotic interaction, was generally and strongly restricted 24 hpi in roots grown in the presence of high nitrate, but it was not completely inhibited. This suggests that nitrate effects in the inhibition of nodulation is upstream of *ENOD11* but that is not associated with changes in the levels of callose, at least at 24 hpi.

Research by van Noorden et al (2016) shows that normal roots hairs curling occurs after inoculation under high nitrate conditions, suggesting that available

forms of nitrate and ammonium do not affect the early stages of the signalling process. If early signalling is what triggers the regulation of callose, it is not surprising that in full-nitrate conditions callose remains unaffected. More research is required to understand how callose regulation is integrated with other factors to coordinate specific responses to nitrate conditions. Understanding how infection and nodulation markers are regulated in response to nitrate and in relation to callose metabolic enzymes and symplastic connectivity would help to elucidate these questions.

Chapter 4

Chapter 4 -Altering callose turnover affects infection and nodulation in *M. truncatula*-rhizobia interaction

4.1 Summary

In the previous chapter, it was demonstrated that the inoculation of *M. truncatula* roots with *S. meliloti* leads to a rapid reduction of callose deposition as early as 24 hours post inoculation. The studies described in this chapter were performed to understand the role of callose in the establishment of the symbiotic relationship, specifically how modifying the patterns of callose deposition at the cell wall prior inoculation affect infection and nodulation processes.

To achieve this, the inhibitor of callose biosynthesis, 2-Deoxy-D Glucose (DDG), was used to chemically inhibit callose synthases in the cell wall of *Medicago* roots prior inoculation with the bacteria. In the 2-Deoxy-D-glucose (DDG) molecule the 2-hydroxyl group of glucose is replaced by hydrogen so it cannot undergo further glycolysis, hence it is not suitable as a monomer for polysaccharides such as callose. DDG is known to inhibit biosynthesis of callose in several plant species (Jaffe and Leopold, 1984; Li et al., 2012). Results from these assays are shown in section 1.2.1.

In section 1.2.2, genetically modified *M. truncatula* roots ectopically expressing the glucanase *MtBG2*, identified in Chapter 3, were used to assess how callose degradation affects the nodulation formation and infection processes.

Interestingly, modification of callose deposition by the two methods mentioned above not only lead to a significantly higher number of infection events and number of developing nodules, but also to a significantly weaker inhibition of nodulation and infection by nitrate.

In the discussion section, these results are interpreted in light of the current literature on the regulation of nodulation and infection. Suggestions for future work are also included in this section.

4.2 Results

4.2.1 Effect of the callose synthase inhibitor 2-Deoxy-D-Glucose in rhizobial infection and nodulation

4.2.1.1 Plant growth and rhizobia infectability are not significantly affected by DDG treatment

To establish whether DDG could inhibit callose synthesis in *M. truncatula* seedlings were treated with 100 μ M DDG for 24 hours. Concentrations of DDG of 250 μ M have been successfully used in infiltration experiments in leaves of soybean plants (Li et al., 2012). Since the treatment would be applied in young seedlings for a long duration, a lower concentration (100 μ M DDG) was tested to avoid prejudicial phenotypic effects in the roots. Callose deposition was quantified by immunolocalisation using fluorescence values collected from at least three roots per condition. *M. truncatula* seeds were germinated and grown in unmodified FP media for 5 days prior applying DDG for 24 hours. Sections of the treated root in the infection zone were fixed and callose immunolocalisation was performed to reveal callose deposition (Figure 4.1). Callose deposition was inferred in these roots as described in Materials and Methods. After 24 hours of treatment with 100 μ M DDG green fluorescence was generally lower in plants treated compared to plants growing in the presence of water, suggesting that the inhibitor is acting at that concentration in *M. truncatula*. All experiments were carried out using 100 μ M DDG.

Next, the effect of 100 μ M DDG treatment in root development and bacterial growth was assessed. Root length and architecture (including root hair formation) and bacterial growth in the presence of 100 μ M DDG were studied. No significant difference was seen in primary root length between control plants (growing in the presence of water) and plants treated with DDG (Figure 4.2). As for root hairs, root hair length, width and quantity were quantified in control plants and in plants treated with DDG for either 24 hours or 5 days. No significant changes in root hair phenotype between control conditions and plants treated with 100 μ M DDG were seen for both treatments (Figure 4.3).

Lateral roots number and lateral root density were also measured. After 5 days of continuous DDG treatment, lateral roots density was increased but not significant change was seen after 24h of treatment (Figure 4.4).

Regarding DDG effect on bacterial growth, a growth curve was performed by measuring the optical density of bacterial cultures growing in the presence of 100 μM DDG and water (control) every 2 hours for 60 hours until stationary phase was reached (Figure 4.5). 100 mM MgCl_2 was used as a positive control for inhibition since it is known that at that particular concentration it strongly inhibits rhizobia growth (Botsford, 1984). Bacterial media with water (the solute for DDG), was used as a negative control. Bacterial cultures growing in the presence of MgCl_2 presented growth inhibition, never reaching the exponential growth phase (Figure 4.5). On the other hand, bacteria growing in the presence of 100 μM DDG did present a very similar growth curve to bacteria growing in the presence of water, suggesting that the chemical is not affecting bacterial growth kinetics.

In addition, the infectability of rhizobia on plants grown on the presence of 100 μM DDG was assessed by using the spot inoculating method. Roots were grown in control and 100 μM DDG containing media and percentage of nodulating plants (percentage of plants showing nodules 7 dpi in relation to the total number of plants) was calculated (Table 4.1). Percentage of infected nodules was also measured by calculating the number of colonized nodules (7 days post inoculation roots were fixed and stained to localise lacZ expressing bacteria within nodules and nodule primordia) in relation to the total number of nodules. The results suggest that there is no significant difference in either the percentage of nodulating plants or of infected nodules between control and DDG treated plants indicating no effect of DDG in either the nodulation capability of the plant (Table 4.1) or the colonization capability of the rhizobia (Table 4.2).

Infectability, or the rhizobia's capacity for infection, was also assessed by growing rhizobia in the presence of 100 μM DDG and using this culture to spot inoculate *Medicago* roots. In parallel, control experiments were carried out using a bacterial culture with no added DDG in the growth media and plants growing in plant media containing DDG. As before, the percentage of nodulating plants was calculated and found not significantly different between these conditions,

suggesting that the infectability of the bacteria is unaffected in the presence of DDG (Table 4.3).

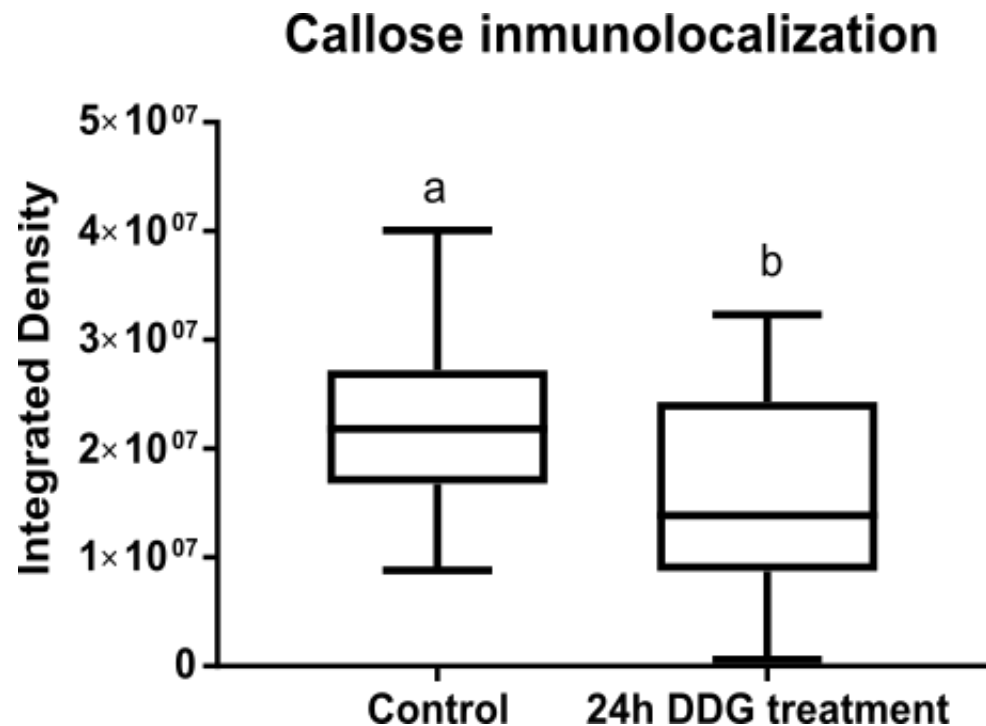


Figure 4.1 2- Deoxy-D Glucose treatment affects callose deposition in *M. truncatula* roots. Callose immunolocalisation in longitudinal sections of *M. truncatula* 5 day-old root growing in the presence of water (control) or 100 μ M DDG for 24h. Callose was localised using monoclonal antibodies and detected with an appropriate Alexa-488nm conjugated secondary antibody. Fluorescence quantification of callose was performed by calculating the integrated density using ImageJ for each image in at least 3 biological repetitions per condition. Fluorescence was quantified in a region of interest of approximately $100\mu\text{m}^2$. A Student's t-test was performed, different letters indicate significant difference ($p < 0.001$).

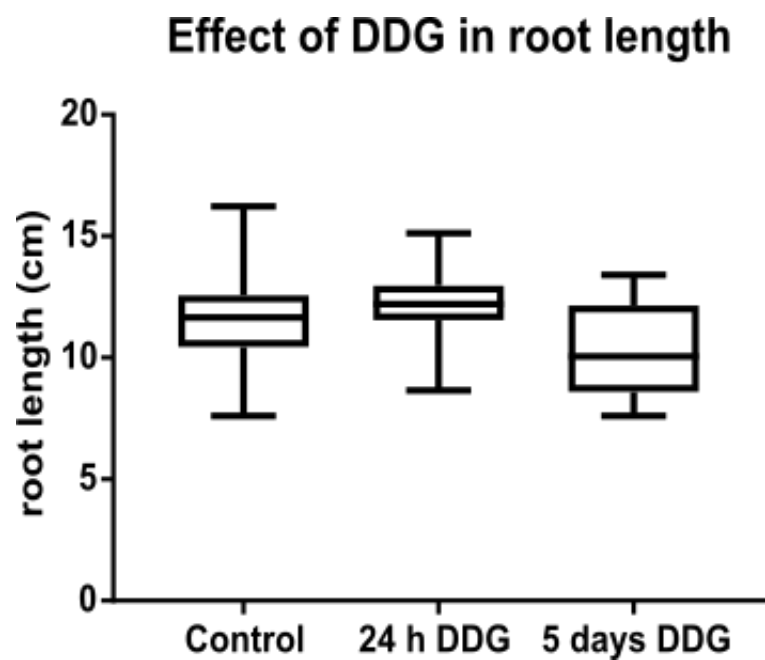


Figure 4.2- Effect of DDG treatment in *Medicago truncatula* root length. 5 days-old *M. truncatula* roots treated with water (control) or with 100 μM DDG (24 hours or 5 days treatment) were measured. A Student's t-test was performed, no significant differences were seen ($p > 0.05$) (N=30).

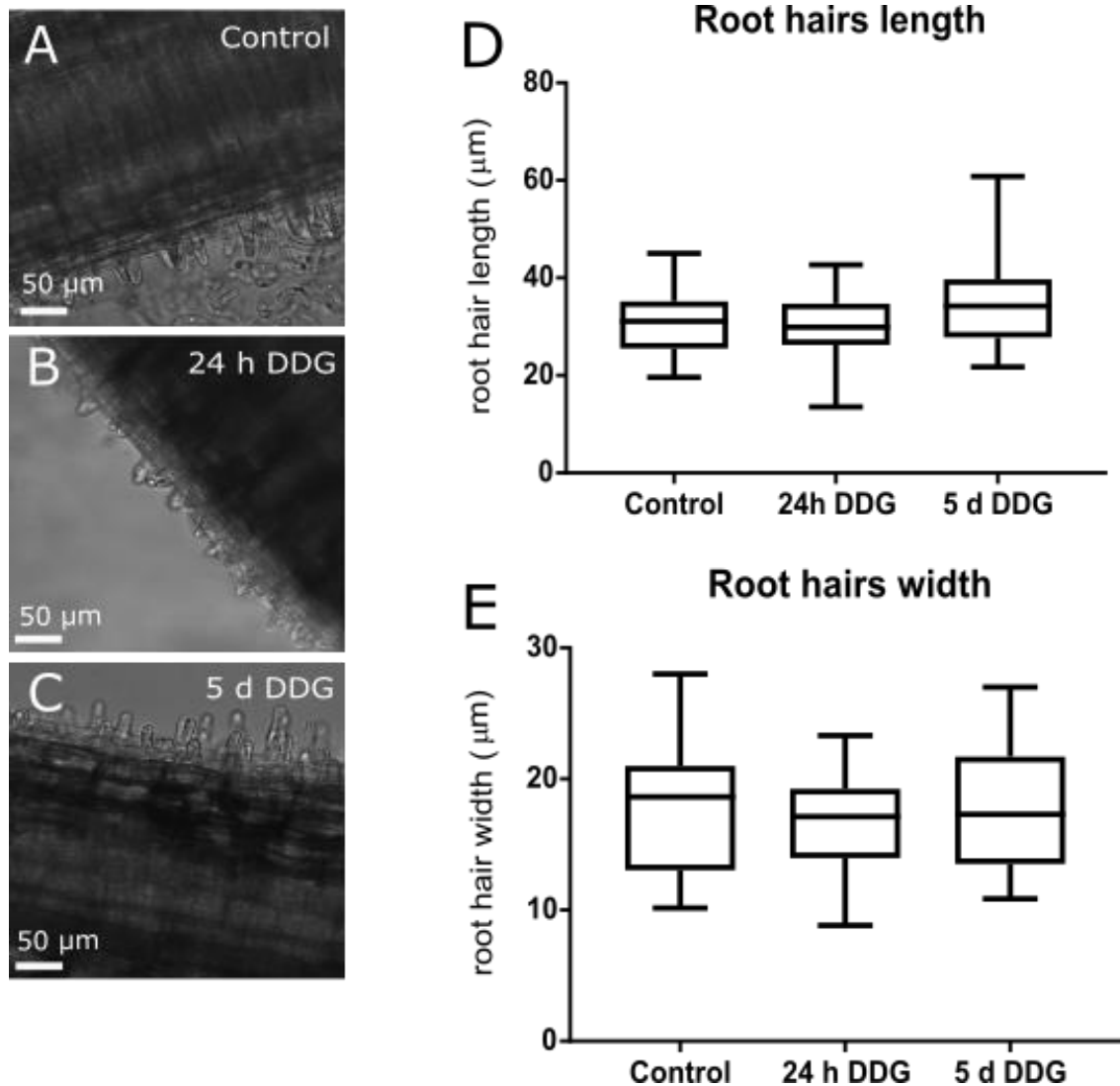


Figure 4.3- DDG does not seem to affect root hair development in *M. truncatula*. A-C Root hairs appear in the infection zone of *M. truncatula* roots (zone of the root where root hairs start to emerge, around 1-3 cm above the root tip). 5 days-old roots were treated with water (control-A) or with DDG for either 24 hours(B) or 5 days(C) and the infection zone was pictured. Root hairs length (D) and width (E) were measured in at least 3 roots per condition and at least 8 root hairs per root using ImageJ. Control picture (A) shows a root growing in the presence of water for 24 hours. A Student's t-test was performed, no significant differences were seen ($p > 0.05$).

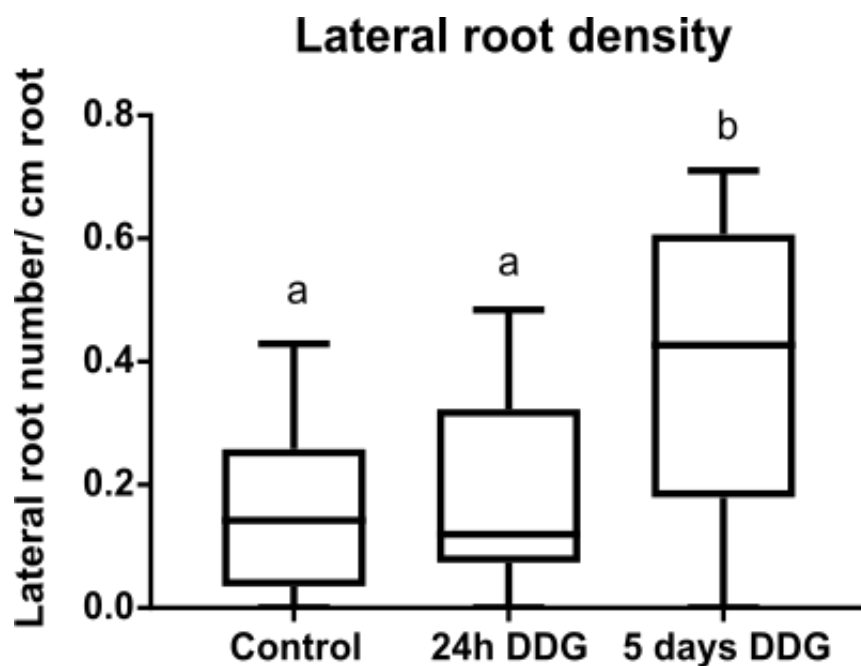


Figure 4.4- Continuous treatment with DDG affects the number of emerged lateral root in *M. truncatula*. 7 days-old plants were treated with either water (control) or with 100 μ M DDG for 24h or for 5 days. The number of emerged lateral roots were counted and divided by the total root length to determine lateral root density. An increase in emerged lateral root density was observed after treatment with DDG for 5 days compared to control conditions (water treated roots) and to 24 hours of treatment. A Student's t-test was performed, different letters indicate significant differences ($p < 0.05$).

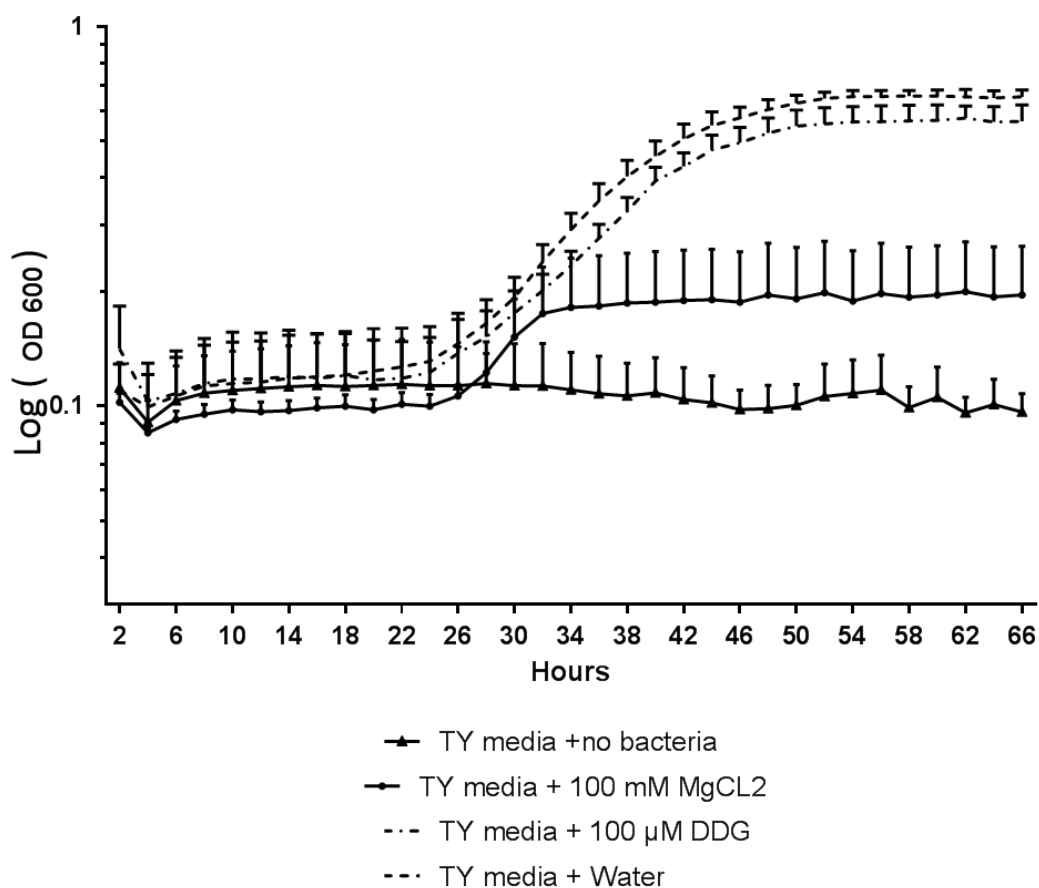
***S. meliloti* growth curve in the presence of DDG**

Figure 4.5- DDG does not affect rhizobia growth. A growth curve for *S. meliloti* pXLGD4 LacZ was performed by measuring optical density (OD₆₀₀) every two hours until cultures reached stationary phase (plateau, from hour 54). Cultures were grown in TY broth 100 mM MgCl₂ as a control for growth inhibition, with water as a negative control, and with 100μM DDG. TY media was used to measure background absorbance. OD₆₀₀ readings were taken in a set of triplicate cultures to calculate the standard deviation. Bacteria growth (LogOD₆₀₀ values) was not significantly different in media supplemented with DDG or with water. Growth was inhibited in 100 mM MgCl₂. Error bars show standard deviation.

Table 4.1- DDG treatment does not affect the percentage of nodulating plants. *M. truncatula* plants growing in either water (control) or 100µM DDG for 24 hours or 5 days were inoculated with rhizobia and number of plants showing one or more nodules 5 days after infection in relation to the total number of plants was used to calculate the percentage of nodulating plants. A Student's t-test was performed to the means with no significant differences seen ($p>0.05$).

| Conditions | Percentage of nodulating plants |
|----------------------------|---------------------------------|
| Control (continuous water) | 85.5% |
| 24 h DDG | 97.5% |
| 5 days DDG | 95% |

Table 4.2- DDG treatment does not affect the percentage of colonised nodules. *M. truncatula* plants treated either with water (control) or with 100 µM DDG for either 24 hours prior inoculation with *S. meliloti* expressing the β -galactosidase protein or 5 days concomitant to the inoculation process 7 days post inoculation roots were fixed and stained to localise bacteria within nodules and nodule primordia. The percentage is calculated dividing blue nodules by a total number of nodule per plant. Student's t-test was performed to the means with no significant differences seen ($p>0.05$).

| Conditions | Percentage of colonised nodules |
|----------------------------|---------------------------------|
| Control (continuous water) | 79.2% |
| 24 h DDG | 69.1% |
| 5 days DDG | 73.3% |

Table 4.3- Infectability of rhizobia is not affected by DDG. Plants growing in control conditions (water) and growing in the presence of 100 μM DDG were spot inoculated with either rhizobia growing in Minimal Media (MM) supplemented with water or DDG to a final concentration of 100 μM . The number of plants growing a nodule in the inoculated spot was divided by the total number of plants inoculated and this referred as percentage of nodulating plants. A Student's t-test was performed to the means with no significant differences seen ($p>0.05$).

| Conditions | Percentage of nodulating plants |
|---|---------------------------------|
| Plants grown in control media and inoculated with bacteria grown in MM media. | 78% |
| Plants grown in DDG and inoculated with bacteria grown in MM media | 75% |
| Plants inoculated with bacteria grown in DDG supplemented MM media | 79% |

4.2.1.2 2-Deoxy-D-Glucose affects nodulation and rhizobial infection in both nitrate depleted and sufficient conditions

Plants pre-treated with 100 μM DDG for 24h prior to inoculation and plants growing in the presence of 100 μM DDG for 5 days were inoculated with rhizobia expressing the β -galactosidase gene (*S. meliloti* strain 1021 pXLGD4 lacZ). Roots were stained to reveal infection sites, nodule primordia and nodules which were counted in at least 20 plants per condition. The number of nodules (including nodule primordia and mature nodules) and infection threads (including infection threads and infection pockets) divided by the root length was used to calculate the density of events (Figure 4.6). Our results indicate a significant increase in infection thread and nodule density in DDG-treated plants in both conditions, pre-treatment and with constant exposure to DDG (Figure 4.6). Infection threads and frequency of colonized nodules in plants treated with DDG were similar to control plants grown in the presence of water (Figure 4.7). Roots were fixed and stained at the same time point post inoculation (7 dpi in this case) but notice that the extent to which the colonization of the nodule has occurred is different between control and DDG treated plants (Figure 4.7). It is difficult to

discern if these differences relay in a true phenotype (late colonization, for example) or if this is just the case of a slight older nodule primordia (control) compared to the DDG treated primordia. In any case, for the calculation of percentage of colonized nodules, all nodules, regardless of age or extent of colonization that presented blue staining were considered as 'colonized'.

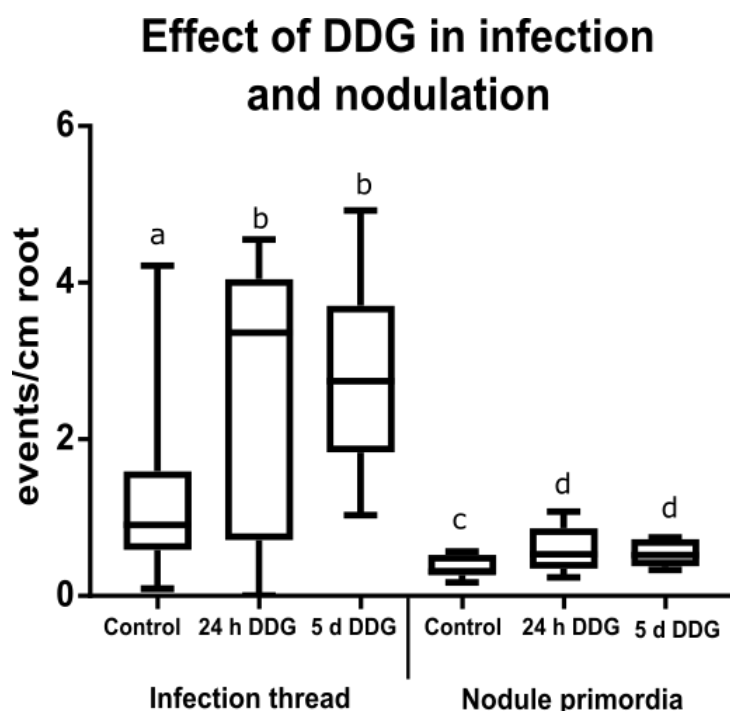


Figure 4.6- DDG treatment affects the density of nodules and infection threads in *M. truncatula* roots inoculated with rhizobia. 100 μ M DDG was applied either 24 hours prior inoculation or 5 days concomitant with the inoculation and infection process. Control plants were treated with water. Both, infection thread and nodule density were calculated by counting the number of events per cm of root length. Significant differences in comparison to control were detected in nodule density and infection thread density in both DDG treatments. A Student's t-test was performed, different letters indicate significant differences ($p < 0.01$).

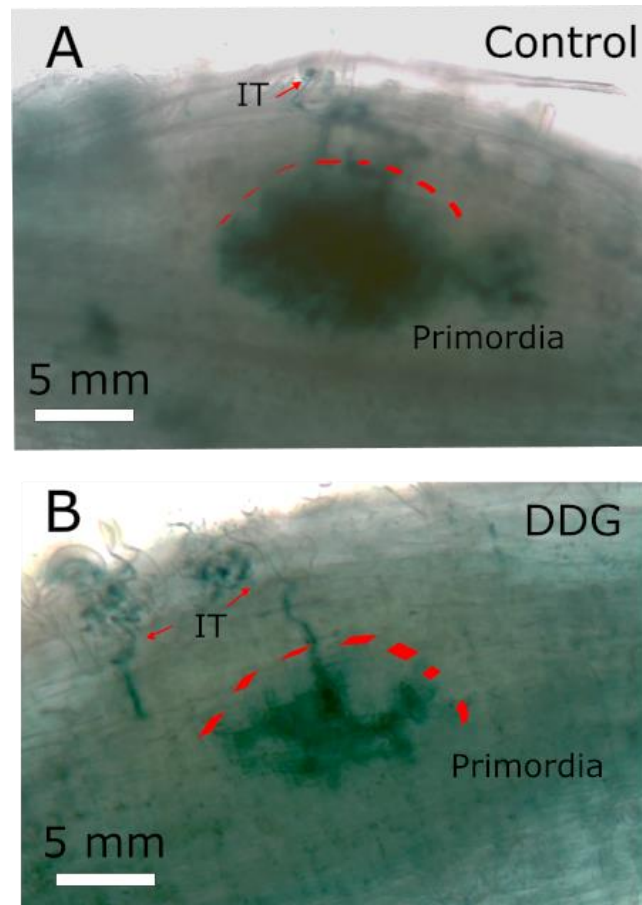


Figure 4.7 Examples of nodule primordia and infection threads (IT) in wild-type *M. truncatula* treated with 100 μ M DDG for 5 days or water (**control**) (A) 5 days old *Medicago* roots were grown in water and inoculated with rhizobia expressing lacZ. Infection threads (IT) are marked with a red arrow and nodule primordia delimited by red discontinuous lines. (B) 5 days old *Medicago* roots were grown in the presence of 100 μ M DDG concomitantly to inoculation with lacZ expressing rhizobia. IT are marked with a red arrow and nodule primordia delimited by red discontinuous lines. Roots were fixed and stained at the same time point post inoculation (7 dpi in this case) but notice that the extent to which the colonization of the nodule has occurred is different between these particular control and DDG treated plants.

Nodules are not efficiently formed in *M. truncatula* plants growing in the presence of 2 mM or 5 mM nitrate 7 dpi (Chapter 3- figure 3.3) but callose levels resembled non-nitrate conditions (lower at 24h after rhizobia inoculation) (Chapter 3-figure 3.5 and figure 3.6). DDG affects infection and nodulation in *M. truncatula* (Figure 4.6), thus its effects in nitrate conditions were evaluated. Plants were grown in

full nitrate and no-nitrate conditions for 5 days prior DDG application 24 hours prior inoculation or exposed for 5 days concomitant with rhizobia. Interestingly, plants treated with DDG appear to produce more infection threads than the untreated plants. Remarkably, DDG treatment in nitrate conditions was able to restore infection threads and nodule density to the same levels as untreated plants in no nitrate conditions (Figure 4.8). These results suggest that changes in callose levels prior infection might compensate for the inhibitory effect of nitrate in nodule formation in *M. truncatula*.

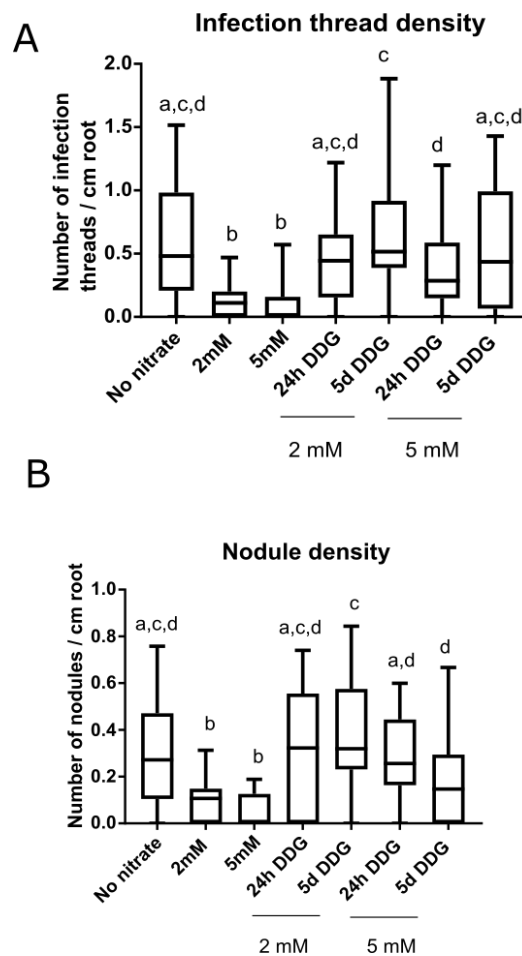


Figure 4.8- DDG treatment can recover infection and nodulation phenotype in nitrate sufficient conditions. *M. truncatula* plants were grown in FP media supplemented with potassium nitrate (0, 2mM and 5 mM final concentration) for 5 days. Plants were treated with 100 μ M DDG either for 24 h prior inoculation or for 5 days concomitant with infection. Control plants were grown in FP media (0, 2mM and 5mM nitrate) and treated with water as a control. 5 days post infection plants were stained to localise infection threads (IT), nodules and nodule primordia. (A) IT density (IT and infection pockets) in plants inoculated while growing in nitrate sufficient conditions and treated with 100 μ M DDG showed no significant difference to the control plants growing in no nitrate media and treated with water. (B) Nodules (primordia and mature nodules) density was not significantly different in control and nitrate condition (both with pre-treatment and concomitant exposure to DDG). A Student's t-test was performed, different letters refer to significant differences ($p < 0.01$).

4.2.2 Ectopic expression of a plasmodesmata-located callose degrading enzyme affects infection and nodulation

4.2.2.1 Ectopic expression of *MtBG2* affects the number of nodules and infection threads

After demonstrating in previous chapters of this thesis that *MtBG2* has callose degrading activity, and to further support the idea that callose plays a role in the establishment of symbiotic interactions, the *M. truncatula* gene was overexpressed in transgenic roots using a constitutive promoter and infection and nodulation phenotypes were studied.

M. truncatula roots transformed with a construct with *MtBG2* driven by the Ubiquitin promoter (*pUb-MtBG2-mcherry*) were inoculated with a saturated solution of *S. meliloti* (expressing *LacZ*) and stained to identify infection sites and nodule primordia 7 dpi. As control of transformation an empty backbone vector was used. Number of infection threads and nodules was higher in *M. truncatula* transgenic plants overexpressing *MtBG2* in comparison to transgenic plants expressing the empty vector as a control. Percentage of infected nodules was also calculated by counting blue (rhizobia containing) nodules in relation to the total number of nodules per plant (Table 4.4).

To assess the effect of constitutive *MtBG2* expression in root and nodule development, root length and the general aspect of composite plants were recorded. An average of 27 independent roots from composite plants were measured with no significant difference among control (empty vector transgenic) and *MtBG2* overexpressing plants (Figure 4.10). No obvious developmental abnormality was seen, apart from the higher number of nodules in these composite plants (Figure 4.11).

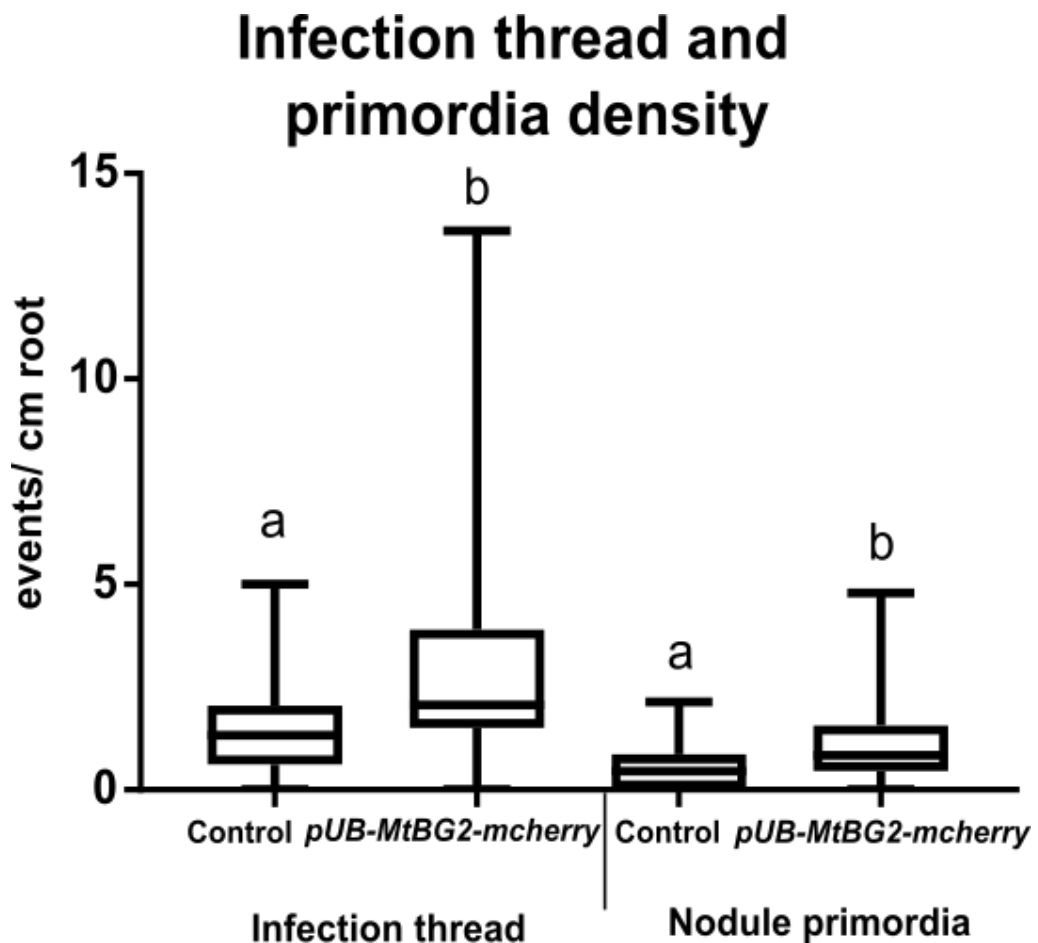


Figure 4.9- *M. truncatula* transgenic roots constitutively expressing MtBG2 show higher density of infection thread and nodule primordia compared to control roots expressing an empty vector. Roots were inoculated with *S. meliloti* expressing the β -galactosidase gene. 7 days post inoculation roots were stained to localise infection sites and nodule primordia. Roots expressing *MtBG2-mcherry* showed a higher number of both infection threads and nodule primordia compared to the control plants expressing an empty vector. A Student's t-test was performed, different letters refer to significant differences ($p < 0.05$).

Table 4.4- Percentage of infected nodules in composite plants expressing *pUb-MtBG2-mcherry* construct. *M. truncatula* roots were infected with *Sinorhizobium meliloti* expressing *lacZ*. 7 days post inoculation, plants were stained to localise bacteria within nodules and nodule primordia. The percentage of blue nodules in relation to the total number of nodules per plant was calculated. A Student's t-test was performed to the means with no significant differences seen ($p>0.05$).

| Composite plants expressing vector | Percentage of infected nodules |
|------------------------------------|--------------------------------|
| Control (empty backbone vector) | 78% |
| <i>pUb- MtBG2-mcherry</i> | 81% |

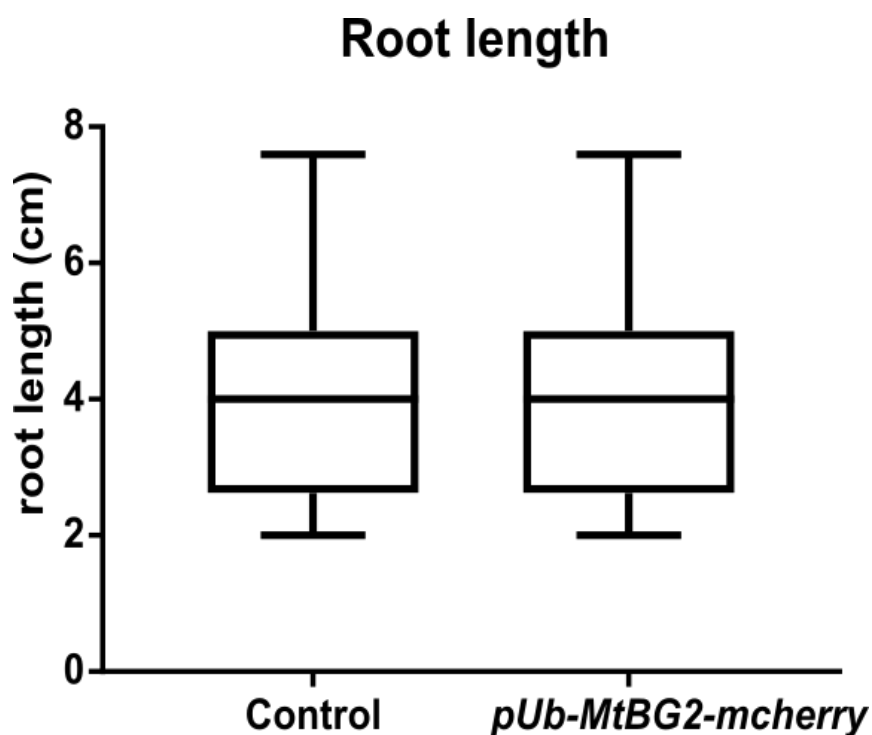


Figure 4.10- Root length is not affected by the expression of *pUb-MtBG2-mcherry*. *M. truncatula* transgenic roots transformed with the *pUb- MtBG2-mcherry* or an empty vector (control) were grown in plates and root length of the composite plants measured. A Student's t-test was performed, no significant differences were seen ($p>0.05$). (N=25).

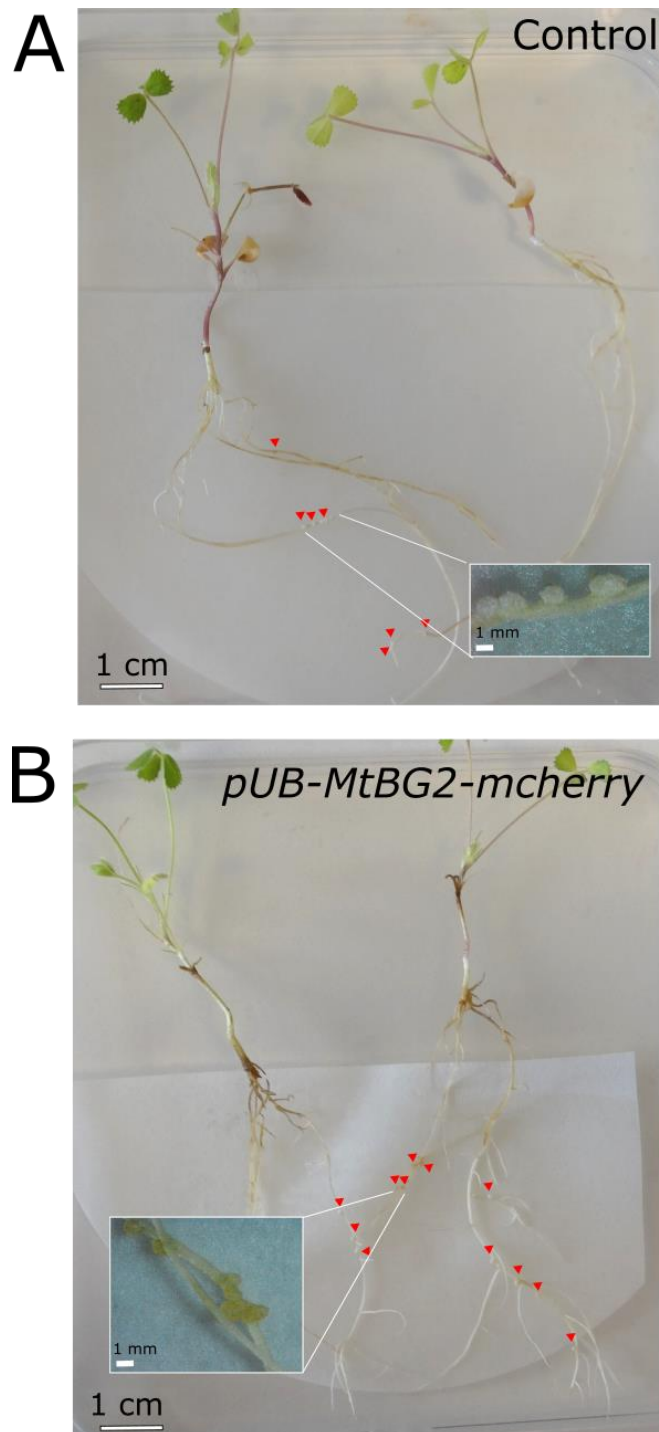


Figure 4.11- *M. truncatula* composite roots 14 days post inoculation. Composite plants were grown in FP media and inoculated with *S. meliloti*. Red triangles mark nodules. (A) *M. truncatula* transgenic roots expressing an empty vector as a control. (B) *M. truncatula* transgenic roots constitutively expressing *pUb-MtBG2-mcherry*

4.2.2.2 Ectopic expression of *MtBG2* is sufficient to offset the inhibition of nodulation by nitrate

M. truncatula transgenic roots expressing either an empty vector as a control or *pUb-MtBG2-mcherry* were grown in the presence of 5 mM nitrate for 9 days prior inoculation with rhizobia expressing the galactosidase gene. Roots were stained 7 dpi to localise infection sites and nodule primordia. Nitrate did not affect root length in either of the transgenic roots (Figure 4.12). Roots expressing the *pUb-MtBG2-mcherry* showed a higher number of nodules at 7 dpi in both nitrate and no-nitrate conditions, when compared to transgenic roots expressing an empty backbone vector (Figure 4.13). Infection success was very similar in plants expressing *pUb-MtBG2-mcherry* grown in nitrate-full conditions and plants infected in no nitrate (Figure 4.13-A). Nodule formation appears reduced by nitrate in both transgenic roots (expressing either *pUb-MtBG2-mcherry* or empty vector) (Figure 4.13-B) in comparison to plants growing and inoculated under no nitrate conditions, but roots overexpressing *MtBG2* in nitrate conditions showed similar nodule density as control plants in nitrate-depleted media (Figure 4.13-B). Given that number of nodules was already higher in plants overexpressing *MtBG2* compared to control plants expressing an empty vector, the 'inhibition rate' was calculated by dividing the number of events (both infection threads and nodules) in no nitrate conditions by the number in nitrate (5mM) conditions. By these means, it was shown that the inhibitory effect of nitrate was two times stronger in plants overexpressing *MtBG2* compared to plants expressing an empty vector as a control (Table 4.5).

The general aspect of composite plants was similar among control and plants expressing *pUb-MtBG2-mcherry* construct 14 dpi grown in full nitrate conditions (Figure 4.14). Percentage of infected nodules in nitrate-replete media was also calculated but not significant difference was observed (Table 4.6).

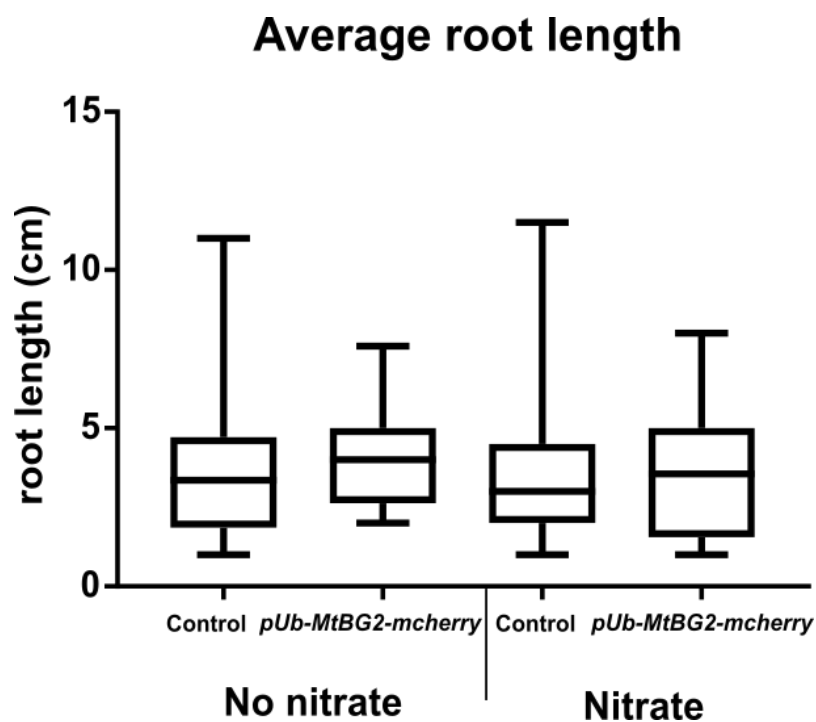


Figure 4.12- Nitrate does not affect root length in *M.* roots expressing *pUb-MtBG2-mcherry*. Roots expressing either an empty vector as a control or *pUb-MtBG2-mcherry* were measured in 5mM nitrate or no nitrate conditions. A Student's t-test was performed, no significant differences were seen ($p > 0.05$). (N=35)

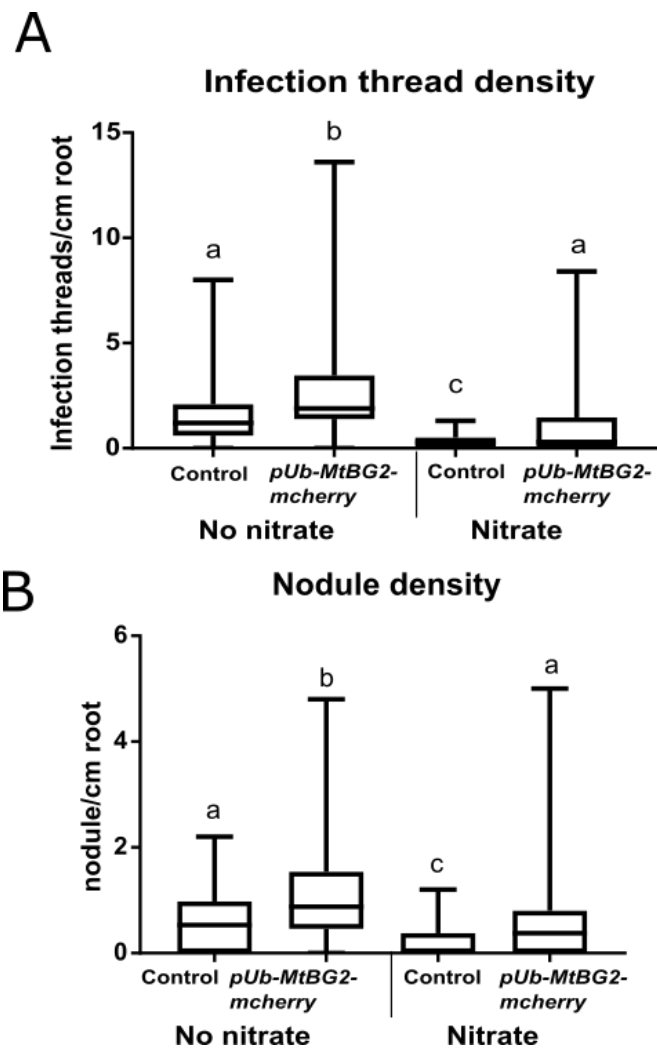


Figure 4.13- *M. truncatula* roots constitutively expressing MtBG2 show inhibition of nodulation and in infection thread in high nitrate conditions. Composite plants expressing an empty vector (control) or *pUb-MtBG2-mcherry* were grown in media supplemented with no nitrate or 5mM nitrate and inoculated with *S. meliloti* expressing the β -galactosidase gene. 7 days post inoculation roots were stained to localise infection sites and nodule primordia. (A) The density of infection threads (IT) is affected by nitrogen availability in the growing media in both control roots and in roots expressing *pUb-MtBG2-mcherry*. Infection threads density in plants overexpressing *MtBG2* growing in high nitrate conditions was similar to control (empty vector) plants growing under no nitrate. (B) The density of nodules (primordia and young nodules) is affected by nitrogen availability in the growing media in both control roots and roots expressing *pUb-MtBG2-mcherry*. Nodule density in plants overexpressing *MtBG2* growing in high nitrate conditions was similar to control (empty vector) plants growing under no nitrate. A Student's t-test was performed, different letters refer to significant differences ($p < 0.05$).

Table 4.5-Effect of nitrate in infection and nodulation in control and overexpressing *MtBG2* plants. The 'inhibition rate' was calculated by dividing the number of events (infection threads and nodule) in no nitrate conditions by the number of events in 5mM nitrate conditions.

| Composite plant expressing vector | Infection threads inhibition rate | Nodules inhibition rate |
|--|--|--------------------------------|
| Control (empty backbone vector) | 2.2 | 1.5 |
| <i>pUb-MtBg2-mcherry</i> | 5.4 | 3 |

Table 4.6- Percentage of infected nodules in composite plants expressing *pUb-MtBG2-mcherry* construct and growing in 5mM potassium nitrate. *M. truncatula* roots were infected with *S. meliloti* expressing the galactosidase gene. 7 days post inoculation plants were stained to localise bacteria within nodules and nodule primordia. The percentage of blue nodules in relation to the total number of nodules per plant was calculated. A Student's t-test was performed to the means with no significant differences seen ($p>0.05$).

| Composite plant expressing vector | Percentage of infected nodules |
|--|---------------------------------------|
| Control (empty backbone vector) | 77% |
| <i>pUb- MtBG2-mcherry</i> | 79% |

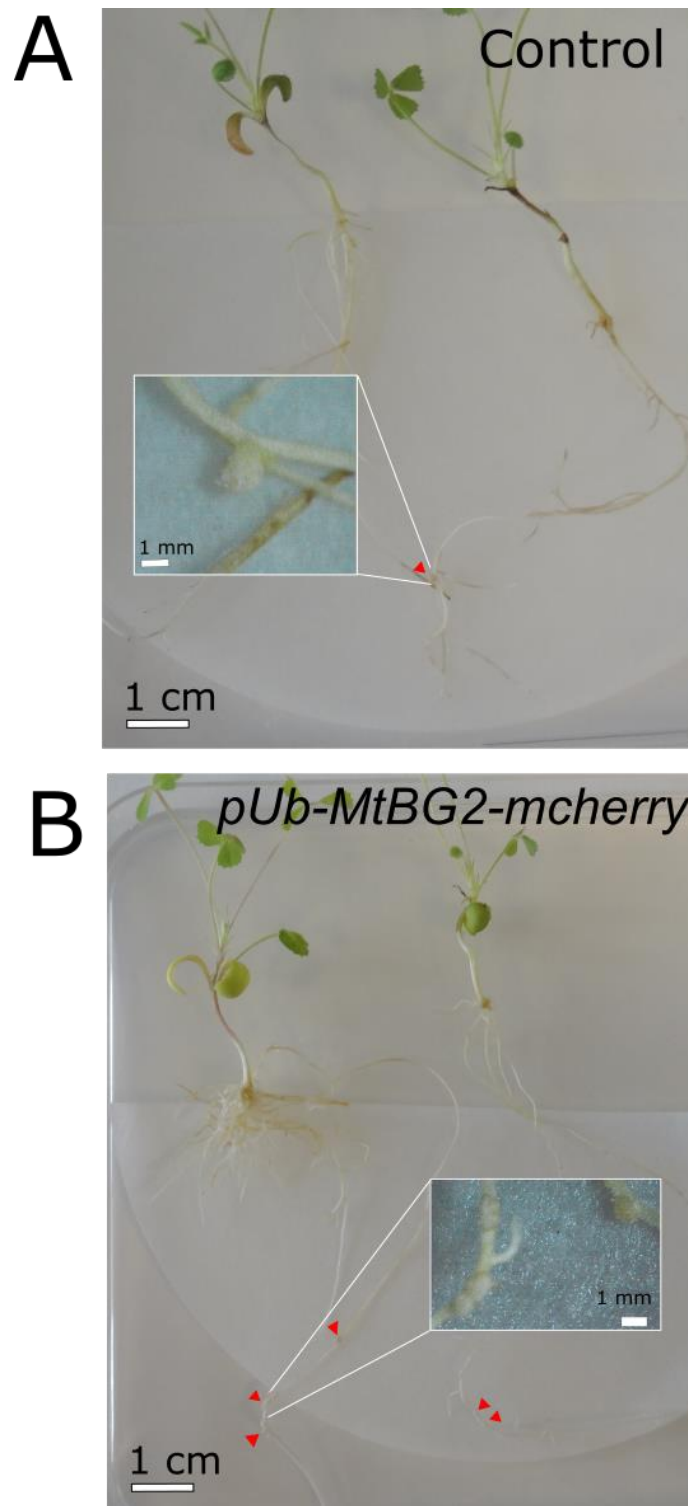


Figure 4.14- *M. truncatula* transgenic roots 14 days post inoculation in nitrate conditions. Composite plants were grown in FP media supplemented with 1 μ M of AVG and 5mM potassium nitrate and inoculated with *S. meliloti*. Red triangles mark nodules. (A) *M. truncatula* roots expressing the empty vector as a control. (B) *M. truncatula* roots constitutively expressing *pUb-MtBG2-mcherry*.

MtBG2 ectopic expression reduces callose levels in no nitrate conditions in comparison to control (root expressing an empty vector) (Chapter 3, Figure 3.7). To determine if the effect in nodulation and infection seen in nitrate conditions was linked to a further reduction in callose levels, callose immunolocalisation was performed. Longitudinal section of plants grown in no nitrate (0 mM) or nitrate (5mM) expressing *pUb-MtBG2-mcherry* 24 hpi with mock (water) or rhizobia cultures were used for these experiments. Just as in control plants, there was not a significant difference in callose labelling between un-inoculated plants expressing *pUb-MtBG2-mcherry* and growing in no nitrate and nitrate media (Figure 4.15). Furthermore, and contrarily to what has been seen in control plants, no further downregulation in callose levels after inoculation was seen, neither in nitrate-depleted conditions nor in full nitrate conditions (Figure 4.15).

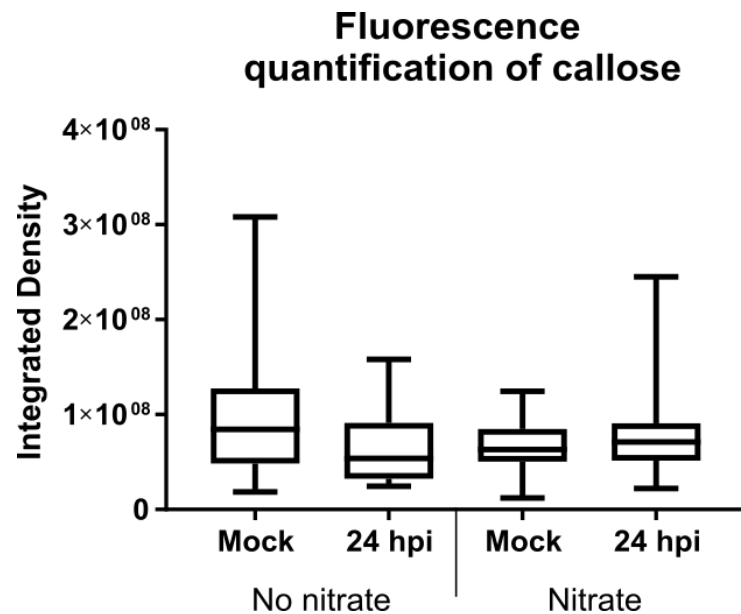


Figure 4.15- Callose remains the same in *M. truncatula* transgenic roots expressing *pUb-MtBG2-mcherry* inoculated with mock or rhizobia cultures in no nitrate and nitrate sufficient conditions. *M. truncatula* roots expressing *pUb-MtBG2-mcherry* and grown in 5mM nitrate or no nitrate media were either inoculated with water (mock) or with *S. meliloti* suspension (24 hpi). Callose immunolocalisation was performed 24 hours post inoculation (hpi) with monoclonal antibodies and the fluorescent signal detected after incubation with an Alexa-488 conjugated secondary antibody. Callose deposition was inferred by calculating the integrated density in ImageJ in at least 3 biological repetitions per condition. Fluorescence was quantified in a region of interest of approximately $100\mu\text{m}^2$. A Student's t-test was performed, no significant differences were seen ($p > 0.05$).

4.3 Discussion

4.3.1 The regulation of callose is probably required to control nodule number in both nitrate depleted and sufficient conditions

In Chapter 3 of this thesis it was shown how callose is downregulated upon inoculation of *M. truncatula* roots with rhizobia and it was also reported the discovery of a novel *M. truncatula* callose-degrading enzyme, which expression appears up-regulated upon rhizobia inoculation. In this section it is presented that *M. truncatula* plants treated with the callose biosynthesis inhibitor 2-Deoxy-D Glucose (DDG) showed an increase in the number of nodules and the number of infection sites. As far as it was seen, DDG treated plants were not phenotypically different from wild type, but the infection process was significantly more efficient. 24 hours of treatment prior to inoculation was sufficient to see an effect in the number of nodules and infection sites, strongly supporting our hypothesis that callose plays a role in the very early stages of infection, probably in the regulation of signalling.

Moreover, *M. truncatula* transgenic roots ectopically expressing the newly identified plasmodesmata-located glucanase *MtBG2* showed an increase in infection and nodule number. *Medicago* transgenic roots constitutively expressing *MtBG2* presented a similar phenotype in terms of root length and general aspect of the composite plant to plants transformed with the empty vector as a control. Nodules and infection threads did not appear phenotypically different from wildtype and the percentage of infected nodules did not vary either. These results suggest that endosymbiotic colonization of the nodule is not affected in the composite plants, but instead there is an increase capacity to form these relations.

M. truncatula plants expressing the viral movement protein (MP) of the Tobacco Mosaic Virus (TMV) under a constitutive promoter also showed increased number of nodules (Complainville et al., 2003). Tobamoviral MPs have been largely linked to plasmodesmata and changes in its connectivity (Ding et al., 1992; Beachy and Heinlein, 2000; Amari et al., 2010; Yuan et al., 2016). MPs

are known to increase plasmodesmata aperture through, among other mechanisms, activation of β -1, 3-glucanases. In light of the results reported in this chapter, it can be proposed that changing callose levels and plasmodesmata connectivity using either the callose synthase inhibitor DDG or the overexpression of a *M. truncatula* glucanase, before rhizobia inoculation is sufficient to improve the success of infection and to manipulate nodule number. Further studies are required to discern whether nitrogenase activity remains unaltered in the composite plants, or if an increase in the number of nodules improves nitrogen assimilation.

Constitutive *MtBG2* expression reduces callose levels in cell walls in comparison to control transgenic expressing an empty vector (Chapter 3, Figure 3.17). Analysis of inoculated roots indicates that transgenic roots ectopically expressing *MtBG2* did not regulate callose further upon inoculation with rhizobia. This might suggest that callose regulation upon inoculation only occurs when callose levels at the cell wall are above a certain threshold or that the technique used is not sensitive enough to detect these differences.

The number of nodules seen in plants treated with DDG or transgenic roots expressing the *pUb- MtBG2-mcherry* construct, although significantly higher compared to plants untreated (growing in water) or transformed with an empty vector, are not close to those found in supernodulation mutants (Schnabel et al., 2005; Lim et al., 2010; Schnabel et al., 2010). Autoregulation of nodulation (AON) is a tightly controlled process by which the plant regulates the number of nodules that will form depending on their nutritional status. Environmental and genetics cues such as nitrate concentration in the soil, hormonal signals and number of infection threads and nodule primordia play a role in regulating the number of final nodules (Ferguson et al., 2010; Kassaw et al., 2015). Our results suggest that callose regulation might contribute to some of the steps of the non-essential AON pathway thus, different from wildtype, plants impaired in callose regulation might be able to overcome to some extent the shoot-derived signals and not trigger a negative regulatory feedback, leading to a higher number of nodules but not to supernodulating mutant phenotypes.

Alternatively, the number of nodules and infection threads reported in plants treated with DDG and overexpressing *MtBG2* plants are more similar to plants overexpressing the *ENOD40* gene (reviewed in more detailed in section 4.3.2) (Charon et al., 1999) and in the *Lotus japonicus* mutant *ein1-2* (Breakspear et al., 2014), involved in ethylene signalling. Both cases have in common the role of ethylene and potentially cytokinins (Charon et al., 1999; Roberts and Oparka, 2003; Benitez-Alfonso et al., 2010). It is possible that modifying callose either by DDG or overexpressing a callose degrading enzyme is affecting the balance of hormones that controls number of nodules, affecting the total number of nodules in plants with altered callose deposition pattern.

The experiments presented in this chapter showed that plants with reduced callose levels, either through chemical or genetics approaches, did not respond to nitrate availability similarly to wild-type plants in terms of nodulation. *MtBG2* overexpressing plants showed a higher N-inhibition rate than control plants in the same conditions (Table 4.5). Although the N-inhibition rate is higher in these plants the total number of nodules 7 dpi and after treatment is still higher. The effect of callose regulation described above might also be linked to nitrate perception which also contributes to control of nodulation, explaining why plants overexpressing *MtBG2* show a higher number of nodule even in the presence of higher concentration of nitrate in the media. It might also be possible that the effect seen is due to the fact that overexpressing *MtBG2* plants are already developing more nodules, hence the total number of nodules after nitrate inhibition would also be higher. Proportionally, the overexpressor was more sensitive to nitrate but, in terms of absolute nodule number, *MtBG2* overexpression plants can tolerate higher levels of nitrate. However, it is also important to remember that inhibition of nodulation might not be acting in a linear and proportional way. A more thorough analysis of the nodulation process under high nitrate conditions would reveal if plants overexpressing *MtBG2* present any kind of insensitivity to nitrate. For example, studying growth rates of the nodules (do they grow faster?), size of nodule primordia or arrested infection threads could help determine to what extent is callose downregulation affecting control of nodulation by nitrate.

Additionally, all experiments exploring the effect of nitrate in nodulation were done in plates, it is therefore possible that this phenotype is not maintained in plants growing in soil. Furthermore, nitrate was applied from the germination stage and throughout the infection and nodulation processes, hence the effect of applied nitrate in the media of plants at later stages of nodulation and infection was not assessed. Future experiments in soil and/or applying nitrate treatments in different stages of the symbiotic process would enrich our understanding of the role of callose in this response.

Nitrate availability inhibits nodule growth and nitrogenase activity and also the formation of new infection sites and nodules (Streeter, 1985a, b). Several authors have identified legumes mutants that showed both a supernodulation phenotype and a tolerance to nitrate availability. For example, *har1*, *nark*, *sym29* and *sun* mutants are able to nodulate in the presence of high nitrate in the environment (Carroll et al., 1985a; Sagan and Duc, 1996; Sagan and Gresshoff, 1996; Wopereis et al., 2000; Penmetsa et al., 2003; Oka-Kira et al., 2005; Schnabel et al., 2005; Magori et al., 2009). These results suggest that nitrate tolerance and the AON in legumes might share some of the regulatory signals or steps in the signalling pathway in *M. truncatula*. On the other hand, the nitrate-tolerant phenotype in these mutants might also be a secondary phenotype. For example, nitrate might negatively regulate the transport of auxin or other signals needed for the control of nodulation, ultimately affecting the number of nodules that are generated. Auxin has also been identified as an important mediator of nitrate effect on root branching in Arabidopsis (Zhang et al., 1999). Interestingly, accumulation of auxin in the infection zone of *M. truncatula* roots in response to rhizobia 24 hpi occurred in both the absence or in the presence of nitrate (van Noorden et al., 2016). Although nitrate does not prevent auxin accumulation, at least at this time point, these plants failed to form a defined auxin maximum in the cortex, which was seen in plants grown in no-nitrate conditions. Cortical cell division could not be seen either (van Noorden et al., 2016). It is still not known if the supernodulating mutants that present a nitrate-insensitive phenotype allow auxin to be accumulated at the nodule primordia site when grown in nitrate. It would also be interesting to characterise the auxin accumulation of plants grown in nitrate and treated with DDG or overexpressing MtBG2. Future experiments

addressing this will shed some light into the mechanisms behind control of nodulation by nitrate in these plants.

Nitrate is also known to affect levels of cytokinin, an essential factor for nodule formation in legumes (Caba et al., 2000; Mathesius et al., 2000). The downregulation of callose deposition might affect cytokinin levels and/or movement, affecting nodule formation. The role for the symplastic pathway in the transport of cytokinins through the phloem has been proposed in Arabidopsis plants. An Arabidopsis line with an over-accumulation of callose in phloem cells was loaded with radioactive cytokinin by the hypocotyl, leading to a 4-fold reduction of cytokinin concentration in the root meristem compared to wild type treated in the same conditions (Absmanner et al., 2013). Further studies analysing whether the accumulation of hormones, such as auxin and/or cytokinin, is differently regulated when callose is depleted could indicate a link with the increase in nodulation observed in full nitrate conditions.

4.3.2 The increase in infection thread formation in callose depleted roots suggests a positive feedback linking infection and nodulation

Autoregulation of nodulation does not only involve the regulation of the number of nodules, but also infection threads that will develop and reach the cortex (Mortier et al., 2012). Plants overexpressing the callose degrading enzyme *MtBG2* did not only show a higher number of nodules, but the number of infection threads that developed from rhizobia inoculation was higher.

Similar effects were seen in *M. truncatula* transgenic plants overexpressing the early nodulin gene *ENOD40*. A higher number of both infection threads and nodules were seen. Nodules also developed faster, since nodule primordia appeared bigger at the same developmental stage compared to control plants (Charon et al., 1999). Interestingly, plants overexpressing *ENOD40* showed a higher number of infection threads and nodules at 18 dpi, but the numbers reached wild type levels at 30 dpi (Charon et al., 1999). Infection and nodulation were never assessed after 14 dpi in plants overexpressing *MtBG2*, hence whether the increase in the number of infection thread and nodules seen at that

time point is maintained or it will eventually stabilise is not known. The developmental stage of nodule primordia was not examined, so it would also be interesting to assess whether nodule primordia grow faster or the infection rate (infection events/time) is affected in these plants.

Several other mutants affected in the number of nodules have been characterised also have changes in the number of infection threads. For example, mutants in the *SUNN* receptor also show a higher number of infection threads compared to wild type plants (Parniske, 2004). On the other hand, the supernodulating mutant *astray* in *L. japonicus* shows a higher number of nodules but the number of infection threads remained unaltered (Nishimura et al., 2002).

Based on our results we can propose two hypotheses: 1) degradation of callose might trigger a signalling pathway that improves root hair infection success, leading to a higher number of nodule primordia and mature nodules. Additionally, a degradation of callose in the cell wall could lead to a weakened root hair, making easier for the rhizobia to enter the epidermis. Alternatively, 2) the negative feedback that occurs in wild type where nodule primordia inhibit the formation of new infection threads (Reid et al., 2011b; Kassaw et al., 2015) might be compromised in plants with modified callose patterns, explaining why it is also seen an increased number of infection threads.

In order to dissect among these two hypotheses, infection and nodulation can be characterised in *M. truncatula* mutants affected in the cell wall to determine if it plays a role in the infection success. Alternatively, the use of a mutant that is able to undergo infection but impaired in the formation of nodules would be useful to determine if the higher number of infection threads is an effect of a compromised negative feedback from the nodule primordia or an actual phenotype from the downregulation of callose.

Chapter 5

Chapter 5 – Using symbiotic promoters to determine the temporal and spatial requirements for callose regulation during nodulation

5.1 Summary

Reducing callose through the constitutive expression of a *M. truncatula* β -1, 3-glucanase or via treatment with the callose synthase inhibitor DDG leads to a significant increase in infection threads and nodule primordia (Chapter 4). These two approaches target general callose deposition throughout the root but do not allow to temporarily or spatially control the modification of the polysaccharide.

The role of Arabidopsis β -1, 3-glucanases in the regulation of callose and plasmodesmata during different developmental processes has been reported in the past years (Neale et al., 1990; Morohashi and Matsushima, 2000; Benitez-Alfonso et al., 2013; Maule et al., 2013). In this chapter, an heterologous β -1, 3-glucanase (identified in Arabidopsis and named PdBG1 (Benitez-Alfonso et al., 2013) was expressed under infection and nodulation-specific promoters. These promoters in the early stages of symbiosis are regulated at different stages of the infection and nodulation process and in different cell layers. The activity of these promoters is mainly epidermal and infection-related for *MtERN1* and *MtNFB*, whereas *MtNIN* is activated both in the epidermal and cortical cell layer to regulate during infection and nodule organogenesis processes (Andriankaja et al., 2007; Marsh et al., 2007; Plet et al., 2011; Vernie et al., 2015). The role of these genes in symbiotic colonization is described in the Introduction (Chapter 1, sections 1.2.2.1 and 1.2.2.2). The aim was to ectopically modify callose at different infection and nodulation stages.

In sections 5.2.2 and 5.2.3 the results of studying nodulation and infection phenotypes in these transgenic lines are presented. In brief, nodulation and infection improved in all the transgenic plants although with different efficiency levels.

In the discussion section, these results are integrated with those obtained in Chapter 4 and with current literature in the regulation of the cell wall architecture

during plant-microbes interactions. Suggestions for future work are also included in this section.

5.2 Results

5.2.1 PDBG1, a bona-fide β -1,3-glucanase as a tool to reduce plasmodesmata-associated callose in *M. truncatula*

Callose degrading activity for the plasmodesmata located β -1, 3-glucanase PdBG1, involved in secondary root organogenesis (lateral root formation) in *A. thaliana*, has been demonstrated (Benitez-Alfonso et al., 2013). The protein displays a high degree of similarity (67%) and the same conserved domain as *MtBG2*, and was selected here as a tool to ectopically modify plasmodesmata-associated callose in *M. truncatula*.

To verify the localisation of PdBG1 in *M. truncatula*, a fusion version of the protein with eGFP was created and ectopically expressed under the infection specific promoter *pMtERN1* in *M. truncatula* roots (Figure 5.1). Co-localisation with callose deposits, revealed with aniline blue staining (as described in Materials and Methods), showed a punctate pattern in the cell periphery resembling plasmodesmata localisation.

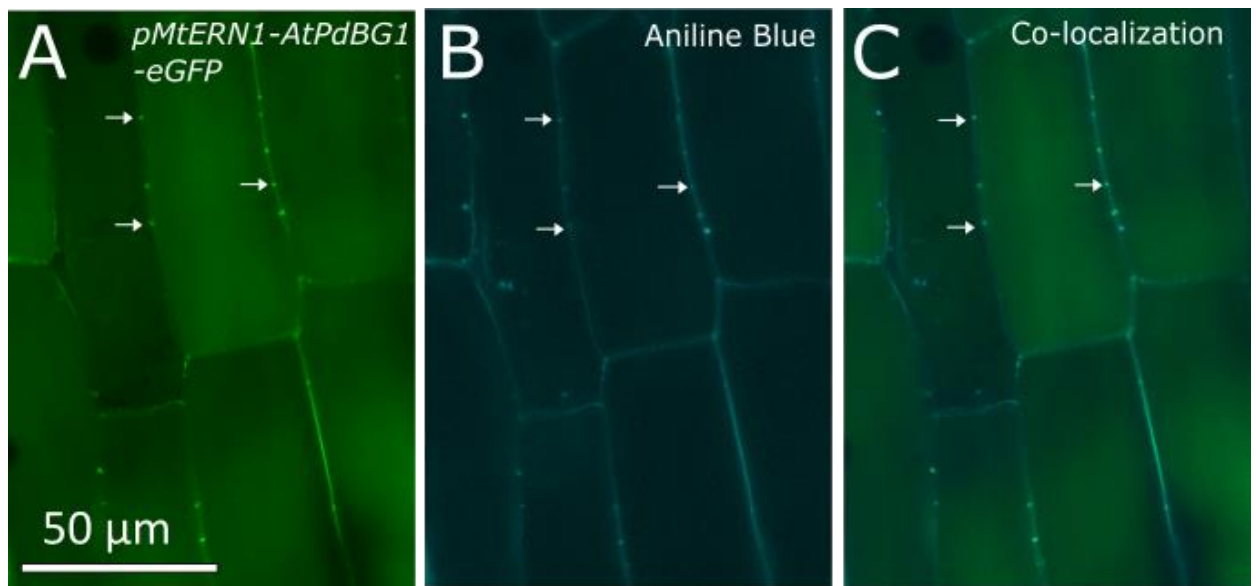


Figure 5.1- *Arabidopsis thaliana* β -1, 3-glucanase PdBG1 localises in the cell periphery in a pattern that resembles plasmodesmata sites in *M. truncatula* roots. (A) Confocal microscopy of roots cortical cells expressing the *pMtERN1-AtPdBG1-eGFP* construct 24 hours post inoculation with rhizobia shows PdBG1 (green channel) localization in the cell periphery (arrows). (B) Callose revealed by aniline blue staining (cyan channel) in the same region of the root shows similar localization pattern (C) Green and cyan channel pictures superimposed revealed co-localisation of PdBG1 and callose (arrows) suggesting plasmodesmata targeting.

In order to determine PdBG1 glucanase activity in *M. truncatula* roots, PdBG1 was expressed under the constitutive p35S promoter and callose immunolocalisation was carried out using roots expressing an empty vector as a control. Antibody signal was quantified to infer callose levels. A strong downregulation of callose deposition was seen in transgenic roots expressing the p35S-*AtPdBG1* vector compared to control plants, suggesting that PdBG1 function as a callose degrading enzyme in *M. truncatula*.

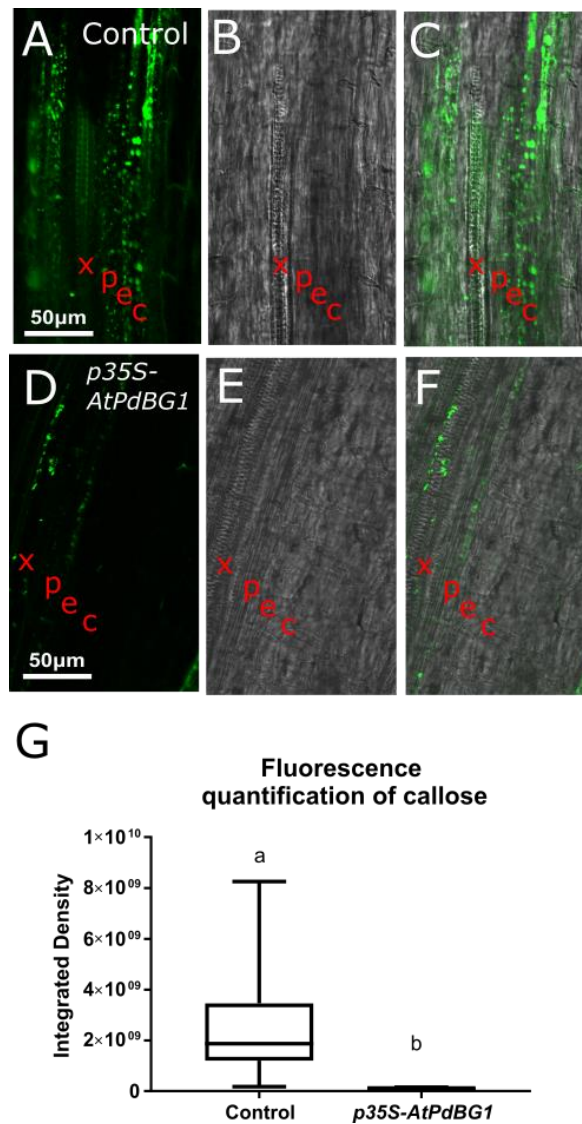


Figure 5.2- Arabidopsis PdBG1 displays callose degrading activity in *M. truncatula*. Immunolocalisation of callose revealed a down-regulation of the polysaccharide at the cell wall of *M. truncatula* over-expressing Arabidopsis *PdBG1* (A-C) compared to control plants expressing an empty vector (D-F). Callose was detected using a monoclonal anti-callose antibody and Alexa-488 (green) conjugated secondary antibody (A and C). Bright field (B and E) and composite image are shown to help section localisation (C and F). (G) Fluorescence quantification of callose was performed by calculating the integrated density using ImageJ for each image in at least 3 biological repetitions per conditions. Fluorescence was quantified in a region of interest of approximately $100\mu\text{m}^2$. Symbols in A to F refer to xylem vessel (x), pericycle (p), endodermis (e), and cortex (c). A Student's t-test was performed, different letters indicate significant differences ($p < 0.001$).

5.2.2 Expressing *PdBG1* under infection and nodulation promoters leads to a higher number of nodules

To discern if temporal and spatial regulation of callose affect *Medicago*-rhizobia interaction, transgenic plants expressing the *Arabidopsis* glucanase *PdBG1* under *MtERN1*, *MtNIN* and *MtNFB* promoters were generated using Goldengate technology. These were inoculated with mock (water) or rhizobia cultures and nodules were identified and counted 14 dpi as described in Material and Methods (Section 2.1.3). Roots carrying either the *pMtERN1-AtPdBG1*, *pMtNIN-AtPdBG1* or *pMtNFB-AtPdBG1* constructs showed a significant increase in the number of nodules (Figure 5.3) in comparison to control roots transformed with an empty (backbone) vector. The results suggest that nodule organogenesis is improved by ectopic expression of *PdBG1* with similar efficiency regardless of the promoter. Composite plants were divided into categories depending on the number of nodules in each plant. Most composite plants showed 4 or more nodules (Figure 5.4) but there is a clear increase in the (>80%) of *pMtERN1-AtPdBG1* transgenic plants that fall in this category in relation to control and other transgenic lines.

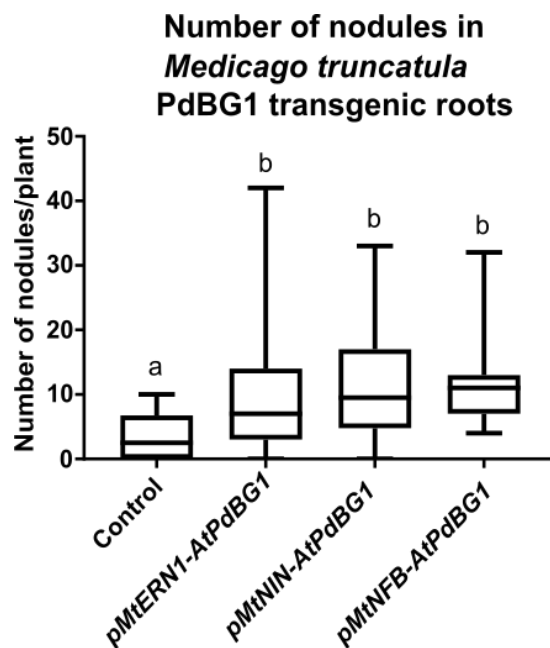


Figure 5.3- Ectopic expression of the Arabidopsis β -1, 3- glucanase PdBG1 improves nodulation. The total number of nodules was counted in *M. truncatula* roots expressing Arabidopsis PdBG1 under infection and nodulation- promoters (*pMtERN1*, *pMtNFB* and *pMtNIN*) 14 days post inoculation with *S. meliloti* and compared to transgenic carrying an empty vector (control). Only mature nodules were counted. A Student's t-test was performed, different letters indicate significant differences ($p < 0.001$).

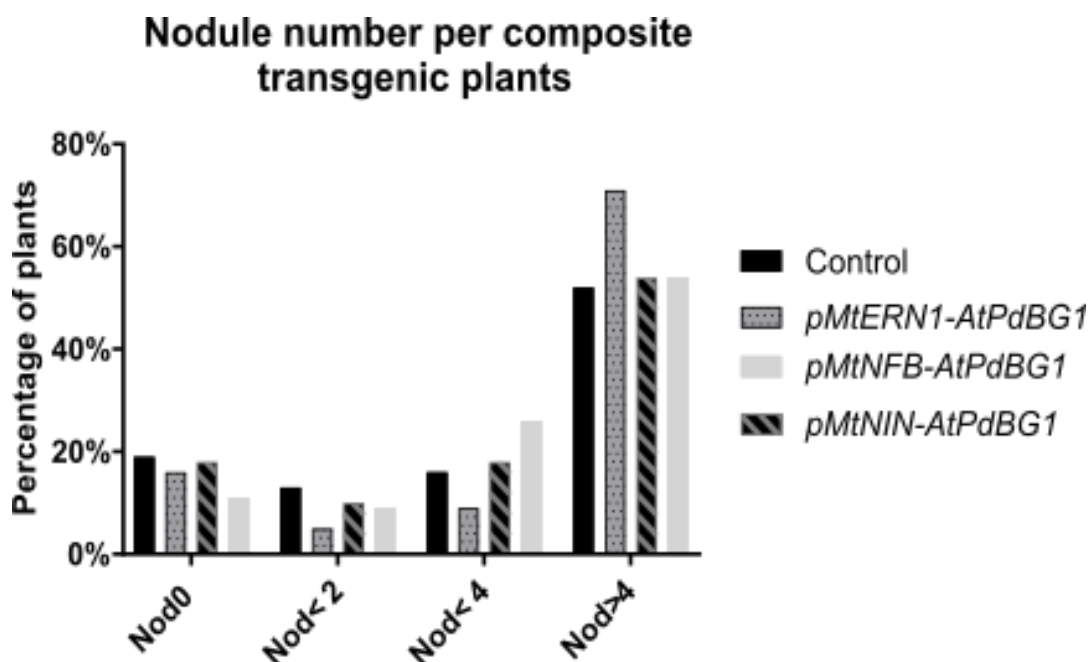


Figure 5.4- The majority of *M. truncatula* plants show more than 4 nodules per plant. The number of plants showing no nodules, 2 or fewer nodules, 4 or fewer nodules or more than 4 nodules in control (expressing an empty vector) and *PdBG1* transgenic plants (expressing from either the *MtERN1*, *MtNFB* or *MtNIN* promoters) was counted 14 days post inoculation with rhizobia. The numbers are expressed in percentage (%) relative to the total number of plants.

5.2.3 Roots expressing the *pMtERN1-AtPdBG1* construct show a higher number of infection threads

Transgenic roots expressing the *pMtERN1-AtPdBG1* construct showed a higher percentage of plants forming more than 4 nodules despite this promoter being associated with infection. To more clearly dissect this phenotype, the formation of infection pockets and threads were evaluated after X-Gal staining of *pMtERN1-AtPdBG1* roots 7 dpi (Figure 5.5). A higher density (number of events per cm of root length) in infection threads was observed in transformed roots when compared to control roots carrying the empty vector (Figure 5.5). At that specific time point and inoculation conditions, no differences were found in the nodule primordia density, contrasting with results obtained 14 days post inoculation (Figure 5.3).

The percentage of infected nodules in roots transformed with the vector *pMtERN1-AtPdBG1* does not significantly differ from control conditions, suggesting a normal colonisation of the nodule (Table 5.1).

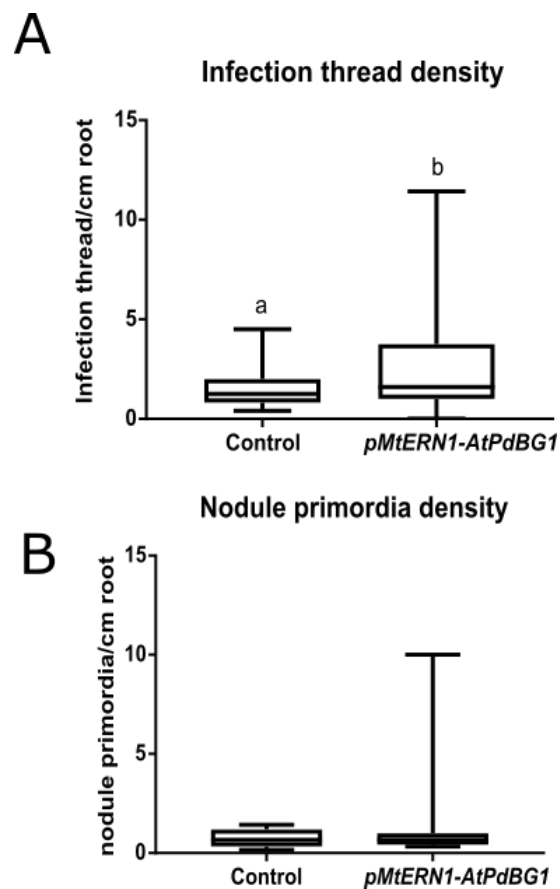


Figure 5.5- PdBG1 expression in *M. truncatula* affects the number of infection threads. (A) Infection threads and infection pockets were counted together 7 days post inoculation with rhizobia expressing the *LacZ* gene. After X-gal staining, the total number of events was used to calculate density (total number of infection threads and infection pockets/cm of root). Differences were significant. A Student's t-test was performed, different letters indicate significant difference ($p < 0.05$). (B) Nodule primordia were counted in the same roots 7dpi. Only infected primordia (stained blue or uninfected primordia but with a clear infection thread above it) were counted. A Student's t-test was performed, with no significant differences ($p > 0.05$).

Table 5.1- Percentage of infected nodules in composite plants expressing pMtERN1-AtPdBG1 construct. *M. truncatula* roots were infected with *S. meliloti* expressing the β -galactosidase gene. 14 dpi plants were stained to localise bacteria within nodules and nodule primordia. The percentage of blue nodules in relation to the total number of nodules per plant was calculated. A Student's t-test was performed to the means with no significant differences seen ($p>0.05$).

| Composite plant expressing vector | Percentage of infected nodules |
|-----------------------------------|--------------------------------|
| Control (backbone vector) | 72.4% |
| pMtERN1-AtPdBG1 | 77.8% |

5.2.4 Root phenotype, nodule development and colonisation are not affected in roots expressing PdBG1

In order to discern if plants expressing AtPdBG1 showed defects in root development plant weight (both root and shoot), length, width, nodule maturity (assessed by pink colouration and size) and nodule colonisation were measured.

No significant differences were seen in root development, morphology or weight compared to the control with the exception of composite plants expressing the pMtNIN-AtPdBG1 construct, that showed a higher root weight (Figure 5.6 and Figure 5.7). Nodule size and general appearance are normal in transgenic roots expressing AtPdBG1 (Figure 5.8), suggesting a normal function of the nodule. Inoculated plants were stained to reveal nodule primordia and infection threads (Figure 5.9). The general aspect of infection thread, pockets and root hairs appeared normal in plants expressing pMtERN1-AtPdBG1 (Figure 5.9).

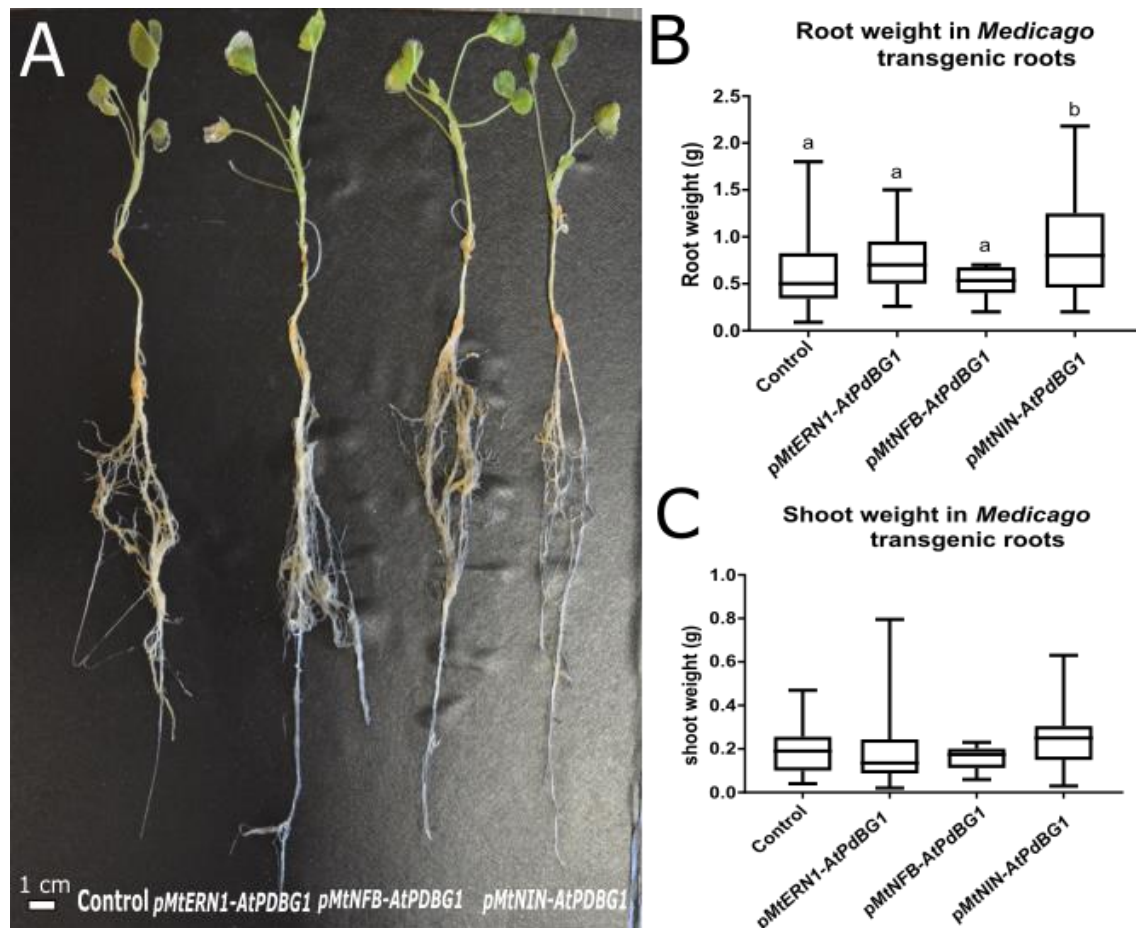


Figure 5.6- Phenotype of *Medicago* transgenic roots expressing PdBG1 under different promoters. (A) The general aspect of the root and shoot of *M. truncatula* 24 days post-transplant to the soil. (B) Root weight was measured for 40 roots per transgenic. Only plants expressing pMtNIN- PdBG1 had a significantly higher root weight. A Student's t-test was performed, different letters indicate significant differences ($p < 0.05$). (C) Shoots were also weighed (N=40). No significant difference was found among the different transgenic.

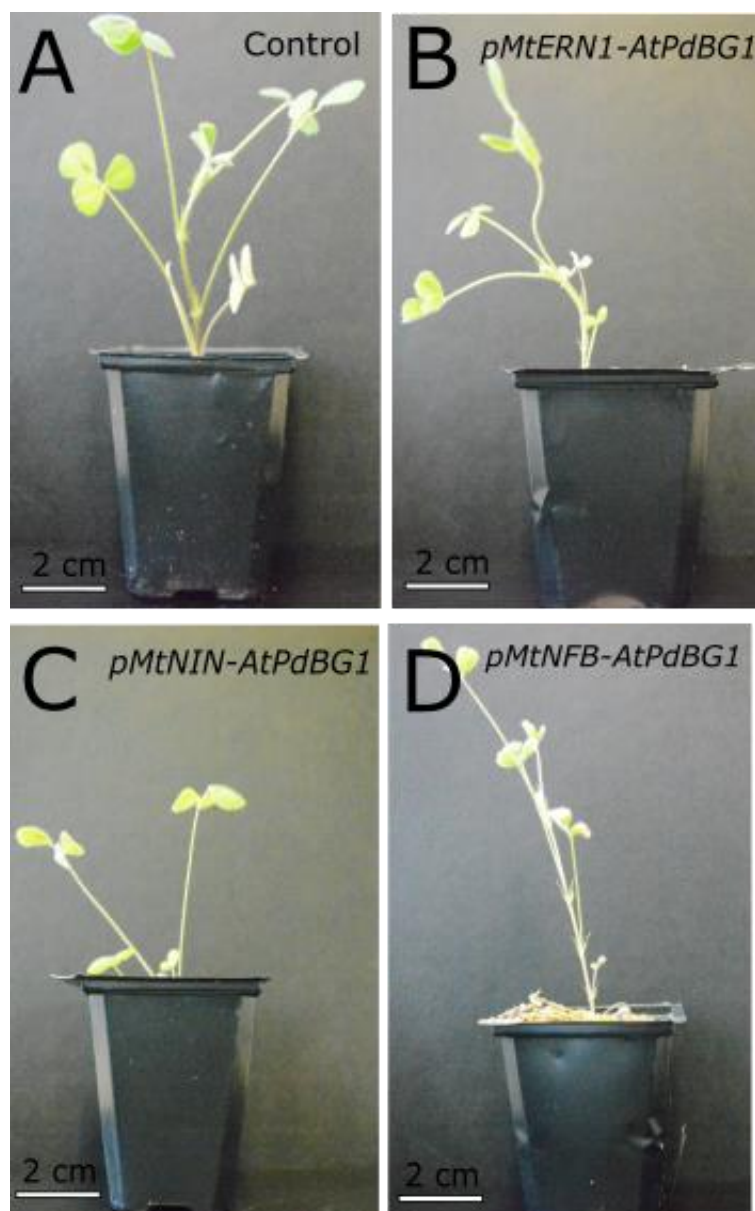


Figure 5.7- *M. truncatula* shoots appear normal in *PdBG1* transgenic. Pictures were taken of the general aspect of *M. truncatula* composite plants growing for 24 days in pots containing an equal mixture of sand and Terragreen.

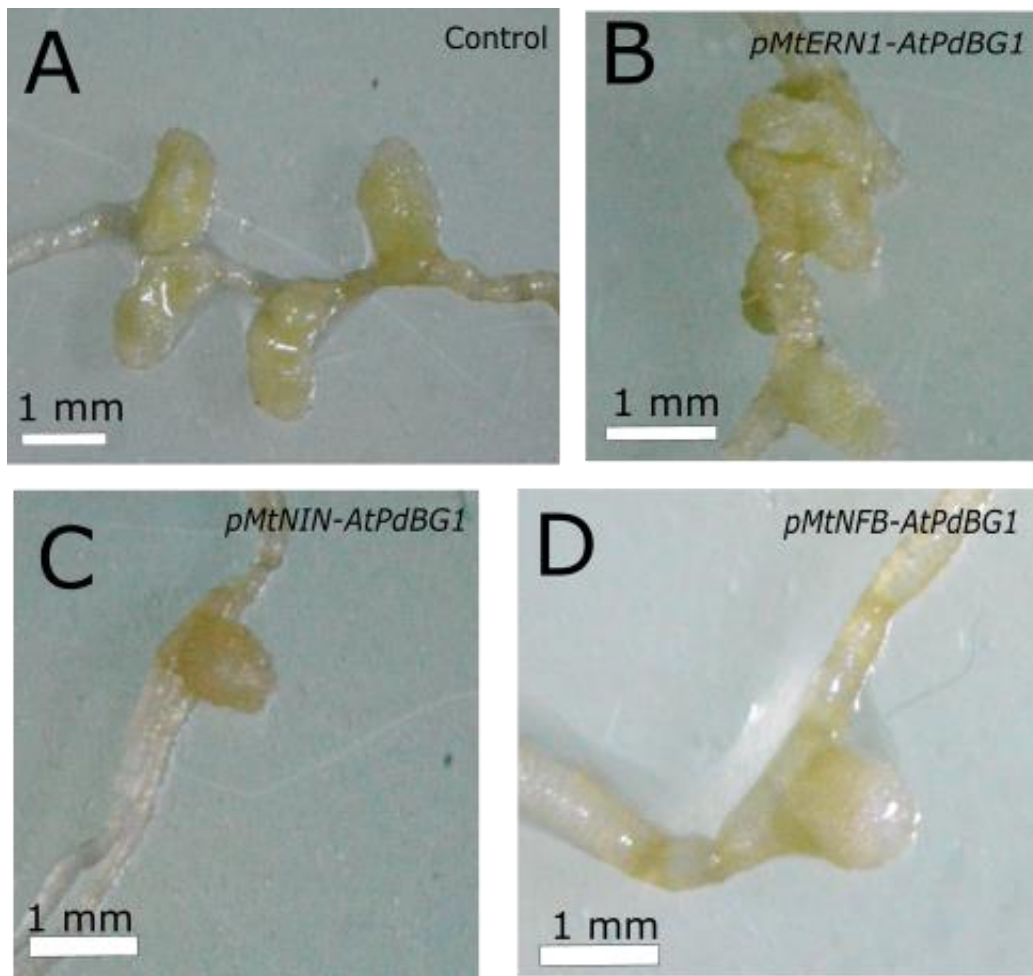


Figure 5.8- Example of nodule architecture 14 days post inoculation in in *M. truncatula* control and roots expressing Arabidopsis PdBG1. Nodules could be seen growing in an alternate pattern (A), in clusters (B) or in isolation (C, D). All three types of nodule architecture were seen in composite plants expressing the four constructs indistinctly. (A) picture was taken in control (empty vector), (B) in roots expressing pMtERN1- AtPdbG1 construct, Individual young rounded-shaped nodules in roots expressing pMtNIN- AtPdBG1 (C) and pMtNFB- AtPdBG1 (D).

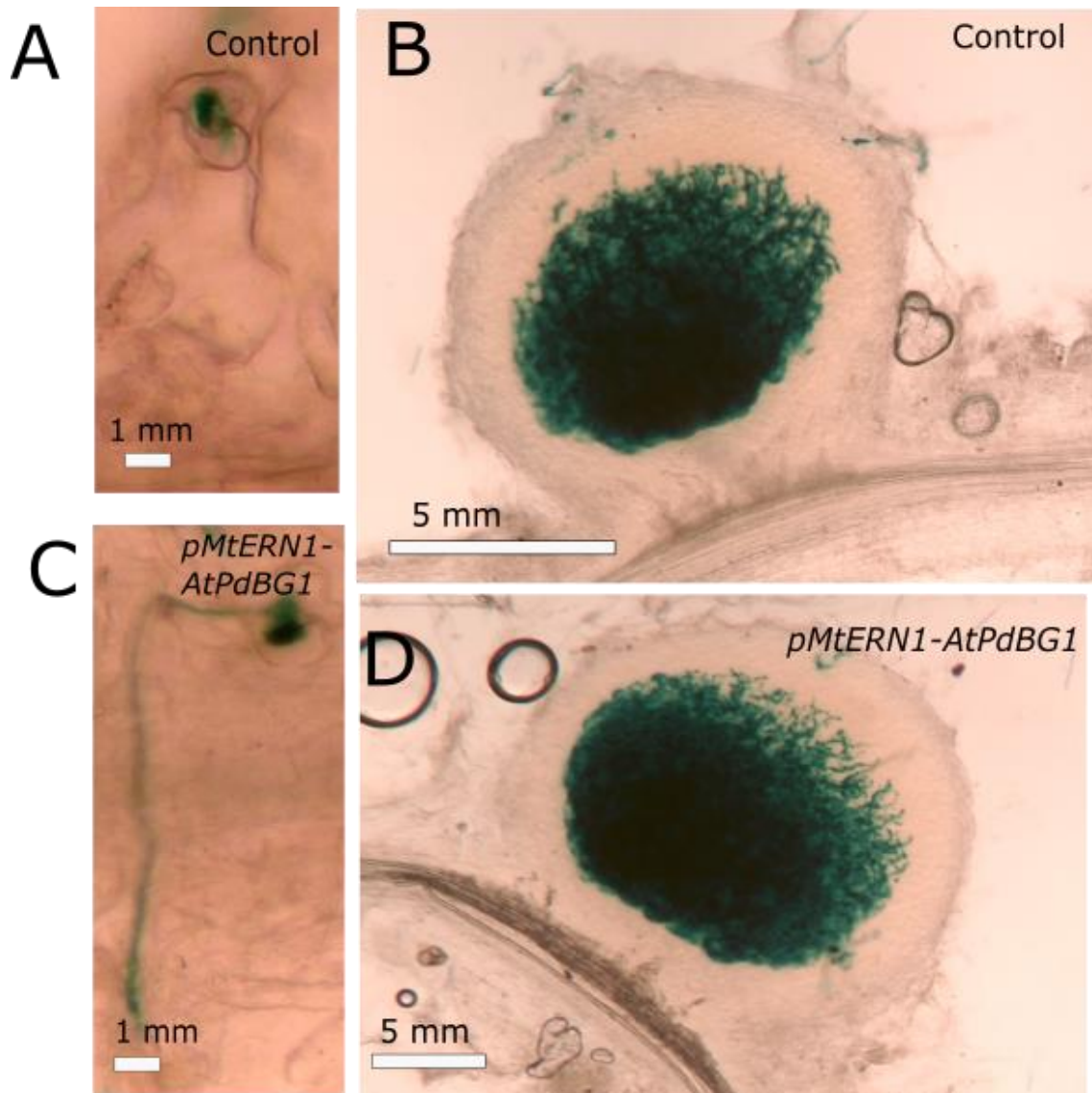


Figure 5.9- Example pictures of infection thread, infection pocket, nodule primordia and nodule in *M. truncatula* roots 14 days post inoculation with *lacZ* expressing rhizobia. (A) Infection pocket in *Medicago* transgenic roots expressing an empty vector as a control. (B) Older infected nodule in a control root expressing the empty vector. (C) Infection thread entering the epidermal cell layer in *Medicago* transgenic roots expressing *pMtERN1-AtPdBG1*. (D) Older infected nodule in a root expressing *pMtERN1-AtPdBG1*.

5.3 Discussion

5.3.1 Ectopic degradation of callose in rhizobia infected epidermal tissues is sufficient to regulate nodulation

Ectopic expression of callose degrading enzyme MtBG2 leads to changes in callose deposition in *M. truncatula* roots and these transgenic appear to develop more nodules and infection threads (Chapter 4).

In this chapter, the Arabidopsis β -1,3-glucanase *PdBG1* was used as a tool to establish the spatial and temporal profiles where callose degradation is required to control nodulation.

Composite plants expressing *PdBG1* under a constitutive promoter showed a plasmodesmata protein localisation and a reduction in callose deposition, which suggests that the protein remains active in the heterologous system. Intriguingly, all transgenic (expressing either the nodulation promoter *pMtNIN*, the infection *pMtNFB* or the infection and nodulation promoter *pMtERN1*) appeared normal in root and shoot development, despite research linking *PdBG1* to changes in lateral root patterning. This is a good indication of the specificity of the promoters, which function mainly in symbiotic infection and nodulation.

Among all the transgenic, roots expressing *pMtERN1-AtPdBG1* showed the strongest effect on nodulation.

ERN1 is a well-studied transcription factor required in early infection events and *ERN1* expression is induced in the epidermis 1 to 3 hpi and during root hair curling (based on GUS-fusion proteins, RNAseq and Affymetrix arrays) (Middleton et al., 2007; Plet et al., 2011; Cerri et al., 2012; Larrainzar et al., 2015). Later, as the nodule develops *ERN1* expression appears in cortical cells (Cerri et al., 2012). Driven by the *ERN1* promoter, it is expected that *PdBG1* expression would be upregulated from the first events involved in NF signalling and infection thread formation. Consistent with this expression profile, roots expressing *PdBG1* under the *pMtERN1* promoter showed more infection pockets and infection threads at 7 dpi than control plants transformed with the empty vector. The number of nodule primordia and young nodules at 7 dpi was, however, not affected in the transformed roots, in contradiction with the results

obtained at 14 dpi. In every experiment only infected primordia (blue after lacZ staining of the rhizobia) and non-infected primordia, but with a clear infection thread above the bump were counted. Very early nodule primordia might have been excluded with this method and this might be the cause why there is a difference at 14 dpi (where more primordia would be infected) but not at 7 dpi. Alternatively, this might be an indication of a possible role for the promoter at later stages of nodule development. A repetition of the experiment using a nodule primordia marker, such as the WD-repeat protein, *CCS52A*, that regulates endoreduplication of the cortical cells (Li et al., 2009) would help bypass this difficulty. Another possibility is that the primary response to PdBG1 expression in the *ERN1* domain is an increase in the number of infection threads formed at an early time frame which indirectly affects the number of primordia at a later stage. Alternatively, and since *ERN1* expression also appears in cortical cells, it is possible that the higher number of nodules is just a direct effect of the expression of PdBG1 in cortical cell layers. The expression of PdBG1 under epidermal/cortical specific promoters, such as *pLeEXT1* and *pCO2* (successfully used in *M. truncatula*) (Rival et al., 2012), could help characterising the possible tissue-specific role of the protein.

Additionally, the high deviation of the nodule primordia density data set in plants expressing the *pMtERN1-PdBG1* (Figure 5.5) might indicate that there is a strong expression difference between transgenic roots, with roots expressing the construct at higher levels developing more nodules. To discern if this is the case, RT-PCR could be performed in roots showing a number of nodules in both extremes of the data set and confirm if the number of nodules correlates with gene expression. Further experiments exploring the expression patterns of infection and nodulation genetic markers in the *pMtERN1-PdBG1* transgenic lines, such as *NIN*, *ENOD11* or *ERN1* itself, could shed some light on which step of the process is primarily affected in these plants.

Although significantly higher compared to control plants, infection thread density in *pMtERN1-AtPdBG1* was not as high as in plants expressing the *pUb-MtBG2-mcherry* vector. This might be due to differences in the expression patterns or in the strength of the promoters. *MtBG2* driven by the strong ubiquitin promoter would affect callose generally around the root and at all times, while *PdBG1*

under the *pMtERN1* promoter, will only be activated in the early stages of infection and in the *ERN1* expression domains. Differences can also be linked to the activity of the specific proteins (*PdBG1* vs *MtBG2*). *M. truncatula* transgenic roots overexpressing *PdBG1* showed a massive downregulation of callose and this effect was used to infer callose regulation in *pMtERN1*, *pMtNIN* and *pMtNFB* transgenic roots.

Important research from collaborators has also shown how the expression of a hyperactive callose synthase (*cals3m* (Vaten et al., 2011) driven by *pMtERN1* dramatically increase callose deposition and reduced the number of infected nodules⁶. Root hair infection was however not as strongly affected compared to control roots. Interestingly, the expression of the same callose synthase under an epidermis specific promoter (*pEXP*) did not significantly affect nodule development, suggesting that the effect is tightly linked to the promoter strength or expression domain. This result suggest that symplastic connectivity is not essential for infection thread formation. Regardless, the effect of *pMtERN1*-*PdBG1* in infection can be explained by a couple of possibilities. As presented in Chapter 4, ectopic callose degradation might contribute to bacterial entrapment by modifying root hairs cell walls or to the ectopic transport of signals (normally restricted to underlying cell layers in early stages of symbiosis) that enhance infection in the epidermis. In *pMtERN1*-*cals3m* the signal will remain restricted thus infection thread will form as normal. In these plants, other signals important for nodule colonization and infection thread progression might instead be restricted.

Although one of the outcomes of changing callose deposition is the regulation of symplastic connectivity (Li et al., 2012; De Storme and Geelen, 2014) there is not enough data to demonstrate that this is happening in *PdBG1* transgenic plants. Further investigation on changes in symplastic communication needs to be done to reveal if in this system, callose downregulation is causing an increase in plasmodesmata permeability and if this modifies signalling between the epidermis, the underlying cell layers and the phloem. Several genes (including

⁶ Personal communication: Martina Beck and Fernanda de Carvalho-Niebel (LIPM, Université de Toulouse, INRA, CNRS, 31326 Castanet-Tolosan, France)

NIN, ENOD40 and DMI3) have been found essential for the epidermis/cortex layers cross-talk (as described more deeply in Chapter 1 section 1.2.2.2) (Charon et al., 1999; Rival et al., 2012). Now it's timely to study if any of their pattern of expression or function is modified in the *PdBG1*, *cals3m* or *MtBG2* overexpressing transgenic roots.

Chapter 6

Chapter 6 -A novel receptor-like kinase targets plasmodesmata to regulate nodulation in nitrogen sufficient conditions

6.1 Summary

In previous chapters, it was discussed how nitrate availability can change the root response to rhizobia, through a signalling pathway that involves local and systemic communication. Transgenic roots expressing the plasmodesmata-located β -1,3- glucanase *PdBG1* or *MtBG2* are partially able to offset inhibition by nitrate thus a role for callose and plasmodesmata in regulating nodulation in response to nitrate can be proposed. In this chapter, phylogenetic and molecular approaches were used to identify a receptor-like kinase (RLK) *M. truncatula* homolog of the *A. thaliana* Plasmodesmata located protein family, PDLP (Thomas et al., 2008; Lee et al., 2011).

The PDLP protein family plays a function in signal perception and/or transduction and is proposed to regulate callose deposition at plasmodesmata (Thomas et al., 2008; Lee et al., 2011). PDLPs are induced in response to viruses and other pathogens (Amari et al., 2010) and are also involved in pathogen recognition and signalling during systemic acquired resistance and immune response in *Arabidopsis* (Caillaud et al., 2014; Carella et al., 2015). PDLPs control symplastic communication (Thomas et al., 2008; De Storme and Geelen, 2014), presumably via activation of CALS at plasmodesmata (Wang et al., 2013; Cui and Lee, 2016). RLK proteins also play a role in development by coordinating cell fate in meristematic tissue and organ differentiation through regulating signalling at plasmodesmata (Stahl and Simon, 2013). A more in-depth review of the role of PDLP in the symplastic pathway can be found in Chapter 1, 1.3.2 and 1.3.3.1

The newly identified RLK (PDLP-like) protein in *Medicago* was found upregulated in the epidermal cell layer after exposure to Nod factors, suggesting an important role in early stages of signalling (Jardinaud et al., 2016). In this chapter, it is explored whether this PDLP-like protein is also involved in the generation and/or maintenance of the nodule meristem and/or in signal perception/response to nitrate sufficient conditions. It is also discussed the implication of the results in

the signalling process that lead to the inhibition of nodulation by nitrate availability in the growth media.

6.2 Results

6.2.1 Phylogenetic analysis identifies MtPDLP1 (Medtr1g073320) as evolutionary related to PDLP proteins

The role of PDLP in plant-microbe interactions and in the regulation of callose at plasmodesmata has been reported. To identify novel PDLP-like proteins that regulate symbiosis in *M. truncatula*, phylogenetic trees were generated using three search algorithms: Bayesian inference (Bayesian), Maximum Likelihood (ML) and Neighbour Joining (NJ). Features such as the characteristic DUF26 domain were analysed to identify potential PDLP orthologues (Figure 6.1).

All proteins identified had predicted signal peptide (SP), transmembrane and DUF26 domain (Appendix 3). The tree topology was generally well supported by all 3 methods (Appendix 8, 9, 16, 17 and 18). *MtPDLP2* (Medtr7g098410) and *MtPDLP1* (Medtr1g073320) were found closely related to Arabidopsis PDLP proteins which target plasmodesmata to regulate cell-to-cell communication and response to a pathogen (Amari et al., 2010; Caillaud et al., 2014). Specifically, *MtPDLP1* shares high homology with Arabidopsis PDLP3 (66% homology) and *PDLP2* (71% homology) and the DUF26 and transmembrane domain are conserved (Figure 6.2).

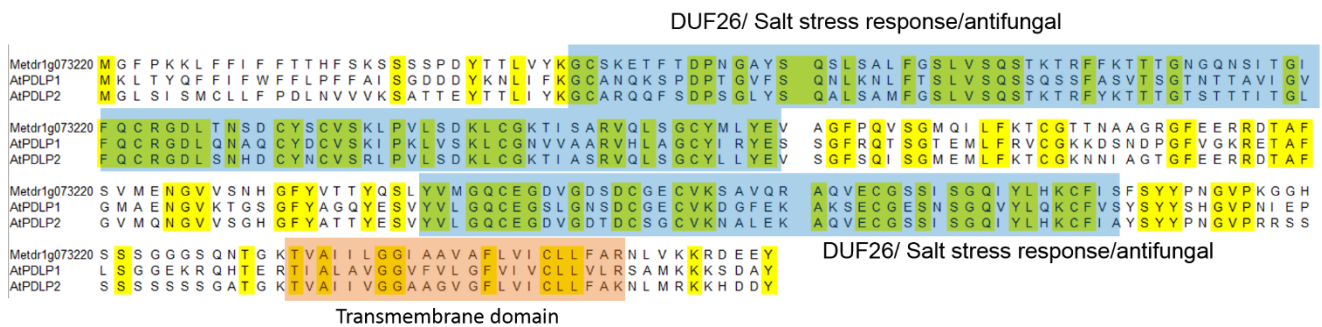


Figure 6.2- Alignment of the *M. truncatula* PDLP-like protein-1 (Medtr1g073320), and the *Arabidopsis thaliana* PDLP proteins AtPDLP1 and AtPDLP2 sequences. The conserved domains DUF26/salt stress/antifungal are shaded in blue. The transmembrane domain is shaded in orange. Residues conserved in all three proteins are indicated in yellow

6.2.2 MtPDLP1 co-localises with callose deposits around plasmodesmata in *M. truncatula* roots

In order to confirm the plasmodesmata localisation of MtPDLP1, a YFP C-terminal protein fusion was generated and expressed under the 35S promoter. *M. truncatula* roots were transformed to express the fusion protein and localisation was assessed by confocal microscopy. The protein showed a punctate localisation pattern (Figure 6.3-A) which co-localised with callose deposits revealed by aniline blue staining (Figure 6.3-B and C), suggesting that this newly identified protein is, very likely, located in plasmodesmata.

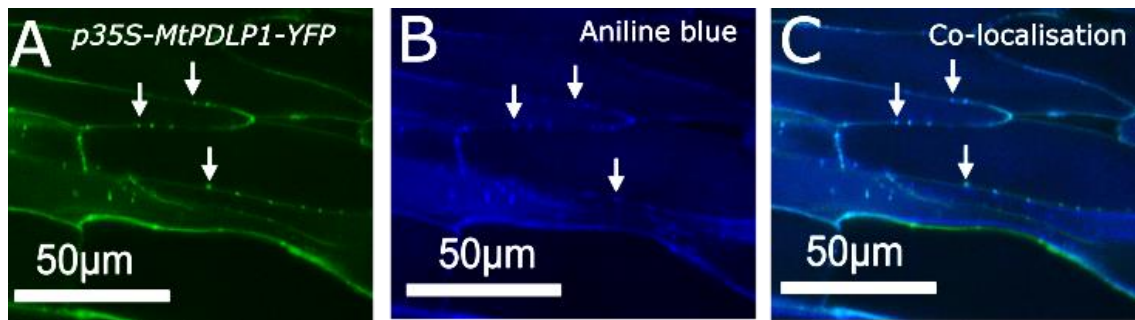


Figure 6.3- Intercellular localisation of MtPDLP1 in *M. truncatula* roots. (A) Shows a confocal picture of a *M. truncatula* transgenic root expressing MtPDLP1 fused to YFP under p35S promoter (green-yellow signal). (B) Blue channel shows callose deposits revealed by aniline blue staining in the same section of root. (C) Co-localisation of the green-yellow signal for *MtPDLP1-YFP* with the blue signal for callose deposits at plasmodesmata (white arrows).

6.2.3 Expression profile indicates up-regulation of MtPDLP1 after rhizobial infection.

Arabidopsis PDLP proteins are known to act in signalling and recognition of pathogens (Amari et al., 2010; Bricchi et al., 2013). *MtPDLP1* appears upregulated in root hairs 3 dpi, as shown by microarray data (Figure 6.4). Therefore, we tested whether *MtPDLP1* was involved in the signalling and recognition of rhizobia as a symbiotic partner. Roots inoculated with rhizobia and mock cultures were collected and total RNA retrotranscribed into cDNA using polydT. Gene-specific primers for *MtPDLP1* were designed to amplify around 200 base pairs. Actin was used as housekeeping gene to control for variations in the RT or PCR efficiency. The results show that *MtPDLP1* is induced at 16hpi and expression maintained high at 24hpi (Figure 6.5).

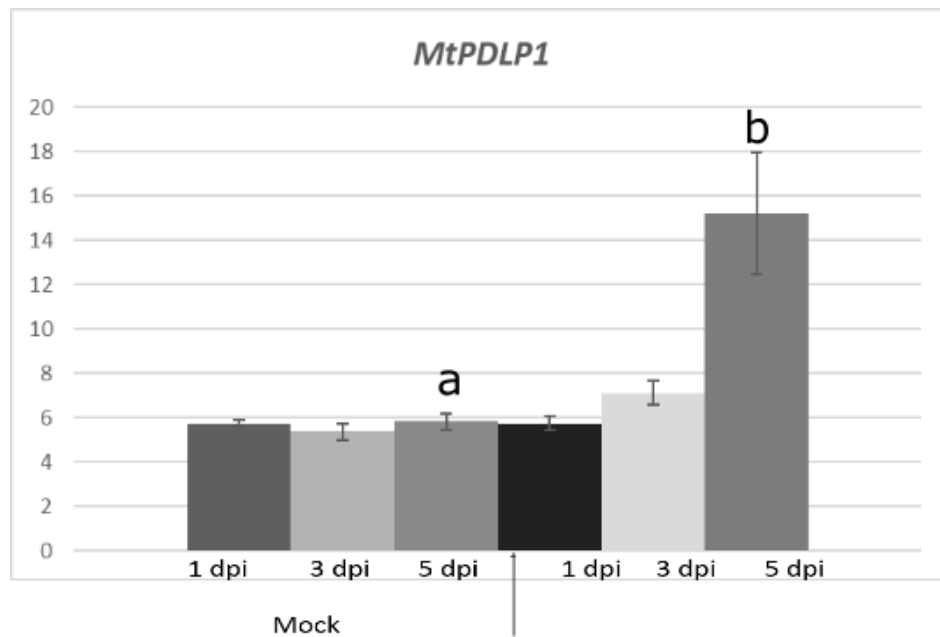


Figure 6.4-Expression profile of *MtPDLP1* in *M. truncatula* inoculated root hairs. *MtPDLP1* relative expression in root hairs inoculated with a mutant rhizobia strain (unable to form symbiosis, mock) and a wild-type strain. Notice increase in expression at 5dpi. Image adapted from <http://mtgea.noble.org/v3/>. Data published by (Breakspear et al., 2014).

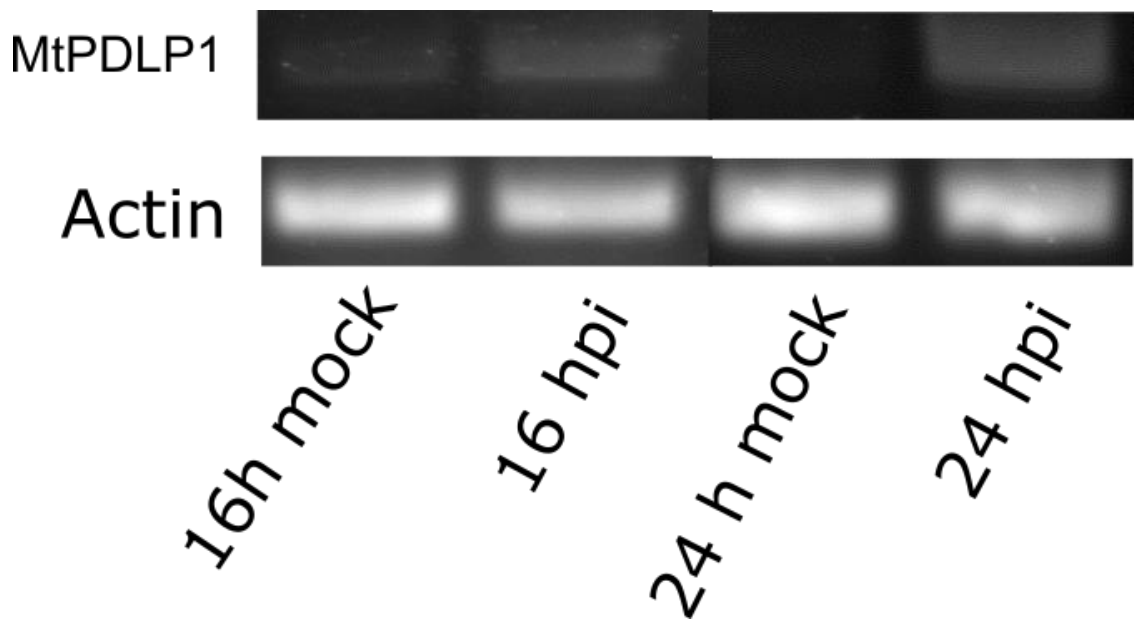


Figure 6.5- *MtPDLP1* is upregulated upon inoculation in *M. truncatula* roots. *M. truncatula* roots were spot-inoculated with *S. meliloti* and samples retrieved at 16 and 24 hours post inoculation (hpi). RNA was extracted and cDNA synthesized. PCR was performed using. Actin was used as a housekeeping gene. *MtPDLP1* shows an upregulation at 16 and 24 hpi.

6.2.4 Constitutive expression of *MtPDLP1* improves plant biomass in soil

Overexpression of members of the PDLP family in *Arabidopsis* leads to over accumulation of callose at plasmodesmata, cell death and chlorosis (in the case of PDLP5), affecting plant growth and development even at the seedling phase (Lee et al., 2011) and/or leading to a dwarf phenotype (reported for PDLP1) (Thomas et al., 2008). To assess whether the over-expression of *MtPDLP1* affects root and shoot development in *M. truncatula* we measured root length and shoot/root biomass of composite plants. We grew control (expressing an empty vector) and *MtPDLP1* overexpressing plants (transformed with p35S-*MtPDLP1*-YFP construct) for 17 days on plates. An average of 27 independent composite roots was measured but no significant difference among control and *MtPDLP1* overexpressing plants was found (Figure 6.6). On the other hand, when transplanted to pots in an equal mixture of sand and terragreen, plants

expressing the p35S- *MtPDLP1-YFP* construct showed an increase in biomass, both at the shoots and roots (Figure 6.7). These differences might mean that *MtPDLP1* overexpression improves plant development when growing in soil or that this effect is only seen at a later stage of development. Additionally, root weight was not measured in plants 20-days old, hence a direct comparison of both developmental stages can not be made. Further phenotyping should be made to fully understand the timely effect of the overexpression of *MtPDLP1* in plant development. Since transformed plants only express the vector in the roots, it can also be inferred that shoot growth is influenced by the root phenotype.

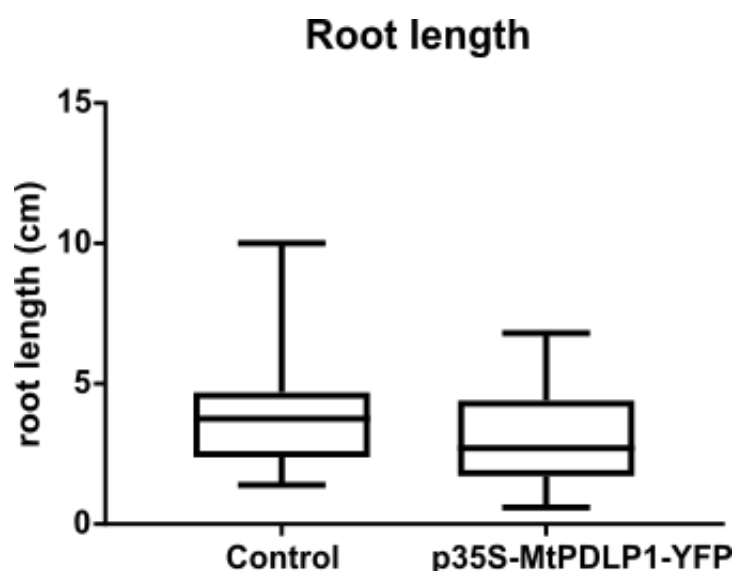


Figure 6.6- *MtPDLP1* overexpression does not affect root length in *M. truncatula*. *M. truncatula* roots transformed with p35S-*MtPDLP1-YFP* or with an empty vector (control) were grown for 20 days post-transformation and root length was measured. A Student's t-test was performed; no significant differences were seen ($p > 0.05$). (N=24).

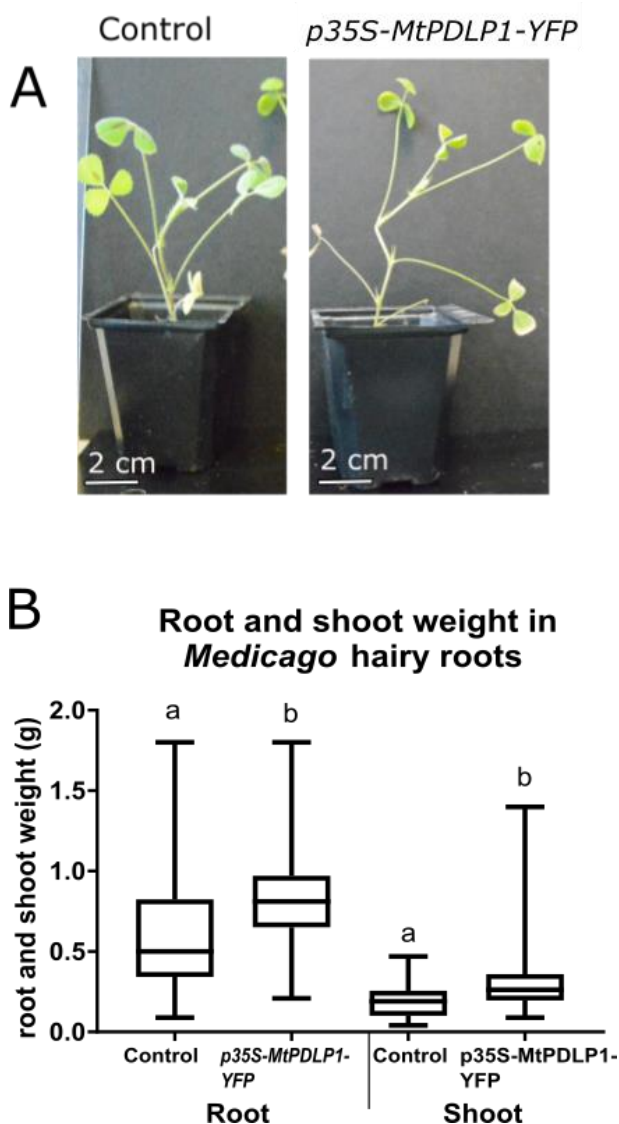


Figure 6.7- *MtPDLP1* overexpression affects plant development. (A) The general aspect of *M. truncatula* composite plants shoots expressing an empty vector (control) or *p35S-MtPDLP1-YFP* driven by a constitutive 35S promoter. 44 days post-transformation the composite plants were photographed growing in an equal mixture of sand and terragreen. (B) Shoot and root weight of composite *M. truncatula* plants expressing an empty vector (control) or *p35S-MtPDLP1-YFP* 44 days post-transformation. A Student's t-test was performed; different letters refer to significant differences ($p < 0.05$), (N=20).

6.2.5 Over-expression of *MtPDLP1* does not affect callose, nodule number or infection threads in nitrogen-depleted conditions

As overexpression of the Arabidopsis orthologue results in over-accumulation of callose (Caillaud et al., 2014) callose immunolocalisation was performed in transgenic roots expressing *p35S-MtPDLP1-YFP*. In contrast to what it was expected, *M. truncatula* roots constitutively expressing *MtPDLP1* did not show a strong regulation of callose in cell walls (Figure 6.8).

MtPDLP1 is upregulated early after inoculation (Figure 6.5) (Jardinaud et al., 2016), so we wondered whether the ectopic expression of *MtPDLP1* would affect infection and/or nodulation. In order to discern this, we inoculated *Medicago* transgenic roots, overexpressing the protein, with mock and rhizobia cultures and counted infection sites and nodule primordia 7 dpi in plates. We also inoculated composite roots in soil and measured nodule density (number of nodules per gr of root weight) at 14 dpi. We could not see a significant difference in infection threads, nodule primordia or mature nodules in either of these conditions (Figure 6.9). Percentage of infected nodules in composite plants expressing *p35S-MtPDLP1-YFP* was also similar to transgenic roots expressing an empty vector (Table 6.1).

Callose immunolocalisation upon inoculation with rhizobia was also performed. Similar to control roots (transformed with an empty vector) downregulation of callose was observed 24 hpi with rhizobia in *p35S-MtPDLP1-YFP* roots growing in nitrate-depleted conditions (Figure 6.11) in comparison to mock (water) inoculated roots.

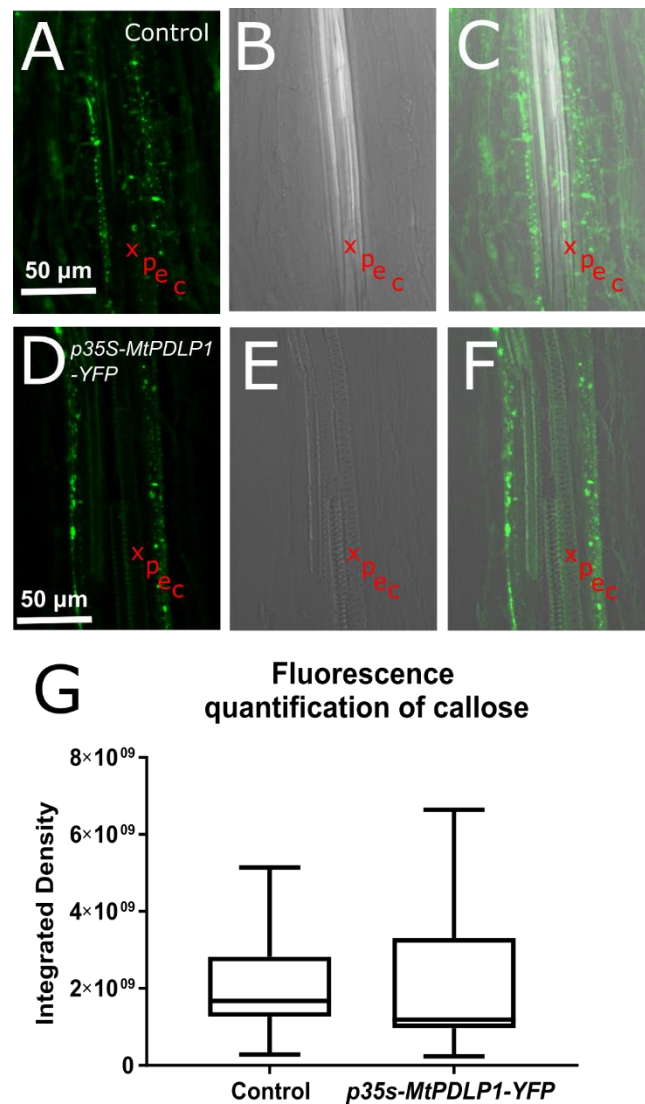


Figure 6.8- Over expression of *MtPDLP1* does not affect callose deposition in *M. truncatula* grown in depleted nitrate. Confocal pictures showing callose detected using a monoclonal antibody and an Alexa-488 conjugated secondary antibody in longitudinal sections of transgenic roots expressing an empty vector as control (A) or *p35S-MtPDLP1-YFP* (D). Bright field (B and E) and composite images (C and F) are shown in the same section were used for localisation. (G) Fluorescence quantification of callose was performed by calculating the integrated density using ImageJ for each image in at least 3 biological repetitions per conditions. Fluorescence was quantified in a region of interest of approximately $100\mu\text{m}^2$. Symbols in A to F refer to xylem vessel (x), pericycle (p), endodermis (e), and cortex (c). A Student's t-test was performed, no significant differences were seen ($p > 0.05$).

Infection thread and nodule primordia density

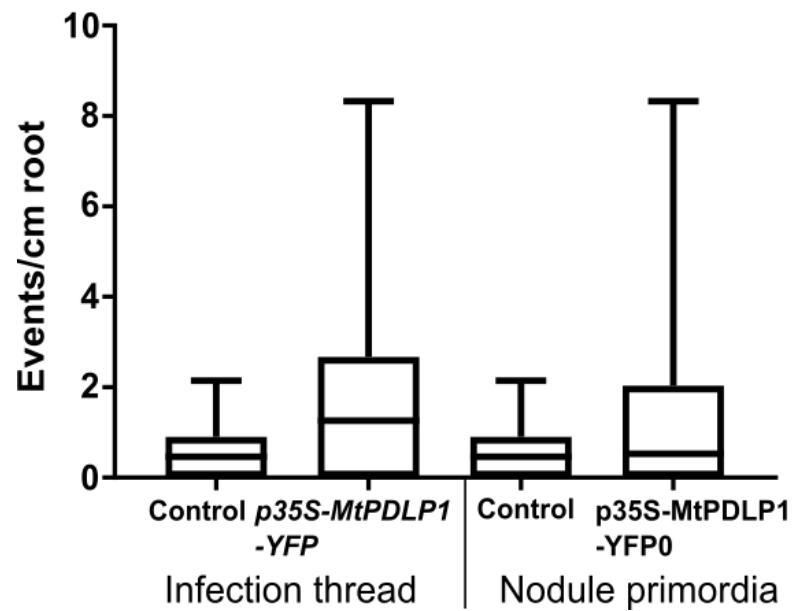


Figure 6.9- Plants expressing *p35S-MtPDLP1-YFP* are not affected in infection or nodulation 7 days post inoculation in low nitrate conditions. Transgenic roots were inoculated with *S. meliloti* expressing the β -galactosidase gene. 7 days post inoculation roots were stained to localise infection sites and nodule primordia. Roots overexpressing MtPDLP1 did not show a significant difference in infection thread or nodule primordia density when compared to control roots expressing an empty vector. A Student's t-test was performed, with no significant differences ($p > 0.05$).

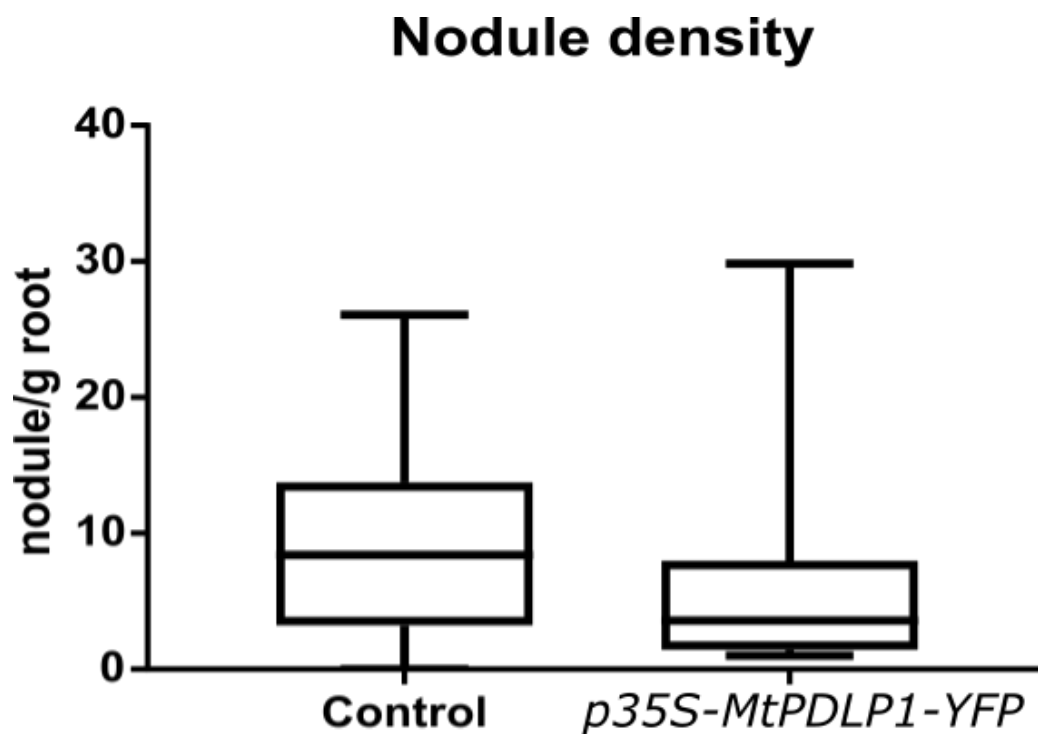


Figure 6.10- Plants overexpressing *MtPDLP1* nodulate normally in soil in low nitrate conditions. Transformed plants were transplanted to soil and infected with rhizobia. 14 days post-inoculation, nodule density was calculated by dividing the total number of nodules per plant by root weight. Only mature nodules visible without the aid of a microscope were counted. A Student's t-test was performed, with no significant differences ($p>0.05$).

Table 6.1- Percentage of infected nodules in composite plants expressing p35S- MtPDLP1-YFP construct. *M. truncatula* roots were infected with *S. meliloti* expressing the β -galactosidase gene. 7 days post inoculation plants were fixed and stained to localise bacteria within nodules and nodule primordia. The percentage of blue nodules/primordia in relation to the total number of nodules per plant was calculated. A Student's t-test was performed to the means with no significant differences seen ($p>0.05$).

| Composite plant expressing vector | Percentage of infected nodules |
|--|---------------------------------------|
| Control (empty backbone vector) | 85.5% |
| p35S- MtPDLP1-YFP | 86.2% |

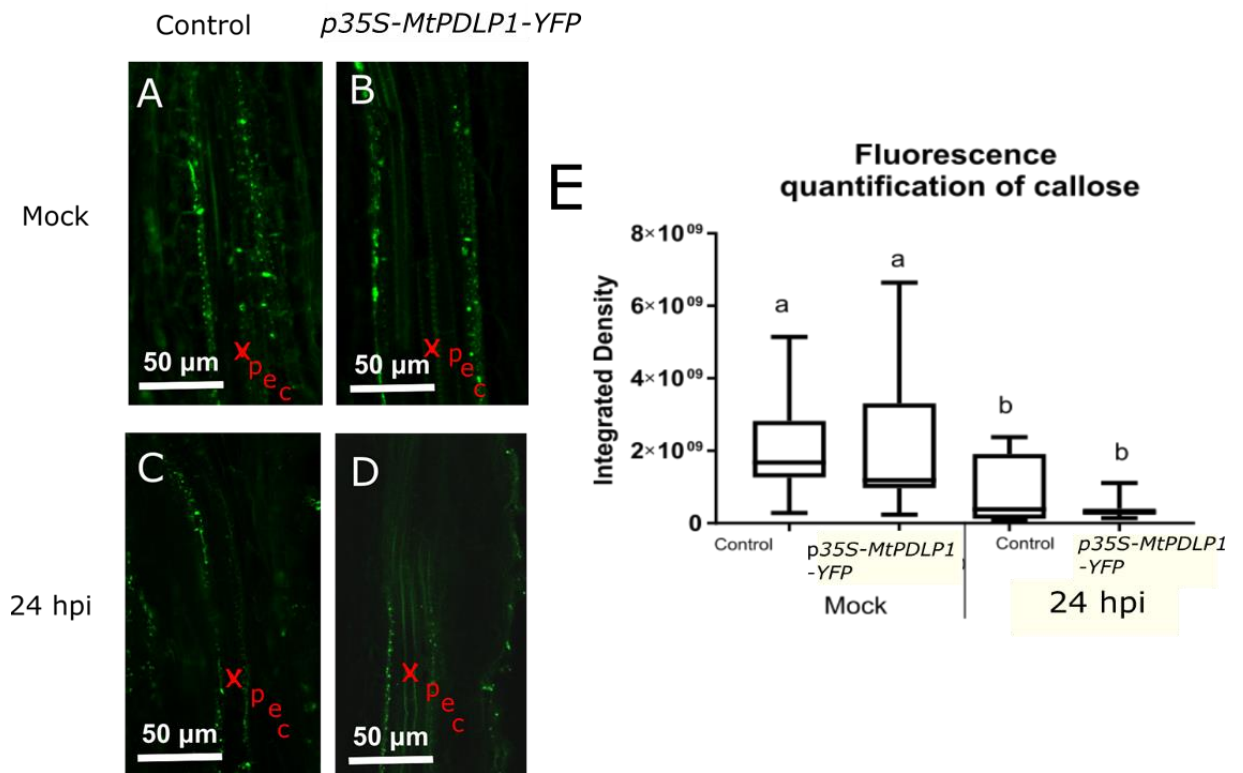


Figure 6.11- *MtPDLP1* plants experience callose downregulation upon inoculation in *M. truncatula* in nitrate-depleted conditions. Callose immunolocalisation was performed in longitudinal sections of *M. truncatula* hairy roots expressing an empty vector (control) (A,C) or *p35S-MtPDLP1-YFP* (B,D) and either mock inoculated (A, B) or rhizobia inoculated and growing in media containing no nitrate (C,D). Samples were retrieved 24 hpi. Callose was localised with monoclonal antibodies (Biosupplies) and detected with a conjugated secondary antibody (Alexa 488). E) Integrated Density was calculated using ImageJ for each image in at least 3 different roots per condition. The region of interests was approximately 100μm². The region of interests was approximately 100μm². Symbols in A to F refer to xylem vessel (x), pericycle (p), endodermis (e), and cortex (c). A Student's t-test was performed, different letters refer to statistic differences ($p < 0.05$).

6.2.6 Constitutive expression of *MtPDLP1* affects response to rhizobia in nitrate sufficient conditions

Despite regulation early after infection, overexpressing *MtPDLP1* did not show any infection or nodulation phenotype under nitrate depleted conditions. A laser dissection-RNAseq analysis of the epidermal cell layer of *Medicago* roots treated with Nod factors identified *MtPDLP1* and CLE-related peptide among several genes up-regulated soon after the treatment (Jardinaud et al., 2016). CLE-

related peptides are essential in the regulation of the AON pathway in full nitrogen conditions, therefore it was hypothesized a role for *MtPDLP1* in this pathway.

Callose regulation was assessed, infection and nodulation in transgenic roots constitutively expressing *MtPDLP1* under full nitrate conditions and compared with nitrate depleted conditions. Shockingly, the characteristic downregulation of callose after infection was not maintained in *MtPDLP1* overexpressing roots grown and inoculated in plates containing full nitrate media (Figure 6.12). Moreover, composite plants overexpressing *MtPDLP1* were not affected in infection (Figure 6.13-A) or nodulation (Figure 6.13-B) in full nitrate conditions in contrast to plants transformed with an empty vector which displayed an inhibition in both infection thread and nodule density in full nitrate. Indeed, there were no significant differences in infection and nodulation between *MtPDLP1* overexpressing roots inoculated in full nitrate or depleted nitrate conditions. Composite plants overexpressing *MtPDLP1* did not show developmental differences when grown in the presence of nitrate compared to plants expressing the empty vector (Figure 6.14), apart from a higher number of nodules. Percentage of infected nodules was also higher in *MtPDLP1* overexpressing transgenic roots in full nitrate (Table 6.2). The results suggest that the protein might be part of the signalling process controlling nodulation in full nitrate conditions, hence the ectopic expression of the protein is probably alleviating the inhibitory effect of nitrate in nodulation.

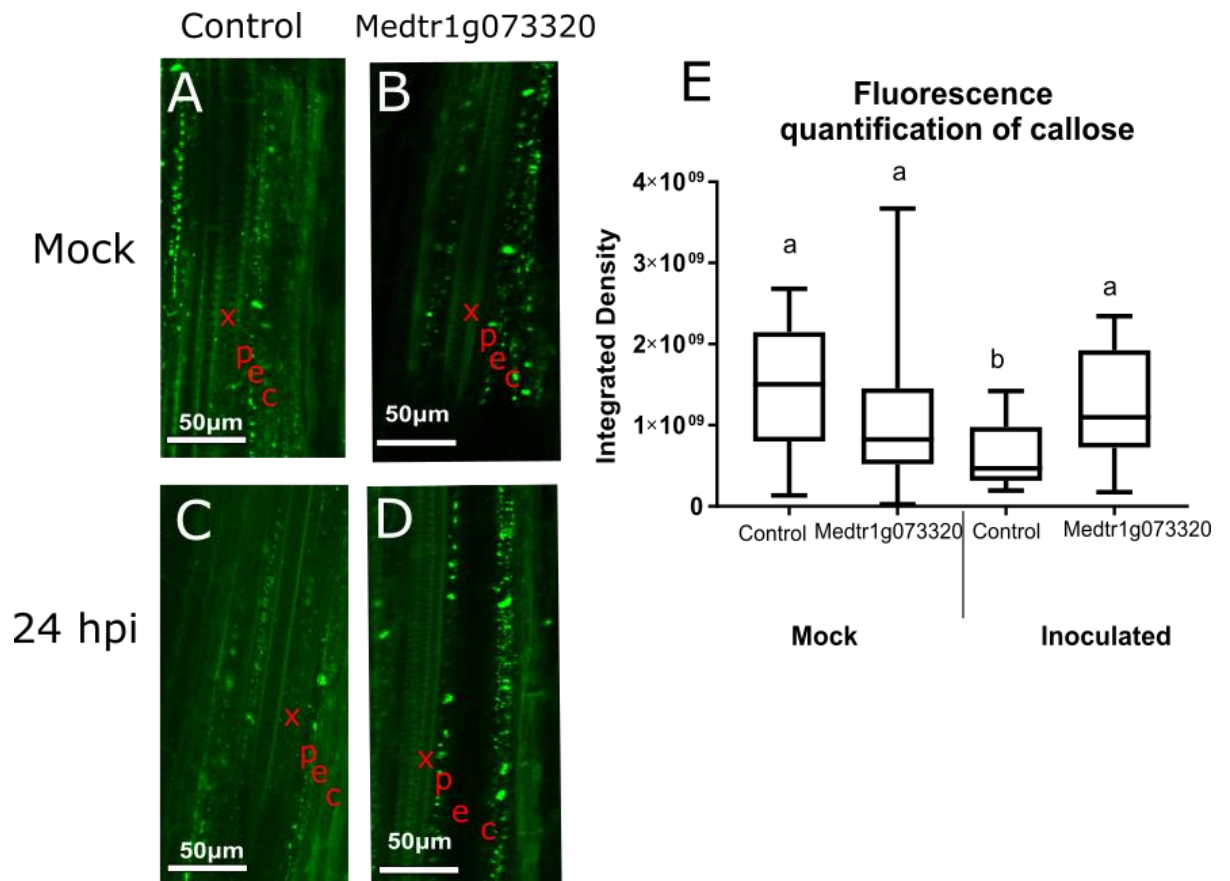


Figure 6.12 *MtPDLP1* affects callose regulation upon inoculation in full-nitrate conditions. *M. truncatula* roots expressing an empty vector (control) (A-B) or *p35S-MtPDLP1-YFP* (C-D) were grown in 5mM nitrate and either mock inoculated (A-C) or rhizobia inoculated (B,D). Samples were fixed 24 hpi and callose was localised with monoclonal antibodies and detected with a conjugated secondary antibody (Alexa-488). (A-D) shows confocal pictures of a section of the root in the green channel where the vasculature (v) is indicated. (E) Integrated density was calculated using ImageJ for each image in at least 3 biological repetitions. Boxes delimit minimum to maximum integrated density values. Note that quantification was performed in a pool of z-stack images, quantifying several sections of the same root. Notice downregulation of callose after rhizobia inoculation of control roots but no effect in *p35S-MtPDLP1-YFP* roots. The region of interests was approximately 100μm². Symbols in A to F refer to xylem vessel (x), pericycle (p), endodermis (e), and cortex (c). A Student's t-test was performed, different letters refer to statistical differences ($p < 0.05$).

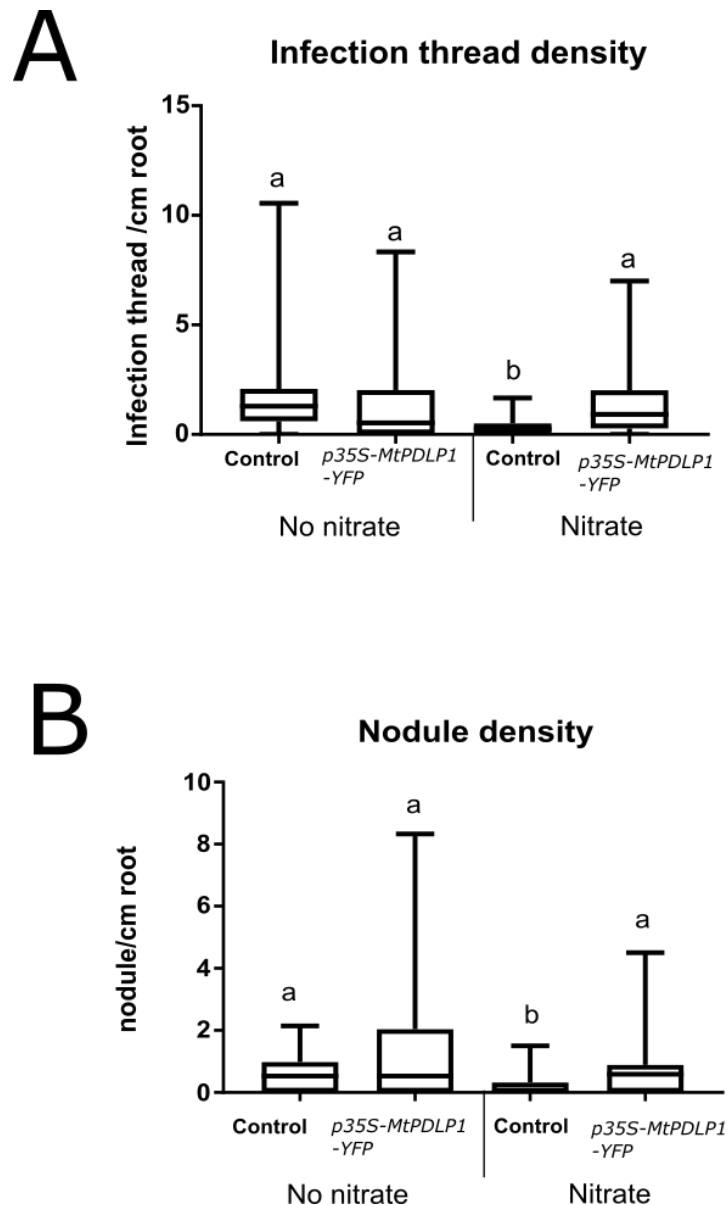


Figure 6.13- *M. truncatula* roots constitutively expressing *MtPDLP1* do not show inhibition of nodulation and infection in full nitrate conditions. *M. truncatula* roots expressing *p35S-MtPDLP1-YFP* were inoculated with a *S. meliloti lacZ* strain and analysed 7 dpi. Composite plants expressing an empty vector (control) were also inoculated as a control. Plants were grown in nitrate depleted (no nitrate) and 5mM nitrate (nitrate) conditions. (A) Infection thread density is represented for the transgenic in nitrate and no nitrate conditions. (B) The nodule density was also calculated. Notice that different to control, infection and nodulation do not appear affected by nitrate in plants overexpressing *MtPDLP1*. A Student's t-test was performed, different letters refer to statistic differences ($p < 0.05$).

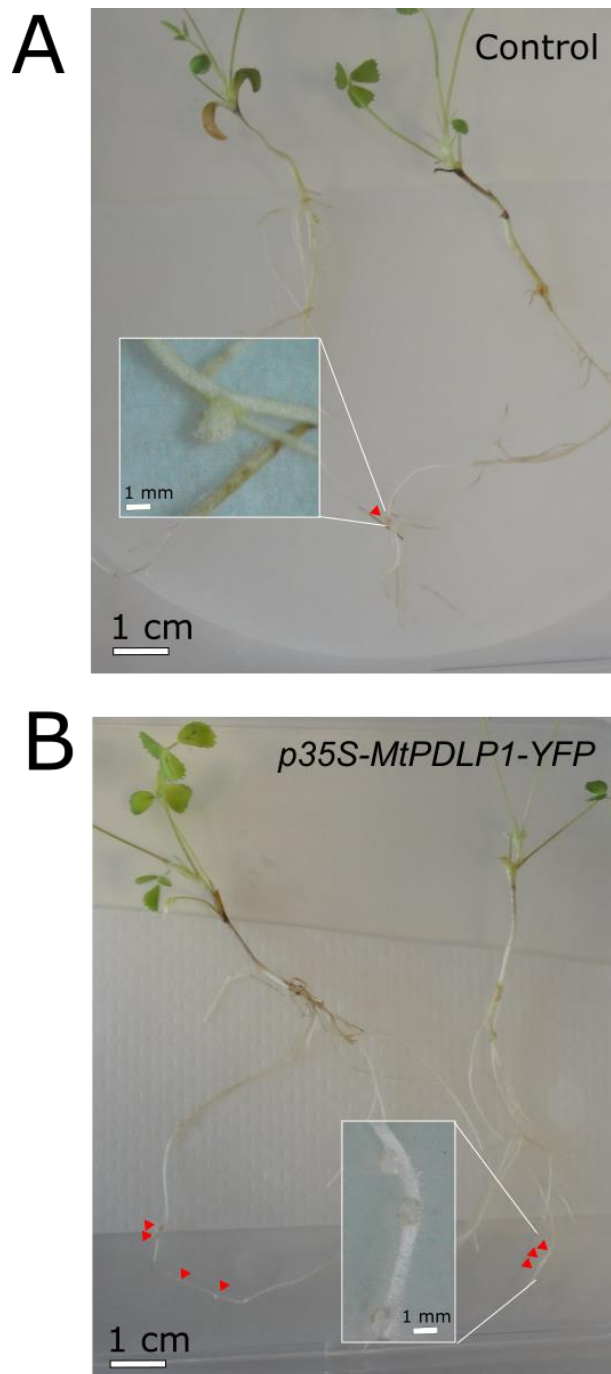


Figure 6.14- Root phenotype of infected *M. truncatula* transgenic roots expressing *p35S- MtPDLP1-YFP*. Composite plants were grown in FP media supplemented with 1 μ M of AVG and 5mM nitrate and inoculated with *S. meliloti*. Pictures were taken 14 days post inoculation. Red triangles mark nodules. (A) *M. truncatula* roots expressing the empty vector as a control. (B) *M. truncatula* roots constitutively expressing *MtPDLP1*.

Table 6.2- Percentage of infected nodules in composite plants expressing *p35S- MtPDLP1-YFP* construct and growing in full nitrate conditions. *M. truncatula* roots were infected with *S. meliloti* expressing the galactosidase gene. 7 days post inoculation plants were fixed and stained to localise bacteria within nodules and nodule primordia. The percentage of blue nodules in relation to the total number of nodules per plant is calculated. A Student's t-test was performed to the means, showing significant differences ($p < 0.05$).

| Composite plant expressing vector | Percentage of infected nodules |
|--|---------------------------------------|
| Control (empty backbone vector) | 80% |
| <i>p35S- MtPDLP1-YFP</i> | 97% |

6.3 Discussion

6.3.1 Overexpression of the receptor-like kinase MtPDLP1 positively regulates plant growth

M. truncatula plants overexpressing *MtPDLP1* show a higher biomass compared to control plants expressing an empty vector. This difference is only seen when plants were transferred to an equal mixture of sand and Terragreen and were grown in that substrate for 14 days. We could not see any developmental phenotype in plants growing in plates but root and shoot weight were not measured in this case. Another reason why differences only appear in soil might be because *MtPDLP1* affects mature stages of development or because of the different growth support systems which mean that different nutrients are available. Although transgenic expression was restricted to the root, both root and shoot biomass were increased in transgenic plants overexpressing *MtPDLP1*, suggesting a systemic root-to-shoot effect.

Overexpression of members of the PDLP family protein in *Arabidopsis* leads to strong developmental defects (Thomas et al., 2008; Lee et al., 2011) (reviewed in Chapter 1 sections 1.3.1 and 1.3.2). Overexpression of PDLP1 and PDLP5 leads to an over accumulation of callose at plasmodesmata, thus changes in symplastic transport probably underlie their effects on plant development and growth (Thomas et al., 2008; Lee et al., 2011; Cui and Lee, 2016). *Medicago* transgenic plants expressing the *p35S-MtPDLP1-YFP* construct did not have affected callose deposition. Experiments expressing *Arabidopsis*' PDLP in *Medicago* plants (or the other way around) to characterise callose deposition could help discern if *MtPDLP1* and PDLPs in *Arabidopsis* are true functional orthologues.

The role for several PDLPs proteins in the immune response of *A. thaliana* has been largely demonstrated (Lee et al., 2011; Wang et al., 2013; Caillaud et al., 2014) (reviewed in section 1.3.3.1 of Chapter 1). It remains unknown whether *MtPDLP1* also plays a role in the immune response to pathogens in *M. truncatula* or if it is involved in the establishment of other symbiotic interactions, such as with AMF. Mutated versions of the protein could be used to determine the

possible dual role of the protein in deciphering the signalling pathway that determines the plant response to different microorganisms.

6.3.2 *MtPDLP1* plays a role in signalling responses to full-nitrate conditions

Based on the nature of *MtPDLP1* and its expression profile, a role for the protein in signalling during the establishment of infection, perhaps influencing the development of nodules was hypothesised. Previous research has shown that *MtPDLP1* is upregulated as early as 4 hpi in the epidermal cell layer (Jardinaud et al., 2016), our results suggest that this upregulation is maintained at least until 24 hpi and in root hairs microarray induction appears at 5 dpi (Figure 6.14) (Breakspear et al., 2014) .

We could not see an effect in the number of nodules and infection threads (either 7 dpi or later at 14 dpi) when *MtPDLP1* was overexpressed in nitrogen depleted conditions. Furthermore, overexpression of *MtPDLP1* does not regulate callose in *M. truncatula* roots, as Arabidopsis orthologues do (Lee et al., 2011).

In addition to the systemic AON pathway (autoregulation of nodulation, reviewed in Chapter 1, section 1.2.3), the number of nodules is also controlled by nitrogen availability (Reid et al., 2011a; Reid et al., 2011b). Several research lines in different plant systems have proved that control of nodulation by rhizobia infection and by nitrate availability act through independent pathways (Jeudy et al., 2010; Reid et al., 2011a). Nevertheless, the fact that several supernodulating mutants are also nitrate insensitive suggest that they share some genetic regulatory mechanisms (Carroll et al., 1985a; Schnabel et al., 2005; Reid et al., 2011a). In *G. max* and *L. japonicus*, for example, nitrate induces a specific CLE peptide that is perceived in the root by the same receptor (NARK and HAIR1 respectively) that perceives the rhizobia-induced CLE peptide in the shoot, (Reid et al., 2011a). So far, CLE peptides induced by nitrate have not been identified in *Medicago* species and only two CLE peptides have been characterized in *M. truncatula* to have a role in regulating the number of nodules induced by rhizobia but not by nitrate, MtCLE12 and MtCLE13 (Mortier et al., 2010). Expression profiles of *MtPDLP1* and MtCLE13 peptides were found co-regulated at similar

timings post-inoculation in root hairs (Breakspear et al., 2014; Jardinaud et al., 2016) (Figure 6.4 and Figure 6.15).

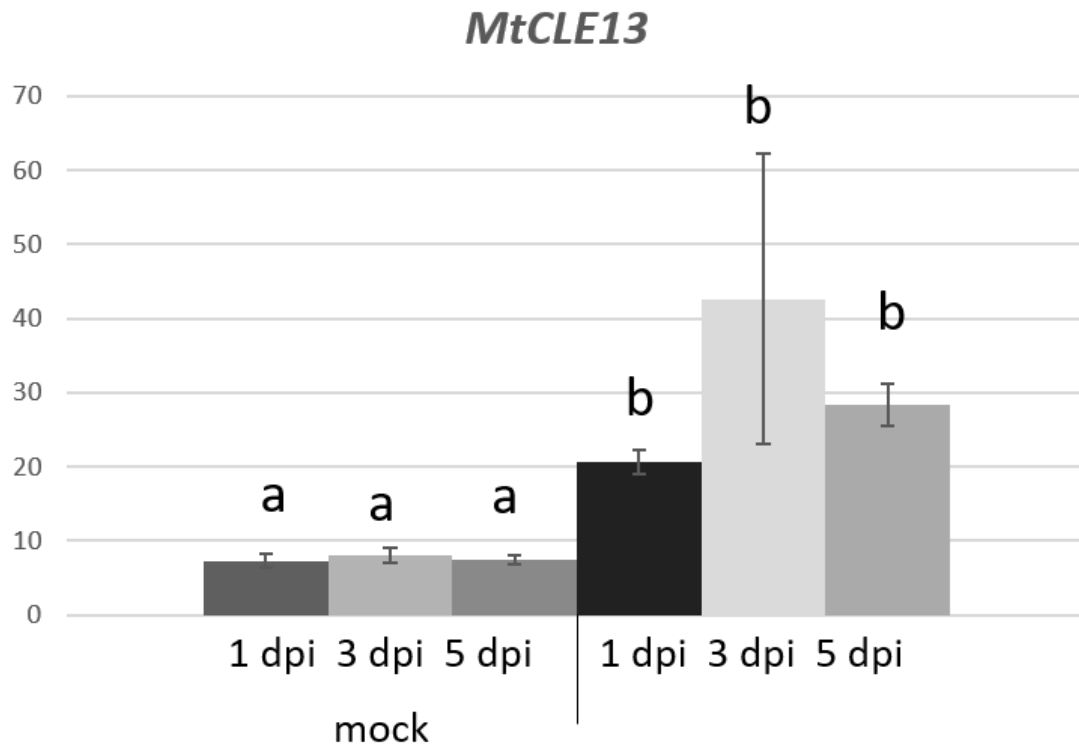


Figure 6.15-Expression pattern of *MtCLE13* in response to rhizobia.

Expression profile in root hairs 1, 2 and 5 days after infection (dpi) with a mutant *S. meliloti* unable to inoculate roots (mock) and 1, 3 and 5 days post infection with wild type *S. meliloti* (dpi). Image adapted from <http://mtgea.noble.org/v3/>. Data published by (Breakspear et al., 2014).

Contrasting with the results obtained in nitrogen-starved conditions, *M. truncatula* transgenic roots overexpressing the newly identified plasmodesmata-located protein *MtPDLP1* formed infection threads and nodules at a rate that resembled wildtype roots in no-nitrate (Figure 6.9). These plants appear to be, at least partially, nitrate insensitive in regards of the inhibition of nodulation in full-nitrate.

In Chapter 3 it was shown that nitrate concentrations as high as 5mM do not affect callose deposition in *M. truncatula* roots in the absence or presence of rhizobia. Callose is not downregulated after inoculation of *MtPDLP1* overexpressing roots in full nitrate conditions. The results suggest that *MtPDLP1* plays a role in the regulation of callose post-inoculation and that this pathway is important to inhibit the formation of nodules when nitrate is available. Callose deposition was not assessed in transgenic plants overexpressing *MtPDLP1* under full nitrate at 7 dpi (when the nodulation phenotype was reported) nor at a later stage of the inoculation stage than 24 hpi. Therefore, it is not possible to know if callose miss-regulation is compensated at later stages of the process.

The potential role of *MtPDLP1* in the transduction/sensing of nitrate signals is supported by its expression profile. The gene is downregulated in full nitrate and downregulated even further in the supernodulating mutant *sun*, in both nitrate depleted and sufficient conditions (Figure 6.16) (Schnabel et al., 2005; Moreau et al., 2011). The reduced *MtPDLP1* expression suggest that this protein contributes to the SUNN-CLE signalling pathway that controls number of nodules in response to CLE (or CLE derived) signals induced by nitrate and/or rhizobia inoculation and that acts downstream of SUNN.

Interestingly and consistent with a signalling function, recent research demonstrated that SUNN localises at the plasmamembrane, predominantly in a punctate pattern resembling plasmodesmata (Crook et al., 2016). Other LRR-RLKs have been located at plasmodesmata (Lucas and Lee, 2004; Sagi et al., 2005; Stahl and Simon, 2013) including Arabidopsis' SUNN orthologue, CLAVATA1 (Stahl and Simon, 2013), which has also been identified as a key partner in the response to nitrate by regulating the outgrowth of lateral roots and expansion of plant root systems (Araya et al., 2014).

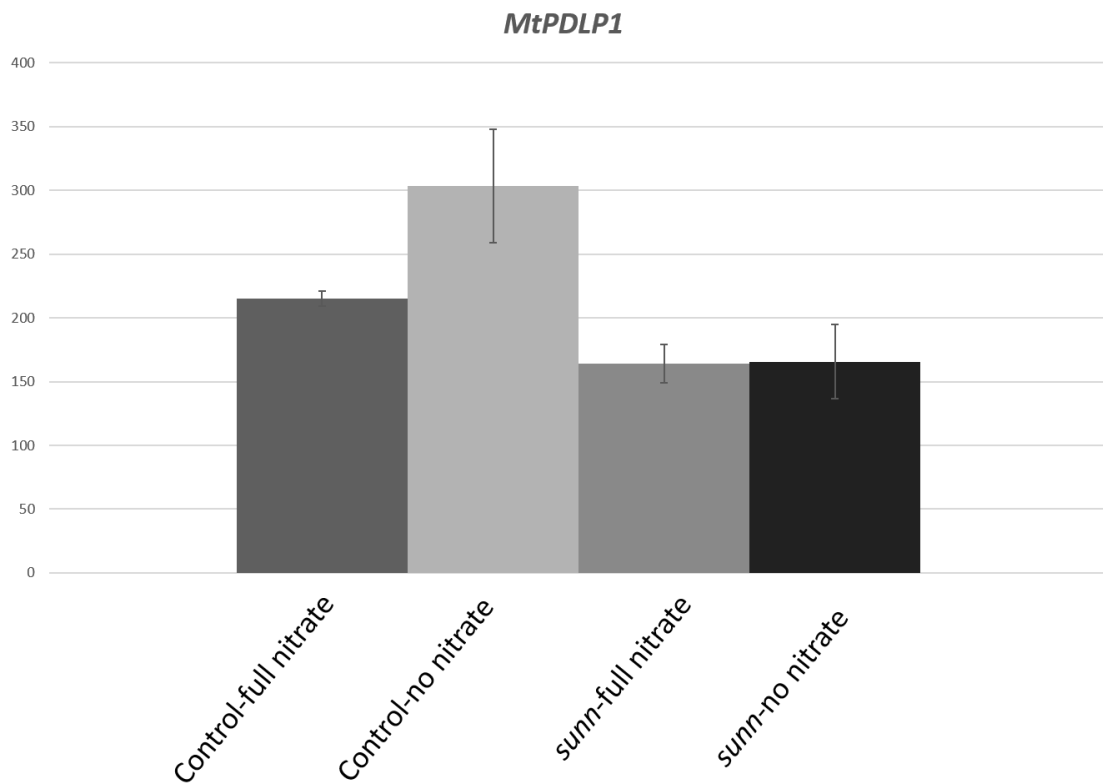


Figure 6.16- Expression pattern of *MtPDLP1* in response nitrate. Expression profile in root in the absence or 10 days-post inoculation with rhizobia and in full or depleted nitrate media. Image adapted from <http://mtgea.noble.org/v3/>. Data published by (Moreau et al., 2011).

Together these results suggest that *MtPDLP1* plays a role in the control of nodulation under full nitrate conditions and that this is mediated by changes in callose turnover. Whether it also plays a role in the regulation of nodulation by rhizobia remains still to be proven, but expression data of the gene in the *sunn* background and SUNN localisation at plasmodesmata suggest that potentially these two receptor proteins (SUNN and *MtPDLP1*), and/or the pathways that they regulate, interact.

A proposed model of the role of *MtPDLP1* is schematised in Figure 6.17. Receptor proteins SUNN and *MtPDLP1* are located at plasmodesmata when both proteins are in homeostasis CLE peptides can be sensed and trigger a secondary signal that control nodulation under high nitrate conditions. On the other hand, when *MtPDLP1* is overexpressed the balance is altered and all

SUNN receptors are engaged with a copy of its partner, not allowing the receptors to sense CLE peptides, blocking downstream signalling. Alternatively, the partner for SUNN in this pathway might be another RLK from the same protein family than *MtPDLP1* and when the latter is overexpressed does not allow SUNN to interact with its true partner, blocking downstream signalling.

Composite plants used in this work presented a wild type number of copies of *MtPDLP1* in the shoot and an overexpression in the roots. Little is yet known about the control of nodulation by nitrate in *Medicago*, but if the regulatory system is anything like regulatory pathway in *G. max*, control of nodulation by nitrate happens mainly locally and AON systemically (Reid et al., 2011a). Following that premise, SUNN/ *MtPDLP1* interaction (or SUNN interaction with other RLKs) is not affected in the shoot, allowing AON to function normally (Figure 6.17-C). Alternatively, *MtPDLP1* might not be playing any role in AON, but instead, it plays an important role in the root at early stages of inoculation (potentially in the transduction of Nod factor signalling).

Further research to identify the signals controlling the regulation of nodulation by nitrate in *M. truncatula* is required to fully understand the mechanism behind it and to determine their role in the hypothetical SUNN/ *MtPDLP1* signalling pathway. Experiments to explore the potential interaction of both proteins at plasmodesmata as part of the control of nodulation (both AON and regulation by nitrate) can help to understand the function of this new receptor-like kinase in these regulatory pathways. Co-immunoprecipitation, bimolecular fluorescence complementation or yeast two-hybrid system could be used to determine if they interact. Additionally, the use of mutants, a stable transgenic line overexpressing *MtPDLP1* and/or grafting experiments are required to understand the possible role of the receptor-like kinase in the systemic control of nodulation.

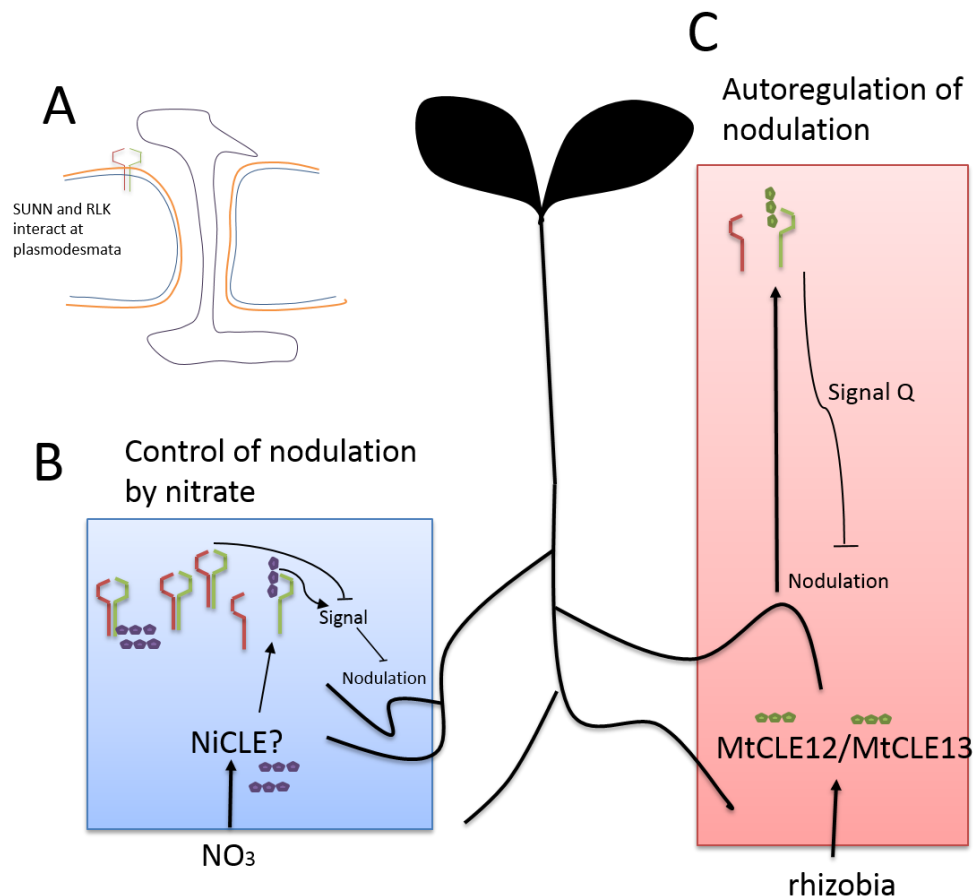


Figure 6.17 Schematic proposed model of the role of *MtPDLP1* in the control of nodulation in *M. truncatula*. (A) Based on the localisation of orthologues, we propose that, upon rhizobia perception or in response to nitrogen, SUNN interacts with specific RLKs at plasmodesmata to trigger downstream intracellular signalling pathways. (B) Nitrate availability triggers the regulation of nodulation by nitrate by inducing a signalling molecule, likely a CLE peptide (Nitrate-induced CLE-NiCLE) in the roots that are locally perceived by SUNN and/or its homologues to trigger inhibition of nodulation. This signal cannot be perceived efficiently when SUNN is engaged in interactions with *MtPDLP1* (or other RLKs). In transgenic roots overexpressing *MtPDLP1*, the inhibition of nodulation by nitrate appears blocked. (C) Rhizobia inoculation induces the expression of MtCLE12 and MtCLE13 in the roots. These signals are transported to the shoot where they are received by SUNN, triggering the expression of an unknown signal Q that stop further nodules and infection threads from developing. In the case of composite transgenic plants (where only the roots are transformed), and since the autoregulation of nodulation is shoot-dependant, AON would not be affected, allowing for an efficient signalling pathway.

Chapter 7

Chapter 7 -General discussion and conclusions

7.1 Callose regulates symplastic communication in *M. truncatula* roots upon rhizobia inoculation

Nodulation and infection are finely tuned processes that are controlled by complex mechanisms regulating the amount of nodules generated (Day et al., 1989; Li et al., 2009; Okamoto et al., 2009; Crook et al., 2016). In this thesis, evidence is presented supporting that callose-regulated symplastic communication actively controls root colonization by the symbiotic bacteria and nodule organogenesis during the establishment of the symbiotic interaction.

The results indicate that callose levels are downregulated in inner pericycle/cortical root tissue as soon as 24 hours after inoculation with the bacteria (Figure 3.1), and this downregulation coincides in time and tissue localisation with the changes in expression of a newly identified plasmodesmata located glucanase *MtBG2* (Figure 3.12, Figure 3.13 and Figure 3.15). Based on the expression profile, it is proposed that this protein plays a role in creating, maintaining and/or modifying symplastic domains to connect the phloem and cells undergoing reprogramming for nodule development concomitant with or prior to root hair infection. The regulation of symplastic connectivity by callose degrading enzymes was previously reported to control lateral root formation and patterning in *A. thaliana* (Benitez-Alfonso et al., 2013). In addition to its regulation in nodule primordia, *MtBG2* expression was also found in lateral root primordia, suggesting a dual role for this protein⁷, potentially linked to the development of post-embryonic organs. The possibility that lateral roots and nodules have a common evolutionary past has been proposed by several authors (Papadopoulou et al., 1996; Charon et al., 1999; Bensmihen, 2015), and the expression pattern of this callose-degrading enzyme opens new research possibilities to identify possible shared developmental pathways.

⁷ Personal communication: Martina Beck and Fernanda de Carvalho-Niebel (LIPM, Université de Toulouse, INRA, CNRS, 31326 Castanet-Tolosan, France)

The use of a symplastic tracer (CFDA) also showed that after rhizobia inoculation symplastic communication is established between the phloem and inner root tissues (Complainville et al., 2003). Using similar tools, it was found by our collaborators that, after inoculation, proteins and small molecules can move symplastically from epidermal cell layers into outer cortical cells⁸. In addition to its early expression in dividing cells (nodule primordia) *MtBG2* expression extends to the outer cortex and epidermal cell layers as the symbiotic process progress (8 dpi)⁷, but the regulation in the symplastic pathway was seen at earlier stages of the process (3 dpi). Together these results suggest that these changes are potentially regulated by other glucanase(s). In Chapter 3, we identified a pool of putative glucanases, among these *MtBG2* was also upregulated upon inoculation (Figure 3.12). Future experiments characterising *MtBG2* are required. Callose immunolocalisation of overexpressor lines and transport assays in mutants would shed some light into the role of the protein in establishing the symplastic continuum seen at 3 dpi. Additionally, electromicroscopy experiments could also help to clarify if the changes in symplastic permeability are due to callose regulation or a change in plasmodesmata structure, such as a change from single to branched plasmodesmata (or to both).

7.2 The ectopic expression of callose degrading enzymes in rhizobia infected and nodulating tissues increases the number of nodules

The importance of the symplastic regulation in the symbiotic process was assessed by evaluating the infection and nodulation phenotypes in transgenic roots constitutively expressing *MtBG2* and the expression of the Arabidopsis orthologous gene *PdBG1* under symbiotic regulated promoters. Both strategies lead to an increase in infection threads and nodule number (Figure 4.9 and Figure 5.3). Conversely, increasing callose via the expression of *cals3m* gain-of-function driven by the *ERN1* promoter strongly affected nodule development and

⁸ Personal communication: Martina Beck and Fernanda de Carvalho-Niebel (LIPM, Université de Toulouse, INRA, CNRS, 31326 Castanet-Tolosan, France)

rhizobia colonization⁷. Although infection was enhanced in transgenic plants when callose was down-regulated, infection threads were not affected in the opposite case. This suggests that regulation of the symplastic connectivity by callose is crucial to control nodule development but is not essential for infection thread formation in *M. truncatula*. It is proposed that this regulatory communication system controls the movement of signalling molecules between infected root hairs and cortical tissues to activate nodule organogenesis and colonization (Figure 7.1).

The mobile signals, which movement might be regulated by callose-mediated symplastic communication, are yet unknown, but gene expression studies in *M. truncatula* transgenic roots expressing p*MtERN1*-cals3m show that *NIN* and the expression of the genes encoding the regulatory peptides *MtCLE12/13* expression are reduced⁹. This indicates that blocking the symplastic pathway through the over-accumulation of callose affects *NIN* and *MtCLE12/13* expression, hence the signalling pathways in which they are involved. The results support a model where *NIN*, or regulators of *NIN*, are transported through plasmodesmata from the epidermis to the cortex to promote the expression of *NIN* or downstream factors that initiate nodule organogenesis. It would be interesting to study the spatial and temporal regulation of *NIN* and *MtCLE12/13* (at gene and protein level) in transgenic roots expressing p*MtERN1*-PdBG1 or overexpressing *MtBG2*. Increased gene expression or changes in protein localization will provide insights into the potential molecular mechanism underlying the increase in nodule number observed in these plants.

Future research is required to elucidate the identity of this putative mobile factor(s) and establish the molecular mechanism and crosstalk among root cell layers that orchestrate nodule organogenesis. For example, complementation studies using a *nin* background transformed with constructs that express *NIN* in the epidermis (for example under the p*EXP* promoter) could be used to test whether *NIN* acts non-cell autonomously. Co-expression of p*MtERN1*-cals3m

⁹ Personal communication: Martina Beck and Fernanda de Carvalho-Niebel (LIPM, Université de Toulouse, INRA, CNRS, 31326 Castanet-Tolosan, France)

(induced callose in infected tissues and restricted transport) will indicate if symplastic communication is required for *nin* complementation. Immuno-probing these lines with NIN antibodies should be able to discern if NIN itself is the mobile signal and if it requires the symplastic pathway for its function. Alternatively, using RNAseq and proteomics analysis, the transcriptome and proteome of p*MtERN1*-cals3m and p*MtERN1*-PdBG1 transgenic roots before and after infection can be compared. Genes which are differentially regulated, or proteins differently enriched, in these transgenic would potentially belong to a mechanism involved in the generation or transmission of the mobile signal orchestrating infection and nodulation.

7.3 A plasmodesmata-located RLK regulated signalling affecting nodule number under high nitrate conditions

Additionally, the study of homologous proteins of Arabidopsis PDLPs (reviewed in Chapter 1, sections 1.3.1, 1.3.2 and 1.3.3.1) identified a novel receptor like kinase targeted to plasmodesmata, *MtPDLP1*. The overexpression of this RLK in *M. truncatula* roots did not lead to changes in callose under nitrate depleted conditions (Figure 6.8) and, as in control plants, downregulation of the polysaccharide after rhizobia infection was also observed (Figure 6.8). Although *MtPDLP1* was rapidly regulated post-rhizobia inoculation, suggesting an infection/nodulation related function (Figure 6.5), transgenic plants did not show any infection or nodulation phenotype under nitrate-depleted conditions (Figure 6.9). On the other hand, callose was not regulated in response to rhizobia in *MtPDLP1* overexpressing plants grown under high nitrate concentrations, suggesting that *MtPDLP1* interferes with callose metabolism or with the signals that control this response. Surprisingly, these plants were nitrate insensitive, meaning that they nodulated as effectively under high nitrate conditions as they did in nitrogen depleted media (Figure 6.13). Alternatively, downregulation of callose might just be delayed (it didn't occur at the measured time point) or there is an over-production of callose (by activation of CALS, for example) that mask the effects of rhizobia in nitrate conditions. Future experiments characterising the callose levels of nodulating plants and expression profile of callose modifying enzymes under full nitrate conditions are required to fully understand the

possible role of callose in this process. In any case, even without considering the effects on callose, the fact remains that transgenic plants overexpressing *MtPDLP1* presented a nitrate insensitive phenotype suggesting that regulated expression of this protein is important for proper nitrate responses.

Based on nodulation phenotypes, *MtPDLP1* might be playing completely different roles under nitrate-deprived and full nitrate conditions

In the case of nitrate-depleted conditions, *MtPDLP1* is upregulated rapidly in the epidermal cell layer upon inoculation with rhizobia (Jardinaud et al., 2016). This upregulation might be necessary for a signal transduction necessary for infection, maybe involving the induction of *MtBG2* in inner root cell layers, leading to the downregulation of callose upon inoculation reported in Chapter 3 (Figure 7.1). No phenotype under nitrate-depleted conditions was seen in plants overexpressing *MtPDLP1*, meaning that either it does not play any role in the regulation of nodulation by rhizobia, that the role of the protein in this pathway is limited to the shoot (hindering the phenotype in this case) or that *MtPDLP1* requires a partner for proper functioning that is either not present or not present at the required levels to produce a phenotype.

When growing in full nitrate, *MtPDLP1* expression is downregulated, and this regulation seems to be SUNN-dependent (Figure 6.16). It can be proposed that *MtPDLP1* plays a role in regulating number of nodules and infection threads under full nitrate conditions, and it does so potentially by interacting with SUNN in the root (Figure 6.17).

To discern among these hypotheses, mutants in *MtPDLP1* could be generated and studied to determine the specific role of this protein in infection or nodulation and in the regulation of callose in response to rhizobia or nitrate signal (are these plants unable to nodulate/infect? Are the number of nodules affected? Is callose deposition regulated upon inoculation?). Additionally, stable lines overexpressing *MtPDLP1* can be generated to study the role of the shoot on nodule number. Grafting experiments combining wild type and *MtPDLP1* (mutant/overexpressor) root and shoot-stocks can also be used to determine the role of root-to-shoot-to root signalling.

Finally, determining the domain of expression of *MtPDLP1* would shed some light on the function of the protein and its role in symbiosis. A *pMtPDLP1-GUS* reporter line could be generated to spatially and timely locate *MtPDLP1* expression pattern. Complementarily, immunolocalisation experiments using antibodies raised against the protein will also help to determine protein levels and localisation. Both approaches would allow the characterisation of the protein function at different time points of the symbiotic process and under different nitrate conditions.

7.4 Conclusions

In conclusion, this work has contributed to the understanding of the role of callose and the symplastic pathway in the establishment and control of the mutualistic symbiotic interaction between *M. truncatula* and *S. meliloti*. Future work has been proposed throughout this thesis to address the questions that arise from this research, and that will help to dissect the signalling molecules and other components using or regulating the symplastic pathway as a medium to orchestrate the infection and nodulation processes.

The results presented in this thesis could be the foundation for more extensive work in economically important legumes, such as soybean or common beans. This work also directly impacts the agro-industry, since it helps in the search for biotechnological tools to improve nodulation and, potentially nitrogen fixation, in legumes. For example, collaborations with agro-companies could be established to transform PdBG1 in the symbiotic domains in economic and agricultural important legumes to tackle the challenge of food security.

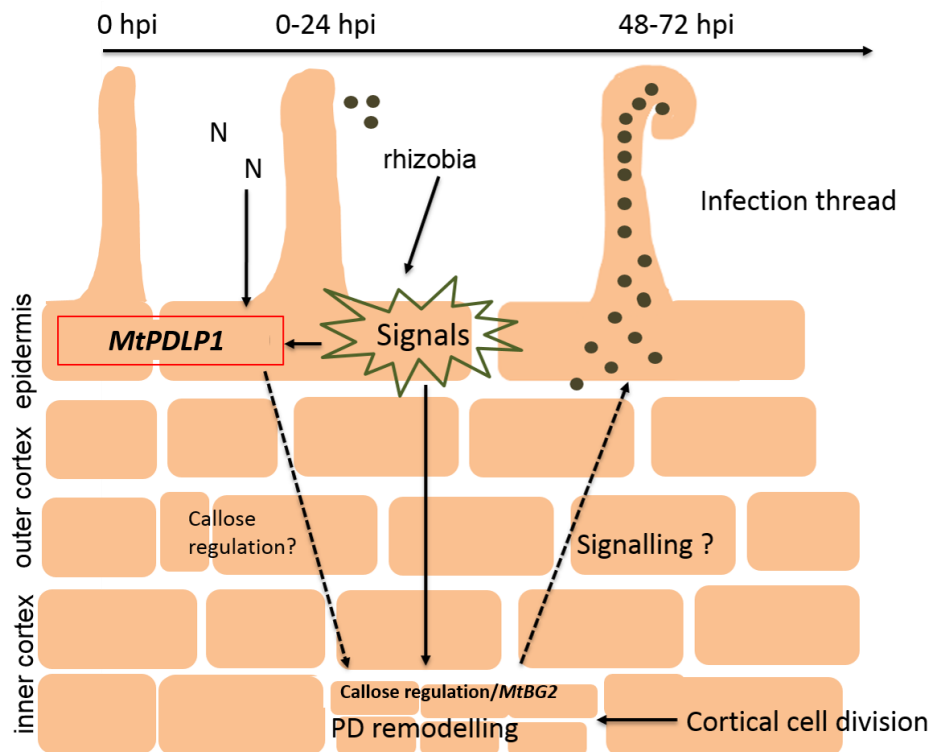


Figure 7.1-Schematic model of callose-mediated regulation of root nodule development in *M. truncatula*. Early signalling (either in response to rhizobia or to nitrogen availability) are perceived in the epidermal cell layer by RLKs including *MtPDLP1* that will trigger further signalling to control infection and nodulation. Callose appears downregulated in pericycle and cortical cell layers coincident with a reported increase in symplastic transport. This process is at least partially regulated by the expression of *MtBG2* in cortical cell layers. Altering callose regulation by ectopic expression of *MtBG2* affects both nodule number and infection thread suggesting interactions between processes occurring in the cortex and epidermal tissues.

Appendices

Appendix 1 List of sequences used in the phylogenetic analysis of β -1,3-glucanases from the GHL17 protein family in *Arabidopsis thaliana* and *M. truncatula*. *Picea sitchensis* sequence was included as an outgroup. Table includes predicted domains (See Material and Methods)

| Organism | Sequence | Identifier | SP | GP I | GHI17 | x8 |
|----------------------|---------------|------------|----|------|-------|----|
| <i>M. truncatula</i> | Medtr8g085720 | MtBG_1 | X | X | X | X |
| <i>M. truncatula</i> | Medtr3g083580 | MtBG_2 | X | X | X | X |
| <i>M. truncatula</i> | Medtr4g132280 | MtBG_3 | X | X | X | X |
| <i>M. truncatula</i> | Medtr5g078200 | MtBG_4 | X | | X | X |
| <i>M. truncatula</i> | Medtr3g065460 | MtBG_5 | X | X | X | X |
| <i>M. truncatula</i> | Medtr5g015720 | MtBG_6 | X | X | x | x |
| <i>M. truncatula</i> | Medtr8g102340 | MtBG_7 | X | | X | X |
| <i>M. truncatula</i> | Medtr4g010200 | MtBG_8 | X | X | X | |
| <i>M. truncatula</i> | Medtr5g081720 | MtBG_9 | X | | X | |
| <i>M. truncatula</i> | Medtr4g069940 | MtBG_10 | X | | X | X |
| <i>M. truncatula</i> | Medtr5g085580 | MtBG_11 | X | | X | X |
| <i>M. truncatula</i> | Medtr3g116510 | MtBG_12 | X | | X | X |
| <i>M. truncatula</i> | Medtr1g007810 | MtBG_13 | | | X | |
| <i>M. truncatula</i> | Medtr3g116510 | MtBG_14 | X | | X | X |
| <i>M. truncatula</i> | Medtr7g026340 | MtBG_15 | X | | X | X |
| <i>M. truncatula</i> | Medtr2g034480 | MtBG_16 | X | | X | X |
| <i>M. truncatula</i> | Medtr2g034470 | MtBG_17 | X | | X | |
| <i>M. truncatula</i> | Medtr2g027560 | MtBG_18 | X | X | X | X |
| <i>M. truncatula</i> | Medtr4g134280 | MtBG_19 | X | | X | X |
| <i>M. truncatula</i> | Medtr4g076470 | MtBG_20 | X | | X | |
| <i>M. truncatula</i> | Medtr4g076430 | MtBG_21 | X | | X | |
| <i>M. truncatula</i> | Medtr4g076440 | MtBG_22 | X | | X | |
| <i>M. truncatula</i> | Medtr4g076490 | MtBG_23 | | | X | |
| <i>M. truncatula</i> | Medtr4g076500 | MtBG_24 | | | X | |
| <i>M. truncatula</i> | Medtr4g076570 | MtBG_25 | X | X | X | |
| <i>M. truncatula</i> | Medtr2g034480 | MtBG_26 | X | | X | |
| <i>M. truncatula</i> | Medtr2g034440 | MtBG_27 | X | | X | |
| <i>M. truncatula</i> | Medtr7g085390 | MtBG_28 | X | X | X | X |
| <i>M. truncatula</i> | Medtr3g108600 | MtBG_29 | X | X | X | X |
| <i>M. truncatula</i> | Medtr4g124440 | MtBG_30 | X | X | X | X |
| <i>M. truncatula</i> | Medtr4g083500 | MtBG_31 | X | X | X | X |
| <i>M. truncatula</i> | Medtr3g095050 | MtBG_32 | X | X | X | X |

| | | | | | | |
|----------------------|---------------|---------|---|---|---|---|
| <i>M. truncatula</i> | Medtr8g092070 | MtBG_33 | X | | X | X |
| <i>M. truncatula</i> | Medtr6g032820 | MtBG_34 | | | X | X |
| <i>M. truncatula</i> | Medtr7g081350 | MtBG_35 | X | | X | |
| <i>M. truncatula</i> | Medtr3g080410 | MtBG_36 | X | | X | |
| <i>M. truncatula</i> | Medtr2g034440 | MtBG_37 | X | | X | |
| <i>M. truncatula</i> | Medtr5g081720 | MtBG_38 | X | | X | |
| <i>M. truncatula</i> | Medtr4g114850 | MtBG_39 | X | X | X | |
| <i>M. truncatula</i> | Medtr7g081370 | MtBG_40 | X | | X | |
| <i>M. truncatula</i> | Medtr8g012400 | MtBG_42 | X | | X | X |
| <i>A. thaliana</i> | At2g05790 | | X | | X | X |
| <i>A. thaliana</i> | At4g26830 | | X | | X | X |
| <i>A. thaliana</i> | At5g55180 | | X | | X | X |
| <i>A. thaliana</i> | At4g18340 | | X | X | X | |
| <i>A. thaliana</i> | At1g30080 | | X | X | X | |
| <i>A. thaliana</i> | At2g26600 | | X | X | X | |
| <i>A. thaliana</i> | At3g15800 | | X | X | X | |
| <i>A. thaliana</i> | At2g27500 | | X | X | X | |
| <i>A. thaliana</i> | At5g42100 | | X | X | X | |
| <i>A. thaliana</i> | At1g32860 | | X | X | X | |
| <i>A. thaliana</i> | At5g24318 | | X | | X | X |
| <i>A. thaliana</i> | At3g46570 | | X | | X | |
| <i>A. thaliana</i> | At2g39640 | | X | | X | X |
| <i>A. thaliana</i> | At3g55430 | | X | | X | X |
| <i>A. thaliana</i> | At5g42720 | | X | | X | |
| <i>A. thaliana</i> | At4g34480 | | X | | X | |
| <i>A. thaliana</i> | At2g16230 | | X | | X | X |
| <i>A. thaliana</i> | At3g13560 | | X | X | X | X |
| <i>A. thaliana</i> | At1g11820 | | X | | X | |
| <i>A. thaliana</i> | At1g66250 | | X | X | X | X |
| <i>A. thaliana</i> | At2g01630 | | X | X | X | X |
| <i>A. thaliana</i> | At4g29360 | | X | X | X | X |
| <i>A. thaliana</i> | At5g56590 | | X | | X | X |
| <i>A. thaliana</i> | At3g55780 | | X | | X | X |
| <i>A. thaliana</i> | At3g61810 | | X | | X | |
| <i>A. thaliana</i> | At3g07320 | | X | | X | X |
| <i>A. thaliana</i> | At3g23770 | | X | | X | X |
| <i>A. thaliana</i> | At4g14080 | | X | | X | X |
| <i>A. thaliana</i> | At5g58480 | | X | X | X | X |
| <i>A. thaliana</i> | At4g17180 | | X | X | X | X |
| <i>A. thaliana</i> | At5g64790 | | X | X | X | X |
| <i>A. thaliana</i> | At3g04010 | | X | X | X | X |
| <i>A. thaliana</i> | At5g18220 | | X | X | X | X |
| <i>A. thaliana</i> | At1g64760 | | X | X | X | X |
| <i>A. thaliana</i> | At2g19440 | | X | X | X | X |
| <i>A. thaliana</i> | At3g24330 | | X | X | X | X |
| <i>A. thaliana</i> | At5g20870 | | X | X | X | X |

| | | | | | | |
|-------------------------|------------|--|---|---|---|---|
| <i>A. thaliana</i> | At5g58090 | | X | X | X | X |
| <i>A. thaliana</i> | At4g31140 | | X | X | X | X |
| <i>A. thaliana</i> | At1g77790 | | X | | X | |
| <i>A. thaliana</i> | At1g77780 | | X | X | X | |
| <i>A. thaliana</i> | At5g20390 | | X | | X | |
| <i>A. thaliana</i> | At5g20560 | | X | | X | |
| <i>A. thaliana</i> | At1g33220 | | X | | X | |
| <i>A. thaliana</i> | At5g20340 | | X | | X | |
| <i>A. thaliana</i> | At5g20330 | | X | | X | |
| <i>A. thaliana</i> | At4g16260 | | X | | X | |
| <i>A. thaliana</i> | At3g57270 | | X | | X | |
| <i>A. thaliana</i> | At3g57240 | | X | | X | |
| <i>A. thaliana</i> | At3g57260 | | X | | X | |
| <i>Picea sitchensis</i> | BT070278.1 | | X | | X | X |

Appendix 2- List of sequences used in the phylogenetic analysis of callose synthase protein family in *Arabidopsis thaliana* and *Medicago truncatula*.

| Organism | Sequence | Identifier |
|----------------------|---------------|------------|
| <i>M. truncatula</i> | Medtr2g013580 | MtGSL1 |
| <i>M. truncatula</i> | Medtr4g078220 | MtGSL2 |
| <i>M. truncatula</i> | Medtr2g090375 | MtGSL3 |
| <i>M. truncatula</i> | Medtr3g096200 | MtGSL4 |
| <i>M. truncatula</i> | Medtr8g093630 | MtGSL5 |
| <i>M. truncatula</i> | Medtr2g061380 | MtGSL6 |
| <i>M. truncatula</i> | Medtr3g075180 | MtGSL7 |
| <i>M. truncatula</i> | Medtr1g116370 | MtGSL8 |
| <i>M. truncatula</i> | Medtr3g047390 | MtGSL9 |
| <i>M. truncatula</i> | Medtr7g005950 | MtGSL10 |
| <i>M. truncatula</i> | Medtr3g075180 | MtGSL11 |
| <i>M. truncatula</i> | Medtr1g116470 | MtGSL12 |
| <i>M. truncatula</i> | Medtr2g072160 | MtGSL13 |
| <i>A. thaliana</i> | AT4G04970 | AtGSL1 |
| <i>A. thaliana</i> | AT2G13680 | AtGSL2 |
| <i>A. thaliana</i> | AT2G31960. | AtGSL3 |
| <i>A. thaliana</i> | AT3G14570 | AtGSL4 |

| | | |
|--------------------|-----------|---------|
| <i>A. thaliana</i> | AT4G03550 | AtGSL5 |
| <i>A. thaliana</i> | AT1G05570 | AtGSL6 |
| <i>A. thaliana</i> | AT1G06490 | AtGSL7 |
| <i>A. thaliana</i> | AT2G36850 | AtGSL8 |
| <i>A. thaliana</i> | AT5G36870 | AtGSL9 |
| <i>A. thaliana</i> | AT3G07160 | AtGSL10 |
| <i>A. thaliana</i> | AT3G59100 | AtGSL11 |
| <i>A. thaliana</i> | AT5G13000 | AtGSL12 |

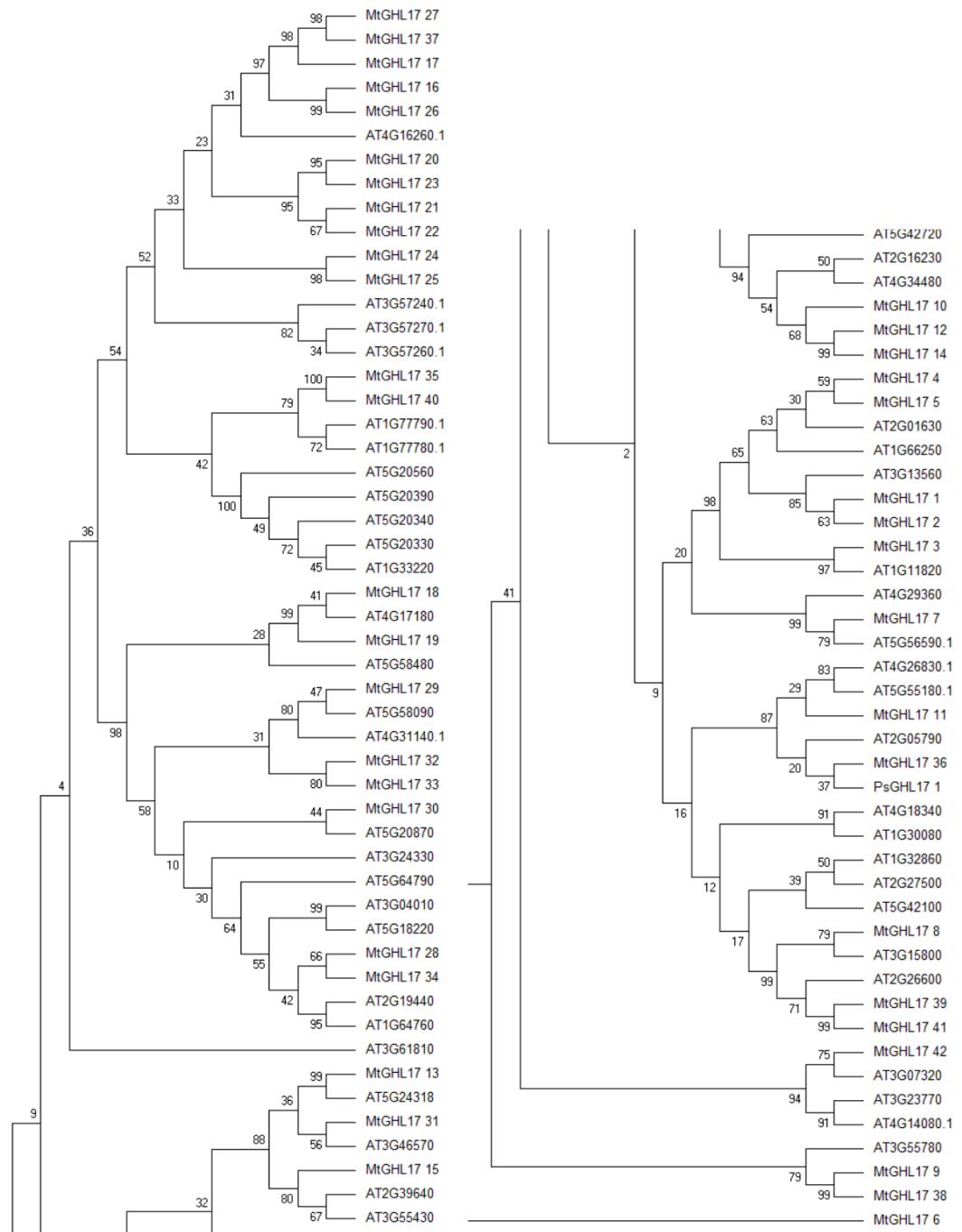
Appendix 3 List of sequences used in the phylogenetic analysis of PDLP protein family in *Arabidopsis thaliana* and *M.truncatula*. *Picea sitchensis* was included as an outgroup. Table include predicted domains (See Material and Methods).

| Organism | Sequence | Identifier | SP | Transmembrane | DUF26/ Salt stress response-antifungal | Other domains |
|----------------------|---------------|-----------------|----|---------------|--|-----------------|
| <i>M. truncatula</i> | Medtr1g073320 | Mt_PDL P-like1 | X | X | X | |
| <i>M. truncatula</i> | Medtr7g098410 | Mt_PDL P-like2 | X | X | X | |
| <i>M. truncatula</i> | Medtr1g080350 | Mt_PDL P-like3 | X | X | X | |
| <i>M. truncatula</i> | Medtr8g104990 | Mt_PDL P-like4 | X | X | X | |
| <i>M. truncatula</i> | Medtr5g078030 | Mt_PDL P-like5 | X | X | X | |
| <i>M. truncatula</i> | Medtr3g065370 | Mt_PDL P-like6 | X | X | X | |
| <i>M. truncatula</i> | Medtr5g005480 | Mt_PDL P-like7 | X | X | X | pkina se_tyr |
| <i>M. truncatula</i> | Medtr5g005530 | Mt_PDL P-like8 | X | X | X | pkina se_tyr |
| <i>M. truncatula</i> | Medtr3g064090 | Mt_PDL P-like9 | X | X | X | pkina se_tyr |
| <i>M. truncatula</i> | Medtr6g463660 | Mt_PDL P-like10 | X | X | X | |
| <i>M. truncatula</i> | Medtr1g104890 | Mt_PDL P-like11 | X | X | X | pkina se_tyr |
| <i>M. truncatula</i> | Medtr2g088930 | Mt_PDL P-like12 | X | X | X | |

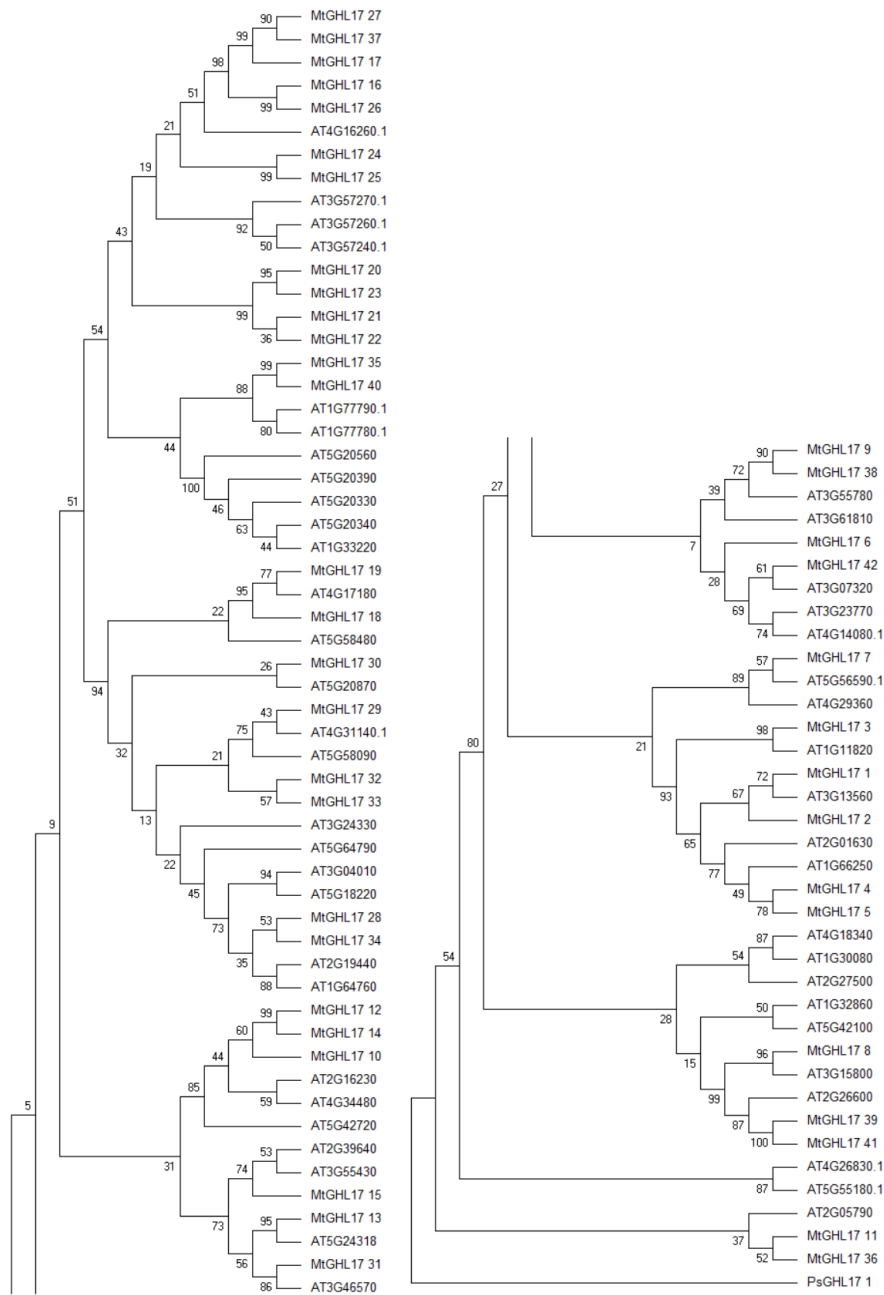
| | | | | | | |
|----------------------|---------------|-----------------|---|---|---|------------------------|
| <i>M. truncatula</i> | Medtr8g041690 | Mt_PDL P-like13 | X | X | X | pkina se_tyr |
| <i>M. truncatula</i> | Medtr1g105650 | Mt_PDL P-like14 | X | X | X | pkina se_tyr |
| <i>M. truncatula</i> | Medtr1g105655 | Mt_PDL P-like15 | X | X | X | pkina se_tyr |
| <i>M. truncatula</i> | Medtr8g041710 | Mt_PDL P-like16 | X | X | X | pkina se_tyr |
| <i>M. truncatula</i> | Medtr2g010730 | Mt_PDL P-like17 | X | X | X | pkina se_tyr |
| <i>M. truncatula</i> | Medtr1g105700 | Mt_PDL P-like18 | X | X | X | S_TY KC |
| <i>M. truncatula</i> | Medtr5g065130 | Mt_PDL P-like19 | X | X | X | pkina se_tyr |
| <i>M. truncatula</i> | Medtr1g105700 | Mt_PDL P-like20 | X | X | X | pkina se_tyr |
| <i>M. truncatula</i> | Medtr1g105800 | Mt_PDL P-like21 | X | X | X | pkina se_tyr |
| <i>M. truncatula</i> | Medtr5g005450 | Mt_PDL P-like22 | X | X | X | pkina se_tyr |
| <i>M. truncatula</i> | Medtr8g028065 | Mt_PDL P-like23 | X | X | X | |
| <i>M. truncatula</i> | Medtr1g105860 | Mt_PDL P-like24 | X | X | X | |
| <i>M. truncatula</i> | Medtr1g105585 | Mt_PDL P-like25 | X | X | X | pkina se_tyr |
| <i>M. truncatula</i> | Medtr8g041870 | Mt_PDL P-like26 | X | X | X | SCOP - BLAS T |
| <i>M. truncatula</i> | Medtr1g105820 | Mt_PDL P-like27 | X | X | X | S_TY KC |
| <i>M. truncatula</i> | Medtr5g068260 | Mt_PDL P-like28 | X | X | X | pkina se_tyr |
| <i>M. truncatula</i> | Medtr8g041650 | Mt_PDL P-like29 | X | X | X | pkina se_tyr |
| <i>M. truncatula</i> | Medtr3g079850 | Mt_PDL P-like30 | X | X | X | pkina se_tyr |
| <i>M. truncatula</i> | Medtr8g041660 | Mt_PDL P-like31 | X | X | X | pkina se_tyr |
| <i>M. truncatula</i> | Medtr1g105615 | Mt_PDL P-like32 | X | X | X | S_TY KC |
| <i>A. thaliana</i> | AtPDLP_1 | | X | X | X | |
| <i>A. thaliana</i> | AtPDLP_2 | | X | X | X | |

| | | | | | | |
|-----------------------------|---------------|--|---|---|---|------------|
| <i>A. thaliana</i> | AtPDLP_3 | | X | X | X | |
| <i>A. thaliana</i> | AtPDLP_4 | | X | X | X | |
| <i>A. thaliana</i> | AtPDLP_5 | | X | X | X | |
| <i>A. thaliana</i> | AtPDLP_6 | | X | X | X | |
| <i>A. thaliana</i> | AtPDLP_7 | | X | X | X | |
| <i>A. thaliana</i> | AtPDLP_8 | | X | X | X | |
| <i>A. thaliana</i> | AT5G48540 | | X | | X | |
| <i>A. thaliana</i> | AT1G63580.1 | | X | X | X | |
| <i>A. thaliana</i> | AT4G23140 | | X | X | X | S_TYK C |
| <i>Picea sitchensis</i> | PsPDLP-like_1 | | X | X | X | |

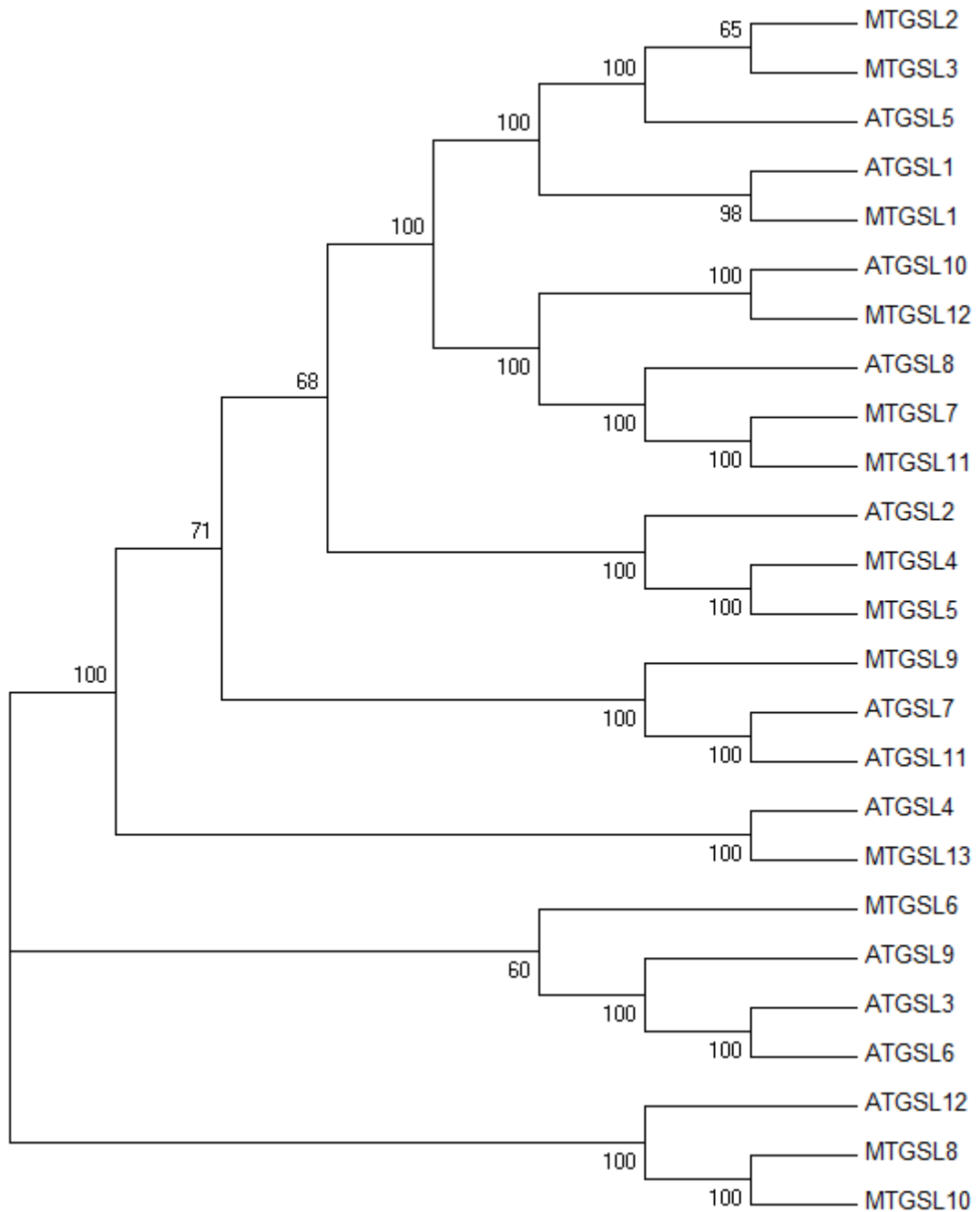
Appendix 4- Phylogenetic reconstruction using β -1,3-glucanases from GHL17 family protein sequences isolated from *A. thaliana* and *M. truncatula* orthologues generated by Maximum Likelihood algorithm. Bootstrap values for 500 repetitions are included.



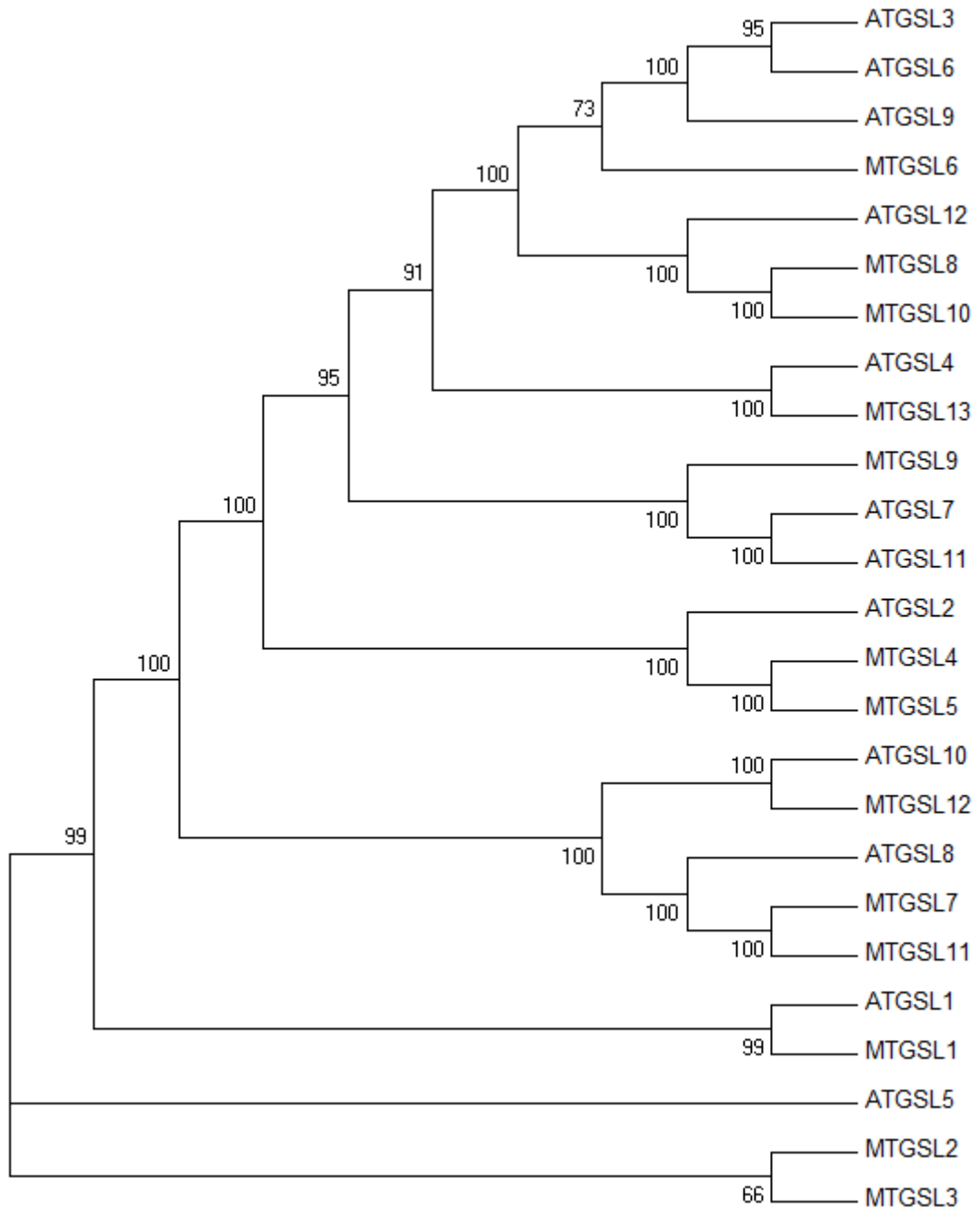
Appendix 5- Phylogenetic reconstruction using β -1,3-glucanases from GHL17 family protein sequences isolated from *A. thaliana* and *M. truncatula* orthologues generated by Neighbour Joining algorithm. Bootstrap values for 500 repetitions are included.



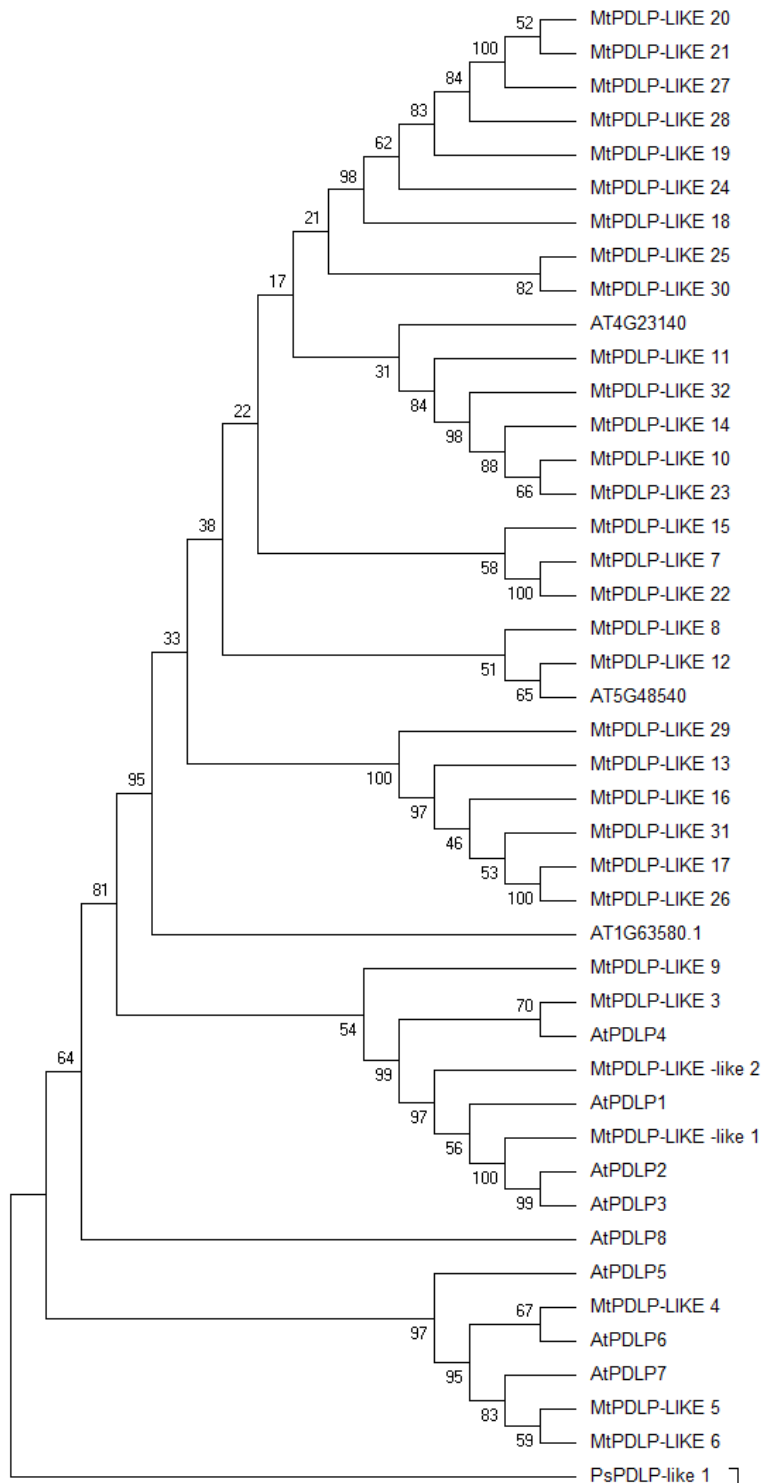
Appendix 6- Phylogenetic reconstruction using CALs sequences isolated from *A. thaliana* and *M. truncatula* orthologues generated by Maximum Likelihood algorithm. Bootstrap values for 500 repetitions are included.



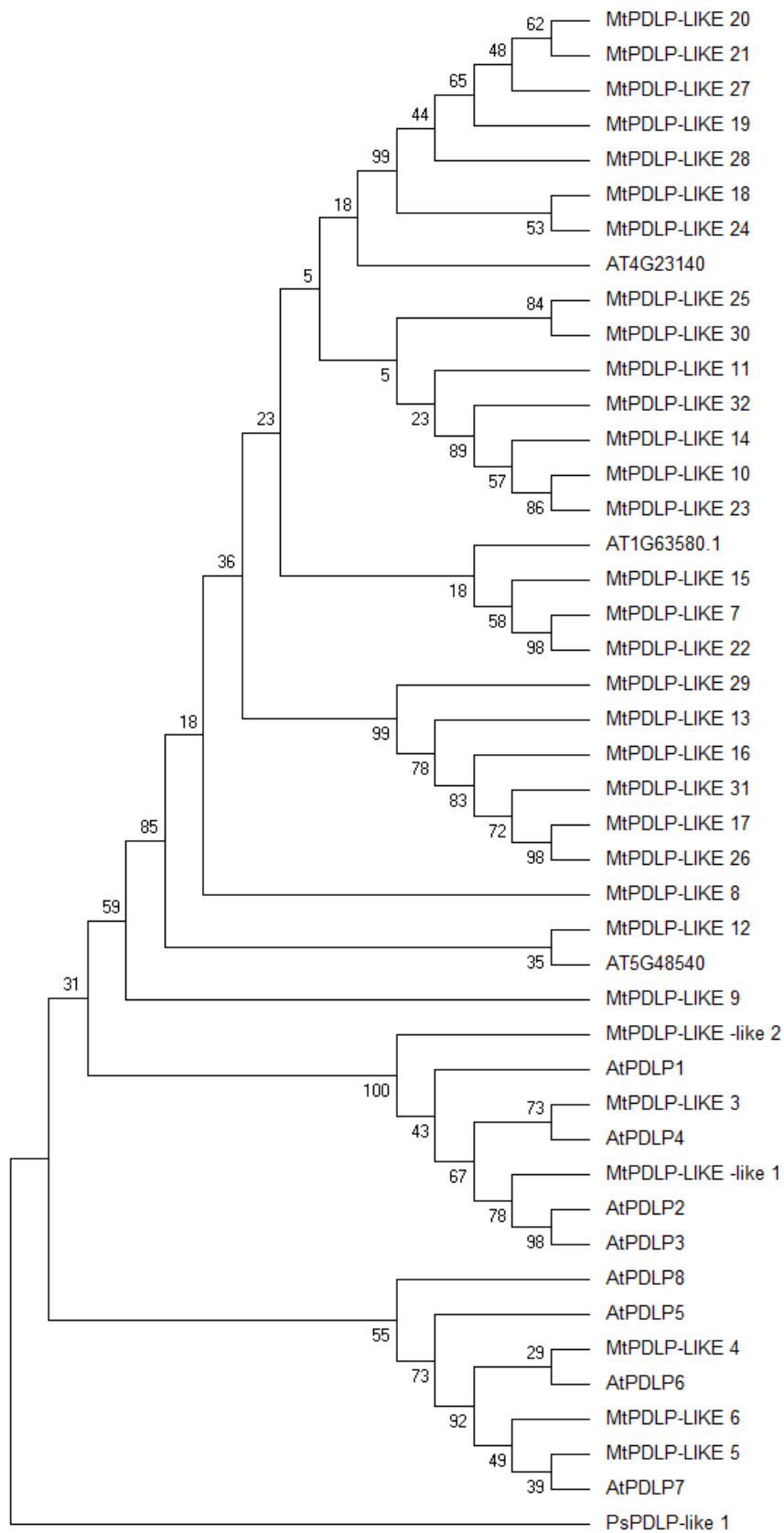
Appendix 7- Phylogenetic reconstruction using CALs sequences isolated from *A. thaliana* and *M. truncatula* orthologues generated by Neighbour Joining algorithm. Bootstrap values for 500 repetitions are included.



Appendix 8- Phylogenetic reconstruction using PDLPs sequences isolated and *A. thaliana* and *M. truncatula* orthologues generated by Maximum Likelihood algorithm. Bootstrap values for 500 repetitions are included.



Appendix 9- Phylogenetic reconstruction using PDLPs sequences isolated and *A. thaliana* and *M. truncatula* orthologues generated by Neighbour Joining algorithm. Bootstrap values for 500 repetitions are included.



Appendix 10- Phylogenetic reconstruction using β -1,3-glucanases from GHL17 family protein sequences isolated from *A. thaliana* and *M. truncatula* orthologues generated by Neighbour Joining algorithm in Newick format. Bootstrap values for 500 repetitions are included.

(((((MtGHL17_27,MtGHL17_37)0.9120,MtGHL17_17)0.9900,(MtGHL17_16,MtGHL17_26)0.9980)0.9780,AT4G16260.1,(MtGHL17_24,MtGHL17_25)0.9920,(AT3G57270.1,(AT3G57260.1,AT3G57240.1)0.5160)0.9140,((MtGHL17_20,MtGHL17_23)0.9560,MtGHL17_21,MtGHL17_22)0.9980,((MtGHL17_35,MtGHL17_40)0.9960,(AT1G77790.1,AT1G77780.1)0.8000)0.8780,(AT5G20560,(AT5G20390,(AT5G20330,AT5G20340,AT1G33220)0.6500)0.5060)0.9960)0.5860,(((MtGHL17_19,AT4G17180)0.7720,MtGHL17_18)0.9580,AT5G58480,MtGHL17_30,AT5G20870,(MtGHL17_29,AT5G58090,AT4G31140.1)0.7760,(MtGHL17_32,MtGHL17_33)0.5900,AT3G24330,AT5G64790,((AT3G04010,AT5G18220)0.9400,(MtGHL17_28,MtGHL17_34)0.6020,(AT2G19440,AT1G64760)0.8980)0.7460)0.9520)0.5200,(((MtGHL17_12,MtGHL17_14)0.9980,MtGHL17_10)0.6240,(AT2G16230,AT4G34480)0.6200,AT5G42720)0.8360,(((AT2G39640,AT3G55430)0.5480,MtGHL17_15)0.7320,((MtGHL17_13,AT5G24318)0.9580,(MtGHL17_31,AT3G46570)0.8440)0.5460)0.7100,((MtGHL17_9,MtGHL17_38)0.8800,AT3G55780)0.6380,AT3G61810,MtGHL17_6,((MtGHL17_42,AT3G07320)0.6160,(AT3G23770,AT4G14080.1)0.7420)0.7000,((MtGHL17_7,AT5G56590.1)0.5700,AT4G29360)0.9180,((MtGHL17_3,AT1G11820)0.9820,(((MtGHL17_1,AT3G13560)0.7160,MtGHL17_2)0.6920,(AT2G01630,AT1G66250,(MtGHL17_4,MtGHL17_5)0.7940)0.7480)0.6420)0.9300(((MtGHL17_11,MtGHL17_36)0.5280,AT2G05790,PsgHL17_1)0.5900,(AT4G26830.1,AT5G55180.1)0.8900)0.8400,((AT4G18340,AT1G30080)0.8720,AT2G27500)0.5040,(AT1G32860,AT5G42100)0.5240,((MtGHL17_8,AT3G15800)0.9760,(AT2G26600,(MtGHL17_39,MtGHL17_41)1.0000)0.8560)0.9900);

Appendix 11: Phylogenetic reconstruction using β -1,3-glucanases from GHL17 family protein sequences isolated from *A. thaliana* and *M. truncatula* orthologues generated by Maximum likelihood algorithm in Newick format. Bootstrap values for 1000 repetitions are included.

(((((((((Medtr4g076470,Medtr4g076490)0.7720,(Medtr4g076430,Medtr4g076440)0.6860)0.9980,(Medtr4g076500,Medtr4g076570)0.7960)0.8780,AT4G16260.1,(Medtr2g034480,(Medtr2g034470,Medtr2g034440)0.9940)0.9900)0.6960,(AT3G57270.1,(AT3G57260.1,AT3G57240.1)0.5280)0.8580)0.9440,(((Medtr7g081350,Medtr7g081370)1.0000,(AT1G77790.1,AT1G77780.1)0.8080)0.6980,(AT5G20390,(AT5G20560,(AT5G20330,AT5G20340,AT1G33220)0.6780)0.6160)1.0000)0.7380)0.5800,(((Medtr2g027560,Medtr4g134280)0.6580,AT4G17180)0.9980,AT5G58480,AT3G24330,(Medtr4g124440,AT5G20870)0.9780,((Medtr3g108600,AT4G31140.1)0.8680,AT5G58090)0.7920,(Medtr3g095050,Medtr8g092070)0.9740,AT5G64790,(Medtr7g085390,Medtr6g032820,(AT2G19440,AT1G

64760)0.9900,(AT3G04010,AT5G18220)1.0000)0.7820)0.9840)0.7640,((Medtr8g012400,AT3G07320)0.7200,(AT3G23770,AT4G14080.1)0.9340)0.9700,Medtr5g015720,((Medtr5g081720,AT3G55780)0.9920,AT3G61810)0.7080,((Medtr8g102340,AT5G56590.1)0.7160,AT4G29360)0.9960,(((Medtr8g085720,Medtr3g083580)0.9020,AT3G13560)0.9960,((Medtr4g132280,AT1G11820)0.9980,(AT2G01630,(AT1G66250,(Medtr5g078200,Medtr3g065460)0.6140)0.6640)0.8040)0.7460)0.9960((((AT2G39640,AT3G55430)0.7480,Medtr7g026340)0.8160,(Medtr4g083500,AT3G46570)0.7120)0.7420,(Medtr1g007810,AT5G24318)0.9500)0.9820,(AT5G42720,((Medtr4g069940,Medtr3g116510)0.9940,(AT2G16230,AT4G34480)0.5780)0.7280)0.9800)0.5560,((((Medtr5g085580,Medtr3g080410)0.6340,AT2G05790)0.7680,(AT4G26830.1,AT5G55180.1)0.9940)0.6040,PsGHL17_1)0.9940,(((Medtr4g010200,AT3G15800)0.5300,(Medtr4g114850,AT2G26600)0.9380)1.0000,((AT4G18340,AT1G30080)0.9960,(AT2G27500,(AT1G32860,AT5G42100)0.9260)0.7420)0.6900)0.6580);

Appendix 12 Phylogenetic reconstruction using β -1,3-glucanases from GHL17 family protein sequences isolated from *A. thaliana* and *M. truncatula* orthologues generated by Bayesian inference of phylogeny algorithm in Newick format. Posterior probabilities are included.

[&u]((((((((('Medtr8g085720 ':0.2451718,'Medtr3g083580 ':0.3567908)100/63/-:0.1688186,AT3G13560:0.3212505)100/85/67:0.4019434,((Medtr4g132280:0.286619,AT1G11820:0.1435538)100/97/98:0.4091283,(((Medtr5g078200:0.1686494,Medtr3g065460:0.2955645)100/59/78:0.1168971,AT1G66250:0.3421259)100/-/49:0.1123388,AT2G01630:0.3382803)100/63/77:0.1380525)100/98/-:0.2344625)100//98:0.4327319,((Medtr8g102340:0.3794693,AT5G56590:0.3384021)100/79/57:0.2325957,AT4G29360:0.3902925)100/99/89:0.5939619)62:0.07911399,((Medtr5g081720:1.0579590650000001,AT3G55780:0.7397673)100/79/72:1.098395,AT3G61810:0.9020489)100//39:0.4649695)99:0.146332,((((Medtr2g034480:0.593956632,AT4G16260:0.4746813)100/31/:0.2235576,(((Medtr4g076470:0.09123974,(Medtr4g076430:0.114744,Medtr4g076440:0.10452)100/67/:0.09487228)87:0.08260917,Medtr4g076490:0.2599281)100/95/99:0.46304,(Medtr4g076500:0.4639144,Medtr4g076570:0.4951869)95/98/99:0.2281664)99:0.3263931)77:0.2055857,(AT3G57270:0.5705425,(AT3G57260:0.4471974,AT3G57240:0.3722345)100//50:0.2403836)99/82/92:0.2437161)100:0.4824156,(((Medtr7g081350:0.02951908,Medtr7g081370:0.05420437)100/100/99:0.6107463,(AT1G77790:0.5472504,AT1G77780:0.7087391)100/72/80:0.5538367)99/79/88:0.2450762,(((AT5G20340:0.09934253,AT5G20330:0.08202446,AT

1G33220:0.1259088)100:0.1229591,AT5G20560:0.5254377)63:0.0521365,AT5G20390:0.2866365)100/100/100:0.9051601)100:0.2873382)100:0.3086235,((Medtr2g027560:0.255826,Medtr4g134280:0.2761864,AT4G17180:0.343659)100//22:0.5361114,((((Medtr7g085390:0.2102179,Medtr6g032820:0.2339699)100/66/53:0.1272722,((AT2G19440:0.141505,AT1G64760:0.08508985)100/95/88:0.184707,(AT3G04010:0.1902218,AT5G18220:0.215089)100/99/94:0.2540444)99:0.08166961)100:0.2477163,((Medtr3g095050:0.3773551,Medtr8g092070:0.37521)100//53:0.3190731,AT5G64790:0.7138696)100:0.2361998)100:0.1570121,AT3G24330:0.7039902)100//22:0.1780755,(((Medtr3g108600:0.3674803,AT4G31140:0.33413)100//43:0.1310195,AT5G58090:0.4714849)100/80/75:0.1692552,(Medtr4g124440:0.43931,AT5G20870:0.4419246)100//26:0.3907251)95:0.1200231)99:0.1907452)100:0.2615124,AT5G58480:0.9034783)100:0.8510162)100:0.2121045,((Medtr8g012400:0.4214229,AT3G07320:0.4260039)100/75/:0.2087235,(AT3G23770:0.1573043,AT4G14080:0.3058904)100/91/:0.429232)100/94/:0.6324538)98:0.1636142)96:0.09895947,((((Medtr4g010200:0.47522,AT3G15800:0.4021781)57/79/96:0.1401989,(Medtr4g114850:0.47858499000000004,AT2G26600:0.3814075)100/71/87:0.292555)100/99:0.7424901,(AT4G18340:0.4561857,AT1G30080:0.5399337)100/91/87:0.4750784)72:0.2114849,((AT1G32860:0.6504422,AT5G42100:0.6488768)100//50:0.2590848,AT2G27500:0.8256317)100/39/:0.3088017)100:0.2780484,((((Medtr4g069940:0.235391,Medtr3g116510:0.23976077):0.2132022,(AT2G16230:0.3079788,AT4G34480:0.2070718)100/54/59:0.1664568)96/68:0.1046872,AT5G42720:0.7923359)100/94/85:0.4393021,((Medtr1g007810:0.6024769,AT5G24318:0.5121537)100/99/95:0.197601,((Medtr7g026340:0.4511523,(AT2G39640:0.7036196,AT3G55430:0.3514873)100/67/59:0.3203555)100/80/:0.2659633,(Medtr4g083500:0.4171561,AT3G46570:0.5708262)100/56/:0.209823)100:0.1254081)100:0.3219886)100:0.2772366)97:0.07885147)87:0.1228173,Medtr5g015720:2.587738)100:0.3620433,(((Medtr5g085580:0.2951973,Medtr3g080410:0.8314089)61//52:0.04973965,AT2G05790:0.3423013)100//37:0.1796912,(AT4G26830:0.2343617,AT5G55180:0.328803)100//87:0.2695614)100:0.1651451):0.20069045,'PsGHL17 1':0.20069045):0.0;

Appendix 13- Phylogenetic reconstruction using CALs sequences isolated from *A. thaliana* and *M. truncatula* orthologues generated by Neighbour Joining algorithm in Newick format. Bootstrap values for 500 repetitions are included.

((((((((((ATGSL3,ATGSL6)0.9570,ATGSL9)1.0000,Medtr2g061380)0.7330,(ATGSL12,(Medtr1g116370,Medtr7g005950)1.0000)1.0000)1.0000,(ATGSL4,Medtr2g072160)1.0000)0.9120,(Medtr3g047390,(ATGSL7,ATGSL11)1.0000)1.0000)0.9560,(ATGSL2,(Medtr3g096200,Medtr8g093630)1.0000)1.0000)1.0000,((AT

GSL10,Medtr1g116470)1.0000,(ATGSL8,(Medtr3g075180,Medtr3g075180)1.0000)1.0000)1.0000)1.0000,(ATGSL1,Medtr2g013580)0.9990)0.9970,ATGSL5,(Medtr4g078220,Medtr2g090375)0.6640);

Appendix 14-Phylogenetic reconstruction using CALs sequences isolated from *Arabidopsis thaliana* and *M. truncatula* orthologues generated by Maximum Likelihood algorithm in Newick format. Bootstrap values for 500 repetitions are included.

((((((((Medtr4g078220,Medtr2g090375)0.6500,ATGSL5)1.0000,(ATGSL1,Medtr2g013580)0.9800)1.0000,((ATGSL10,Medtr1g116470)1.0000,(ATGSL8,(Medtr3g075180,Medtr3g075180)1.0000)1.0000)1.0000)1.0000,(ATGSL2,(Medtr3g096200,Medtr8g093630)1.0000)1.0000)0.6820,(Medtr3g047390,(ATGSL7,ATGSL11)1.0000)1.0000)0.7120,(ATGSL4,Medtr2g072160)1.0000)1.0000,(Medtr2g061380,(ATGSL9,(ATGSL3,ATGSL6)1.0000)1.0000)0.6020,(ATGSL12,(Medtr1g116370,Medtr7g005950)1.0000)1.0000);

Appendix 15- Phylogenetic reconstruction using CALs sequences isolated from *Arabidopsis thaliana* and *M. truncatula* orthologues generated by Bayesian inference of phylogeny algorithm in Newick format. Posterior probabilities are included.

(ATGSL1:0.300099,Medtr2g013580:0.2351849,(((ATGSL2:0.1427671,(Medtr3g096200:0.08205553,Medtr8g093630:0.1094132)100:0.0528233)100:0.2121195,(((ATGSL3:0.04095976,ATGSL6:0.04348255)99:0.01722926,ATGSL9:0.4151319):0.09709551,Medtr2g061380:0.1796305)100:0.05406835,(ATGSL12:0.09537064,(Medtr1g116370:0.06044139,Medtr7g005950:0.07479403)100:0.04659432)100:0.04479113)100:0.2161742,((ATGSL4:0.2106318,Medtr2g072160:0.3375866)100:0.4615765,((ATGSL7:0.1735286,ATGSL11:0.1984245)100:0.1139442,Medtr3g047390:0.2776077)100:0.3558181)100:0.08466711)100:0.1098251)100:0.3509958,((ATGSL8:0.184856,(Medtr3g075180:6.905382E4,Medtr3g075180:0.0147327)100:0.1521995)100:0.1856737,(ATGSL10:0.1744449,Medtr1g116470:0.1618575)100:0.2274695)100:0.6504952)100:0.692501,(ATGSL5:0.2490029,(Medtr4g078220:0.1006829,Medtr2g090375:0.2317417)100:0.05144233)100:0.0642969)100:0.09835613);

Appendix 16- Phylogenetic reconstruction using PDLPs sequences isolated and *A. thaliana* and *M. truncatula* orthologues generated by Neighbour Joining algorithm in Newick format. Bootstrap values for 500 repetitions are included.

((((((((((((((((Medtr1g105700,Medtr1g105800)0.6200,Medtr1g105820)0.4860,Medtr5g065130)0.6560,Medtr5g068260)0.4440,(Medtr1g105700,Medtr1g105860)0.5320)0.9920,AT4G23140)0.1890,((Medtr1g105585,Medtr3g079850)0.8430,(Medtr1g104890,(Medtr1g105615,(Medtr1g105650,(Medtr6g463660,Medtr8g0280650.8690)0.5710)0.8900)0.2310)0.0550)0.0550,(AT1G63580.1,(Medtr1g105655,(Medtr5g005480,Medtr5g005450)0.9860)0.5860)0.1800)0.2340,(Medtr8g041650,(Medtr8g041690,(Medtr8g041710,(Medtr8g041660,(Medtr2g010730,Medtr8g041870)0.9800)0.7220)0.8350)0.7810)0.9990)0.3690,Medtr5g0055300.1870,(Medtr2g088930,AT5G48540)0.3550)0.8530,Medtr3g064090)0.5940,(Medtr7g098410,(AtPDLP1,((Medtr1g080350,AtPDLP4)0.7350,(Medtr1g073320,(AtPDLP2,AtPDLP3)0.9850)0.7890)0.6720)0.4360)1.0000)0.3120,(AtPDLP8,(AtPDLP5,((Medtr8g104990,AtPDLP6)0.2950,(Medtr3g0653706,(Medtr5g078030,AtPDLP7)0.3940)0.4930)0.9250)0.7300)0.5500)0.0000,PsPDLP-like_1);

Appendix 17- Phylogenetic reconstruction using PDLPs sequences isolated and *A. thaliana* and *M. truncatula* orthologues generated by Maximun Likelihood algorithm in Newick format. Bootstrap values for 500 repetitions are included.

((((((((((((((((Medtr1g105700,Medtr1g105800)0.5220,Medtr1g105820)1.0000,Medtr5g068260)0.8450,Medtr5g065130)0.8310,Medtr1g105860)0.6260,Medtr1g105700)0.9890,(Medtr1g105585,Medtr3g079850)0.8290)0.2130,(AT4G23140,(Medtr1g104890,(Medtr1g105615,(Medtr1g105650,(Medtr6g463660,Medtr8g028065)0.6600)0.8840)0.9860)0.8470)0.3150)0.1720,(Medtr1g105655,(Medtr5g005480,Medtr5g005450)1.0000)0.5890)0.2240,(Medtr5g0055308,(Medtr2g088930,AT5G48540)0.6560)0.5110)0.3850,(Medtr8g041650,(Medtr8g041690,(Medtr8g041710,(Medtr8g041660,(Medtr2g010730,Medtr8g041870)1.0000)0.5390)0.4610)0.9770)1.0000)0.3350,AT1G63580.1)0.9500,(Medtr3g064090,((Medtr1g080350,AtPDLP4)0.7090,(Medtr7g098410,(AtPDLP1,(Medtr1g0733201,(AtPDLP2,AtPDLP3)0.9950)1.0000)0.5640)0.9750)0.9980)0.5400)0.8170,AtPDLP8)0.6460,(AtPDLP5,((Medtr8g104990AtPDLP6)0.6710,(AtPDLP7,(Medtr5g078030,Medtr3g065370)0.5910)0.8300)0.9570)0.9760)0.0000,PsPDLP-like_1);

Appendix 18- Phylogenetic reconstruction using PDLP sequences isolated from *Arabidopsis thaliana* and *Medicago truncatula* orthologues generated by Bayesian inference of phylogeny algorithm in Newick format. Posterior probabilities are included.

```

((((('Medtr1g073320':0.1893951,(AtPDLP2:0.0959477,AtPDLP3:0.1349284)10
0:0.158642):0.2201806,('Medtr7g098410':0.3667274,AtPDLP1:0.3786872
)100:0.1731097):0.1806229,('Medtr1g080350':0.6704144,AtPDLP4:0.7200
153)99:0.2160614):0.4970965,((((('Medtr5g005480':0.3348081,'Medtr5
g005450':0.3540556)100:0.302001, (('Medtr1g105585':0.5943211,'Medtr3
g079850':0.6772901)62:0.05071878,AT163580.1:1.361351)99:0.0828642
9)99:0.06504876,'Medtr1g105655':0.5519695)91:0.05710796, (('Medtr6g
463660':0.5076711,'Medtr8g028065':0.5674215)100:1.098892,'Medtr1g10
5615':0.4537923)84:0.08441025,'Medtr1g105650':0.2841128)95:0.15523
4,'Medtr1g104890':0.4570452,AT4G23140:0.5949421)95:0.08568302)99:
0.08738445,('Medtr1g105700':0.6449607,'Medtr5g065130':0.4414775, (('
Medtr1g105700':0.156555,'Medtr1g105800':0.1027344)100:0.04706876,'
Medtr1g105820':0.03606886)100:0.2648813,'Medtr5g068260':0.3839742)
53:0.03899846,'Medtr5g068260':1.991098)100:0.30058)100:0.1232128, (('
Medtr5g005530':0.7668514,'Medtr2g088930':0.6599428)51:0.07224065, (('
Medtr8g041690':0.2992259,'Medtr8g041710':0.1956196)100:0.0693817
6,'Medtr8g041660':0.2045865)100:0.04653429,('Medtr2g010730':0.10027
43,'Medtr8g041870':0.3639162)100:0.1363752)100:0.2201923,'Medtr8g0
41650':0.4317114)100:0.3699142)81:0.1310593)91:0.1359005,AT5G485
40:0.8828821)99:0.1948364,'Medtr3g064090':1.273588):0.3984391):0.18
14648, (('Medtr8g104990':0.3255435,AtPDLP6:0.2706075)99:0.0934141
7, (('Medtr5g078030':0.284187,'Medtr3g065370':0.2953186)100:0.149804
8,AtPDLP7:0.2948461)100:0.1451248)98:0.1163457,AtPDLP5:0.5568149
)100:0.2842443,AtPDLP8:0.5789527)84:0.1427195):0.28969,'PsPDLP-
like 1':0.28969):0.0;

```

Bibliography

- Abd-Alla, M.H., Koyro, H.W., Yan, F., Schubert, S., and Peiter, E.** (2000). Functional structure of the indeterminate *Vicia faba* L. root nodule: implications for metabolite transport. *Journal of Plant Physiology* **157**, 335-343.
- Absmanner, B., Stadler, R., and Hammes, U.Z.** (2013). Phloem development in nematode-induced feeding sites: the implications of auxin and cytokinin. *Front Plant Sci* **4**, 241-255.
- Adamowski, M., and Friml, J.** (2015). PIN-dependent auxin transport: action, regulation, and evolution. *Plant Cell* **27**, 20-32.
- Allen, E.K., Allen, O.N., and Newman, S.** (1953). Pseudonodulation of Leguminous Plants Induced by 2-Bromo-3,5- Dichlorobenzoic Acid. *American Journal of Botany* **40**, 429-435.
- Amari, K., Boutant, E., Hofmann, C., Schmitt-Keichinger, C., Fernandez-Calvino, L., Didier, P., Lerich, A., Mutterer, J., Thomas, C.L., Heinlein, M., Mely, Y., Maule, A.J., and Ritzenthaler, C.** (2010). A family of plasmodesmal proteins with receptor-like properties for plant viral movement proteins. *PLoS Pathog* **6**, e1001119.
- Andersen, J.H., Fossing, H., Hansen, J.W., Manscher, O.H., Murray, C., and Petersen, D.L.** (2014). Nitrogen inputs from agriculture: towards better assessments of eutrophication status in marine waters. *Ambio* **43**, 906-913.
- Andriankaja, A., Boisson-Dernier, A., Frances, L., Sauviac, L., Jauneau, A., Barker, D.G., and de Carvalho-Niebel, F.** (2007). AP2-ERF transcription factors mediate Nod factor dependent Mt ENOD11 activation in root hairs via a novel cis-regulatory motif. *Plant Cell* **19**, 2866-2885.
- Araya, T., Miyamoto, M., Wibowo, J., Suzuki, A., Kojima, S., Tsuchiya, Y.N., Sawa, S., Fukuda, H., von Wiren, N., and Takahashi, H.** (2014). CLE-CLAVATA1 peptide-receptor signaling module regulates the expansion of plant root systems in a nitrogen-dependent manner. *Proc Natl Acad Sci U S A* **111**, 2029-2034.
- Arrighi, J.F., Barre, A., Ben Amor, B., Bersoult, A., Soriano, L.C., Mirabella, R., de Carvalho-Niebel, F., Journet, E.P., Gherardi, M., Huguet, T., Geurts, R., Denarie, J., Rouge, P., and Gough, C.** (2006). The *Medicago truncatula* lysin [corrected] motif-receptor-like kinase gene family includes NFP and new nodule-expressed genes. *Plant Physiol* **142**, 265-279.
- Barker, D., Bianchi, S., Blondon, F., Dattée, Y., Duc, G., Essad, S., Flament, P., Gallusci, P., Génier, G., Guy, P., Muel, X., Tourneur, J., Dénarié, J., and Huguet, T.** (1990). *Medicago truncatula*, a Model Plant for Studying the Molecular Genetics of Therhizobium-Legume Symbiosis. *Plant Molecular Biology Reporter* **8**, 40-49.
- Beachy, R.N., and Heinlein, M.** (2000). Role of P30 in replication and spread of TMV. *Traffic* **1**, 540-544.

- Bederska, M., Borucki, W., and Znojek, E.** (2012). Movement of fluorescent dyes Lucifer Yellow (LYCH) and carboxyfluorescein (CF) in *Medicago truncatula* Gaertn. roots and root nodules. *Symbiosis* **58**, 183-190.
- Benedito, V.A., Torres-Jerez, I., Murray, J.D., Andriankaja, A., Allen, S., Kakar, K., Wandrey, M., Verdier, J., Zuber, H., Ott, T., Moreau, S., Niebel, A., Frickey, T., Weiller, G., He, J., Dai, X., Zhao, P.X., Tang, Y., and Udvardi, M.K.** (2008). A gene expression atlas of the model legume *Medicago truncatula*. *Plant J* **55**, 504-513.
- Benitez-Alfonso, Y.** (2014). Symplastic intercellular transport from a developmental perspective. *J Exp Bot* **65**, 1857-1863.
- Benitez-Alfonso, Y., Faulkner, C., Ritzenthaler, C., and Maule, A.J.** (2010). Plasmodesmata: gateways to local and systemic virus infection. *Mol Plant Microbe Interact* **23**, 1403-1412.
- Benitez-Alfonso, Y., Faulkner, C., Pendle, A., Miyashima, S., Helariutta, Y., and Maule, A.** (2013). Symplastic intercellular connectivity regulates lateral root patterning. *Dev Cell* **26**, 136-147.
- Bensmihen, S.** (2015). Hormonal Control of Lateral Root and Nodule Development in Legumes. *Plants (Basel)* **4**, 523-547.
- Bernhardt, E.S., Likens, G.E., Buso, D.C., and Driscoll, C.T.** (2003). In-stream uptake dampens effects of major forest disturbance on watershed nitrogen export. *Proc Natl Acad Sci U S A* **100**, 10304-10308.
- Bhuvaneshwari, T.V., Bhagwat, A.A., and Bauer, W.D.** (1981). Transient susceptibility of root cells in four common legumes to nodulation by rhizobia. *Plant Physiol* **68**, 1144-1149.
- Boisson-Dernier, A., Andriankaja, A., Chabaud, M., Niebel, A., Journet, E.P., Barker, D.G., and de Carvalho-Niebel, F.** (2005). MtENOD11 gene activation during rhizobial infection and mycorrhizal arbuscule development requires a common AT-rich-containing regulatory sequence. *Mol Plant Microbe Interact* **18**, 1269-1276.
- Bonfante-Fasolo, P., Vian, B., Perotto, S., Faccio, A., and Knox, J.P.** (1990). Cellulose and pectin localization in roots of mycorrhizal *Allium porrum*: labelling continuity between host cell wall and interfacial material. *Planta* **180**, 537-547.
- Bonfante, P., and Genre, A.** (2010). Mechanisms underlying beneficial plant-fungus interactions in mycorrhizal symbiosis. *Nat Commun* **1**, 48-59.
- Botsford, J.L.** (1984). Osmoregulation in *Rhizobium meliloti*: inhibition of growth by salts. *Archives of Microbiology* **137**, 124-127.
- Breakspear, A., Liu, C., Roy, S., Stacey, N., Rogers, C., Trick, M., Morieri, G., Mysore, K.S., Wen, J., Oldroyd, G.E., Downie, J.A., and Murray, J.D.** (2014). The root hair "infectome" of *Medicago truncatula* uncovers changes in cell cycle genes and reveals a requirement for Auxin signaling in rhizobial infection. *Plant Cell* **26**, 4680-4701.
- Bricchi, I., Occhipinti, A., Berteaux, C.M., Zebelo, S.A., Brillada, C., Verrillo, F., De Castro, C., Molinaro, A., Faulkner, C., Maule, A.J., and Maffei, M.E.** (2013). Separation of early and late responses to herbivory in *Arabidopsis* by changing plasmodesmal function. *Plant J* **73**, 14-25.
- Bucher, G.L., Tarina, C., Heinlein, M., Di Serio, F., Meins, F., Jr., and Iglesias, V.A.** (2001). Local expression of enzymatically active class I beta-1, 3-glucanase enhances symptoms of TMV infection in tobacco. *Plant J* **28**, 361-369.

- Burch-Smith, T.M., Stonebloom, S., Xu, M., and Zambryski, P.C.** (2011). Plasmodesmata during development: re-examination of the importance of primary, secondary, and branched plasmodesmata structure versus function. *Protoplasma* **248**, 61-74.
- Caba, J.M., Recalde, L., and Ligeró, F.** (1998). Nitrate-induced ethylene biosynthesis and the control of nodulation in alfalfa. *Plant Cell and Environment* **21**, 87-94.
- Caba, J.M., Centeno, M.L., Fernández, B., Gresshoff, P.M., and Ligeró, F.** (2000). Inoculation and nitrate alter phytohormone levels in soybean roots: differences between a supernodulating mutant and the wild type. *Planta* **211**, 98-104.
- Caetano-Anolles, G., and Gresshoff, P.M.** (1991). Efficiency of nodule initiation and autoregulatory responses in a supernodulating soybean mutant. *Appl Environ Microbiol* **57**, 2205-2210.
- Caillaud, M.C., Wirthmueller, L., Sklenar, J., Findlay, K., Piquerez, S.J., Jones, A.M., Robatzek, S., Jones, J.D., and Faulkner, C.** (2014). The plasmodesmal protein PDL1 localises to haustoria-associated membranes during downy mildew infection and regulates callose deposition. *PLoS Pathog* **10**, e1004496.
- Cardenas, L., Dominguez, J., Quinto, C., Lopez-Lara, I.M., Lugtenberg, B.J., Spaink, H.P., Rademaker, G.J., Haverkamp, J., and Thomas-Oates, J.E.** (1995). Isolation, chemical structures and biological activity of the lipo-chitin oligosaccharide nodulation signals from *Rhizobium etli*. *Plant Mol Biol* **29**, 453-464.
- Carella, P., Wilson, D.C., and Cameron, R.K.** (2015). Mind the gap: Signal movement through plasmodesmata is critical for the manifestation of SAR. *Plant Signal Behav* **10**, e1075683.
- Carlsbecker, A., Lee, J.Y., Roberts, C.J., Dettmer, J., Lehesranta, S., Zhou, J., Lindgren, O., Moreno-Risueno, M.A., Vaten, A., Thitamadee, S., Campilho, A., Sebastian, J., Bowman, J.L., Helariutta, Y., and Benfey, P.N.** (2010). Cell signalling by microRNA165/6 directs gene dose-dependent root cell fate. *Nature* **465**, 316-321.
- Carroll, B.J., McNeil, D.L., and Gresshoff, P.M.** (1985a). Isolation and properties of soybean [*Glycine max* (L.) Merr.] mutants that nodulate in the presence of high nitrate concentrations. *Proc Natl Acad Sci U S A* **82**, 4162-4166.
- Carroll, B.J., McNeil, D.L., and Gresshoff, P.M.** (1985b). A Supernodulation and Nitrate-Tolerant Symbiotic (nts) Soybean Mutant. *Plant Physiol* **78**, 34-40.
- Cerri, M.R., Frances, L., Laloum, T., Auriac, M.C., Niebel, A., Oldroyd, G.E., Barker, D.G., Fournier, J., and de Carvalho-Niebel, F.** (2012). *Medicago truncatula* ERN transcription factors: regulatory interplay with NSP1/NSP2 GRAS factors and expression dynamics throughout rhizobial infection. *Plant Physiol* **160**, 2155-2172.
- Charon, C., Sousa, C., Crespi, M., and Kondorosi, A.** (1999). Alteration of *enod40* expression modifies *medicago truncatula* root nodule development induced by *sinorhizobium meliloti*. *Plant Cell* **11**, 1953-1966.
- Chaumont, F., and Tyerman, S.D.** (2014). Aquaporins: highly regulated channels controlling plant water relations. *Plant Physiol* **164**, 1600-1618.

- Chen, X.Y., Liu, L., Lee, E., Han, X., Rim, Y., Chu, H., Kim, S.W., Sack, F., and Kim, J.Y.** (2009). The Arabidopsis callose synthase gene *GSL8* is required for cytokinesis and cell patterning. *Plant Physiol* **150**, 105-113.
- Cho, M.J., and Harper, J.E.** (1991). Effect of localized nitrate application on isoflavonoid concentration and nodulation in split-root systems of wild-type and nodulation-mutant soybean plants. *Plant Physiol* **95**, 1106-1112.
- Clark, S.E., Running, M.P., and Meyerowitz, E.M.** (1993). *CLAVATA1*, a regulator of meristem and flower development in Arabidopsis. *Development* **119**, 397-418.
- Combiér, J.P., Kuster, H., Journet, E.P., Hohnjec, N., Gamas, P., and Niebel, A.** (2008). Evidence for the involvement in nodulation of the two small putative regulatory peptide-encoding genes *MtRALFL1* and *MtDVL1*. *Mol Plant Microbe Interact* **21**, 1118-1127.
- Complainville, A., Brocard, L., Roberts, I., Dax, E., Sever, N., Sauer, N., Kondorosi, A., Wolf, S., Oparka, K., and Crespi, M.** (2003). Nodule initiation involves the creation of a new symplasmic field in specific root cells of medicago species. *Plant Cell* **15**, 2778-2791.
- Coronado, C., Zuanazzi, J., Sallaud, C., Quirion, J.C., Esnault, R., Husson, H.P., Kondorosi, A., and Ratet, P.** (1995). Alfalfa Root Flavonoid Production Is Nitrogen Regulated. *Plant Physiol* **108**, 533-542.
- Criscuolo, G., Valkov, V.T., Parlati, A., Alves, L.M., and Chiurazzi, M.** (2012). Molecular characterization of the *Lotus japonicus* *NRT1(PTR)* and *NRT2* families. *Plant Cell Environ* **35**, 1567-1581.
- Crook, A.D., Schnabel, E.L., and Frugoli, J.A.** (2016). The systemic nodule number regulation kinase *SUNN* in *Medicago truncatula* interacts with *MtCLV2* and *MtCRN*. *Plant J* **88**, 108-119.
- Cui, W., and Lee, J.Y.** (2016). Arabidopsis callose synthases *CalS1/8* regulate plasmodesmal permeability during stress. *Nat Plants* **2**, 16034.
- D'Haese, W., and Holsters, M.** (2002). Nod factor structures, responses, and perception during initiation of nodule development. *Glycobiology* **12**, 79R-105R.
- Day, D., Carroll, B., Delves, A., and Gresshoff, P.** (1989). Relationship between autoregulation and nitrate inhibition of nodulation in soybeans. *Physiologia Plantarum* **75**, 37-42.
- De Storme, N., and Geelen, D.** (2014). Callose homeostasis at plasmodesmata: molecular regulators and developmental relevance. *Front Plant Sci* **5**, 138-161.
- Delay, C., Imin, N., and Djordjevic, M.A.** (2013). *CEP* genes regulate root and shoot development in response to environmental cues and are specific to seed plants. *J Exp Bot* **64**, 5383-5394.
- Denarie, J., Debelle, F., and Prome, J.C.** (1996). Rhizobium lipochitooligosaccharide nodulation factors: signaling molecules mediating recognition and morphogenesis. *Annu Rev Biochem* **65**, 503-535.
- Doxey, A.C., Yaish, M.W., Moffatt, B.A., Griffith, M., and McConkey, B.J.** (2007). Functional divergence in the Arabidopsis beta-1,3-glucanase gene family inferred by phylogenetic reconstruction of expression states. *Mol Biol Evol* **24**, 1045-1055.
- Doyle, J.J.** (2011). Phylogenetic perspectives on the origins of nodulation. *Mol Plant Microbe Interact* **24**, 1289-1295.

- Dudley, M.E., Jacobs, T.W., and Long, S.R.** (1987). Microscopic studies of cell divisions induced in alfalfa roots by *Rhizobium meliloti*. *Planta* **171**, 289-301.
- Ehlers, K., and Kollmann, R.** (2001). Primary and secondary plasmodesmata: structure, origin, and functioning. *Protoplasma* **216**, 1-30.
- Ehrhardt, D.W., Atkinson, E.M., and Long, S.R.** (1992). Depolarization of alfalfa root hair membrane potential by *Rhizobium meliloti* Nod factors. *Science* **256**, 998-1000.
- Ehrhardt, D.W., Wais, R., and Long, S.R.** (1996). Calcium spiking in plant root hairs responding to *Rhizobium* nodulation signals. *Cell* **85**, 673-681.
- Eisenhaber, B., Wildpaner, M., Schultz, C.J., Borner, G.H., Dupree, P., and Eisenhaber, F.** (2003). Glycosylphosphatidylinositol lipid anchoring of plant proteins. Sensitive prediction from sequence- and genome-wide studies for *Arabidopsis* and rice. *Plant Physiol* **133**, 1691-1701.
- Ellinger, D., and Voigt, C.A.** (2014). Callose biosynthesis in *Arabidopsis* with a focus on pathogen response: what we have learned within the last decade. *Ann Bot* **114**, 1349-1358.
- Engler, C., Kandzia, R., and Marillonnet, S.** (2008). A one pot, one step, precision cloning method with high throughput capability. *PLoS One* **3**, e3647.
- Engvild, K.C.** (1987). Nodulation and nitrogen fixation mutants of pea, *Pisum sativum*. *Theor Appl Genet* **74**, 711-713.
- Fankhauser, N., and Maser, P.** (2005). Identification of GPI anchor attachment signals by a Kohonen self-organizing map. *Bioinformatics* **21**, 1846-1852.
- Farkas, A., Maroti, G., Durgo, H., Gyorgypal, Z., Lima, R.M., Medzihradzsky, K.F., Kereszt, A., Mergaert, P., and Kondorosi, E.** (2014). *Medicago truncatula* symbiotic peptide NCR247 contributes to bacteroid differentiation through multiple mechanisms. *Proc Natl Acad Sci U S A* **111**, 5183-5188.
- Faulkner, C., Petutschnig, E., Benitez-Alfonso, Y., Beck, M., Robatzek, S., Lipka, V., and Maule, A.J.** (2013). LYM2-dependent chitin perception limits molecular flux via plasmodesmata. *Proc Natl Acad Sci U S A* **110**, 9166-9170.
- Felle, H.H., Kondorosi, E., Kondorosi, A., and Schultze, M.** (1999). Elevation of the cytosolic free $[Ca^{2+}]$ is indispensable for the transduction of the Nod factor signal in alfalfa. *Plant Physiol* **121**, 273-280.
- Ferguson, B.J., Indrasumunar, A., Hayashi, S., Lin, M.H., Lin, Y.H., Reid, D.E., and Gresshoff, P.M.** (2010). Molecular analysis of legume nodule development and autoregulation. *J Integr Plant Biol* **52**, 61-76.
- Ferguson, B.J., Li, D., Hastwell, A.H., Reid, D.E., Li, Y., Jackson, S.A., and Gresshoff, P.M.** (2014). The soybean (*Glycine max*) nodulation-suppressive CLE peptide, GmRIC1, functions interspecifically in common white bean (*Phaseolus vulgaris*), but not in a supernodulating line mutated in the receptor PvNARK. *Plant Biotechnol J* **12**, 1085-1097.
- Fernandez-Calvino, L., Faulkner, C., Walshaw, J., Saalbach, G., Bayer, E., Benitez-Alfonso, Y., and Maule, A.** (2011). *Arabidopsis* plasmodesmal proteome. *PLoS One* **6**, e18880.
- Field, K.J., Rimington, W.R., Bidartondo, M.I., Allinson, K.E., Beerling, D.J., Cameron, D.D., Duckett, J.G., Leake, J.R., and Pressel, S.** (2016). Functional analysis of liverworts in dual symbiosis with *Glomeromycota*

- and Mucoromycotina fungi under a simulated Palaeozoic CO₂ decline. *ISME J* **10**, 1514-1526.
- Fisher, R.F., and Long, S.R.** (1992). Rhizobium--plant signal exchange. *Nature* **357**, 655-660.
- Fournier, J., Teillet, A., Chabaud, M., Ivanov, S., Genre, A., Limpens, E., de Carvalho-Niebel, F., and Barker, D.G.** (2015). Remodeling of the infection chamber before infection thread formation reveals a two-step mechanism for rhizobial entry into the host legume root hair. *Plant Physiol* **167**, 1233-1242.
- Frugier, F., Kosuta, S., Murray, J.D., Crespi, M., and Szczyglowski, K.** (2008). Cytokinin: secret agent of symbiosis. *Trends Plant Sci* **13**, 115-120.
- Gage, D.J.** (2004). Infection and invasion of roots by symbiotic, nitrogen-fixing rhizobia during nodulation of temperate legumes. *Microbiol Mol Biol Rev* **68**, 280-300.
- Gaudioso-Pedraza, R., and Benitez-Alfonso, Y.** (2014). A phylogenetic approach to study the origin and evolution of plasmodesmata-localized glycosyl hydrolases family 17. *Front Plant Sci* **5**, 212-226.
- Geurts, R., and Bisseling, T.** (2002). Rhizobium nod factor perception and signalling. *Plant Cell* **14 Suppl**, S239-249.
- Gherbi, H., Markmann, K., Svistoonoff, S., Estevan, J., Autran, D., Giczey, G., Auguy, F., Peret, B., Laplaze, L., Franche, C., Parniske, M., and Bogusz, D.** (2008). SymRK defines a common genetic basis for plant root endosymbioses with arbuscular mycorrhiza fungi, rhizobia, and Frankiacteria. *Proc Natl Acad Sci U S A* **105**, 4928-4932.
- Gleason, C., Chaudhuri, S., Yang, T., Munoz, A., Poovaiah, B.W., and Oldroyd, G.E.** (2006). Nodulation independent of rhizobia induced by a calcium-activated kinase lacking autoinhibition. *Nature* **441**, 1149-1152.
- Gollotte, A., Gianinazzi-Pearson, V., Giovannetti, M., Sbrana, C., Avio, L., and Gianinazzi, S.** (1993). Cellular localization and cytochemical probing of resistance reactions to arbuscular mycorrhizal fungi in a 'locus a' myc-mutant of *Pisum sativum* L. *Planta* **191**, 112-121.
- Gonzalez-Rizzo, S., Crespi, M., and Frugier, F.** (2006). The *Medicago truncatula* CRE1 cytokinin receptor regulates lateral root development and early symbiotic interaction with *Sinorhizobium meliloti*. *Plant Cell* **18**, 2680-2693.
- Gray, W.M.** (2004). Hormonal regulation of plant growth and development. *PLoS Biol* **2**, E311.
- Gresshoff, P.M., Lohar, D., Chan, P.K., Biswas, B., Jiang, Q., Reid, D., Ferguson, B., and Stacey, G.** (2009). Genetic analysis of ethylene regulation of legume nodulation. *Plant Signal Behav* **4**, 818-823.
- Guenther, J.C., and Trail, F.** (2005). The development and differentiation of *Gibberella zeae* (anamorph: *Fusarium graminearum*) during colonization of wheat. *Mycologia* **97**, 229-237.
- Guinel, F.C.** (2015). Ethylene, a Hormone at the Center-Stage of Nodulation. *Front Plant Sci* **6**, 1121.
- Guinel, F.C., and Larue, T.A.** (1992). Ethylene Inhibitors Partly Restore Nodulation to Pea Mutant E 107 (brz). *Plant Physiol* **99**, 515-518.
- Guseman, J.M., Lee, J.S., Bogenschutz, N.L., Peterson, K.M., Virata, R.E., Xie, B., Kanaoka, M.M., Hong, Z., and Torii, K.U.** (2010). Dysregulation

- of cell-to-cell connectivity and stomatal patterning by loss-of-function mutation in *Arabidopsis thaliana* *glucan synthase-like 8*. *Development* **137**, 1731-1741.
- Haag, A.F., Arnold, M.F., Myka, K.K., Kerscher, B., Dall'Angelo, S., Zanda, M., Mergaert, P., and Ferguson, G.P.** (2013). Molecular insights into bacteroid development during *Rhizobium-legume* symbiosis. *FEMS Microbiol Rev* **37**, 364-383.
- Han, X., Hyun, T.K., Zhang, M., Kumar, R., Koh, E.J., Kang, B.H., Lucas, W.J., and Kim, J.Y.** (2014). Auxin-callose-mediated plasmodesmal gating is essential for tropic auxin gradient formation and signaling. *Dev Cell* **28**, 132-146.
- Hao, P., Liu, C., Wang, Y., Chen, R., Tang, M., Du, B., Zhu, L., and He, G.** (2008). Herbivore-induced callose deposition on the sieve plates of rice: an important mechanism for host resistance. *Plant Physiol* **146**, 1810-1820.
- Haupt, S., Cowan, G.H., Ziegler, A., Roberts, A.G., Oparka, K.J., and Torrance, L.** (2005). Two plant-viral movement proteins traffic in the endocytic recycling pathway. *Plant Cell* **17**, 164-181.
- He, J., Benedito, V.A., Wang, M., Murray, J.D., Zhao, P.X., Tang, Y., and Udvardi, M.K.** (2009). The *Medicago truncatula* gene expression atlas web server. *BMC Bioinformatics* **10**, 441-450.
- Heckmann, A.B., Sandal, N., Bek, A.S., Madsen, L.H., Jurkiewicz, A., Nielsen, M.W., Tirichine, L., and Stougaard, J.** (2011). Cytokinin induction of root nodule primordia in *Lotus japonicus* is regulated by a mechanism operating in the root cortex. *Mol Plant Microbe Interact* **24**, 1385-1395.
- Heinlein, M., Padgett, H.S., Gens, J.S., Pickard, B.G., Casper, S.J., Epel, B.L., and Beachy, R.N.** (1998). Changing patterns of localization of the tobacco mosaic virus movement protein and replicase to the endoplasmic reticulum and microtubules during infection. *Plant Cell* **10**, 1107-1120.
- Helariutta, Y., Fukaki, H., Wysocka-Diller, J., Nakajima, K., Jung, J., Sena, G., Hauser, M.T., and Benfey, P.N.** (2000). The *SHORT-ROOT* gene controls radial patterning of the *Arabidopsis* root through radial signaling. *Cell* **101**, 555-567.
- Held, M., Hou, H., Miri, M., Huynh, C., Ross, L., Hossain, M.S., Sato, S., Tabata, S., Perry, J., Wang, T.L., and Szczyglowski, K.** (2014). *Lotus japonicus* cytokinin receptors work partially redundantly to mediate nodule formation. *Plant Cell* **26**, 678-694.
- Hill, J.** (2000). *Jester*. *Plant Variety Journal* **13**.
- Hirsch, A.M.** (1992). Developmental biology of legume nodulation. *New Phytologist* **122**, 26.
- Hirsch, A.M., Bhuvaneshwari, T.V., Torrey, J.G., and Bisseling, T.** (1989). Early nodulin genes are induced in alfalfa root outgrowths elicited by auxin transport inhibitors. *Proc Natl Acad Sci U S A* **86**, 1244-1248.
- Hofmann, J., Youssef-Banora, M., de Almeida-Engler, J., and Grundle, F.M.** (2010). The role of callose deposition along plasmodesmata in nematode feeding sites. *Mol Plant Microbe Interact* **23**, 549-557.
- Huang, Z., Andrianov, V.M., Han, Y., and Howell, S.H.** (2001). Identification of *Arabidopsis* proteins that interact with the cauliflower mosaic virus (CaMV) movement protein. *Plant Mol Biol* **47**, 663-675.

- Huault, E., Laffont, C., Wen, J., Mysore, K.S., Ratet, P., Duc, G., and Frugier, F.** (2014). Local and systemic regulation of plant root system architecture and symbiotic nodulation by a receptor-like kinase. *PLoS Genet* **10**, e1004891.
- Iglesias, V.A., and Meins, F.** (2000). Movement of plant viruses is delayed in a beta-1,3-glucanase-deficient mutant showing a reduced plasmodesmatal size exclusion limit and enhanced callose deposition. *Plant Journal* **21**, 157-166.
- Imin, N., Mohd-Radzman, N.A., Ogilvie, H.A., and Djordjevic, M.A.** (2013). The peptide-encoding CEP1 gene modulates lateral root and nodule numbers in *Medicago truncatula*. *J Exp Bot* **64**, 5395-5409.
- Ishida, T., Kurata, T., Okada, K., and Wada, T.** (2008). A genetic regulatory network in the development of trichomes and root hairs. *Annu Rev Plant Biol* **59**, 365-386.
- Ishikawa, K., Yokota, K., Li, Y.Y., Wang, Y., Liu, C., Suzuki, S., Aono, T., and Oyaizu, H.** (2008). Isolation of a novel root-determined hypernodulation mutant *rdh1* of *Lotus japonicus*. *Soil Science and Plant Nutrition* **54**, 259–263.
- Jaffe, M.J., and Leopold, A.C.** (1984). Callose deposition during gravitropism of *Zea mays* and *Pisum sativum* and its inhibition by 2-deoxy-D-glucose. *Planta* **161**, 20-26.
- Jardinaud, M.F., Boivin, S., Rodde, N., Catrice, O., Kisiala, A., Lepage, A., Moreau, S., Roux, B., Cottret, L., Sallet, E., Brault, M., Emery, R.J., Gouzy, J., Frugier, F., and Gamas, P.** (2016). A Laser Dissection-RNAseq Analysis Highlights the Activation of Cytokinin Pathways by Nod Factors in the *Medicago truncatula* Root Epidermis. *Plant Physiol* **171**, 2256-2276.
- Jeudy, C., Ruffel, S., Freixes, S., Tillard, P., Santoni, A.L., Morel, S., Journet, E.P., Duc, G., Gojon, A., Lepetit, M., and Salon, C.** (2010). Adaptation of *Medicago truncatula* to nitrogen limitation is modulated via local and systemic nodule developmental responses. *New Phytol* **185**, 817-828.
- Jones, K.M., Kobayashi, H., Davies, B.W., Taga, M.E., and Walker, G.C.** (2007). How rhizobial symbionts invade plants: the *Sinorhizobium-Medicago* model. *Nat Rev Microbiol* **5**, 619-633.
- Journet, E.P., El-Gachtouli, N., Vernoud, V., de Billy, F., Pichon, M., Dedieu, A., Arnould, C., Morandi, D., Barker, D.G., and Gianinazzi-Pearson, V.** (2001). *Medicago truncatula* ENOD11: a novel RPRP-encoding early nodulin gene expressed during mycorrhization in arbuscule-containing cells. *Mol Plant Microbe Interact* **14**, 737-748.
- Kankanala, P., Czymmek, K., and Valent, B.** (2007). Roles for rice membrane dynamics and plasmodesmata during biotrophic invasion by the blast fungus. *Plant Cell* **19**, 706-724.
- Karimi, M., De Meyer, B., and Hilson, P.** (2005). Modular cloning in plant cells. *Trends Plant Sci* **10**, 103-105.
- Kassaw, T., Jr, W.B., and Frugoli, J.** (2015). Multiple Autoregulation of Nodulation (AON) Signals Identified through Split Root Analysis of *Medicago truncatula* *sun* and *rdn1* Mutants. *Plants (Basel)* **4**, 209-224.
- Katzen, F.** (2007). Gateway((R)) recombinational cloning: a biological operating system. *Expert Opin Drug Discov* **2**, 571-589.

- Kawaharada, Y., Kelly, S., Nielsen, M.W., Hjuler, C.T., Gysel, K., Muszynski, A., Carlson, R.W., Thygesen, M.B., Sandal, N., Asmussen, M.H., Vinther, M., Andersen, S.U., Krusell, L., Thirup, S., Jensen, K.J., Ronson, C.W., Blaise, M., Radutoiu, S., and Stougaard, J. (2015). Receptor-mediated exopolysaccharide perception controls bacterial infection. *Nature* **523**, 308-312.
- Kereszt, A., Mergaert, P., and Kondorosi, E. (2011). Bacteroid development in legume nodules: evolution of mutual benefit or of sacrificial victims? *Mol Plant Microbe Interact* **24**, 1300-1309.
- Kitagawa, M., and Jackson, D. (2017). Plasmodesmata-Mediated Cell-to-Cell Communication in the Shoot Apical Meristem: How Stem Cells Talk. *Plants (Basel)* **6**.
- Knoblauch, M., Vendrell, M., de Leau, E., Paterlini, A., Knox, K., Ross-Elliott, T., Reinders, A., Brockman, S.A., Ward, J., and Oparka, K. (2015). Multispectral phloem-mobile probes: properties and applications. *Plant Physiol* **167**, 1211-1220.
- Knox, J.P., and Benitez-Alfonso, Y. (2014). Roles and regulation of plant cell walls surrounding plasmodesmata. *Curr Opin Plant Biol* **22**, 93-100.
- Kosslak, R.M., and Bohlool, B.B. (1984). Suppression of nodule development of one side of a split-root system of soybeans caused by prior inoculation of the other side. *Plant Physiol* **75**, 125-130.
- Kraner, M.E., Link, K., Melzer, M., Ekici, A.B., Uebe, S., Tarazona, P., Feussner, I., Hofmann, J., and Sonnewald, U. (2017). Choline transporter-like1 (CHER1) is crucial for plasmodesmata maturation in *Arabidopsis thaliana*. *Plant J* **89**, 394-406.
- Krouk, G., Lacombe, B., Bielach, A., Perrine-Walker, F., Malinska, K., Mounier, E., Hoyerova, K., Tillard, P., Leon, S., Ljung, K., Zazimalova, E., Benkova, E., Nacry, P., and Gojon, A. (2010). Nitrate-regulated auxin transport by NRT1.1 defines a mechanism for nutrient sensing in plants. *Dev Cell* **18**, 927-937.
- Krusell, L., Madsen, L.H., Sato, S., Aubert, G., Genua, A., Szczyglowski, K., Duc, G., Kaneko, T., Tabata, S., de Bruijn, F., Pajuelo, E., Sandal, N., and Stougaard, J. (2002). Shoot control of root development and nodulation is mediated by a receptor-like kinase. *Nature* **420**, 422-426.
- Laffont, C., Rey, T., Andre, O., Novero, M., Kazmierczak, T., Debelle, F., Bonfante, P., Jacquet, C., and Frugier, F. (2015). The CRE1 Cytokinin Pathway Is Differentially Recruited Depending on *Medicago truncatula* Root Environments and Negatively Regulates Resistance to a Pathogen. *Plos One* **10**, e0116819.
- Laloum, T., Baudin, M., Frances, L., Lepage, A., Billault-Penneteau, B., Cerri, M.R., Ariel, F., Jardinaud, M.F., Gamas, P., de Carvalho-Niebel, F., and Niebel, A. (2014). Two CCAAT-box-binding transcription factors redundantly regulate early steps of the legume-rhizobia endosymbiosis. *Plant J* **79**, 757-768.
- Laplaze, L., Lucas, M., and Champion, A. (2015). Rhizobial root hair infection requires auxin signaling. *Trends Plant Sci* **20**, 332-334.
- Laplaze, L., Benkova, E., Casimiro, I., Maes, L., Vanneste, S., Swarup, R., Weijers, D., Calvo, V., Parizot, B., Herrera-Rodriguez, M.B., Offringa, R., Graham, N., Dumas, P., Friml, J., Bogusz, D., Beeckman, T., and

- Bennett, M.** (2007). Cytokinins act directly on lateral root founder cells to inhibit root initiation. *Plant Cell* **19**, 3889-3900.
- Larrainzar, E., Riely, B.K., Kim, S.C., Carrasquilla-Garcia, N., Yu, H.J., Hwang, H.J., Oh, M., Kim, G.B., Surendrarao, A.K., Chasman, D., Siahpirani, A.F., Penmetza, R.V., Lee, G.S., Kim, N., Roy, S., Mun, J.H., and Cook, D.R.** (2015). Deep Sequencing of the *Medicago truncatula* Root Transcriptome Reveals a Massive and Early Interaction between Nodulation Factor and Ethylene Signals. *Plant Physiol* **169**, 233-265.
- Lee, J.Y., Wang, X., Cui, W., Sager, R., Modla, S., Czymmek, K., Zybaliov, B., van Wijk, K., Zhang, C., Lu, H., and Lakshmanan, V.** (2011). A plasmodesmata-localized protein mediates crosstalk between cell-to-cell communication and innate immunity in *Arabidopsis*. *Plant Cell* **23**, 3353-3373.
- Letunic, I., Doerks, T., and Bork, P.** (2012). SMART 7: recent updates to the protein domain annotation resource. *Nucleic Acids Res* **40**, D302-305.
- Levy, A., Erlanger, M., Rosenthal, M., and Epel, B.L.** (2007). A plasmodesmata-associated beta-1,3-glucanase in *Arabidopsis*. *Plant J* **49**, 669-682.
- Levy, J., Bres, C., Geurts, R., Chalhoub, B., Kulikova, O., Duc, G., Journet, E.P., Ane, J.M., Lauber, E., Bisseling, T., Denarie, J., Rosenberg, C., and Debelle, F.** (2004). A putative Ca²⁺ and calmodulin-dependent protein kinase required for bacterial and fungal symbioses. *Science* **303**, 1361-1364.
- Li, D., Kinkema, M., and Gresshoff, P.M.** (2009). Autoregulation of nodulation (AON) in *Pisum sativum* (pea) involves signalling events associated with both nodule primordia development and nitrogen fixation. *J Plant Physiol* **166**, 955-967.
- Li, W., Zhao, Y., Liu, C., Yao, G., Wu, S., Hou, C., Zhang, M., and Wang, D.** (2012). Callose deposition at plasmodesmata is a critical factor in restricting the cell-to-cell movement of Soybean mosaic virus. *Plant Cell Rep* **31**, 905-916.
- Lim, C.W., Lee, Y.W., and Hwang, C.H.** (2011). Soybean nodule-enhanced CLE peptides in roots act as signals in GmNARK-mediated nodulation suppression. *Plant Cell Physiol* **52**, 1613-1627.
- Lim, C.W., Park, J.Y., Lee, S.H., and Hwang, C.H.** (2010). Comparative proteomic analysis of soybean nodulation using a supernodulation mutant, SS2-2. *Biosci Biotechnol Biochem* **74**, 2396-2404.
- Lim, G.H., Shine, M.B., de Lorenzo, L., Yu, K., Cui, W., Navarre, D., Hunt, A.G., Lee, J.Y., Kachroo, A., and Kachroo, P.** (2016). Plasmodesmata Localizing Proteins Regulate Transport and Signaling during Systemic Acquired Immunity in Plants. *Cell Host Microbe* **19**, 541-549.
- Liu, C.W., Breakspear, A., Roy, S., and Murray, J.D.** (2015). Cytokinin responses counterpoint auxin signaling during rhizobial infection. *Plant Signal Behav* **10**, e1019982.
- Locascio, A., Roig-Villanova, I., Bernardi, J., and Varotto, S.** (2014). Current perspectives on the hormonal control of seed development in *Arabidopsis* and maize: a focus on auxin. *Front Plant Sci* **5**, 412.
- Lohar, D., Stiller, J., Kam, J., Stacey, G., and Gresshoff, P.M.** (2009). Ethylene insensitivity conferred by a mutated *Arabidopsis* ethylene

- receptor gene alters nodulation in transgenic *Lotus japonicus*. *Ann Bot* **104**, 277-285.
- Lucas, W.J., and Lee, J.Y.** (2004). Plasmodesmata as a supracellular control network in plants. *Nat Rev Mol Cell Biol* **5**, 712-726.
- Luna, E., Pastor, V., Robert, J., Flors, V., Mauch-Mani, B., and Ton, J.** (2011). Callose deposition: a multifaceted plant defense response. *Mol Plant Microbe Interact* **24**, 183-193.
- Madsen, E.B., Madsen, L.H., Radutoiu, S., Olbryt, M., Rakwalska, M., Szczyglowski, K., Sato, S., Kaneko, T., Tabata, S., Sandal, N., and Stougaard, J.** (2003). A receptor kinase gene of the LysM type is involved in legume perception of rhizobial signals. *Nature* **425**, 637-640.
- Magori, S., Oka-Kira, E., Shibata, S., Umehara, Y., Kouchi, H., Hase, Y., Tanaka, A., Sato, S., Tabata, S., and Kawaguchi, M.** (2009). Too much love, a root regulator associated with the long-distance control of nodulation in *Lotus japonicus*. *Mol Plant Microbe Interact* **22**, 259-268.
- Maillet, F., Poinot, V., Andre, O., Puech-Pages, V., Haouy, A., Gueunier, M., Cromer, L., Giraudet, D., Formey, D., Niebel, A., Martinez, E.A., Driguez, H., Becard, G., and Denarie, J.** (2011). Fungal lipochitooligosaccharide symbiotic signals in arbuscular mycorrhiza. *Nature* **469**, 58-63.
- Mao, G., Turner, M., Yu, O., and S, S.** (2013). miR393 and miR164 influence indeterminate but not determinate nodule development. *Plant Signaling & Behavior* **8**.
- Marsh, J.F., Rakocevic, A., Mitra, R.M., Brocard, L., Sun, J., Eschstruth, A., Long, S.R., Schultze, M., Ratet, P., and Oldroyd, G.E.** (2007). *Medicago truncatula* NIN is essential for rhizobial-independent nodule organogenesis induced by autoactive calcium/calmodulin-dependent protein kinase. *Plant Physiol* **144**, 324-335.
- Mathesius, U., Charon, C., Rolfe, B.G., Kondorosi, A., and Crespi, M.** (2000). Temporal and spatial order of events during the induction of cortical cell divisions in white clover by *Rhizobium leguminosarum* bv. *trifolii* inoculation or localized cytokinin addition. *Mol Plant Microbe Interact* **13**, 617-628.
- Mathesius, U., Schlaman, H.R., Spalink, H.P., Of Sautter, C., Rolfe, B.G., and Djordjevic, M.A.** (1998). Auxin transport inhibition precedes root nodule formation in white clover roots and is regulated by flavonoids and derivatives of chitin oligosaccharides. *Plant J* **14**, 23-34.
- Maule, A., Gaudioso-Pedraza, R., and Benitez-Alfonso, Y.** (2013). Callose deposition and symplastic connectivity are regulated prior to lateral root emergence. *Commun Integr Biol* **6**, e26531.
- McGarry, R.C., and Kragler, F.** (2013). Phloem-mobile signals affecting flowers: applications for crop breeding. *Trends Plant Sci* **18**, 198-206.
- Middleton, P.H., Jakab, J., Penmetsa, R.V., Starker, C.G., Doll, J., Kalo, P., Prabhu, R., Marsh, J.F., Mitra, R.M., Kereszt, A., Dudas, B., VandenBosch, K., Long, S.R., Cook, D.R., Kiss, G.B., and Oldroyd, G.E.** (2007). An ERF transcription factor in *Medicago truncatula* that is essential for Nod factor signal transduction. *Plant Cell* **19**, 1221-1234.
- Miller, J.B., Pratap, A., Miyahara, A., Zhou, L., Bornemann, S., Morris, R.J., and Oldroyd, G.E.** (2013). Calcium/Calmodulin-dependent protein kinase is negatively and positively regulated by calcium, providing a

- mechanism for decoding calcium responses during symbiosis signaling. *Plant Cell* **25**, 5053-5066.
- Mitra, R.M., Gleason, C.A., Edwards, A., Hadfield, J., Downie, J.A., Oldroyd, G.E., and Long, S.R.** (2004). A Ca²⁺/calmodulin-dependent protein kinase required for symbiotic nodule development: Gene identification by transcript-based cloning. *Proc Natl Acad Sci U S A* **101**, 4701-4705.
- Mohd-Radzman, N.A., Laffont, C., Ivanovici, A., Patel, N., Reid, D., Stougaard, J., Frugier, F., Imin, N., and Djordjevic, M.A.** (2016). Different Pathways Act Downstream of the CEP Peptide Receptor CRA2 to Regulate Lateral Root and Nodule Development. *Plant Physiol* **171**, 2536-2548.
- Morales-Rayas, R., Ruiz-Medrano, R., and Xoonostle-Cazares, B.** (2011). Macromolecular trafficking between a vesicular arbuscular endomycorrhizal fungus and roots of transgenic tobacco. *Plant Signal Behav* **6**, 617-623.
- Moreau, S., Verdenaud, M., Ott, T., Letort, S., de Billy, F., Niebel, A., Gouzy, J., de Carvalho-Niebel, F., and Gamas, P.** (2011). Transcription reprogramming during root nodule development in *Medicago truncatula*. *PLoS One* **6**, e16463.
- Moreira, S., Braga, T., Carvalho, H., and Campilho, A.** (2013). The Arabidopsis HP6 gene is expressed in *Medicago truncatula* lateral roots and root nodule primordia. *Plant Signal Behav* **8**, e25262.
- Morohashi, Y., and Matsushima, H.** (2000). Development of beta-1,3-glucanase activity in germinated tomato seeds. *J Exp Bot* **51**, 1381-1387.
- Mortier, V., Holsters, M., and Goormachtig, S.** (2012). Never too many? How legumes control nodule numbers. *Plant Cell Environ* **35**, 245-258.
- Mortier, V., Den Herder, G., Whitford, R., Van de Velde, W., Rombauts, S., D'Haeseleer, K., Holsters, M., and Goormachtig, S.** (2010). CLE peptides control *Medicago truncatula* nodulation locally and systemically. *Plant Physiol* **153**, 222-237.
- Muraro, D., Wilson, M., and Bennett, M.J.** (2011). Root development: cytokinin transport matters, too! *Curr Biol* **21**, R423-425.
- Murray, J.D., Liu, C.W., Chen, Y., and Miller, A.J.** (2017). Nitrogen sensing in legumes. *J Exp Bot* **68**, 1919-1926.
- Murray, J.D., Karas, B.J., Sato, S., Tabata, S., Amyot, L., and Szczyglowski, K.** (2007). A cytokinin perception mutant colonized by *Rhizobium* in the absence of nodule organogenesis. *Science* **315**, 101-104.
- Nakajima, K., Sena, G., Nawy, T., and Benfey, P.N.** (2001). Intercellular movement of the putative transcription factor SHR in root patterning. *Nature* **413**, 307-311.
- Neale, A.D., Wahleithner, J.A., Lund, M., Bonnett, H.T., Kelly, A., Meeks-Wagner, D.R., Peacock, W.J., and Dennis, E.S.** (1990). Chitinase, beta-1,3-glucanase, osmotin, and extensin are expressed in tobacco explants during flower formation. *Plant Cell* **2**, 673-684.
- Nishimura, R., Ohmori, M., and Kawaguchi, M.** (2002). The novel symbiotic phenotype of enhanced-nodulating mutant of *Lotus japonicus*: astray mutant is an early nodulating mutant with wider nodulation zone. *Plant Cell Physiol* **43**, 853-859.
- Novak, K.** (2010). Early action of pea symbiotic gene NOD3 is confirmed by adventitious root phenotype. *Plant Sci* **179**, 472-478.

- Nukui, N., Ezura, H., and Minamisawa, K.** (2004). Transgenic *Lotus japonicus* with an ethylene receptor gene Cm-ERS1/H70A enhances formation of infection threads and nodule primordia. *Plant Cell Physiol* **45**, 427-435.
- Nukui, N., Ezura, H., Yuhashi, K., Yasuta, T., and Minamisawa, K.** (2000). Effects of ethylene precursor and inhibitors for ethylene biosynthesis and perception on nodulation in *Lotus japonicus* and *Macroptilium atropurpureum*. *Plant Cell Physiol* **41**, 893-897.
- Oka-Kira, E., Tateno, K., Miura, K., Haga, T., Hayashi, M., Harada, K., Sato, S., Tabata, S., Shikazono, N., Tanaka, A., Watanabe, Y., Fukuhara, I., Nagata, T., and Kawaguchi, M.** (2005). *klavier (klv)*, a novel hypernodulation mutant of *Lotus japonicus* affected in vascular tissue organization and floral induction. *Plant J* **44**, 505-515.
- Okamoto, S., and Kawaguchi, M.** (2015). Shoot HAR1 mediates nitrate inhibition of nodulation in *Lotus japonicus*. *Plant Signal Behav* **10**, e1000138.
- Okamoto, S., Ohnishi, E., Sato, S., Takahashi, H., Nakazono, M., Tabata, S., and Kawaguchi, M.** (2009). Nod factor/nitrate-induced CLE genes that drive HAR1-mediated systemic regulation of nodulation. *Plant Cell Physiol* **50**, 67-77.
- Oldroyd, G.E., Engstrom, E.M., and Long, S.R.** (2001). Ethylene inhibits the Nod factor signal transduction pathway of *Medicago truncatula*. *Plant Cell* **13**, 1835-1849.
- Oldroyd, G.E., Harrison, M.J., and Udvardi, M.** (2005). Peace talks and trade deals. Keys to long-term harmony in legume-microbe symbioses. *Plant Physiol* **137**, 1205-1210.
- Oparka, K.J., Roberts, A.G., Boevink, P., Santa Cruz, S., Roberts, I., Pradel, K.S., Imlau, A., Kotlizky, G., Sauer, N., and Epel, B.** (1999). Simple, but not branched, plasmodesmata allow the nonspecific trafficking of proteins in developing tobacco leaves. *Cell* **97**, 743-754.
- Otero, S., Helariutta, Y., and Benitez-Alfonso, Y.** (2016). Symplastic communication in organ formation and tissue patterning. *Curr Opin Plant Biol* **29**, 21-28.
- Overvoorde, P., Fukaki, H., and Beeckman, T.** (2010). Auxin control of root development. *Cold Spring Harb Perspect Biol* **2**, a001537.
- Papadopoulou, K., Roussis, A., and Katinakis, P.** (1996). Phaseolus ENOD40 is involved in symbiotic and non-symbiotic organogenetic processes: expression during nodule and lateral root development. *Plant Mol Biol* **30**, 403-417.
- Parniske, M.** (2004). Molecular genetics of the arbuscular mycorrhizal symbiosis. *Curr Opin Plant Biol* **7**, 414-421.
- Pellizzaro, A., Clochard, T., Cukier, C., Bourdin, C., Juchaux, M., Montrichard, F., Thany, S., Raymond, V., Planchet, E., Limami, A.M., and Morere-Le Paven, M.C.** (2014). The nitrate transporter MtNPF6.8 (MtNRT1.3) transports abscisic acid and mediates nitrate regulation of primary root growth in *Medicago truncatula*. *Plant Physiol* **166**, 2152-2165.
- Penmetsa, R.V., and Cook, D.R.** (1997). A Legume Ethylene-Insensitive Mutant Hyperinfected by Its Rhizobial Symbiont. *Science* **275**, 527-530.

- Penmetsa, R.V., Frugoli, J.A., Smith, L.S., Long, S.R., and Cook, D.R.** (2003). Dual genetic pathways controlling nodule number in *Medicago truncatula*. *Plant Physiol* **131**, 998-1008.
- Penmetsa, R.V., Uribe, P., Anderson, J., Lichtenzveig, J., Gish, J.C., Nam, Y.W., Engstrom, E., Xu, K., Sckisel, G., Pereira, M., Baek, J.M., Lopez-Meyer, M., Long, S.R., Harrison, M.J., Singh, K.B., Kiss, G.B., and Cook, D.R.** (2008). The *Medicago truncatula* ortholog of *Arabidopsis* EIN2, *sickle*, is a negative regulator of symbiotic and pathogenic microbial associations. *Plant J* **55**, 580-595.
- Peret, B., Swarup, R., Jansen, L., Devos, G., Auguy, F., Collin, M., Santi, C., Hocher, V., Franche, C., Bogusz, D., Bennett, M., and Laplaze, L.** (2007). Auxin influx activity is associated with *Frankia* infection during actinorhizal nodule formation in *Casuarina glauca*. *Plant Physiol* **144**, 1852-1862.
- Perrot-Rechenmann, C.** (2010). Cellular responses to auxin: division versus expansion. *Cold Spring Harb Perspect Biol* **2**, a001446.
- Peters, N.K., and Crist-Estes, D.K.** (1989). Nodule formation is stimulated by the ethylene inhibitor aminoethoxyvinylglycine. *Plant Physiol* **91**, 690-693.
- Peterson, R.L., and Bonafante, P.** (1994). Comparative structure of vesicular-arbuscular mycorrhizas and ectomycorrhizas *Plant and Soil* **159**, 79-88.
- Pierleoni, A., Martelli, P.L., and Casadio, R.** (2008). PredGPI: a GPI-anchor predictor. *BMC Bioinformatics* **9**, 392-401.
- Plet, J., Wasson, A., Ariel, F., Le Signor, C., Baker, D., Mathesius, U., Crespi, M., and Frugier, F.** (2011). MtCRE1-dependent cytokinin signaling integrates bacterial and plant cues to coordinate symbiotic nodule organogenesis in *Medicago truncatula*. *Plant J* **65**, 622-633.
- Poisson, G., Chauve, C., Chen, X., and Bergeron, A.** (2007). FragAnchor: a large-scale predictor of glycosylphosphatidylinositol anchors in eukaryote protein sequences by qualitative scoring. *Genomics Proteomics Bioinformatics* **5**, 121-130.
- Qin, S., Yeboah, S., Cao, L., Zhang, J., Shi, S., and Liu, Y.** (2017). Breaking continuous potato cropping with legumes improves soil microbial communities, enzyme activities and tuber yield. *PLoS One* **12**, e0175934.
- Reid, D.E., Ferguson, B.J., and Gresshoff, P.M.** (2011a). Inoculation- and nitrate-induced CLE peptides of soybean control NARK-dependent nodule formation. *Mol Plant Microbe Interact* **24**, 606-618.
- Reid, D.E., Li, D., Ferguson, B.J., and Gresshoff, P.M.** (2013). Structure-function analysis of the GmRIC1 signal peptide and CLE domain required for nodulation control in soybean. *J Exp Bot* **64**, 1575-1585.
- Reid, D.E., Ferguson, B.J., Hayashi, S., Lin, Y.H., and Gresshoff, P.M.** (2011b). Molecular mechanisms controlling legume autoregulation of nodulation. *Ann Bot* **108**, 789-795.
- Resendes, C.M., Geil, R.D., and Guinel, F.C.** (2001). Mycorrhizal development in a low nodulating pea mutant. *New Phytologist* **150**, 563-572.
- Rey, T., and Schornack, S.** (2013). Interactions of beneficial and detrimental root-colonizing filamentous microbes with plant hosts. *Genome Biol* **14**, 121-135.
- Rightmyer, A.P., and Long, S.R.** (2011). Pseudonodule formation by wild-type and symbiotic mutant *Medicago truncatula* in response to auxin transport inhibitors. *Mol Plant Microbe Interact* **24**, 1372-1384.

- Rinne, P.L., van den Boogaard, R., Mensink, M.G., Kopperud, C., Kormelink, R., Goldbach, R., and van der Schoot, C.** (2005). Tobacco plants respond to the constitutive expression of the tospovirus movement protein NS(M) with a heat-reversible sealing of plasmodesmata that impairs development. *Plant J* **43**, 688-707.
- Rinne, P.L., Welling, A., Vahala, J., Ripel, L., Ruonala, R., Kangasjarvi, J., and van der Schoot, C.** (2011). Chilling of dormant buds hyperinduces FLOWERING LOCUS T and recruits GA-inducible 1,3-beta-glucanases to reopen signal conduits and release dormancy in *Populus*. *Plant Cell* **23**, 130-146.
- Rival, P., de Billy, F., Bono, J.J., Gough, C., Rosenberg, C., and Bensmihen, S.** (2012). Epidermal and cortical roles of NFP and DMI3 in coordinating early steps of nodulation in *Medicago truncatula*. *Development* **139**, 3383-3391.
- Roberts, A.G., and Oparka, K.J.** (2003). Plasmodesmata and the control of symplastic transport. *Plant, Cell and Environment* **26**, 103–124.
- Roy, S., Robson, F., Lilley, J., Liu, C., Cheng, X., Wen J., Walker, S., Sun, J., Cousins, D., Bone, C., Bennett, M., Downie, A., Swarup, J., Oldroyd, G., Murray, J.D. (2017). MtLAX2, a Functional Homologue of the Arabidopsis Auxin Influx 3 Transporter AUX1, is Required for Nodule Organogenesis. *Plant Physiology* **175**
- Ryu, H., Cho, H., Choi, D., and Hwang, I.** (2012). Plant hormonal regulation of nitrogen-fixing nodule organogenesis. *Mol Cells* **34**, 117-126.
- Sagan, M., and Gresshoff, P.** (1996). Developmental mapping of nodulation events in pea (*Pisum sativum* L) using supernodulating plant genotypes and bacterial variability reveals both plant and *Rhizobium* control of nodulation regulation. *Plant Science* **117**, 167-179.
- Sagan, M., and Duc, G.** (1996). Sym28 and Sym29, two new genes involved in regulation of nodulation in pea (*Pisum sativum* L.). *Symbiosis* **20**, 229-245.
- Sager, R., and Lee, J.Y.** (2014). Plasmodesmata in integrated cell signalling: insights from development and environmental signals and stresses. *J Exp Bot* **65**, 6337-6358.
- Sagi, G., Katz, A., Guenoune-Gelbart, D., and Epel, B.L.** (2005). Class 1 reversibly glycosylated polypeptides are plasmodesmal-associated proteins delivered to plasmodesmata via the golgi apparatus. *Plant Cell* **17**, 1788-1800.
- Saha, S., and DasGupta, M.** (2015). Does SUNN-SYMRK Crosstalk occur in *Medicago truncatula* for regulating nodule organogenesis? *Plant Signal Behav* **10**, e1028703.
- Saha, S., Dutta, A., Bhattacharya, A., and DasGupta, M.** (2014). Intracellular catalytic domain of symbiosis receptor kinase hyperactivates spontaneous nodulation in absence of rhizobia. *Plant Physiol* **166**, 1699-1708.
- Salmon, M.S., and Bayer, E.M.** (2012). Dissecting plasmodesmata molecular composition by mass spectrometry-based proteomics. *Front Plant Sci* **3**, 307-315.
- Santi, C., Bogusz, D., and Franche, C.** (2013). Biological nitrogen fixation in non-legume plants. *Ann Bot* **111**, 743-767.

- Sasaki, N., Park, J.W., Maule, A.J., and Nelson, R.S.** (2006). The cysteine-histidine-rich region of the movement protein of Cucumber mosaic virus contributes to plasmodesmal targeting, zinc binding and pathogenesis. *Virology* **349**, 396-408.
- Schaller, G.E.** (2012). Ethylene and the regulation of plant development. *BMC Biol* **10**, 9.
- Schauser, L., Roussis, A., Stiller, J., and Stougaard, J.** (1999). A plant regulator controlling development of symbiotic root nodules. *Nature* **402**, 191-195.
- Schmittgen, T.D., and Livak, K.J.** (2008). Analyzing real-time PCR data by the comparative C(T) method. *Nat Protoc* **3**, 1101-1108.
- Schnabel, E., Journet, E.P., de Carvalho-Niebel, F., Duc, G., and Frugoli, J.** (2005). The *Medicago truncatula* SUNN gene encodes a CLV1-like leucine-rich repeat receptor kinase that regulates nodule number and root length. *Plant Mol Biol* **58**, 809-822.
- Schnabel, E., Mukherjee, A., Smith, L., Kassaw, T., Long, S., and Frugoli, J.** (2010). The *lss* supernodulation mutant of *Medicago truncatula* reduces expression of the SUNN gene. *Plant Physiol* **154**, 1390-1402.
- Schnabel, E.L., Kassaw, T.K., Smith, L.S., Marsh, J.F., Oldroyd, G.E., Long, S.R., and Frugoli, J.A.** (2011). The ROOT DETERMINED NODULATION1 gene regulates nodule number in roots of *Medicago truncatula* and defines a highly conserved, uncharacterized plant gene family. *Plant Physiol* **157**, 328-340.
- Schubert, M., Koteyeva, N.K., Wabnitz, P.W., Santos, P., Buttner, M., Sauer, N., Demchenko, K., and Pawlowski, K.** (2011). Plasmodesmata distribution and sugar partitioning in nitrogen-fixing root nodules of *Datisca glomerata*. *Planta* **233**, 139-152.
- Searle, I.R., Men, A.E., Laniya, T.S., Buzas, D.M., Iturbe-Ormaetxe, I., Carroll, B.J., and Gresshoff, P.M.** (2003). Long-distance signaling in nodulation directed by a CLAVATA1-like receptor kinase. *Science* **299**, 109-112.
- Searle, P.G.E., Comudom, Y., Shedden, D.C., and Nance, R.** (1981). Effect of maize + legume intercropping systems and fertilizer nitrogen on crop yielding and residual nitrogen. *Field Crops Research* **4**, 15.
- Sevilem, I., Miyashima, S., and Helariutta, Y.** (2013). Cell-to-cell communication via plasmodesmata in vascular plants. *Cell Adh Migr* **7**, 27-32.
- Sevilem, I., Yadav, S.R., and Helariutta, Y.** (2015). Plasmodesmata: channels for intercellular signaling during plant growth and development. *Methods Mol Biol* **1217**, 3-24.
- Signora, L., De Smet, I., Foyer, C.H., and Zhang, H.** (2001). ABA plays a central role in mediating the regulatory effects of nitrate on root branching in *Arabidopsis*. *Plant J* **28**, 655-662.
- Silva, J., Serra, G.E., Moreira, J.R., Concalves, J.C., and Goldemberg, J.** (1978). Energy balance for ethyl alcohol production from crops. *Science* **201**, 903-906.
- Simmons, A.R., and Bergmann, D.C.** (2016). Transcriptional control of cell fate in the stomatal lineage. *Curr Opin Plant Biol* **29**, 1-8.

- Singh, S., Katzer, K., Lambert, J., Cerri, M., and Parniske, M.** (2014). CYCLOPS, a DNA-binding transcriptional activator, orchestrates symbiotic root nodule development. *Cell Host Microbe* **15**, 139-152.
- Soto, M., Nogales, J., Pérez-Mendoza, D., Gallegos, M., Olivares, J., and Sanjuán, J.** (2011). Pathogenic and mutualistic plant-bacteria interactions: ever increasing similarities. *Central European Journal of Biology* **6**, 911–917.
- Soto, M.J., Sanjuan, J., and Olivares, J.** (2006). Rhizobia and plant-pathogenic bacteria: common infection weapons. *Microbiology* **152**, 3167-3174.
- Sousa, C., Johansson, C., Charon, C., Manyani, H., Sautter, C., Kondorosi, A., and Crespi, M.** (2001). Translational and structural requirements of the early nodulin gene *enod40*, a short-open reading frame-containing RNA, for elicitation of a cell-specific growth response in the alfalfa root cortex. *Mol Cell Biol* **21**, 354-366.
- Soyano, T., Kouchi, H., Hirota, A., and Hayashi, M.** (2013). Nodule inception directly targets NF-Y subunit genes to regulate essential processes of root nodule development in *Lotus japonicus*. *PLoS Genet* **9**, e1003352.
- Stahl, Y., and Simon, R.** (2013). Gated communities: apoplastic and symplastic signals converge at plasmodesmata to control cell fates. *J Exp Bot* **64**, 5237-5241.
- Stougaard, J., Abildsten, D. & Marcker, K.A.** (1987). The *Agrobacterium* Rhizogenes Pri TI-DNA Segment as a Gene Vector System for Transformation of Plants. *Mol Gen Genet* **207**, 251–255.
- Streeter, J.G.** (1985). Nitrate inhibition of legume nodule growth and activity : I. Long term studies with a continuous supply of nitrate. *Plant Physiol* **77**, 321-324.
- Su, S., Liu, Z., Chen, C., Zhang, Y., Wang, X., Zhu, L., Miao, L., Wang, X.C., and Yuan, M.** (2010). Cucumber mosaic virus movement protein severs actin filaments to increase the plasmodesmal size exclusion limit in tobacco. *Plant Cell* **22**, 1373-1387.
- Suzaki, T., Ito, M., and Kawaguchi, M.** (2013). Induction of localized auxin response during spontaneous nodule development in *Lotus japonicus*. *Plant Signal Behav* **8**, e23359.
- Svistoonoff, S., Sy, M.O., Diagne, N., Barker, D.G., Bogusz, D., and Franche, C.** (2010). Infection-specific activation of the *Medicago truncatula* *Enod11* early nodulin gene promoter during actinorhizal root nodulation. *Mol Plant Microbe Interact* **23**, 740-747.
- Thomas, C.L., Bayer, E.M., Ritzenthaler, C., Fernandez-Calvino, L., and Maule, A.J.** (2008). Specific targeting of a plasmodesmal protein affecting cell-to-cell communication. *PLoS Biol* **6**, e7.
- Tirichine, L., James, E.K., Sandal, N., and Stougaard, J.** (2006a). Spontaneous root-nodule formation in the model legume *Lotus japonicus*: a novel class of mutants nodulates in the absence of rhizobia. *Mol Plant Microbe Interact* **19**, 373-382.
- Tirichine, L., Sandal, N., Madsen, L.H., Radutoiu, S., Albrechtsen, A.S., Sato, S., Asamizu, E., Tabata, S., and Stougaard, J.** (2007). A gain-of-function mutation in a cytokinin receptor triggers spontaneous root nodule organogenesis. *Science* **315**, 104-107.

- Tirichine, L., Imaizumi-Anraku, H., Yoshida, S., Murakami, Y., Madsen, L.H., Miwa, H., Nakagawa, T., Sandal, N., Albrechtsen, A.S., Kawaguchi, M., Downie, A., Sato, S., Tabata, S., Kouchi, H., Parniske, M., Kawasaki, S., and Stougaard, J.** (2006b). Deregulation of a Ca²⁺/calmodulin-dependent kinase leads to spontaneous nodule development. *Nature* **441**, 1153-1156.
- Tominaga, A., Nagata, M., Futsuki, K., Abe, H., Uchiumi, T., Abe, M., Kucho, K., Hashiguchi, M., Akashi, R., Hirsch, A.M., Arima, S., and Suzuki, A.** (2009). Enhanced nodulation and nitrogen fixation in the abscisic acid low-sensitive mutant enhanced nitrogen fixation1 of *Lotus japonicus*. *Plant Physiol* **151**, 1965-1976.
- Turgeon, R., and Wolf, S.** (2009). Phloem transport: cellular pathways and molecular trafficking. *Annu Rev Plant Biol* **60**, 207-221.
- Vadassery, J., and Oelmuller, R.** (2009). Calcium signaling in pathogenic and beneficial plant microbe interactions: what can we learn from the interaction between *Piriformospora indica* and *Arabidopsis thaliana*. *Plant Signal Behav* **4**, 1024-1027.
- Vaddepalli, P., Herrmann, A., Fulton, L., Oelschner, M., Hillmer, S., Stratil, T.F., Fastner, A., Hammes, U.Z., Ott, T., Robinson, D.G., and Schneitz, K.** (2014). The C2-domain protein QUIRKY and the receptor-like kinase STRUBBELIG localize to plasmodesmata and mediate tissue morphogenesis in *Arabidopsis thaliana*. *Development* **141**, 4139-4148.
- Van de Velde, W., Guerra, J.C., De Keyser, A., De Rycke, R., Rombauts, S., Maunoury, N., Mergaert, P., Kondorosi, E., Holsters, M., and Goormachtig, S.** (2006). Aging in legume symbiosis. A molecular view on nodule senescence in *Medicago truncatula*. *Plant Physiol* **141**, 711-720.
- van Noorden, G.E., Ross, J.J., Reid, J.B., Rolfe, B.G., and Mathesius, U.** (2006). Defective long-distance auxin transport regulation in the *Medicago truncatula* super numeric nodules mutant. *Plant Physiol* **140**, 1494-1506.
- van Noorden, G.E., Verbeek, R., Dinh, Q.D., Jin, J., Green, A., Ng, J.L., and Mathesius, U.** (2016). Molecular Signals Controlling the Inhibition of Nodulation by Nitrate in *Medicago truncatula*. *Int J Mol Sci* **17**, 1060-1078.
- Vaten, A., Dettmer, J., Wu, S., Stierhof, Y.D., Miyashima, S., Yadav, S.R., Roberts, C.J., Campilho, A., Bulone, V., Lichtenberger, R., Lehesranta, S., Mahonen, A.P., Kim, J.Y., Jokitalo, E., Sauer, N., Scheres, B., Nakajima, K., Carlsbecker, A., Gallagher, K.L., and Helariutta, Y.** (2011). Callose biosynthesis regulates symplastic trafficking during root development. *Dev Cell* **21**, 1144-1155.
- Vega-Hernández, M.C., Pérez-Galdona, R., Dazzo, F.B., Jarabo-Lorenzo, A., Alfayate, M.C., and León-Barrios, M.** (2001). Blackwell Science Ltd Novel infection process in the indeterminate root nodule symbiosis between *Chamaecyctis proliferus* (tagasaste) and *Bradyrhizobium sp.* *New Phytologist* **150**, 14.
- Vernie, T., Moreau, S., de Billy, F., Plet, J., Combier, J.P., Rogers, C., Oldroyd, G., Frugier, F., Niebel, A., and Gamas, P.** (2008). EFD Is an ERF transcription factor involved in the control of nodule number and differentiation in *Medicago truncatula*. *Plant Cell* **20**, 2696-2713.
- Vernie, T., Kim, J., Frances, L., Ding, Y., Sun, J., Guan, D., Niebel, A., Gifford, M.L., de Carvalho-Niebel, F., and Oldroyd, G.E.** (2015). The

- NIN Transcription Factor Coordinates Diverse Nodulation Programs in Different Tissues of the *Medicago truncatula* Root. *Plant Cell* **27**, 3410-3424.
- Voigt, C.A.** (2014). Callose-mediated resistance to pathogenic intruders in plant defense-related papillae. *Front Plant Sci* **5**, 168-174.
- Wais, R.J., Keating, D.H., and Long, S.R.** (2002). Structure-function analysis of nod factor-induced root hair calcium spiking in *Rhizobium-legume* symbiosis. *Plant Physiol* **129**, 211-224.
- Wais, R.J., Galera, C., Oldroyd, G., Catoira, R., Penmetsa, R.V., Cook, D., Gough, C., Denarie, J., and Long, S.R.** (2000). Genetic analysis of calcium spiking responses in nodulation mutants of *Medicago truncatula*. *Proc Natl Acad Sci U S A* **97**, 13407-13412.
- Wang, X., Sager, R., Cui, W., Zhang, C., Lu, H., and Lee, J.Y.** (2013). Salicylic acid regulates Plasmodesmata closure during innate immune responses in *Arabidopsis*. *Plant Cell* **25**, 2315-2329.
- Ward, B.M., Medville, R., Lazarowitz, S.G., and Turgeon, R.** (1997). The geminivirus BL1 movement protein is associated with endoplasmic reticulum-derived tubules in developing phloem cells. *J Virol* **71**, 3726-3733.
- Whitford, R., Fernandez, A., De Groot, R., Ortega, E., and Hilson, P.** (2008). Plant CLE peptides from two distinct functional classes synergistically induce division of vascular cells. *Proc Natl Acad Sci U S A* **105**, 18625-18630.
- Wopereis, J., Pajuelo, E., Dazzo, F.B., Jiang, Q., Gresshoff, P.M., De Bruijn, F.J., Stougaard, J., and Szczyglowski, K.** (2000). Short root mutant of *Lotus japonicus* with a dramatically altered symbiotic phenotype. *Plant J* **23**, 97-114.
- Wu, S., O'Lexy, R., Xu, M., Sang, Y., Chen, X., Yu, Q., and Gallagher, K.L.** (2016). Symplastic signaling instructs cell division, cell expansion, and cell polarity in the ground tissue of *Arabidopsis thaliana* roots. *Proc Natl Acad Sci U S A* **113**, 11621-11626.
- Wu, X., Dinneny, J.R., Crawford, K.M., Rhee, Y., Citovsky, V., Zambryski, P.C., and Weigel, D.** (2003). Modes of intercellular transcription factor movement in the *Arabidopsis* apex. *Development* **130**, 3735-3745.
- Xie, B., Wang, X., Zhu, M., Zhang, Z., and Hong, Z.** (2011). CalS7 encodes a callose synthase responsible for callose deposition in the phloem. *Plant J* **65**, 1-14.
- Xie, F., Murray, J.D., Kim, J., Heckmann, A.B., Edwards, A., Oldroyd, G.E., and Downie, J.A.** (2012). Legume pectate lyase required for root infection by rhizobia. *Proc Natl Acad Sci U S A* **109**, 633-638.
- Xu, B., Cheval, C., Laohavisit, A., Hocking, B., Chiasson, D., Olsson, T.S.G., Shirasu, K., Faulkner, C., and Gilliam, M.** (2017). A calmodulin-like protein regulates plasmodesmal closure during bacterial immune responses. *New Phytol* **215**, 77-84.
- Yadav, S.R., Yan, D., Sevilem, I., and Helariutta, Y.** (2014). Plasmodesmata-mediated intercellular signaling during plant growth and development. *Front Plant Sci* **5**, 44-51.
- Yoshida, C., Funayama-Noguchi, S., and Kawaguchi, M.** (2010). plenty, a novel hypernodulation mutant in *Lotus japonicus*. *Plant Cell Physiol* **51**, 1425-1435.

- Zarsky, V., Kulich, I., Fendrych, M., and Pecenkova, T.** (2013). Exocyst complexes multiple functions in plant cells secretory pathways. *Curr Opin Plant Biol* **16**, 726-733.
- Zavaliev, R., Ueki, S., Epel, B.L., and Citovsky, V.** (2011). Biology of callose (beta-1,3-glucan) turnover at plasmodesmata. *Protoplasma* **248**, 117-130.
- Zavaliev, R., Levy, A., Gera, A., and Epel, B.L.** (2013). Subcellular dynamics and role of Arabidopsis beta-1,3-glucanases in cell-to-cell movement of tobamoviruses. *Mol Plant Microbe Interact* **26**, 1016-1030.
- Zhang, H., Jennings, A., Barlow, P.W., and Forde, B.G.** (1999). Dual pathways for regulation of root branching by nitrate. *Proc Natl Acad Sci U S A* **96**, 6529-6534.
- Zhang, J., Subramanian, S., Stacey, G., and Yu, O.** (2009). Flavones and flavonols play distinct critical roles during nodulation of *Medicago truncatula* by *Sinorhizobium meliloti*. *Plant J* **57**, 171-183.
- Zhang, Q., Walawage, S.L., Tricoli, D.M., Dandekar, A.M., and Leslie, C.A.** (2015). A red fluorescent protein (DsRED) from *Discosoma* sp. as a reporter for gene expression in walnut somatic embryos. *Plant Cell Rep* **34**, 861-869.
- Zipfel, C., and Oldroyd, G.E.** (2017). Plant signalling in symbiosis and immunity. *Nature* **543**, 328-336.